Study of carnitine palmitoyltransferase 1A (CPT1A) in adipose tissue.

Effects on obesity, inflammation and insulin resistance

Maria Ida Malandrino

UNIVERSIDAD DE BARCELONA

Departamento de Bioquímica y Biología Molecular

Facultad de Farmacia

STUDY OF CARNITINE PALMITOYLTRANSFERASE 1A (CPT1A) IN ADIPOSE TISSUE. EFFECTS ON OBESITY, INFLAMMATION AND INSULIN RESISTANCE

Maria Ida Malandrino

UNIVERSIDAD DE BARCELONA

Departamento de Bioquímica y Biología Molecular

Facultad de Farmacia

Memoria presentada por María Ida Malandrino, Licenciada en Biología por la Universidad de Perugia (Italia), para optar al grado de Doctora en la Universidad de Barcelona.

Esta tesis ha sido realizada bajo la dirección de los Doctores Laura Herrero Rodríguez y Fausto García Hegardt, en el Departamento de Bioquímica y Biología Molecular de la Facultad de Farmacia de la Universidad de Barcelona.

Director/Tutor	**Director**
Dra. Laura Herrero Rodríguez	**Dr. Fausto G. Hegardt**

Maria Ida Malandrino

Barcelona, 2013

Programa de doctorado: Biotecnología

A mi marido, Vittorio

GRAZIE, GRACIAS, GRACIÉS, THANK YOU

Finalmente llegó ese día tan esperado, un día lleno de emociones muy intensas…
Han sido cuatro años de aprendizaje, de esfuerzos, de risas y lagrimitas; un camino que por suerte no recorrí sola sino rodeada de personas que me han ayudado y querido muchísimo, que me han permitido ser una persona mejor y que *SIEMPRE* agradeceré.

A mis directores de tesis, la *Dra. Laura Herrero y* el *Prof. Fausto G.Hegardt.*
Al *Prof. Fausto G.Hegardt* por darme la oportunidad de desarrollar mi doctorado en ese grupo y de aprender tanto.

A la *Dra. Laura Herrero* por seguirme paso a paso en mi aprendizaje, por ser mi mentor y mi amiga, para enseñarme a encontrar siempre una respuesta a las dudas existenciales de los experimentos, por su pasión por la ciencia y por su optimismo. *GRACIAS Laura!*

A la *Dra. Dolors Serra y Dra. Guillermina Asins* por estar siempre pendiente de nosotros tanto a nivel profesional como a nivel personal, sobre todo y de enseñarme tanto. *GRACIAS!*

A mis queridos compañeros y amigos: Paula, Joan, Pep, Macarena, Kamil, Mar y los últimos "superfichajes" Minéia, Raquel y María porque además de ser un ayuda constante en mis experimentos, siempre han estado a mi lado cuando lo he necesitado, escuchando mis "locuras" y secando unas cuantas lagrimitas. *OS QUIERO UN MONTÓN!!*

A *mis niñas*, Lorea (alias *Bella Ciao*, *Gracias por todo!*), Begoña, Julia y Nina porque vuestra presencia en el lab ha traído mucha alegría y mucho "baile del Nile Red". *Gracias chicas!!*

A *tod@s los chic@s* del departamento que han compartido conmigo estos maravillosos años: Carlota, Elena, Lorena, Nuria, Xenia, Laura R, Elaine, Laura A, Joana, Marina, Mari, Albert, Ana.

A todos los profesores del departamento, los técnicos y las secretarias por ser siempre tan amables conmigo.

A David y Montse por ayudarme con mis "queridos" adipocitos! *Gracias* por vuestra constante disponibilidad.

A los *chic@s from IRB*: Valeria y Alessio, Sebas y Silvana, Eli y Tommy, Emma, Jessi, Rodolfo, Lorena, Sandra, Gonzalo y María, Carlos y Ágata. *Gracias* por las cenas, comidas y excursiones. Nos los pasamos muy bien juntos!

A *tod@s mis queridos amigos* que a lo largo de estos años han acompañado mi vida en BCN: Pauli, Sergi, Johnny, Alejandro, Pep, Xana, Marc, Rosada, Mar, David y Silvia. *GRACIAS por vuestro cariño! OS QUIERO MUCHO!*

A *mis queridos amig@s* de Italia por mantener siempre viva nuestra amistad, a pesar de la distancia, e interesarse siempre a mi vida. *VI VOGLIO BENE!*

A *mis padres* por enseñarme a ser una persona generosa y trabajadora, por agradecer siempre Dios por todo lo que tengo, por apoyarme siempre, en fin por quererme tanto. *GRACIAS POR TODO!*

A *mi hermano, mi abuela y a toda mi familia from Campania and Puglia,* por apoyarme en todo y por recordarme siempre su cariño. *GRACIAS!*

Finalmente, a *mi marido Vittorio*. Esta tesis es también la suya. *GRACIAS* por estar siempre a mi lado, por compartir al 100% las alegrías y las penas de nuestro trabajo, por recordarme que en dos se puede superar todo, por acabar el día siempre con un *"Te quiero". TI AMO.*

Maria Ida

ABBREVIATIONS

AAMs: Alternatively Activated Macrophages

ACC: Acetyl-CoA Carboxylase

AGPAT5: 1-Acylglycerol-3-Phosphate-O-Acyltransferase 5

Akt/PKB: Protein Kinase B

AMP: Adenosine Monophosphate

AMPK: AMP-Activated Protein Kinase

ANGPTL2/4: Angiopoietin-Like 2/4

AP-1: Activation Protein-1

aP2 (or FABP4): Fatty Acid Binding Protein 4

ASK-1: Apoptosis Signal-regulating Kinase 1

AT: Adipose Tissue

ATF4: Activating Transcription Factor 4

ATF6: Activating Transcription Factor 6

ATGL: Adipose Triglyceride Lipase (Desnutrin)

ATMs: Adipose Tissue Macrophages

ATP: Adenosine Triphosphate

AU: Arbitrary Units

BAT: Brown Adipose Tissue

BCL2: B-cell lymphoma 2

BiP/GRP78: Binding Immunoglobulin Protein

BMI: Body Mass Index

BMP7: Bone Morphogenetic Protein 7

BMPD8B: Bone Morphogenetic Protein 8B

CACT: Carnitine Acylcarnitine Transferase

c-Src: proto-oncogene c-Src

C/EBP: CCAAT/Enhancer Binding Protein

CAMs: Classical Activated Macrophages

CAT: Catalase

CD163: Cluster of Differentiation 163

CGI-58: Comparative Gene Identification - 58

CHOP: C/EBP Homologous Protein

Cidea: Cell death-inducing DFFA-like effector a

CLSs: Crown-Like Structures

CNS: Central Nervous System

COT: Carnitine Octanoyltransferase

CPT1A: Carnitine Palmitoyltransferase 1A (liver isoform)

CPT1AM: Carnitine Palmitoyltransferase 1A (mutant form)

CPT2: Carnitine Palmitoyltransferase 2

CrAT: Carnitine Acyltranferase

CREB: cAMP Response Element Binding protein

CRP: C-R eactive Protein

CXCL5: C-X-C motif chemokine 5

DAG: Diacylglycerol

DGAT1: Diacylglycerol Acyltransferase 1

DIO: Diet-Induced Obese

DIO2: Type II Iodothyronine Deiodinase

DMSO: Dimethylsulfoxide

E1: Pyruvate Deydrogenase

ECM: Extracellular Matrix

EDEM: ER Degradation Enhancing α-Mannosidase-like protein

eIF2α: eukaryotic translation Initiation Factor 2α

ER: Endoplasmic Reticulum

ERAD: Endoplasmic-Reticulum-Associated protein Degradation

ETC: Electron Transport Chain

FA(s): Fatty Acid(s)

FAD(H_2): Flavin Adenine Dinucleotide

FAO: Fatty Acid Oxidation

FAS: Fatty Acid Synthase

FFAs: Free Fatty Acids

FGF21: Fibroblast Growth Factor 21

GADD34: Growth Arrest and DNA Damage-inducible protein 34

GATA 2/3: Gata Binding Factor 2/3

GCN2: General Control Nonrepressed 2

GFP: Green Fluorescent Protein

GI: Gastro-Intestinal

GLUT4: Glucose Transporter-4

GM-CSF: Granulocyte-Macrophage Colony-Stimulating Factor

GPAT: Glycerol-3-Phosphate Acyltransferase

GPx: Glutathione Peroxidase

GSK3: Glycogen Synthase Kinase 3

GST4: Glutathione S-Transferase 4

HFD: High Fat Diet

HIF: Hypoxia Inducible Factor

HSL: Hormone Sensitive Lipase

ICAM: Intercellular Adhesion Molecule

IKK: IkB Kinase

IL-18: Interleukin-18

IL-1β: Interleukin-1β

IL-6: Interleukin-6

IMM: Inner Mitochondrial Membrane

IMTG: Intramuscular Triglycerides

iNOS: Inducible Nitric Oxide Synthase

IR: Insulin Receptor

IRE1: Inositol-Requiring protein 1

IRS: Insulin Receptor Substrate

JAK: Janus Kinase

JNK: c-Jun N-terminal Kinase

KLF: Krüppel-like factor

LCAS: Long-Chain Acyl-CoA Synthetase

LCFAs: Long-Chain Fatty Acids

LPA: Lysophosphatidic Acid

LPL: Lipoprotein Lipase

LPS: Lipopolysaccaride

M-CSF: Macrophages Colony-Stimulating Factor

m.o.i.: Multiplicity of Infection

MAG: Monoacylglycerol

MAPK: Mitogen Activated Protein Kinase

MCD: Malonyl-CoA Decarboxylase

MCP-1: Monocyte Chemoattractant Protein-1

MESCs: Mouse Embryonic Stem Cells

MIF: Macrophage migration Inhibitory Factor

MMP2/9: Matrix Metallo-Proteinasas 2/9

mTOR: mammalian Target Of Rapamycin

Myf: Myogenic Factor

NADH: Nicotinamide Adenine Dinucleotide

NAFLD: Nonalcoholic Fatty Liver Disease

NAMPT: Nicotinamide Phosphoribosyltransferase

NEFA: Non-Esterified FAs

NF-κB: Nuclear Factor κ-light-chain-enhancer of activated B cells

NLPR3: NOD-like receptor family, pyrin domain containing 3

NO: Nitric Oxide

NRF2: Nuclear factor (erythroid-derived 2)-like

OMM: Outer Mitochondrial Membrane

OXPHOS: Oxidative Phosphorilation

PA: Palmitate

PAI-1: Plasminogen Activator Inhibitor-1

PC: Pyruvate Carboxylase

PD3B: Phospho-Diesterase 3B

PDI: Protein Disulfide Isomerase

PDK1: 3-phosphoinositide-dependent protein kinase-1

PDK4: Pyruvate Dehydrogenase Kinase 4

PEPCK: Phosphoenolpyruvate Carboxykinase

PERK: PKR- like ER Kinase

PFU: Plaque Forming Unit

PGC-1: Peroxisome proliferator-activated receptor Gamma Coactivator- 1

PKA: Protein Kinase A

PKC: Protein Kinase C

PKR: Protein Kinase R

PP1: Phosphoprotein Phosphatase 1

PP2A: Protein Phosphatase 2A

PPAR: Peroxisome Proliferator Activated Receptor

PRDM16: PR Domain containing 16

PTB: Phosphotyrosine-binding

RBP-4: Retinol Binding Protein-4

RHMs: Recruited Hepatic Macrophages

RIDD: IRE1-Dependent Decay

RIP: Regulated Intramembrane Proteolysis

ROS: Reactive Oxygen Species

SAT: Subcutaneus Adipose Tissue

SCD1: Stearoyl-CoA Desaturase 1

SFAs: Saturated Fatty Acids

SIRT: Sirtuin

SkM: Skeletal Muscle

SOCS3: Suppressor Of Cytokine Signaling 3

SREBP 1c (or SREBF-1): Sterol Regulatory Element-Binding Protein 1c

STAT: Signal Transducer and Activator of Transcription

SVF: Stroma Vascular Fraction

T2DM: Type 2 Diabetes Mellitus

TCA: Tricarboxylic Acid cycle

TFAM: Mitochondrial Transcription Factor A

TG: Triglycerides

TLR4: Toll Like Receptor-4

TNF-α: Tumor Necrosis Factor-α

TRAF2: TNF Receptor Associated Factor 2

TRB3: Tribbles Homolog 3

UCP1: Uncoupling Protein 1

UPR*:* Unfolded Protein Response

VAT: Visceral Adipose Tissue

VCAM: Vascular Cell Adhesion Molecule

VEGF: Vascular Endothelial Growth Factor

WAT: White Adipose Tissue

XBP1: X-box Binding Protein 1

ABSTRACT

Current lifestyle with high-energy diets and little exercise is triggering an alarming growth in obesity. Excess of adiposity is leading to severe increase in associated pathologies, such as insulin resistance, type 2 diabetes (T2DM), atherosclerosis, cancer, arthritis, asthma, and hypertension. This, together with the lack of efficient anti-obesity drugs, is the driving force behind much research.

Obesity is associated with adipocyte dysfunction, macrophage infiltration, inflammation and decreased fatty acid oxidation (FAO) levels. Recent results suggest that enhancing cellular energy expenditure may be an attractive alternative therapy.

In this study, we propose that an increase in adipocytes and macrophages FAO rate could protect from obesity and insulin resistance by a decrease in the lipid content and inflammatory levels**.** Thus, we expressed carnitine palmitoyltransferase 1AM (CPT1AM), a permanently active mutant form of CPT1A (the rate-limiting enzyme in mitochondrial FAO) in 3T3-L1 CARΔ1 adipocytes and RAW 264.7 macrophages by adenovirus infection.

Visceral and subcutaneous adipose tissue (VAT and SAT, respectively) samples from lean, overweight, obese and diabetic patients were studied.

CPT1AM-expressing adipocytes and macrophages had increased FAO and showed a reduction in palmitate-induced increase in triglyceride content, inflammation, endoplasmic reticulum (ER) stress and reactive oxygen species (ROS) levels compared to GFP control cells. CPT1AM expression was able to restore palmitate-induced impairment in adipocyte insulin signaling.

Human data showed that CPT1A is highly expressed in adipose tissue macrophages compared to adipocytes both in VAT and SAT of overweight patients. No differences were seen in adipose tissue CPT1A mRNA expression between controls, overweight, obese and diabetic patients. Interestingly, in control and overweight patients, the more insulin resistant-associated human visceral adipose tissue expressed higher CPT1A levels compared to the subcutaneous depot.

These results points out to an increase in adipocyte and macrophage FAO as a promising strategy for the treatment of the obesity-induced metabolic syndrome.

INDEX

INTRODUCTION

1. OBESITY AND THE METABOLIC SYNDROME 3

1.1 PATHOPHYSIOLOGY OF OBESITY AND INSULIN RESISTANCE 3

2. ADIPOSE TISSUE AND OBESITY 15

2.1 WHITE ADIPOSE TISSUE (WAT) 15

2.2 BROWN ADIPOSE TISSUE (BAT) 24

3. ADIPOSE TISSUE REMODELLING DURING OBESITY 27

4. SUBCUTANEOUS ADIPOSE TISSUE (SAT) *vs* VISCERAL ADIPOSE TISSUE (VAT) IN THE PATHOPHYSIOLOGY OF OBESITY 29

5. MACROPHAGES IN OBESITY 30

5.1 MACROPHAGES SUBPOPULATIONS 30

6. MITOCHONDRIAL BIOENERGETICS 32

6.1 MITOCHONDRIAL BIOENERGETICS AND ROS 33

7. THE ROLE OF MITOCHONDRIA IN WHITE ADIPOSE TISSUE (WAT) 36

7.1 MITOCHONDRIAL DYSFUNCTION IN WAT DURING OBESITY 37

8. BIOENERGETICS AND MITOCHONDRIAL FATTY ACID OXIDATION (FAO) 39

8.1 MITOCHONDRIAL FATTY ACID OXIDATION (FAO) 39

8.2 CARNITINE PALMITOYLTRANSFERASE (CPT) SYSTEM 40

8.3 CPT1 ISOFORMS 41

8.4 CPT1 REGULATION 43

8.5 CPT1AM: ABOLITION OF MALONYL-CoA SENSITIVITY OF CPT1A 46

OBJECTIVES 51

MATERIALS AND METHODS

1. CELL CULTURE 55

1.1 SOLUTIONS AND BASIC PROCEDURES 55

1.2 3T3-L1 CARΔ1 ADIPOCYTES 57

1.3 RAW 264.7 MACROPHAGES 60

1.4 HEK 293 CELLS 61

2. ADENOVIRUS 61

2.1 ADENOVIRUS BIOLOGY 61

2.2 ADENOVIRUS AMPLIFICATION 62

2.3 ADENOVIRUS TITRATION 63

2.4 ADENOVIRUS INFECTION 64

3. PROTEIN ANALYSIS 66

3.1 TOTAL PROTEIN EXTRACTION 66

3.2 BCA PROTEIN QUANTITATION 66

3.3 WESTERN BLOT (WB) 67

4. PROTEIN CARBONYL CONTENT ANALYSIS (OXYBLOT) 72

5. CPT1 ACTIVITY ANALYSIS 73

5.1 MITOCHONDRIA ISOLATION 73

5.2 CPT1 ACTIVITY ASSAY 73

5.3 MALONYL-CoA INHIBITION ASSAY 76

6. CELLULAR METABOLISM ANALYSIS 76

6.1 OLEATE OXIDATION 76

6.2 OLEATE OXIDATION TO ACID SOLUBLE PRODUCT (ASP) 78

6.3 TRYGLICERIDES (TG) CONTENT ANALYSIS 80

6.4 OIL RED O STAINING 80

6.5 NILE RED STAINING 81

7. RNA ANALYSIS 82

7.1 TOTAL RNA EXTRACTION 82

7.2 RT-PCR 82

7.3 qRT-PCR 82

8. ANALYSIS OF CPT1A EXPRESSION IN HUMAN ADIPOSE TISSUE 83

8.1 SELECTION OF PATIENTS 83

8.2 ANTHROPOMETRIC MEASUREMENTS 84

8.3 COLLECTIONS AND PROCESSING OF HUMAN SAMPLES 84

8.4 ADIPOSE TISSUE FRACTIONATION 85
8.5 ANALYTICAL METHODS 85
8.6 WESTERN BLOT (WB) 85
8.7 IMMUNOHISTOCHEMISTRY 86
8.8 IMMUNOFLUORESCENCE 86
8.9 RNA ANALYSIS 88
9. STATISTICAL ANALYSIS 88
RESULTS
1. EFFECT OF CPT1AM EXPRESSION IN 3T3-L1 CARΔ1 ADIPOCYTES ON LIPID METABOLISM, INSULIN RESISTANCE, INFLAMMATION AND ROS DAMAGE DURING FATTY ACIDS OVERLOAD 91
1.1 ADENOVIRUS INFECTION OF 3T3-L1 CARΔ1 ADIPOCYTES 91
1.2 ANALYSIS OF CPT1A mRNA, PROTEIN AND ACTIVITY LEVEL 91
1.3 ANALYSIS OF FATTY ACID OXIDATION (FAO) RATE 93
1.4 ANALYSIS OF TRIGLYCERIDES (TG) CONTENT 94
1.5 ANALYSIS OF INSULIN SENSITIVITY 95
1.6 ANALYSIS OF INFLAMMATORY CYTOKINES LEVELS 96
1.7 ANALYSIS OF ENDOPLASMIC RETICULUM (ER) STRESS 97
1.8 ANALYSIS OF ROS DAMAGE 98
2. EFFECT OF CPT1AM EXPRESSION IN RAW 264.7 MACROPHAGES ON LIPID METABOLISM, INFLAMMATION AND ROS DAMAGE DURING FATTY ACIDS OVERLOAD 98
2.1 ADENOVIRUS INFECTION OF RAW 264.7 MACROPHAGES 99
2.2 EFFECT OF ADENOVIRUS INFECTION ON RAW 264.7 MACROPHAGES 99
2.3 ANALYSIS OF CPT1A mRNA, PROTEIN AND ACTIVITY LEVEL 100
2.4 ANALYSIS OF FATTY ACID OXIDATION (FAO) RATE 101
2.5 ANALYSIS OF TRYGLICERIDES (TG) CONTENT 102
2.6 ANALYSIS OF INFLAMMATORY CYTOKINES LEVELS 103

2.7 ANALYSIS OF ENDOPLASMIC RETICULUM (ER) STRESS 104

2.8 ANALYSIS OF ROS DAMAGE 105

3. CPT1A EXPRESSION IN HUMAN ADIPOSE TISSUE 106

3.1 ANALYSIS OF CPT1A EXPRESSION DURING DIFFERENTIATION OF HUMAN ADIPOCYTES 106

3.2 ANALYSIS OF CPT1A EXPRESSION IN HUMAN ADIPOSE TISSUE MACROPHAGES 107

3.3 ANALYSIS OF CPT1A EXPRESSION IN HUMAN ADIPOSE TISSUE FROM OBESITY COHORT 108

3.4 ANALYSIS OF CPT1A EXPRESSION IN HUMAN ADIPOSE TISSUE FROM T2DM COHORT 111

3.5 BIVARIATE CORRELATION AND MULTIPLE REGRESSION ANALYSIS FOR CPT1A EXPRESSION IN HUMAN ADIPOSE TISSUE OF OBESITY COHORT 112

DISCUSSION 117

CONCLUSIONS 127

REFERENCES 131

PUBLICATIONS 153

INTRODUCTION

1.OBESITY AND THE METABOLIC SYNDROME

Obesity is defined as abnormal or excessive fat accumulation in the adipose tissue and other organs. The World Health Organization (WHO) defines overweight as a body mass index (BMI), calculated as weight [kg] divided by height squared [m^2]) equal to or greater than 25 kg/m^2 and obese as a BMI equal to or greater than 30 kg/m^2 [1, 2].

Current lifestyle trends and continuous nutrient excess are causing obesity to increase at alarming rates, especially in young people. There are more than 500 million obese people worldwide and, more importantly, overweight and obesity are the fifth leading risk for global death [1, 2]. Humanity is facing a new epidemic already dubbed ‘‘Prosperity’s Plague’’ [3]. Therefore, significant research is needed in the race to find effective therapies and to minimize the enormous costs of the related healthcare.

Weight gain is influenced by several factors, such as genetics, maternal and perinatal environment, energy-dense diets, and sedentary lifestyle [4]. Of great concern is the prevalence of Metabolic Syndrome, a cluster of interrelated common clinical disorders, including obesity, insulin resistance, hypertension, and dyslipidemia [5-7] and the concurrent and parallel increase of pathological conditions associated with obesity, which comprise type 2 diabetes mellitus (T2DM), cardiovascular disease, nonalcoholic fatty liver, polycystic ovary syndrome, asthma, Alzheimer’s disease, and some forms of cancer.

Thus, elucidating the causes involved in the pathophysiology of obesity-related disorders is one of the most critical endeavors in modern medical research.

1.1 Pathophysiology of obesity and insulin resistance

Insulin resistance is the key etiologic defect that defines Metabolic Syndrome [6]. After initiation of the insulin-resistant, metabolic syndrome state, many of these patients eventually develop β- cell failure, which triggers the onset of T2DM [8].

Insulin is the most potent anabolic hormone known and is essential for appropriate tissue development, growth, and maintenance of whole-body glucose homeostasis.

Insulin is a member of a gene family which includes insulin-like growth factor (IGF)-I, IGF-II and relaxin. However, unlike the other members of this gene family, expression of insulin is restricted exclusively to the β-cells of the pancreas of Langerhans in response to increased circulating levels of glucose and aminoacids after a meal. Insulin regulates glucose

homeostasis at many sites, reducing hepatic glucose output promoting glycogen synthesis and inhibiting gluconeogenesis and increasing the rate of glucose uptake, primarily into skeletal muscle (SkM) and adipose tissue (AT), serving as the primary regulator of blood glucose concentration. Insulin also profoundly affects lipid metabolism, increasing lipogenesis in liver and AT, glycogen and protein synthesis, and inhibiting lipolysis in SkM and AT, glycogenolysis and protein breakdown [9] **(Fig.1).**

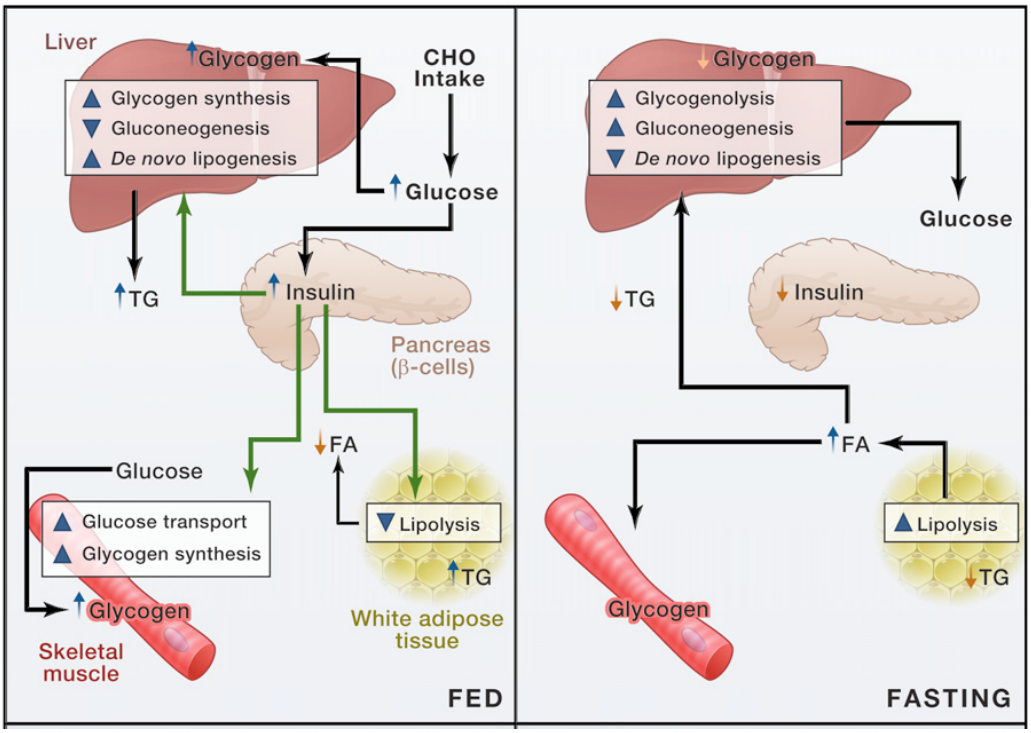

Fig.1. **Main insulin actions in fed and fasted state**
(Left) In the fed state, dietary carbohydrate (CHO) increases plasma glucose and promotes insulin secretion from the pancreatic β-cells. In the skeletal muscle (SkM), insulin increases glucose transport, permitting glucose entry and glycogen synthesis. In the liver, insulin promotes glycogen synthesis and *de novo* lipogenesis while also inhibiting gluconeogenesis. In the adipose tissue, insulin suppresses lipolysis and promotes lipogenesis. (Right) In the fasted state, insulin secretion is decreased. The drop in insulin (as well as the action of other hormones that are not depicted) serves to increase hepatic gluconeogenesis and promote glycogenolysis. Hepatic lipid production diminishes while adipose lipolysis increases. (TG: Triglycerides; FA: Fatty Acids). Adapted from Samuel V. *et al*. *Cell,* 2012 [10].

Furthermore, insulin also acts upon hypothalamic neurons, pancreatic islet cells, and the vasculature to regulate food intake, energy expenditure, hormone production, and blood flow [11, 12].

A key action of insulin is to stimulate glucose uptake into cells (SkM and AT) by inducing translocation of the glucose transporter, GLUT4, from intracellular storage to the plasma membrane. An important signaling molecule in this pathway is protein kinase B (PKB) or Akt [9].

In adipocytes, glucose is stored primarily as lipids, owing to increased uptake of glucose and activation of lipid synthetic enzymes, including pyruvate dehydrogenase (E1), fatty acid synthase (FAS) and acetyl-CoA carboxylase (ACC). Insulin also profoundly inhibits lipolysis in adipocytes, primarily through inhibition of the enzyme hormone-sensitive lipase (HSL). This enzyme is acutely regulated by control of its phosphorylation state, which is activated by protein kinase A (PKA)-dependent phosphorylation, and inhibited as a result of a combination of kinase inhibition and phosphatase activation. Insulin inhibits the activity of the lipase primarily through reductions in cAMP levels, owing to the activation of a cAMP-specific phosphodiesterase in fat cells [9].

When normal circulating concentrations of insulin are insufficient to regulate these processes appropriately in metabolically active organs and tissues, like liver, SkM and AT, insulin resistance occurs. Thus, by definition, insulin resistance is a defect in signal transduction.

The etiology of insulin resistance is very complex. Several mechanisms have emerged in the past two decades to explain the pathogenesis of this multifactorial condition, mainly, the ectopic lipid accumulation, the systemic inflammation, the development of ER stress and more recently, the change of gastrointestinal (GI) microbiota.

Though many additional mechanisms have been offered, these four represent different aspects of metabolic control that ultimately may converge on common pathways to regulate insulin action [10].

1) Ectopic lipid accumulation and lipotoxicity

Normal cellular fatty acids (FAs) homeostasis reflects a balance between processes that generate or deliver FAs and processes that utilize these molecules.

In mammalian cells, free fatty acids (FFAs) are generated through the *de novo* synthetic pathway and liberated when triglycerides (TG) and phospholipids are hydrolyzed by cellular

lipases. FFAs can also be imported into mammalian cells by both protein- and non-protein-mediated mechanisms, either when cellular demand is high or when extracellular FFAs concentrations are high [13]. FFAs derived from each of these processes can be utilized for membrane biosynthesis, energy production through β-oxidation, generation of lipid signaling molecules, post-translational protein modification, and transcriptional regulation. When cells accumulate more FFAs than are required for anabolic or catabolic processes, excess lipid is esterified and stored as TG in lipid droplets. These single-membrane bound compartments are dynamic and FAs stored within may be mobilized through the actions of cellular lipases, in a process regulated by hormones and by droplet-associated proteins. Adipocytes have the capacity to store large amounts of excess FFAs in cytosolic lipid droplets.

During obesity the excessive fat calorie load is so high that it exceeds the buffering capacity and efficiency of adipose tissue storage so that these excess fat calories "overflows" to other tissues like SkM, liver, pancreas and heart [13]. This inappropriate accumulation in non-adipose tissues is defined ectopic lipid accumulation and the resultant cellular dysfunction or cell death is termed lipotoxicity [14, 15].

In T2DM, ectopic lipid accumulation impairs insulin signaling. With accumulation of intramyocellular lipid (IMCL), insulin-mediated SkM glucose uptake is impaired. As a result, glucose is diverted to the liver. In the liver, increased lipid content also impairs the ability of insulin to regulate gluconeogenesis and activate glycogen synthesis. In contrast, lipogenesis remains unaffected and, together with the increased delivery of dietary glucose, leads to increased lipogenesis worsening nonalcoholic fatty liver disease (NAFLD).

Impaired insulin action in the adipose tissue allows for increased lipolysis, which will promote re-esterification of lipids in other tissues (such as liver) and further exacerbates insulin resistance. Coupled with a decline in pancreatic β- cells, hyperglycemia develops.

All these mechanisms are summarized in the **Fig.2**.

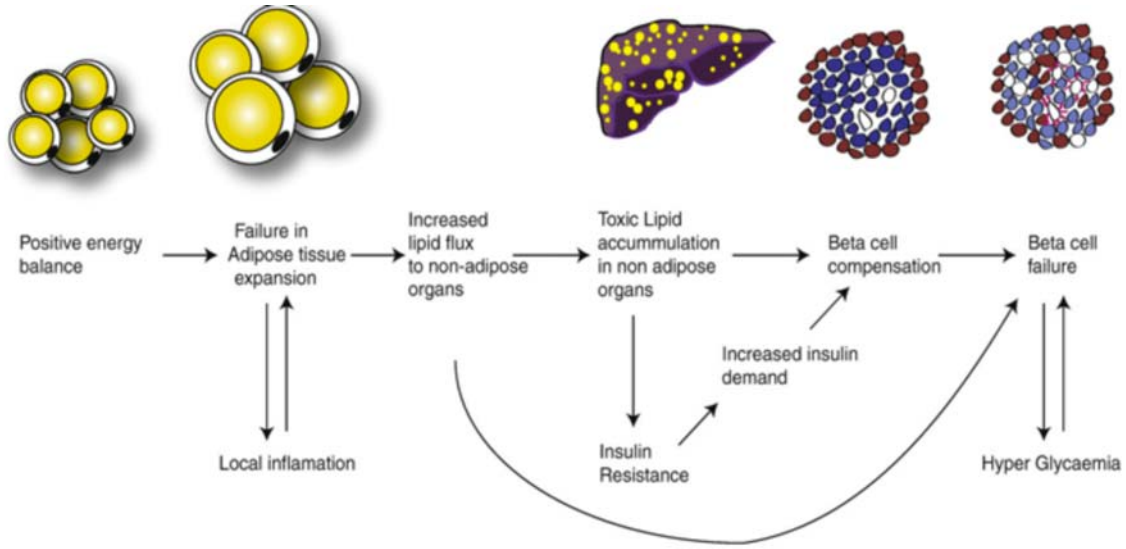

Fig.2 Ectopic lipid accumulation and lipotoxicity
During obesity the excessive fat calorie load is so high that adipose tissue no longer appropriately buffers lipid flux. These excess fat calories "overflows" to tissues other than adipose tissues (*e.g.*, liver, pancreas etc.) resulting in cellular dysfunction (lipotoxicity). Adapted from Virtue S. *et al.*, Biochim Biophys Acta, 2010 [7].

In liver and muscle, insulin action impairment is mediated by intermediaries of FAs metabolism (*e.g.,* DAG, PA, LPA, ceramide). Lysophosphatidic acid (LPA), palmitate (PA), diacilglycerol (DAG), and ceramide can activate the mTOR/ p70S6K, JNK, IKK, and/or the novel PKC/conventional PKC (nPKC/cPKC; e.g., PKC-θ) pathways that negatively regulate insulin action [16-19].

2) Inflammation

Low-grade tissue inflammation is a major and well-known cause of obesity-induced insulin resistance [8]. Initial landmark observations in this area were made by Hotamisligil *et al*., who showed an increase in tumor necrosis factor-α (TNF-α) concentration in obese adipose tissue and that TNF-α neutralization improved insulin sensitivity in obese rodent models [20-22].

Later studies by Weisberg *et al*. and Xu *et al.* demonstrated that adipose tissue from obese humans and mice is characterized by a striking accumulation of macrophages. Indeed, up to 40% of all cells in obese adipose tissue are infiltrating macrophages [23, 24]. Subsequent studies have demonstrated that adipose tissue macrophages (ATMs) are highly activated, with increased expression of a large array of proinflammatory genes [25, 26]. These proinflammatory genes include a set of cytokines, particularly TNF-α, that are excessively

secreted from activated macrophages and directly cause insulin resistance by acting on insulin target cells in local tissues through paracrine mechanisms [20, 27].

TNF-α signaling activates intracellular kinases, such as c-Jun N-terminal kinase (JNK) and IkB kinase (IKK), which inhibit insulin receptor signaling by serine phosphorylation of insulin receptor substrate 1 (IRS-1). Furthermore, activation of the transcription factors, activator Protein-1 (AP-1) and nuclear factor κ-light-chain-enhancer of activated β cells (NF-κB) results in a feed-forward mechanism whereby proinflammatory cytokines production is exacerbated. If the magnitude of cytokines secretion is great enough, they can leak out of the tissue, raising circulating levels, to produce endocrine effects on distant organ systems, such as muscle and liver, exacerbating systemic insulin resistance [28].

However, the adipose tissue concentrations of cytokines are much higher than circulating levels, and it is likely that, in most circumstances, the major effects of these secretory products are local rather than systemic [21].

Although increased adiposity causes insulin resistance, it has long been known that visceral adipose tissue (VAT) has a much greater negative metabolic effect than subcutaneous adipose tissue (SAT). In obesity, increased macrophage accumulation and other signs of inflammation occur in the VAT, but not in the SAT depots, consistent with the negative impact of VAT expansion on insulin sensitivity [8].

Similar etiologic events can also occur in the liver [28, 29]. During obesity, there is a substantial increase in resident hepatic macrophages, termed Kupffer cells and also in recruited hepatic macrophages (RHMs), which migrate into the liver under obese conditions [30]. However, the relative contributions of these different cell types to hepatic inflammation and insulin resistance remain unresolved.

Interestingly, it has been shown that obesity is associated with hypothalamic inflammation [31] and that the resulting local production of proinflammatory cytokines can cause central leptin resistance, a key feature of obesity [29]. In addition, central nervous system (CNS) inflammation can contribute to systemic insulin resistance, particularly in the liver, via a brain-liver neuronal signal [32]. Thus, inflammation in the CNS during obesity may be a key determinant of weight gain and systemic insulin sensitivity.

Increased numbers of macrophages have been observed also in the pancreatic islets of HFD-fed rodents as well as in islets from individuals with T2DM [28, 33]. On the basis of these

findings, it is possible that a heightened inflammatory response in islets has a role in the cell dysfunction characteristic of T2DM.

Obesity does not appear necessarily or uniformly to induce inflammation in muscle tissue, but inflammatory mediators from other sites such as liver and adipose can influence muscle metabolism [29]. For example, morphologically, macrophage infiltration is not observed in muscle fibers *per se* in obese animals, but the adjacent adipose tissue displays increased infiltration compared with lean tissues [23]. Also, unlike adipose or liver tissues, muscle does not express or release significant amounts TNF-α or IL-6 in T2DM patients compared with controls and therefore is not likely to be a source for the rise in inflammatory mediators [34, 35].

The diversity of ATMs, Kupffer cells, and RHMs indicates that tissue macrophages consist of heterogeneous populations with differential functions [8, 36]. In the obese state, the balance is clearly tilted toward the proinflammatory macrophage phenotype [8, 29]. Macrophages are by no means the only immune cell type that participates in the process of inflammation-induced insulin resistance. Neutrophils [37] and mast cells [38] are increased in obese adipose tissue, and studies in mice have indicated that these two cell types can promote insulin resistance. Lymphocytes also play an important role. B lymphocytes [39], CD8+ cytotoxic T lymphocytes [40], and CD4+ TH_1 cells [41] promote insulin resistance, whereas CD4+ regulatory T (Treg) cells are anti-inflammatory [42, 43]. The numbers of Tregs and TH_2 cells are absolutely or relatively decreased in obese adipose tissue [41, 43], and these cells serve an important function in modulating macrophage behavior. Treg and TH_2 cells can inhibit polarization of proinflammatory macrophages and can also prevent their recruitment into tissues. Another checkpoint promoting the anti-inflammatory state is provided by eosinophils [44].

In the *in vivo* situation, it is unlikely that these cell types work in isolation but, rather, are part of an ongoing interactive immune cell conversation.

Amplification of the inflammatory signal

Circulating FFAs levels are often elevated in obese and/or diabetic states, and satured fatty acids (SFAs) can activate cellular proinflammatory pathways through Toll-like receptor 4 (TLR4)-dependent mechanisms, demonstrating the link between this form of lipotoxicity and

inflammatory signaling [45, 46].

Stimulation of TLR4 by SFAs induces activation of JNK and IKK, which directly inhibit insulin signaling via serine phosphorylation of IRS-1. Furthermore, activation of these kinases leads to NF-κB and AP-1 activation and changes in the expression of genes that influence insulin action, providing an additional mechanism for SFAs-induced insulin resistance [47].

Activation of the inflammasome can also be a consequence of SFAs stimulation [48].The inflammasome mediates the caspase-1-driven cleavage of pro-IL-1β and pro-IL-18, leading to the secretion of the active forms of these cytokines; deficiency of inflammasome components (such as NLRP3*)* ameliorates insulin resistance. Thus, SFAs-induced inflammasome activation exacerbates inflammation, resulting in the inhibition of insulin action [8].

SFAs can also be incorporated into specific lipid raft domains of the plasma membrane, where they enhance TLR4 dimerization and c-Src recruitment [49, 50]. This activates downstream stress signaling pathways (such as JNK/AP-1) that inhibit insulin action [50].

The stress-activated protein kinases JNK1 and IKKB are central signal transducers in innate immunity and stress responses that control the expression of several proinflammatory genes. The JNK subgroup of stress-activated kinases belongs to the mitogen-activated protein kinases (MAPK) family, whose constituents are activated in response to growth factors, proinflammatory cytokines, microbial components, such as lipopolysaccharide (LPS), and a variety of stresses. Once activated, the JNKs phosphorylate and activate transcription factors including c-Jun, leading to increased *Jun* and *Fos* gene transcription and increased AP-1 transcription factor activity.

The JNKs have also been implicated in post-transcriptional control of gene expression by causing stabilization of inherently unstable mRNAs encoding cytokines and other inflammatory mediators**.** IKKβ, on the other hand, is one of the 2 catalytic subunits (together with IKKα) of the IkB kinase (IKK) complex, whose activity is rapidly stimulated by proinflammatory cytokines, viral and microbial components, and numerous other inducers. IKK is responsible for activation of the NF-kB/Rel family of transcription factors through its ability to phosphorylate their IkB inhibitors and target them to proteolitic degradation. Once freed from the IkB grasp, NF-kB dimers enter the nucleus and regulate transcription of genes involved in innate immunity and inflammation, as well as the maintenance of cell survival

and tissue homeostasis [51].

Molecular pathway interfacing inflammation and obesity are summarized in **Fig.3.**

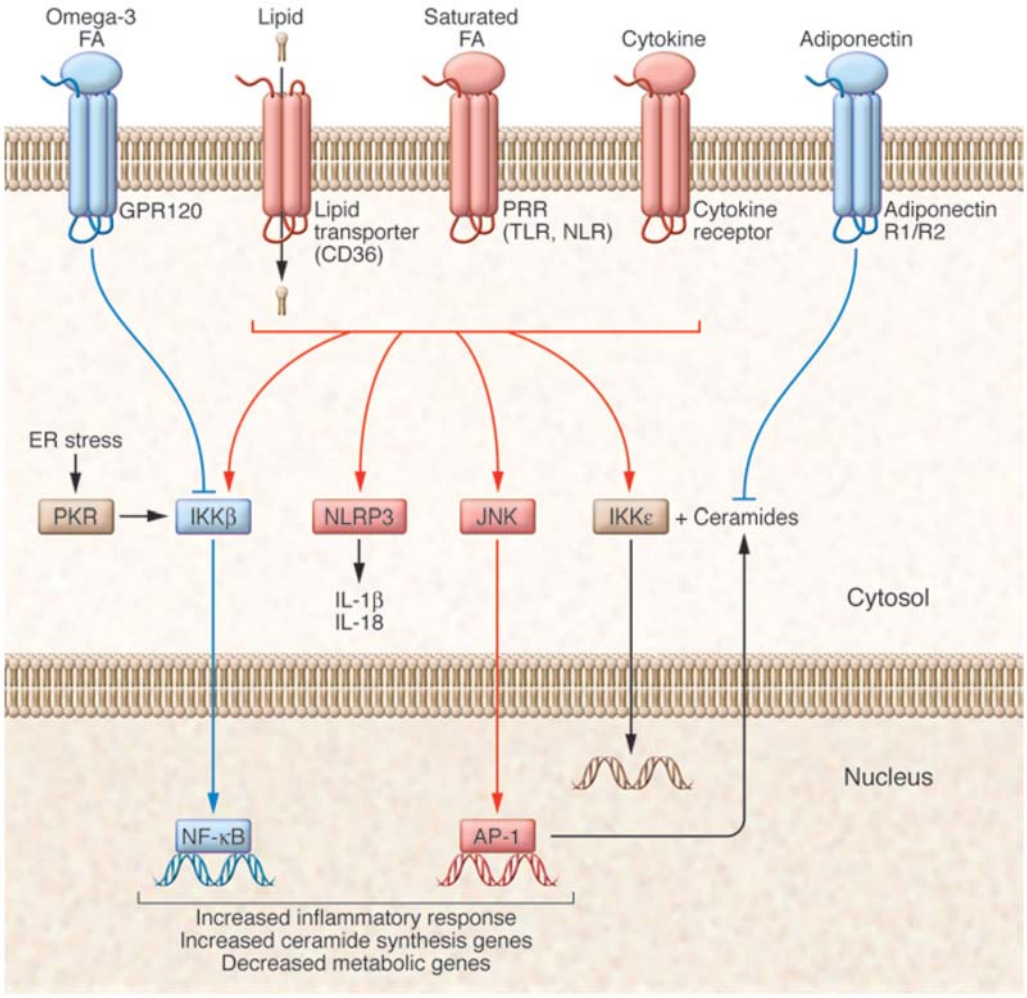

Fig.3 Molecular pathway interfacing obesity and inflammation
Multiple signaling pathways participate in translating obesity-derived nutrient and inflammatory signals into a cellular response relevant in disease. These include proinflammatory and antinflammatory signals from the cells surface that integrate through many common intracellular pathways to generate the coordinated increase in inflammatory genes while repressing genes important in maintaining proper nutrient metabolism. NLPR3*:* NOD-like receptor family, pyrin domain containing 3; PERK: PKR-like ER kinase. From Lumeng C.L. *et al., JCI,* 2011 [52].

3) ER stress

The ER is the site of synthesis, folding and maturation of secreted and transmembrane proteins, storage of Ca^{2+}, and lipid biosynthesis [53].

ER stress is defined as an imbalance between the protein folding capacity of the ER and the client protein load, resulting in the accumulation of misfolded protein. Loss of ER homeostasis activates the ER stress response, also known as the Unfolded Protein Response (UPR). This response is an adaptive mechanism, especially important in secretory cells, that serves to dynamically expand both the size of the ER and its capacity according to the functional demand placed upon the exocytotic pathway.

The sensing of stress in the ER lumen and ER-to-cytoplasm or -nucleus communication is mediated by three canonical ER stress transducers: inositol-requiring 1 (IRE1), PKR-like ER kinase (PERK) and activating transcription factor 6 (ATF6).

In a well-functioning and ‘‘stress-free’’ ER, these three transmembrane proteins are bound by a chaperone, GRP78 (glucose-regulated protein 78), also called BiP (immunoglobulin heavy chain binding protein), in their intralumenal domains (amino-terminal of IRE1 and PERK and carboxy-terminal of ATF6) and rendered inactive [53]. Accumulation of improperly folded proteins and increased protein cargo in the ER results in the recruitment of BiP away from these UPR sensors and consequently cause the activation of IRE1, PERK and ATF6, engage a complex downstream signaling pathway as described in the **Fig.4**. Upon ER stress, PERK phosphorylates the subunit of eukaryotic translation initiation factor 2 (eIF2α) leading to rapid reduction in the initiation of mRNA translation, and thus reducing the load of new proteins in the ER. Paradoxically, phosphorylation of eIF2α by PERK allows the translation of activating transcription factor 4 (ATF4). ATF4 induces transcription of genes involved in amino acids synthesis and apoptosis, such as tribbles homolog 3 (TRB3) and C/EBP homologous protein (CHOP). PERK also phosphorylates the nuclear factor erythroid 2 (NRF2), an antioxidant-response transcription factor. By activating the expression of the growth arrest and DNA damage-inducible protein (GADD34) that targets the protein phosphatase 1 (PP1) to eIF2α for dephosphorylation, ATF4 also participates in the retrocontrol of PERK signaling. In addition to its response to ER stress, eIF2α is phosphorylated by three other kinases: double-stranded RNA (dsRNA)-activated protein kinase (PKR), general control non-derepressible kinase 2 (GCN2), and heme-regulated inhibitor kinase (HRI), that are respectively activated by dsRNA, amino acid depletion, and heme deprivation. Owing to its activation by various stresses, the eIF2α/ATF4 pathway has been designated as the ‘integrated stress response’. Upon ER stress, autophosphorylation of

IRE1 unmasks its endoribonuclease activity that is responsible for the unconventional splicing of the X box-binding protein 1 (XBP1) mRNA and its translation into the transcription factor XBP1s. XBP1s upregulates the transcription of genes encoding ER chaperones, components of the endoplasmic-reticulum-associated protein degradation (ERAD) machinery and phospholipid biosynthesis. IRE1 has also a nonspecific endoribonuclease activity that is responsible for the degradation of ER-localized mRNAs, a process named regulated IRE1-dependent decay (RIDD). This mechanism also contributes to the reduction of protein accumulation in the ER. IRE1 also activates c-jun N-terminal kinase (JNK) by recruiting the scaffold protein tumor necrosis factor receptor-associated factor 2 (TRAF2) as well as the apoptosis signal-regulating kinase (ASK1), and caspase 12, which are proapoptotic. Finally, ATF6 translocates from the ER to the Golgi where it is cleaved by regulated intramembrane proteolysis (RIP) by site 1 and site 2 proteases. The cytoplasmic part of ATF6, an active transcription factor, transactivates genes encoding ER chaperones, ERAD components, and protein foldases [54].

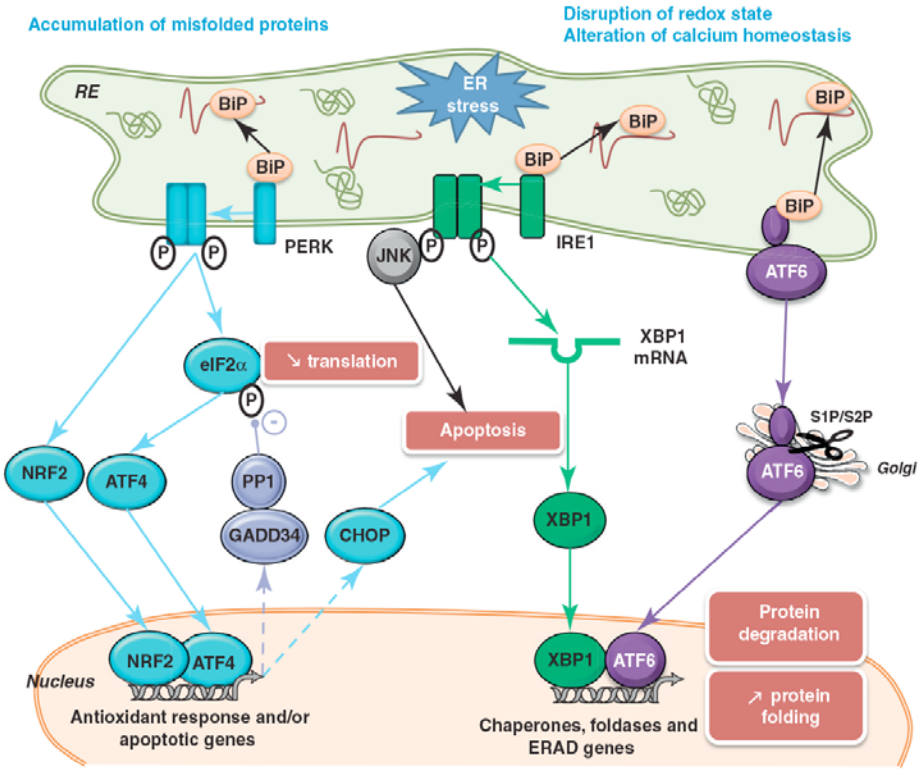

Fig.4 The unfolded protein response (UPR) pathway
In unstressed conditions, the BiP chaperone interacts with the luminal domain of the three

endoplasmic reticulum (ER) transmembrane sensors, ATF6, IRE1, and PERK, and maintains them in an inactive state. Upon ER stress, BiP interacts with unfolded proteins, leading to the activation of the UPR transducers**.** From Flamment M. *et al.*, *Trends in Endocrinol Metab*, 2012 [54].

The ER can be viewed as a ‘‘nutrient- sensing’’ apparatus, establishing specific functional links with metabolic responses including links with endocrine networks that have systemic actions. As explained above, the UPR is closely integrated with stress signaling, inflammation, and JNK activation and given that obesity stresses the ER (due to an increase in synthetic demand, alterations in energy availability, and activation of inflammatory pathways), obesity lead to chronic ER stress in metabolically active tissues such as liver and adipose tissue.

Indeed, ATF6-regulated chaperones are increased in subcutaneous adipose tissue (SAT) from obese individuals [53, 55]. Increased eIF2α phosphorylation in enlarged fat depots possibly reflects PERK activation. IRE1 activation was found in fat of obese, compared with nonobese, volunteers, with JNK1 activation and upregulation of XBP1s mRNA, calreticulin, calnexin and protein disulfide isomerase [53, 56]. In a study comparing various fat depots, BiP and XBP1 expression was higher in VAT compared with SAT, and more so in severe obesity [53, 57]. All these mechanisms contribute to insulin signaling impairment.

In addition to contributing to inflammation, ER stress can modify FFAs and adipokines secretion. Adipocyte ER stress induces basal lipolysis through downregulation of perilipin [58, 59]. Decreased ER disulfide-bond A oxidore-ductase-like (DsbA-L) protein expression in obesity impairs adiponectin folding and multimerization and causes ER stress [60, 61]. Insulin receptor expression and leptin secretion are also decreased upon ER stress, whereas IL-6 is strongly induced [58]. ER stress also inhibits resistin transcription in murine adipocytes through upregulation of CHOP [62].

In summary, excess nutrients during obesity lead to UPR signaling in fat, but also in liver, muscle, hypothalamus and β-cells in obesity and diabetes by mechanisms that are not yet fully elucidated, and several questions remain to be answered.

4) Microbiota and obesity

Recent studies have demonstrated that the microbiota of the gastrointestinal (GI) tract plays an important role in the modulation of obesity and insulin sensitivity [63, 64]. Indeed, in

mouse models of obesity, the composition of the microbiota is altered, a phenomenon referred to as *dysbiosis* [65-67]. In addition, increased levels of circulating bacteria or bacterial products, such as LPS, which are derived from the microbiota, have been associated with insulin resistance [68].

Through their activity in the lumen, the microbiota also produce bioactive metabolites, such as acetate, bile acid derivatives, and hydrogen species, all of which can reach the circulation and influence systemic insulin sensitivity, inflammation, and energy metabolism.

Whether microbial dysbiosis is a cause or consequence of obesity and/or insulin resistance is a matter of ongoing debate [64], given that most studies describe associations of dysbiosis with metabolic disease rather than mechanistic connections. It also remains to be established how well these processes or mechanisms observed in mice can be extrapolated to humans.

2. ADIPOSE TISSUE AND OBESITY

Adipose tissue (AT) has an important role in the maintenance of energy homeostasis and its dysfunction is crucial in the development of the metabolic syndrome [69].

Two types of adipose tissue exist in humans, white adipose tissue (WAT) and brown adipose tissue (BAT).

2.1 White adipose tissue (WAT)

Function and distribution of WAT

WAT has long been recognized as the main storage site for lipids derived from food intake. This long-term energy reservoir stores lipids mainly in the form of triglycerides (TG), which can be mobilized and used to generate ATP through the mitochondrial β-oxidation pathway in peripheral organs during periods of caloric need.

WAT is an active and endocrine organ that secretes a large number of adipokines, cytokines, and chemokines, overall named adipocytokines, and plays a key role in regulating whole-body glucose and lipid metabolism [69].

WAT represents the major proportion of adipose tissue (AT) in humans, although there is increasing evidence that BAT is present in significant quantities and co-exists with WAT within the same depot as described later. In humans, WAT is dispersed throughout the body.

Visceral adipose tissue (VAT) includes the intra-abdominal depots around the omentum, intestines, mesenteric and perirenal areas, whereas subcutaneous adipose tissue (SAT) includes the subcutaneous depots in the buttocks, thighs, and abdomen. About 80% of all body fat is in the subcutaneous areas. Visceral fat accounts for up to 10–20% of total fat in men and 5–8% in women. The amount of visceral fat increases with age in both genders.

Both visceral and subcutaneous adipose depots are well developed at birth and continue to develop throughout adult life [70]. In addition, WAT can be found in many other areas, including in the retro-orbital space, on the face and extremities, and within the bone marrow.

The majority of adipose tissue development is completed in early life, and fat mass expansion in later life is thought to be mainly due to enlargement of the size of white adipocytes. The number of adipocytes is relatively stable, and the turnover rate is approximately 10% per year in adult life. About half of the white adipocytes in humans are replaced every 8.3 years [71].

Some adipose tissue depots are responsive to sex hormones, such as AT in the breasts and thighs, whereas other depots, such as fat on the neck and upper back, are more responsive to glucocorticoids, forming a so-called “buffalo-hump”.

Fat distribution, even in thin individuals with steady body weight and stable BMI, changes with age, decreasing in retro-orbital fat and subcutaneous fat and increasing in intra-abdominal fat [72, 73].

Composition of WAT

WAT is heterogeneous and contains multiple cell types. Adipocytes are the main cellular component of adipose tissue, and they are crucial for both energy storage and endocrine activity. The other cell types that are present are precursor cells (including pre-adipocytes), fibroblasts and immune cells. Furthermore, AT contains cells from the vascular (endotelial and vascular smooth cells) and nervous systems. All these non-adipose cells constitute the stromal vascular fraction (SVF) of adipose tissue. Factors that are secreted by these different cellular components are critical for maintaining homeostasis in adipose tissue and throughout the body.

White adipocytes have a single large cytoplasmic lipid droplet of TG with the nucleus located

to the side of the cell and low mitochondrial density. Lipid droplets in adipocytes are tightly regulated specialized organelles [73, 74].

Regulation of lipolysis and lipogenesis in WAT

In the fed state, insulin is the principal stimulus of TG formation in white adipocytes, stimulating GLUT4 mediated glucose transport and the activity of acetyl CoA-syntase (ACC), the rate-limiting step of FAs synthesis from acetyl-CoA [75]. Insulin, via Akt/PKB mediated phosphorylation and activation of PDE3B (phosphodiesterase 3B), stimulates the breakdown of cAMP, thereby suppressing lipolysis. TG is formed from the esterification of FAs and glycerol-3-phosphate. Glyceroneogenesis is the dominant pathway for TG-glycerol synthesis in WAT [76]. The key enzyme of this metabolic process is the cytosolic isoform of phosphoenolpyruvate carboxykinase (PEPCK), which catalyses decarboxylation of oxaloacetate to form phosphoenolpyruvate. Another important player in the process of glyceroneogenesis is mitochondrial pyruvate dehydrogenase that functions as a metabolic switch between glucose and fatty acids (FAs) utilisation. Its inhibition by pyruvate dehydrogenase kinase 4 (PDK4) enables pyruvate to be used for glyceroneogenesis when the supply of glucose is low [77].

FAs are obtained from circulating lipoproteins by LPL (lipoprotein lipase)-mediated lipolysis and are transported into the adipocyte or synthesized *de novo* by lipogenesis from non-lipid substrates such as glucose [78]. The key transcription factor regulating lipogenic gene expression and thus lipid synthesis is sterol regulatory element-binding protein-1c (SREBP-1c).

In contrast, in the fasted state, or during prolonged physical activity, TG in the lipid droplet is hydrolysed to FAs and glycerol, by the successive action of ATGL (adipose triglyceride lipase; also known as desnutrin), which converts TG into DAG, HSL (Hormone Sensitive Lipase), which converts DAG into MAG (monoacylglycerol) and MAG lipase, which converts MAG into FAs and glycerol for use by other tissues for ATP generation or hepatic gluconeogenesis respectively. In the fasted state noradrenergic stimulation of adipose tissue induces the formation of the second messenger cAMP, with subsequent activation of PKA (cAMP-dependent protein kinase) which phosphorylates and recruits the lipid droplet scaffolding protein perilipin and HSL to the lipid droplet to stimulate lipolysis [74]. HSL is

phosphorylated by PKA at Ser^{563}, which increases its intrinsic activity, and Ser^{659} and Ser^{660}, which are involved in the translocation of HSL from the cytosol to the lipid droplet. In the absence of cAMP, perilipin is associated with the protein CGI-58 (comparative gene identification-58). Upon perilipin phosphorylation by PKA, CGI-58 is released and interacts with ATGL, stimulating lipase activity [79].

Lipolysis of TG in white adipocytes is associated with re-esterification of a part (30–90% at basal state, and 10–20% at stimulated state) of lipolyzed FAs back into adipose TG, *i.e.* futile TG/FA cycling. Substrate cycles could provide a mechanism of variable sensitivity for controlling the flux through a metabolic pathway. Thus, TG/FAs cycle in white adipocytes has the key role in metabolic flexibility of adipocytes, as well as the whole organism.

In response to long-term fasting and other strong hormonal and pharmacological stimuli, the balance between the rates of lipolysis and FAs re-esterification within adipocytes may be affected. Higher activity of TG/FAs cycle in human VAT [80] corresponds with relatively high mitochondrial content and oxidative phosphorylation (OXPHOS) activity in this fat depot as compared with SAT. Moreover, induction of lipolysis in adipocytes is linked to stimulation of mitochondrial FAO. In turn, a decrease in mitochondrial ATP production results in the inhibition of both FA synthesis and lipolytic action of catecholamines.

In the absence of the stimulation of TG/FA cycle, fatty acid oxidation (FAO) is relatively slow, which is consistent with the low carnitine palmitoyltransferase 1 (CPT1) activity in WAT. However, the amount of FAs disposed through oxidative pathway increased about 1.5-fold with the stimulation of lipolysis and TG/FAs cycle by fasting.

5' AMP-activated protein kinase (AMPK) plays a key role in the up-regulation of mitochondrial biogenesis and activation of mitochondrial FAO under various conditions leading to stimulation of lipolysis and TG/FA cycle. AMPKα1 has been reported to be the principal catalytic subunit isoform expressed in human SAT and mouse BAT and it's also the dominant isoform in isolated epididymal rat adipocytes and cultured 3T3- L1 adipocytes [73].

Adipogenesis of WAT

In a human fetus, WAT appears in the six principal fat deposit sites as early as the second trimester, an important period for WAT development. White adipocytes mostly derive from the lateral plate mesoderm from stem cells that are negative for the myogenic factor Myf5.

WAT development begins with an accumulation of a dense mass of mesenchymal stem cells (MESCs) at various sites while angiogenesis occurs. MESCs develop into adipocytes near the networks of capillaries. Early fat cell clusters then develop into WAT, consisting of vascular structures and densely packed white adipocytes. Due to nutrition restriction, WAT development is much slower in the uterus compared to after birth [81, 82].

The transition from preadipocyte to adipocyte involves four stages: growth arrest, clonal expansion, early differentiation, and terminal differentiation. These stages are orchestrated by a transcriptional cascade involving the nuclear receptor PPARγ and members of the C/EBPs family **(Fig.5)**.

PPARγ plays an important role in adipogenesis and has been shown to be necessary and sufficient for adipocyte differentiation. PPAR-γ also appears to be required for maintenance of the terminal differentiated state of adipocytes. Two isoforms of PPARγ (PPARγ1 and PPARγ2) are generated by alternative splicing and promoter usage of the *Pparγ* gene. Although both are expressed in adipocytes, PPARγ2 has been regarded as a specific marker of fat.

The C/EBP family consists of five different members, C/EBPα C/EBPβ, C/EBPδ, C/EBPγ, and CHOP. Sequential expression of these factors is observed during adipocyte differentiation, in which the early expression of C/EBPβ and C/EBPδ promotes expression of C/EBPα and PPARγ [72]. Although both C/EBPα and PPARγ control adipocyte differentiation, PPARγ appears to be dominant.

Other known adipogenic factors, such as, cAMP response element binding protein (CREB), KROX20, and Kruppel- like factors (KLF3, 4, 5, and 15), have been shown to function through direct or indirect induction of PPAR-γ expression [82].

In addition to initiation of adipogenesis in preadipocytes, PPARγ is also critical for inducing expression of a large number of genes crucial for maintaining adipocytes in a differentiated stage for proper lipogenesis and glucose metabolism. PPARγR binding sites have been identified in the regulatory regions of insulin response GLUT4, lipoprotein lipase (LPL), adipocyte fatty acid binding protein (aP2), PEPCK, and adiponectin.

The process of adipogenesis is also negatively regulated by antiadipogenic factors such as GATA2/3 and several members of the Wnt, hedgehog, and KLF families [82, 83]. Many of

these adipogenesis repressors function through protein–protein interactions rather than by directly inhibiting transcription of genes critical for adipocyte differentiation.

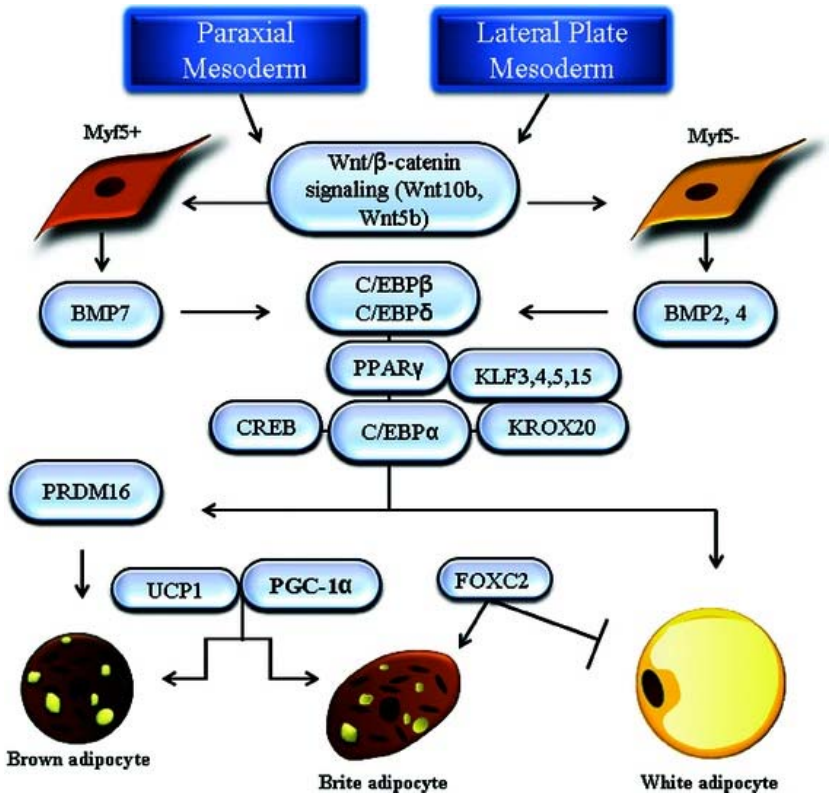

Fig.5 Origin and adipogenesis of white and brown adipocytes
Positive regulators involved in preadipocyte commitment and terminal differentiation of white, brite, and brown adipocytes are outlined. Brite and brown adipocytes differentiation pathway will be detailed later in the text. From Feng B. *et al., Ann. N.Y. Acad. Sci.,* 2013 [82].

Beside protein factors, recent studies in the field demonstrate the involvement of microRNAs (miRNAs), a family of noncoding small RNA molecules containing approximately 22 nucleotides, in regulation of adipogenesis [82]. Further investigations in *in vivo* models are necessary to confirm and clarify the functions of these miRNAs in AT development.

WAT as an endocrine organ: adipocytokines

As mentioned above, WAT is also an active endocrine and paracrine organ and through a communication network with other tissues, sympathetic nervous system and brain can influence appetite, energy balance, immunity, insulin sensitivity, angiogenesis, blood pressure, lipid metabolism and homeostasis, by adipocytokynes secretion. Indeed, over 50

adipocytokines have already been identified [84].

The following sections summarize the function of some key adipocytokines.

- *Leptin.* Leptin was one of the first proteins discovered to be secreted from adipose tissue, by the identification and sequencing of the *ob* gene (also known as *Lep*) from the *ob/ob* mice by positional cloning [85]. It is a hormone secreted mainly by adipocytes and its levels in the blood positively correlate with adipose mass [86]. Once secreted by adipose tissue, in greater amount by SAT than VAT [87], leptin circulates in plasma bound to plasma proteins, enters by diffusion into the CNS, where acts as a satiety signal on hypothalamus, by reducing food intake and increasing energy expenditure.

The main determinant of leptin secretion is glucose metabolism, because the concentration of circulating leptin diminishes under fasting or caloric restriction conditions and increases in response to food intake [88].

Leptin inhibits lipogenesis and stimulates lipolysis, reducing intracellular lipid levels in SkM, liver, and pancreatic β-cells, thereby improving insulin sensitivity.

Obesity is associated with increased leptin levels and hyperleptinemia is a reflection of the leptin resistance associated with obesity [89].

Leptin is structurally similar to the family of helical cytokines that includes IL-2 and growth hormone 1, and is it is generally accepted that leptin acts as a pro-inflammatory adipokine. Indeed, leptin increases the production of TNF-α and IL-6 by monocytes and stimulates the production of CC-chemokine ligands (namely, CCL3, CCL4 and CCL5) by macrophages by activating the JAK2 (Janus kinase 2)–STAT3 (signal transducer and activator of transcription 3) pathway [90, 91]. In monocytes, leptin also stimulates the production of ROS and promotes cell proliferation and migratory responses [90, 92]. Leptin levels in the serum are increased in response to pro-inflammatory stimuli, including TNF-α and LPS [93]. Furthermore, leptin increases the production of the TH_1-type cytokines IL-2 and IFN-γ and suppresses the production of the TH_2-type cytokine IL-4 by T cells or mononuclear cells [94], thus polarizing T cells towards a TH_1 cell phenotype.

- *Adiponectin***.** Adiponectin is almost exclusively synthesized by adipocytes, in a greater amount by SAT than VAT [87], and is present at high levels in the blood [95]. PPAR-γ agonists promote adipocyte differentiation, and adiponectin secretion is stimulated in adipocytes by

the activation of PPAR-γ [95].

Adiponectin levels in the plasma and adipose tissue are decreased in obese individuals compared with lean individuals [96]. Consistent with this, the production of adiponectin by adipocytes is inhibited by pro-inflammatory factors, such as TNF-α and IL-6 [95] as well as by hypoxia and oxidative stress [97].

Several clinical observations support an association between adiponectin levels and obesity-linked metabolic dysfunction: first, plasma adiponectin levels negatively correlate with VAT accumulation [96]; second, plasma adiponectin levels are decreased in patients with T2DM; and third, high adiponectin levels are associated with a lower risk for developing T2DM [95]. High levels of this adipokine are related with weight loss [98] and, in addition, adiponectin improves insulin sensitivity, decreases the flow of FFAs and increases their oxidation, inhibits major gluconeogenic liver enzymes, reduces hepatic release of glucose and muscle, and stimulates glucose utilization and fatty acid oxidation (FAO) [99]. Adiponectin shows high anti-inflammatory and antiatherogenic powers because it inhibits the adhesion of monocytes to endothelial cells, the transformation of macrophages into foam cells and endothelial cell activation. It also abrogates LPS-stimulated TNF-α production by macrophages [100] and inhibits TLR4-mediated NF-κB activation in mouse macrophages [101]. Furthermore, adiponectin stimulates the production of the anti-inflammatory cytokine IL-10 by human macrophages [102]. Its globular isoform inhibits cell proliferation and production of ROS induced by low-density lipoprotein (LDL) oxidase during atheromatous plaque formation [88].

- *TNF-α (Tumor Necrosis Factor-α).* TNF-α is a pro-inflammatory cytokine, and it was the first adipocyte-derived factor that suggested a link between obesity, inflammation and T2DM [20]. Although originally thought to be mainly secreted by adipocytes, it is now thought that the majority of TNF-α is secreted by macrophages [23].

TNF-α expression is increased in the adipose tissue of experimental animal models of obesity and T2DM [20]. Accordingly, neutralization of TNF-α-induced signalling in obese animals leads to an improvement in insulin sensitivity, which is associated with an enhancement of insulin signalling in SkM and adipose tissue [20, 103, 104]. TNF-α levels are increased in the adipose tissue and plasma of obese individuals, and a reduction of body weight in these

individuals is associated with a decrease in TNF-α expression [105].
At a mechanistic level, TNF-α attenuates insulin-stimulated tyrosine phosphorylation of the insulin receptor and IRS1 in SkM and AT, thus promoting insulin resistance [103].

- *IL-6 (Interleukin-6).* IL-6 is secreted by adipocytes but also by macrophages and endothelial cells of WAT. This cytokine appears to have dual functions, depending on the tissue and metabolic state. In SkM, during exercise, it acts to increase glucose uptake resulting in muscle hypertrophy and myogenesis and AMPK-mediated fatty acid oxidation, as well as having an anti-inflammatory effect [106, 107], while in adipose tissue and liver, IL-6 is shown to be a pro-inflammatory adipokine. Indeed, it increases insulin resistance by up-regulating suppressor of cytokine signalling 3 (SOCS3), which, in turn, impairs insulin-induced insulin receptor and IRS1 phosphorylation [108-110]. However, the role of IL-6 in insulin resistance has been controversial because IL-6 deficiency exacerbates hepatic insulin resistance and inflammation in mice on a high-calorie diet [111], whereas reduction of IL-6 in adipose tissue (by ablation of JNK) protects against the development of insulin resistance through modulation of SOCS3 expression in the liver [112]. Thus, the different actions of IL-6 on insulin signaling may be due to its disparate actions in different organs (liver versus muscle) or the different sources of IL-6 (muscle versus fat).

- *CCL2 or MCP-1 (Chemokine CC-motif ligand 2 or Monocyte Chemotactic-1).* MCP-1 is secreted by WAT in a greater amount by VAT than SAT [113]. The expression of this cytokine has been shown to be increased in adipose tissue under conditions of glucose deprivation [114]. In addition, genetically obese (*ob/ob*) mice and diet-induced obese mice have high levels of CCL2 expression in their WAT, and this observation has been extended to humans [115]. In mice, high levels of circulating CCL2 (originating from adipose tissue) are sufficient to induce macrophage recruitment to, and inflammation in adipose tissue, as well as to promote glucose intolerance and insulin insensitivity [114].

Other important adipocytokines and its function are summarized in the **Fig.6**. For more details, see Ouchi N *et al*., *Nat Rev Immunol*, 2011 [84].

Adipokine	Primary source(s)	Binding partner or receptor	Function
Leptin	Adipocytes	Leptin receptor	Appetite control through the central nervous system
Resistin	Peripheral blood mononuclear cells (human), adipocytes (rodent)	Unknown	Promotes insulin resistance and inflammation through IL-6 and TNF secretion from macrophages
RBP4	Liver, adipocytes, macrophages	Retinol (vitamin A), transthyretin	Implicated in systemic insulin resistance
Lipocalin 2	Adipocytes, macrophages	Unknown	Promotes insulin resistance and inflammation through TNF secretion from adipocytes
ANGPTL2	Adipocytes, other cells	Unknown	Local and vascular inflammation
TNF	Stromal vascular fraction cells, adipocytes	TNF receptor	Inflammation, antagonism of insulin signalling
IL-6	Adipocytes, stromal vascular fraction cells, liver, muscle	IL-6 receptor	Changes with source and target tissue
IL-18	Stromal vascular fraction cells	IL-18 receptor, IL-18 binding protein	Broad-spectrum inflammation
CCL2	Adipocytes, stromal vascular fraction cells	CCR2	Monocyte recruitment
CXCL5	Stromal vascular fraction cells (macrophages)	CXCR2	Antagonism of insulin signalling through the JAK–STAT pathway
NAMPT	Adipocytes, macrophages, other cells	Unknown	Monocyte chemotactic activity
Adiponectin	Adipocytes	Adiponectin receptors 1 and 2, T-cadherin, calreticulin–CD91	Insulin sensitizer, anti-inflammatory

Fig. 6 Main adipocytokines and its functions
Adapted from Ouchi N *et al., Nat Rev Immunol,* 2011 [84].

2.2 Brown adipose tissue (BAT)

Function and distribution of BAT

In addition to energy-storing WAT, human fat consists of thermogenic controlling BAT. Brown adipocytes contain multilocular lipid droplets and are rich in mitochondria. In humans, BAT is found mainly in fetuses and newborns localized in axillary, cervical, perirenal, and periadrenal regions but decreases shortly after birth [116]. BAT fades away in adult humans and is mostly replaced by WAT later in life.

The physiological relevance of BAT in adult humans has been unclear until recent identification of metabolically active BAT in healthy adult humans, and the mass of BAT was found to be inversely correlated with age and BMI [117-119].

The result of fluorodeoxyglucose positron emission tomography (FDG-PET) indicates that BAT distributes at many sites in the adult human body, including the neck, supraclavicular depot, paravertebral depot, interscapular depot, mediastinum depot, para-aortic depot, and other depots. The supraclavicular depot is the largest BAT depot in most people. BAT has not

been detected in every adult person under thermoneutral conditions, and according to a recent study, approximately 7.5% of females and 3.1% of males have detectable BAT activities under unstimulated conditions. Enhanced BAT activities are detected in adult humans under certain conditions, such as cold exposure, insulin stimulation, and elevated circulating levels of catecholamines. People who work outdoors in cold temperature have more BAT mass than those who work indoors.

Instead of humans, BAT is commonly found in rodents throughout their lives.

BAT is also highly vascularized and densely innervated by terminal fibers of the sympathetic nervous system [82, 120].

BAT is the only tissue expressing UCP1, a protein found in the inner mitochondrial membrane that orchestrates the uncoupled reaction of allowing protons to re-enter the mitochondrial matrix without generating ATP. The dissipation of energy as heat confers BAT with the capacity to control thermogenesis. In fact, altered UCP1 expression (UCP1- deficient or transgenic mice) leads to dysregulated sensitivity to cold exposure and body weight control [121-124]. Body temperature changes stimulate norepinephrine released by sympathetic nervous endings that activate β-adrenergic receptors and trigger a signal transduction cascade that converts nutrients into acetyl-CoA. The TCA cycle uses this mitochondrial fuel to produce protons and electrons, which generate ATP through the ETC. However, in BAT, UCP1 allows protons to enter the mitochondrial matrix without generating ATP, that is, uncoupled, and heat is produced in this process, counteracting hypothermia, obesity, and diabetes.

Adipogenesis of BAT

In the human fetus, BAT development occurs earlier than WAT development during gestation. Brown adipocytes, are also derived from the mesoderm [72] and along with connecting capillaries, form distinct lobules with dense amounts of connective tissue. These lobules are arranged into lobes that provide the structure of BAT [125]. Existing evidence indicates that BAT is well developed around five months of gestation and peaks at birth [126]. In infants, BAT can account for approximately 5% of body weight and it plays an important role in maintenance of core temperature when newborns face a sudden change from 37°C in an intrauterine environment to a lower temperature of the external

environment [127].

Two types of brown adipocytes have been identified in humans, classic interscapular-like brown adipocytes (iBAT) and inducible brown adipocytes interspersed among white fat depots in response to cold exposure or elevated plasma concentrations of catecholamine (wBAT, brite adipocytes, beige adipocytes) [118]. iBAT is developed from Myf^{5+} stem cells (myf^{-5} muscle-like cellular lineage) originating in the paraxial mesoderm, while brite adipocytes are derived from the lateral plate mesoderm [128] **(Fig.5)**.

The developmental timing is also different for these two types of brown adipocytes. In mice, iBAT is fully differentiated at birth, when coat and WAT are absent. In contrast, brite adipocytes appear around 10 days postbirth, peak around 21 days postbirth, and then regress. The disappearance of brite cells coincides with the appearance of WAT and coat. Brite cells are distinct from white and classic brown adipocytes in relation to gene expression pattern, with brite cells having low UCP1 levels in the basal state but high UCP1 levels and respiration rates in response to cyclic AMP stimulation, similar to those of the classic brown fat cells [129]. Thus, the beige cells have the capability to switch between an energy storage and energy dissipation phenotype in a manner that other fat cells lack.

Brown fat depots identified in adult humans have characteristics of brite adipocytes [129]. At a molecular level, classic brown adipogenesis involves both unique transcription factors/cofactors, such as bone morphogenetic protein 7 (BMP7), PR domain containing 16 (PRDM16), and PGC-1α, and factors that also influence WAT adipogenesis, such as PPARγ and members of the C/EBP family [120, 130]. PRDM16 is exclusively expressed in BAT and plays a critical role in brown preadipocyte commitment and terminal differentiation [131]. When expressed at physiologically relevant levels, PRDM16 promotes almost all of the key features of *bona fide* brown adipocytes, even in the absence of PPAR-γ, including increased expression of PGC-1α and UCP1 and enhanced mitochondrial gene expression and density. PGC-1α is a cold-inducible transcription coactivator that is essential for brown adipocyte mitochondrial thermogenesis but dispensable for brown adipocyte differentiation [132]. Brown adipocytes are also differentiated from white adipocytes because of their high expression of type 2 iodothyronine deiodinase (DIO2), and the lipolytic regulator, cell death-inducing DFFA-like effector a (Cidea) [120, 133].

Recent landmark studies have identified novel secreted proteins, such as liver fibroblast

growth factor 21 (FGF21) [134], cardiac natriuretic peptides [135], and irisin [136]. Especially irisin is a potent inducer of brite cells specifically in subcutaneous WAT.

In addition, recent articles reported that macrophages [137] and the bone morphogenetic protein BMP8B [138] have also the capacity to regulate BAT thermogenesis.

3. ADIPOSE TISSUE REMODELLING DURING OBESITY

Adipose tissue (AT) can respond rapidly and dynamically to alterations in nutrient deprivation and excess through adipocyte hypertrophy (increase of cells mass) and hyperplasia (increase of cells number), thereby fulfilling its major role in whole- body energy homeostasis.

AT remodeling is an ongoing process that is pathologically accelerated in the obese state. This exacerbated expansion can lead to a myriad of effects, including hypoxia, adipocyte cell death, enhanced chemokine secretion, and dysregulation in FAs fluxes [139].

Firstly, as adipocytes grow, they become hypoxic and activate the hypoxia inducible factor (HIF) pathway. Larger fat droplets force nuclei and cytoplasmic compartments of the adipocyte farther from blood vessels and therefore oxygen supply decreases. Hypoxia activates the JNK and IKK/NF-$\kappa\beta$ pathways, which up-regulate the production of chemokines and pro-inflammatory cytokines such as macrophage migration inhibitory factor (MIF), the matrix metalloproteinases MMP2 and MMP9, IL-6, ANGPLT4, PAI-1, VEGF, and leptin in adipocytes. Additionally, physical pressure on adipocytes from the extracellular matrix (ECM) may also stimulate chemokines production. These cytokines promote the immune cells recruitment, first of all adipose tissue macrophages (ATMs), and their activation to M1 phenotype, leading to pro-inflammatory cytokines secretion like TNF-α, IL-6 and IL-1β. Hypertrophy drives also to adipocyte cell death and consequently to the release of cellular contents into the extracellular space. This is a prominent additional stimulus for ATMs infiltration [7]. As “professional” phagocytes, macrophages are extremely proficient in the removal of numerous molecules, ranging from small lipids to colonies of pathogens to dead cells. In this state, they fuse to phagocytose the residual lipid droplet, forming large lipid-laden multinucleated syncytia surrounding dying adipocytes in the process, called Crown-Like Structures (CLS_s) [140]. This process is a commonly accepted hallmark of chronic inflammation that contributes to local and systemic insulin resistance by multiple mechanisms as detailed above **(Fig.7).**

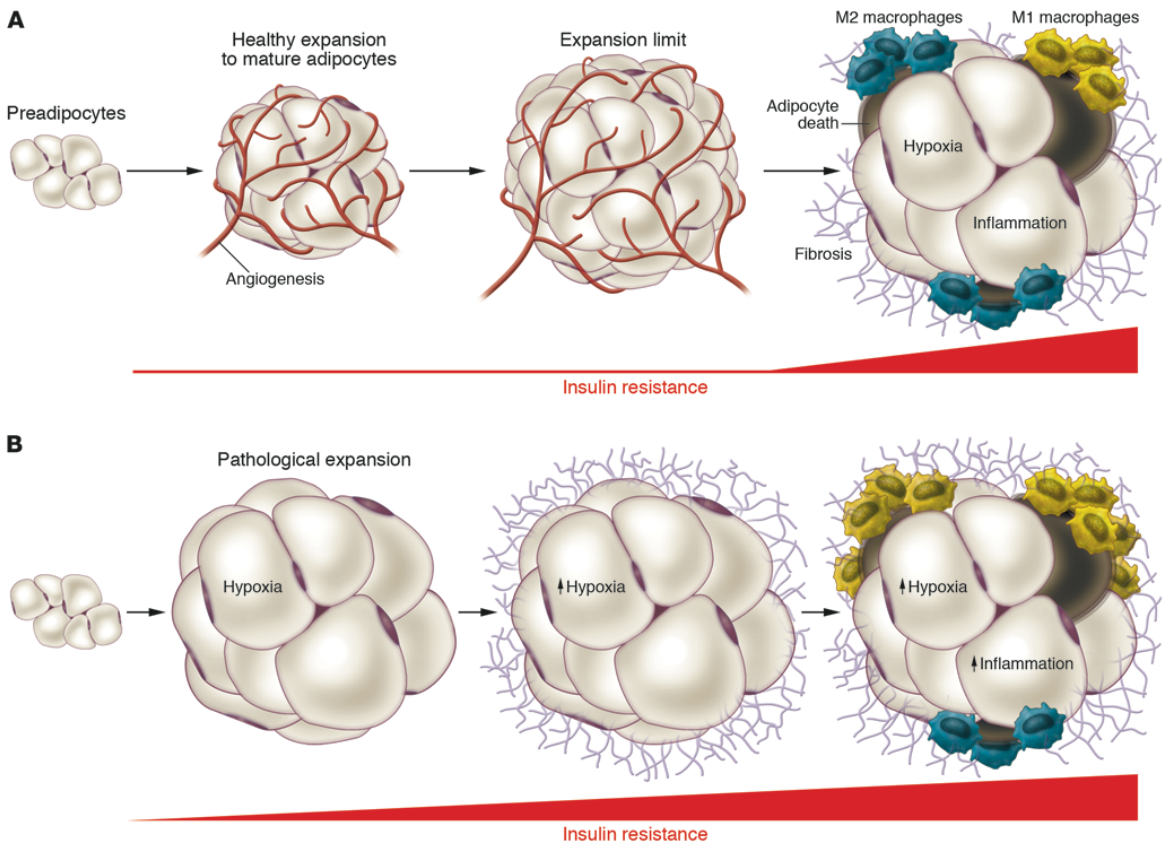

Fig.7 Adipose tissue remodeling during healthy and obesity
A. Healthy AT expansion consists of an enlargement of AT with an adequate angiogenic response and appropriate remodeling of the ECM**. B**. In contrast, pathological AT expansion consists of massive enlargement of existing adipocytes, limited angiogenesis and ensuing hypoxia. Ultimately, M1 macrophages prevail leading to proinflammatory phenotype that is strongly associated with insulin resistance. From Sun K. *et al.*, *JCI*, 2011 [139].

When AT becomes insulin resistant, lipolysis is not suppressed in the post-prandial state and capacity of adipose tissue to take up lipids from the circulation to store into TG fails. These processes lead to elevated serum FFAs and TG and a net flux of lipids to tissues other than AT causing ectopic accumulation and consequently peripheral insulin resistance. Elevated FFAs levels can also directly activate macrophages via TLR4, resulting in an increase production of pro-inflammatory cytokines and ER stress induction via PERK-dependent IKK activation [139]. Recently it has has been demonstrated that FFAs, especially palmitate, also has the potential to directly activate the NLRP3-inflammasome in macrophages. The inflammasome is an important part of our innate immune system that responds to danger

signals that are sensed by a number of different intracellular NOD-like receptors (NLRs). NLRP3 is the most extensively studied inflammasome that, upon its activation, facilitates caspase-1-dependent processing of pro-IL-1β into its active form IL-1β. This cytokine elicits potent proinflammatory actions in various tissues and cell types during obesity that contibutes to insulin resistance [141].

The links between macrophages and AT tissue expansion represent a vicious circle because pro-inflammatory macrophage-released cytokines decrease the formation of 'good' small adipocytes. By reducing new adipocyte formation inflammatory cytokines cause a relative increase in larger insulin resistant adipocytes. The larger adipocytes in turn produce more chemokines secretion and more FFAs. Increased chemokines and FFAs attract and activate yet more macrophages further inhibiting adipocyte function and preadipocyte differentiation, exhacerbating the milieu of obesity-related inflammatory state and systemic insulin resistance.

4. SUBCUTANEOUS ADIPOSE TISSUE (SAT) *vs* VISCERAL ADIPOSE TISSUE (VAT) IN THE PATHOPHYSIOLOGY OF OBESITY

The type of fat cells (adipocytes), their endocrine function, lipolytic activity, response to insulin and other hormones differ between subcutaneous adipose tissue (SAT) and visceral adipose tissue (VAT).

SAT accumulation represents the normal physiological buffer for excess energy intake (high-caloric diet) with limited energy expenditure (physical inactivity). It acts as a metabolic sink where excess FFAs and glycerol are stored as TG in adipocytes [142].

On one hand, SAT contains small adipocytes. Small adipocytes are more insulin-sensitive and have high avidity for FFAs and TG synthesis, preventing their ectopic deposition in non-adipose tissues. When the storage capacity of SAT is exceeded or its ability to generate new adipocytes is impaired because of either genetic predisposition or stresses (physiological and mental stress), fat begins to accumulate in areas outside the subcutaneous tissue, the natural store house for energy. Chronic stress leads to elevated cortisol levels that may lead to accumulation of VAT.

On the other hand, VAT contains greater number of large adipocytes. As adipocytes grow larger, they become dysfunctional. Because of its anatomical position, VAT blood is drained

directly to the liver through the portal vein. This contrasts with SAT where venous drainage is through systemic veins. The portal drainage of VAT provides direct hepatic access to FFAs and adipocytokines secreted by visceral adipocytes. VAT is characterized by being more vascular, rich in blood supply and more heavily innervated than SAT [143].

VAT and SAT also differ in density of glucorticoids receptors. Indeed they are mainly concentrated in VAT, especially adrenergic receptor targets of cathecolamines. Catecholamines have dual effects on the lipolysis rate, both accelerating, through β_3-adrenoceptors, and retarding lipolysis, through α_2-adrenoceptors. Abdominal visceral adipocytes, compared with subcutaneous abdominal, show an elevated rate of lipolysis due to increased number and activity of β_3-adrenoceptors and, partly, to a reduced activity of α_2-adrenoceptors.

The density of insulin receptor in VAT is lower than in SAT, and this makes the abdominal VAT more sensitive to lipolytic stimuli and less sensitive to the inhibitory action of insulin than SAT [143, 144].

All these factors contribute to the critical role of VAT in the development of Metabolic Syndrome.

5. MACROPHAGES IN OBESITY

An important finding that helped to elucidate the cause of tissue inflammation was that adipose tissue, from obese mice and humans, was infiltrated with large numbers of macrophages. These adipose tissue macrophages (ATMs) can comprise up to 40% of the cells in obese adipose tissue [23].

ATMs and adipose tissue inflammation have been extensively studied, and ATMs have been shown to have a key role in systemic insulin resistance, glucose tolerance and the development of metabolic syndrome and T2DM.

5.1 Macrophages subpopulations

Macrophages can be classified into broad subpopulations on the basis of concepts that were derived from *in vitro* experiments in which bone marrow–derived cells (precursor M0 macrophages) were treated with specific growth factors **(Fig.8)**.

Classically activated macrophages (CAMs), termed M1, can be induced *in vitro* by growing

bone marrow–derived hematopoietic cells with granulocyte-macrophage colony–stimulating factor (GM-CSF). These cells, whose differentiation is promoted by agents such as LPS and IFN-γ, display the marker CD11c in addition to F4/80 and CD11b and produce proinflammatory mediators like TNF-α, IL-6, IL-1β, nitric oxide (NO), IL-12, which role in inducing insulin resistance is well known. M1 macrophages also promote TH_1 response and displays strong microbicidal and tumoricidal activity [28, 145]. Alternatively activated macrophages (AAMs), termed M2, can be induced by culturing the bone marrow–derived cells with macrophage colony–stimulating factor (M-CSF), IL-4 and IL-13; they express the cell-surface markers CD11b, F4/80, CD301, and CD206. In contrast to M1 macrophages M2 macrophages secrete anti-inflammatory cytokines such as IL-10, IL-1 receptor antagonist (IL-1Ra) and arginase-1. They are considered to be involved in parasite containment, promotion of tissue remodeling, repair tumor progression and maintenance of insulin sensitivity. M2 macrophage polarization is dependent upon the transcription factors PPARδ and γ as well as the co-activator PGC-1β, known to promote mitochondrial biogenesis and FAO. Indeed M2 macrophages may prefer FAO as fuel, whereas M1 macrophages tend to utilize the glycolytic pathway for energy and metabolite generation [28, 145, 146].

Tissue macrophages respond to changes in the local environment by changing their polarization status, and, thus, the M1 and M2 classifications are oversimplifications of the more dynamic and varied polarization states of macrophages that can be observed *in vivo. In vivo,* it is likely that ATMs span a spectrum, from the M1-like proinflammatory state to the M2-like noninflammatory state. Both M1-like and M2-like populations express F4/80 and CD11b, and the ATMs population of M1-like macrophages also express CD11c.

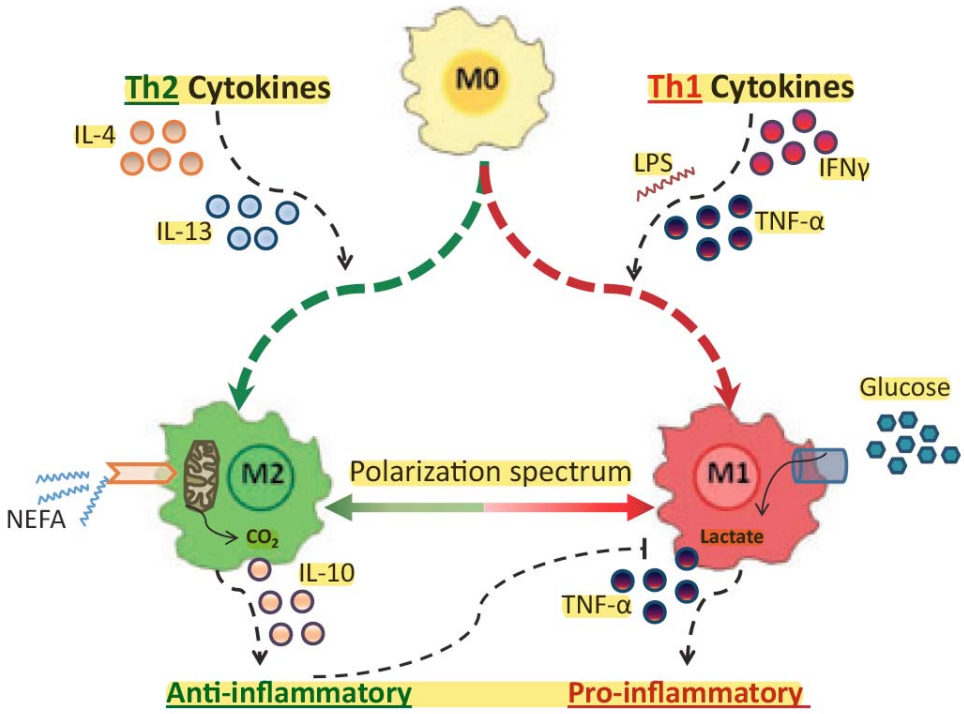

Fig.8 Macrophages subpopulations
Macrophages subtypes exist and can be broadly categorized as pro-inflammatory M1 or alternatively activated M2, polarized from precursor M0 macrophages, although *in vivo* studies reveal that macrophage plasticity results in a spectrum of macrophage phenotypes. Adapted from Johnson A.R. *et al.*, *Immunol Rev,* 2012 [146].

Immune system cells, above all macrophages, accumulate in the VAT (in particular, in the epididymal depot) of both lean and obese individuals. In the lean state, most macrophages have a ‘‘M2 like’’ or ‘‘alternatively activated’’ phenotype. In the obese state, M1-like ATMs can accumulate lipids, taking on a foamy appearance in the AT [147]. Increased numbers of M1-like, CD11c+ recruited macrophages account for the majority of the increase in ATMs in obesity [26, 148], and >90% of recruited monocytes become CD11c+ ATMs.

6. MITOCHONDRIAL BIOENERGETICS

Energy flow in living cells (bioenergetics) takes place mainly in mitochondria. Energy is obtained from FAs and other nutrients in the form of ATP, the chemical currency of life, through the tricarboxylic acid (TCA) cycle, and the electron transport chain (ETC) in a process known as oxidative phosphorylation (OXPHOS) [149]. In the ETC, the energy of electrons

from NADH and $FADH_2$ is used to pump protons (H^+) from the mitochondrial matrix to the intermembrane space and generate the electrochemical gradient necessary for ATP synthesis. However, when these electrons escape the ETC, ROS are produced in the mitochondria.

6.1 Mitochondrial bioenergetics and ROS

The mitochondrial respiratory chain is a major source of ROS within the cell because O_2 is used as the ultimate electron acceptor during respiration. Thus, during the reduction of O_2 to H_2O, reactive intermediates, specifically superoxide ($O_2^{\bullet-}$), hydrogen peroxide (H_2O_2), and hydroxyl radical ($OH^{\bullet}$), are generated.

Major targets for ROS oxidation include bis-allylic double bonds in lipids, cysteine and methione residues in proteins, and the C8 position on deoxyguanosine. Lipid radical intermediates can self-propagate leading to the further formation of lipid radicals, which can severely compromise membrane integrity. End products (*e.g.* 4-Hydroxynonenal) are highly reactive, forming covalent bonds with aminoacid residues that render proteins inactive.

To avoid the potentially damaging effects of ROS (*i.e.* scavenging), cells use a variety of systems to keep ROS within tolerable limits. This scavenging system includes enzymatic and nonenzymatic antioxidant systems, such as superoxide dismutase (SOD), catalase (CAT) and glutathione peroxidase (GPx), peroxiredoxins, thioredoxins, glutathione reductase, glucose-6-phosphate dehydrogenase and vitamins (A, C, E,).

$O_2^{\bullet-}$ generated by mitochondria (by the respiratory chain or other enzymes) is quickly dismutated to hydrogen peroxide (H_2O_2) by either manganese (Mn) or copper/zinc (Cu/Zn)-dependent SOD, which are located in the matrix and intermembrane space environments, respectively. Compared to superoxide, H_2O_2 is far more stable and able to traverse membranes. It is thus the main ROS used in signaling. Catalase also degrades H_2O_2 but only when H_2O_2 reaches high concentrations. The reductive power stored in NADPH, produced by a variety of metabolic enzymes, is then used to rejuvenate the enzymes used to sequester H_2O_2 [150]. This system is indispensable for protecting tissues and organs from oxidative stress.

Although these classical antioxidant mechanisms function to keep ROS in check, recent work has shown that control over ROS production plays an equally important role maintaining cell ROS levels.

ROS emission increases and decreases rapidly from normally functioning mitochondria. These changes coincide with parallel changes in mitochondrial membrane potential. Hence, a mechanism that 'fine tunes' membrane potential may be used to acutely modulate small changes in ROS production from mitochondria. UCP2 and UCP3 proton leak mechanisms represent one such mechanism [151]. Mitochondrial uncoupling proteins (UCPs) uncouple ATP production from mitochondrial respiration, thereby reducing the H^+ gradient across the inner mitochondrial membrane and relieving the formation of ROS. The reversible glutathionylation is required to activate/inhibit UCP2 and UCP3, not UCP1 and these two proteins are well recognized as functioning in a negative feedback loop for mitochondrial ROS emission [152].

The mechanisms detailed above are summarized in **Fig.9**.

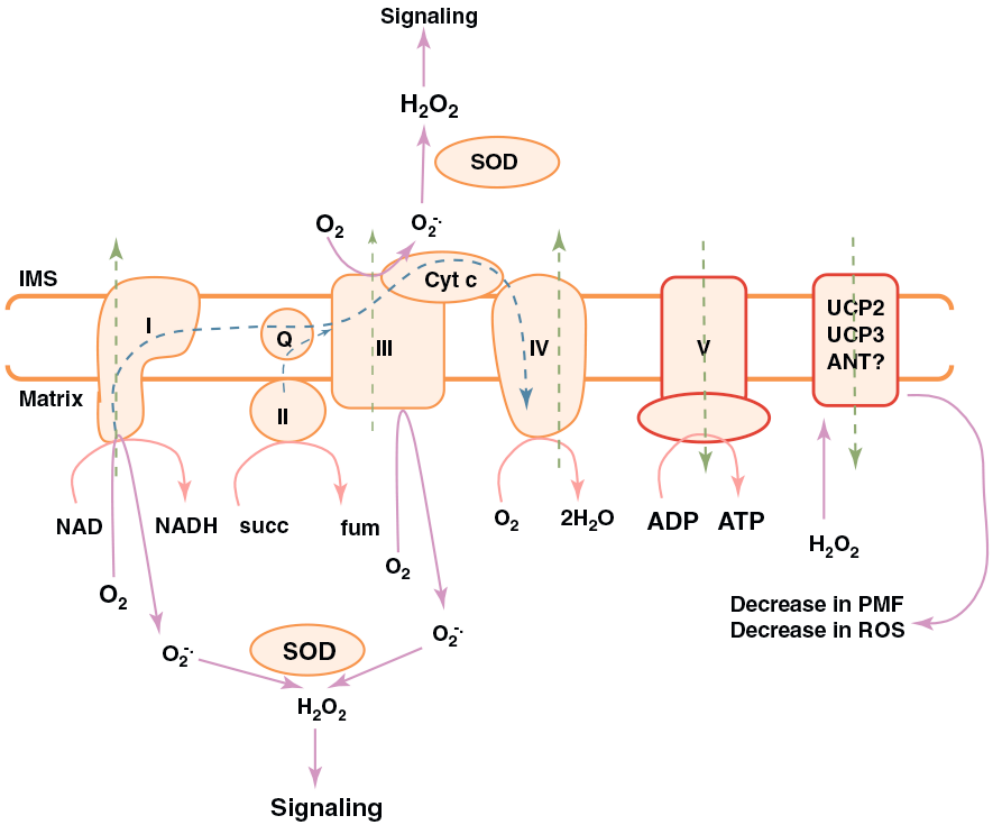

Fig.9 Mitochondrial ROS production

Following NADH (complex I), succinate (complex II), and other fuel oxidations, electrons systematically pass through the respiratory complexes (complexes III and IV) to the terminal electron acceptor, O_2. The difference in redox potential between components of the respiratory chain allows proton extrusion from the matrix at complexes I, III and IV, which establishes proton motive force (PMF). The latter is then used to drive ATP synthesis through

complex V (ATP synthetase). When PMF is high and the components of the respiratory chain are mainly in reduced states, liberated electrons from complexes I and III can univalently reduce O_2 to superoxide ($O_2^{\bullet-}$). In contrast to complex I, complex III generates ROS on both the intermembrane space (IMS) and matrix side of the membrane. The production of $O_2^{\bullet-}$ by mitochondria is self-regulated through the activation of uncoupling proteins (UCPs) 2 and 3, which decrease the PMF and thus decrease ROS production. Direction of electron flow is indicated by the blue-dotted line. Proton extrusion or import is indicated by green-dotted arrows. ANT: adenine nucleotide translocase. Adapted from Mailloux R.J. *et al.*, *Trends Endocrinol Metab*, 2012 [150].

ROS production is necessary for cell redox signalling that normally provides feedback for the regulation of mitochondrial metabolism. The direction of many cellular processes, such as phosphorylation and dephosphorylation and regulation of the cell cycle, can be determined by the redox state. Increases in ROS can lead to an imbalance of the cellular oxidation state, disrupting the redox balance.

When produced in a controlled fashion, ROS play very important signaling roles, especially in insulin pathway. Indeed, millimolar ROS concentrations have been shown to play a physiological role in insulin signaling via an NADPH oxidase-dependent mechanism. Upon insulin stimulation there is a burst in H_2O_2 production, creating a short- term and low dose exposure to ROS. This enhances the insulin cascade by inhibiting tyrosine phosphatase activity, leading to an increase in the basal tyrosine phosphorylation level of both the insulin receptor and its substrates.

In the metabolic syndrome, nutrient overload leads to redox imbalance, oxidative stress occurs causing mitochondrial dysfunction and contributes to pathology [153].

The primary tissues most negatively influenced by suboptimal mitochondrial performance are those that rely most heavily on mitochondrial function, such as SkM and cardiac muscle, liver, and AT [154].

Several mechanisms have been described to explain the pathological role of ROS during obesity. Indeed, ROS impairs insulin signaling inducing IRS serine/threonine phosphorylation, disturbing cellular redistribution of insulin signaling components, decreasing GLUT4 gene transcription, or altering mitochondrial activity. Other serine/threonine kinases involved in insulin signaling can also be directly activated by ROS. Among these are PKC, PKB, mTOR, and GSK3, all of which can act synergistically to desensitize the insulin signal by phosphorylating IR or IRSs on select serine/threonine residues.

Chronic oxidative stress can also induce to induce a number of stress sensitive and inflammatory signaling pathways, such as NF-κB, JNK/SAPK, and p38 MAPK, that are well know to impair insulin signaling [153].

Another important obesity-associated pathway involving ROS is ER stress. Indeed there's an interconnection between ROS production, Unfolded Protein Response (UPR) and inflammation through various mechanisms [155].

7. THE ROLE OF MITOCHONDRIA IN WHITE ADIPOSE TISSUE

Although a major role has been established for white adipose tissue (WAT) in regulating energy intake, energy expenditure, and insulin resistance, the functional role of WAT mitochondria has received less attention. Over the past decade, several studies have highlighted the potential relevance of mitochondria in the cellular physiology of the adipocyte in WAT and its impact on systemic metabolic regulation. Indeed any obesity-induced changes in WAT mitochondria can substantially disrupt whole-body energy homeostasis.

Despite containing relatively low mitochondrial mass compared to its overall size, the adipocyte interprets nutritional and hormonal cues in its microenvironment. Mitochondria play an essential role in many different pathways in the adipocyte. The synchronized initiation of adipogenesis and mitochondrial biogenesis indicates that mitochondria play a pertinent role in the differentiation and maturation of adipocytes. Indeed, mitochondrial content of mature white adipocytes is several-fold higher as compared with preadipocytes [156].

Furthermore, the early events of enhanced mitochondrial metabolism, biogenesis and ROS production [specifically through complex III of ETC], are crucial for the initiation and promotion of adipocyte differentiation in an mTORC1-dependent manner [157]. ROS, primarily in the form of H_2O_2, are essential to initiate the PPARγ transcriptional machinery necessary to evoke adipocyte differentiation. Alternatively, ROS may play an important role in insulin signal transduction.

In white adipocytes, similarly as in most other cells, mitochondria represent the main site of ATP production. Especially in fully differentiated white adipocytes, mitochondria must generate sufficient ATP to support various energy-consuming processes, *i.e.* lipolysis, *de*

novo FAs synthesis, TG synthesis, glyceroneogenesis, and FAs re-esterification.

7.1 Mitochondria dysfunction in WAT during obesity

During the development of obesity and T2DM, WAT expansion and adipocyte hypertrophy persist, to accommodate surplus nutrient intake.

Preadipocytes initiate adaptive responses to such metabolic challenges by adjusting the abundance and/or morphology of mitochondria, and mitochondrial DNA (mtDNA) content, ultimately to remodel their highly organized mitochondrial networks within the cell. However, how these adipocyte-specific pathways are altered and how the adipocyte adapts to substantial adjustments in mitochondrial demand is not clear.

Key contributors to mitochondrial dysfunction include excessive nutrient supply, which subsequently contributes to ROS formation and toxic lipid species production, genetic factors, ER stress, aging and/or proinflammatory processes, and altered mitochondrial fission that severely disrupts the dynamic mitochondrial network fission process; all single-handedly or collectively contribute to insulin resistance.

High levels of glucose and FFAs have been reported to stimulate mitochondrial dysfunction directly in 3T3-L1 adipocytes [158]. Moreover, studies have documented that mitochondrial loss in WAT correlates with the development of T2DM. Indeed, mitochondrial levels in white adipocytes derived from epididymal fat-pads of *ob/ob* mice are approximately 50% lower than in lean control mice [159]. Furthermore, Choo and colleagues demonstrated a reduction in mitochondrial number and function, and a decrease in mtDNA content and ETC enzymatic activity, in addition to an altered mitochondrial network; all contributing to a decline in OXPHOS and β-oxidation in WAT of diabetic mice [160]. Moreover, elegant microarray profiling studies have revealed that several mitochondrial genes crucial for mitochondrial function and OXPHOS, in addition to PPARα, ERR-α, and PGC1-α, are downregulated in obese, HFD-fed, insulin-resistant mice, and in *db/db* mice [161, 162]. These findings suggest that mitochondrial biogenesis is highly compromised in WAT of obese insulin-resistant mouse models.

Similarly, in patients with insulin resistance, T2DM, and severe obesity, the abundance of mitochondria and the expression of key genes pertinent to mitochondrial function are

significantly reduced in WAT [163], in concert with decreased adipocyte oxygen consumption rates and ATP production [164].

In vitro studies demonstrate that, under hyperglycemic conditions, non-esterified FAs (NEFAs) or TNF-α treatment of 3T3-L1 adipocytes lead to ROS accumulation [165, 166], reduced mitochondrial biogenesis, decreased insulin sensitivity [158, 167], and enhanced proinflammatory cytokine secretion [165]. Such effects result in an oxidative stress state, which further leads to downregulation of PPARγ and adiponectin [168].

By contrast, De Pauw and colleagues noted that mild uncoupling of 3T3-L1 adipocytes mitochondria, increased ROS production but did not alter mitochondrial biogenesis [169]. Instead, the abundance of adipocyte pyruvate carboxylase, a major enzyme that participates in *de novo* FAs synthesis and glyceroneogenesis, was significantly downregulated; this was accompanied by a reduction in adipocyte TG content [169].

Oxidative stress has further been described clinically, as well as in WAT of many additional mouse models of obesity, such as diet-induced obesity (DIO), and *db/db* mice [167, 168, 170].

Microarray analyses of human adipose tissue revealed that glutathione-S-transferase alpha 4 (GSTA4) expression is downregulated in omental and subcutaneous depots of obese insulin-resistant individuals. Furthermore, both GST4A-silenced 3T3-L1 adipocytes and WAT from GST4A knockout mice display a significant impairment in OXPHOS with increased ROS formation [170].

Despite a persistently high burden of FFAs even under normal physiological conditions, the adipocyte displays tolerance to unusually high levels of ROS under basal conditions, without concomitant cell damage; in fact, the majority of other cell types cannot sustain such a high level of ROS without undergoing apoptosis. The onset of obesity, however, promotes relatively sluggish behavior of the scavenging system within the adipocyte. This exacerbates the existing high basal levels of ROS, leading to inhibition of oxygen consumption. Consequently, substrates cannot be oxidized efficiently and TG storage is favored.

8. BIOENERGETICS AND MITOCHONDRIAL FATTY ACID OXIDATION (FAO)

8.1 Mitochondrial fatty acid oxidation (FAO)

Hormones, such as insulin, glucagon, and noradrenaline, control the extracellular uptake and intracellular release of the main cell fuels; namely, carbohydrates and FAs.

FFAs are produced by lipolysis, transported bound to albumin in blood and taken up by tissues in a process mediated by transport proteins present in the plasma membrane [171]. Once within the cell, FFAs are bound to fatty acid binding proteins, which are present in the cytosol in high amounts [172]. Depending on the tissue and its metabolic demand, FAs are either converted to TG or membrane phospholipids or oxidized in the mitochondria for energy production.

The β-oxidation of activated FAs occurs within the mitochondrial matrix and is catalysed by the sequential action of four enzyme families (acyl-CoA dehydrogenase, enoyl-CoA hydratase, 3-hydroxyacyl-CoA dehydrogenase and 3-ketoacyl-CoA thiolase), each with different substrate specificity for short-, medium- and long chain-CoAs [173]. Before being directed into storage, membranes or oxidation, FAs are first activated to acyl-CoAs. This reaction is catalyzed by long-chain acyl-CoA synthetase (LCAS), which is abundant in microsomes and mitochondria [174]. LCAS is associated with the outer mitochondrial membrane (OMM) and appears to be a transmembrane protein with the active site exposed to the cytosol [175]. This orientation of LCAS gives rise to cytosolic production of long-chain acyl-CoA (LC-CoA), which must cross both mitochondrial boundary membranes for β-oxidation. Esterification of carboxylic acids to coenzyme A (CoA) through a thioester bond is a common strategy used in metabolic processes to 'activate' the relevant metabolite. This activation has two universal consequences: 1) it renders the acyl-CoA ester impermeant through cellular membranes, and 2) it sequesters CoA from the limited pools that exist in individual subcellular compartments. As a result, the pools of acyl-CoA esters are maintained separate in the different cellular compartments, which is imperative due to the high biological activity displayed by some of them. Consequently, the cell has two requirements: 1) a mechanism for the control of CoA ester concentrations that is rapid and does not involve the energetically expensive hydrolysis and resynthesis of the esters from FFAs, and 2) a system that, after the initial synthesis of the CoA ester, enables the acyl moiety to

permeate membranes without the need to re-expend energy. The cell achieves all these requirements through a single mechanism, the transesterification between acyl-CoA esters and L-carnitine to form the corresponding carnitine ester and regenerate unesterified CoA:

RCO-S-CoA + carnitine-OH ⇔ RCO-O-carnitine + CoA-SH

These reactions are catalysed by a family of carnitine acyltransferases [176]. They enable the cell to move the required moieties between intracellular compartments while keeping its pools of CoA esters distinct in their respective compartments. The enzyme involved depends on the length of the fatty acyl moiety to be transported. Carnitine acetyltransferase (CrAT) [177] acts with acetyl-CoA as substrate, while carnitine octanoyltransferase (COT) facilitates the transport of medium-chain FAs (C8- C10) from peroxisomes to mitochondria through the conversion of shortened fatty acyl- CoA from peroxisomal β-oxidation into fatty acylcarnitine [178]. Peroxisomal β-oxidation does not directly provide energy but is able to shorten very long-chain FAs, thus allowing their subsequent mitochondrial β-oxidation. It also has a detoxifying action by oxidizing molecules such as eicosanoids and xenobiotics. Finally, carnitine palmitoyltransferases (CPTs) [179] 1 and 2 facilitate the transport of long-chain acyl groups (C16) into the mitochondrial matrix, where they undergo β-oxidation. One characteristic that differentiates the various carnitine acyltransferases activities is their sensitivity to inhibition by malonyl-CoA. CPT1 and COT are sensitive to malonyl-CoA, while CrAT and CPT2 are not.

8.2 Carnitine Palmitoyltransferase (CPT) System

The carnitine-dependent transport of activated FAs precedes their β-oxidative chain shortening. This transport system consists of three proteins [180], CPT1, carnitine-acylcarnitine translocase (CACT) and CPT2, each with different submitochondrial localization. As a first step, long-chain acyl-CoA (LC-CoAs) formed by the catalytic action of LCAS in the outer mitochondrial membrane (OMM) are converted to acylcarnitines. This transesterification is catalyzed by transmembrane CPT1 protein, also localized in the OMM. The reaction products, LC-acylcarnitines, are then translocated into the mitochondrial matrix in an exchange reaction catalyzed by CACT, an integral inner membrane protein. Within the matrix the acylcarnitines are then reconverted to the respective acyl-CoAs by CPT2, an enzyme associated with the inner leaflet of the inner mitochondrial membrane (IMM).

CPT1 is tightly regulated by its physiological inhibitor malonyl-CoA, and thus CPT1 is the most physiologically important regulatory step in mitochondrial FAO [181]. This process allows the cell to signal the relative availability of lipid and carbohydrate fuels in liver, heart, SkM and pancreatic β-cells [182, 183].

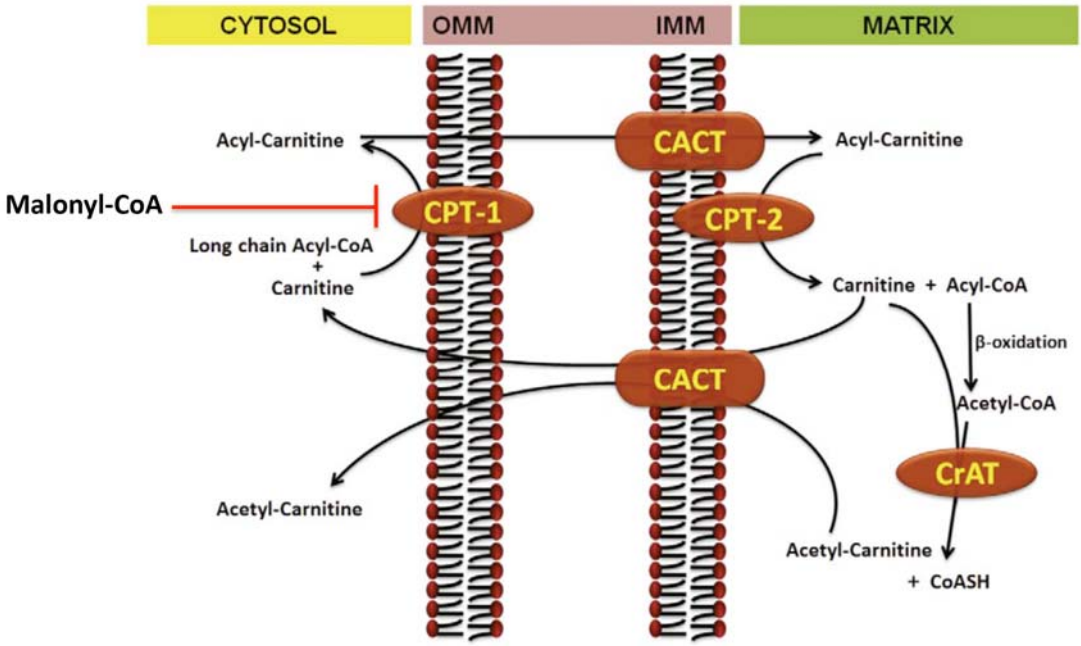

Fig.11 CPT1 system
The CPT system operates body-wide to permit the entry of long-chain fatty acids (LCFA) into the mitochondrial matrix, where they undergo β-oxidation as a source of energy. Fatty acids do not permeate through the mitochondrial membrane, but their entry is facilitated by the CPT system. The first component of the system, **CPT1,** located at the outer mitochondrial membrane **(OMM**), converts a fatty-acyl group from CoA to carnitine. The acylcarnitine product crosses the inner mitochondrial membrane in a reaction catalysed by a specific carnitine/acylcarnitine translocase. The transesterification is then reversed to regenerate fatty acyl-CoA by the action of a distinct enzyme denoted **CPT2**, loosely bound to the matrix face of the inner mitochondrial membrane **(IMM)**. The regulation of fatty-acid flux through the CPT system takes place at the level of CPT1. Malonyl-CoA, derived from glucose metabolism and the first intermediate in lipogenesis, regulates fatty-acid oxidation by inhibiting CPT1. Adapted from Sharma S *et al., Drug Discovery Today: Disease Mechanisms, 2009.*

8.3 CPT1 isoforms

In mammals, there are three isoforms of CPT1: CPT1A (also called liver isoform or L-CPT1), CPT1B (also called muscle isoform or M-CPT1) and CPT1C.

CPT1A is expressed in liver, kidney, WAT (mouse) [184, 185], testis, ovary, pancreatic islet, lung, spleen, brain, intestine [184, 186], and at much lower levels in heart [185].

In contrast, CPT1B is expressed in SkM, heart, testis, BAT and WAT (humans) [187, 188]. CPT1C was discovered recently and is expressed predominantly in brain and in testes [189].

In humans, the different isoforms of CPT1 are encoded on separate chromosomes: CPT1A gene is localized at the 11q13 chromosome, CPT1B at 22q13.3 chromosome and CPT1C at 19q13.33 [189, 190].

CPT1A protein contains 773 amino acids (88 kDa) and CPT1B is a protein of 772 amino acids (88 kDa). The identity in aminoacids residues is high (62%) but they are differentially regulated by malonyl-CoA. CPT1A isoform is inhibited by malonyl-CoA to a much lesser extent than the CPT1B isoform (the IC_{50} value for CPT1B is about 2 orders of magnitude lower than for CPT1B) [187]. Although the protein sequence is highly similar to that of the other two isozymes, CPT1C expressed in yeast or HEK293T cells displays no catalytic activity with common acyl-CoA esters as substrates. Expression studies indicate that CPT1C is localized exclusively in the CNS, with homogeneous distribution in all areas (hippocampus, cortex, hypothalamus, and others). The pattern resembles that of FAS, ACC1 rather than CPT1A or ACC2 [189, 191]. The capacity of CPT1C to bind malonyl-CoA has been demonstrated, and it has been suggested that CPT1C regulates malonyl-CoA availability in the brain cells [192]. While CPT1A and CPT1B are localized in the outer mitochondrial membrane with the N and C termini facing to the cytosolic side, it has recently been demonstrated that CPT1C is localized in the ER of the cells and less in mitochondria and that shows carnitine palmitoyltransferase activity [192]. The wide distribution of the protein in the brain suggests a more general, ubiquitous function, not only in the control of energy homeostasis [193] and food intake, related with ceramides metabolism in leptin hypothalamic control of feeding [194, 195].

The distribution and kinetics of the mitochondrial CPT1 enzymes are summarized in the next table:

	CPT1A	CPT1B	CPT1C	CPT2
Mass	88 kDa	88 kDa	88 kDa	70 kDa
Malonyl-CoA IC_{50}	2,5 μM	0,03 μM		-
Carnitine K_m	30 μM	500 μM		120 μM
Human chromosome locus	11q13	22q13.3	19q13.33	1p32
Tissue expression				
Liver	++++	-		+
SkM	(+)	+++++		+
Heart	+	+++		+
Kidney	+++++	(+)		+
Lung	+++++	(+)		+
Spleen	+++++	-		+
Intestine	+++++	-	(+)	+
Pancreas	+++++	-		+
BAT	(+)	++++		+
WAT	+	++++		+
Ovary	+++++	(+)	(+)	+
Testis	(+)	+++++	(+)	+
Human fibroblasts	+++++	-		+
Brain			+	
Cerebellum	-	++++++	+	-
Human deficiency described	yes	no	no	yes

Table 1. Overview of distribution and kinetics of the mitochondrial CPT1 enzymes.
Relative levels of CPT1 isoforms expression for each organ are based on northern blot analysis (and in some cases [^{3}H] etomoxir-CoA labelling), but do not indicate precise ratios. (+), traces expression compared with the alternative isoform; −, undetected. Tissue expression data refer to the rat, except in the case of fibroblasts and brain. Adapted from McGarry JD *et al*. Eur. J. Biochem., 1997 [179].

8.4 CPT1 regulation

- **Malonyl-CoA-Independent Regulation of CPT1 Activity**

The complexity of the mechanisms involved in determining the precise sensitivity of CPT1 (particularly CPT1A) to malonyl-CoA inhibition tends to obscure the fact that the activity of

the enzyme is also regulated by malonyl-CoA-independent mechanisms.

Gene expression is important, although induction (*e.g.*, by PPARα and PGC-1α and β [196]) is modest, as are likely changes in activity associated with changes in substrate concentrations (particularly of carnitine in muscle).

However, there are direct and indirect post-translational protein modification mechanisms that could alter catalytic activity. Several phosphorylation sites have been described on CPT1A, at least two of which affect the kinetic characteristics of the enzyme, particularly its malonyl-CoA sensitivity and mechanism of inhibition [197]. However, no evidence exists that their phosphorylation state is altered by physiological state; consequently, such phosphorylation may be constitutive (perhaps co-translational). This conclusion is strengthened by the observation that only an intramitochondrial protein phosphatase released *in vitro* upon freeze-thawing of isolated mitochondria is able to dephosphorylate the enzyme.

Heart CPT1 may become nitrated *in vivo* during sepsis [198], a condition known to result in the lowering of FAO in the heart. This modification resulted in the inhibition specifically of CPT1B, and not of the smaller amount of CPT1A also expressed in the heart [199]. However, in those experiments nitration was only identified using an anti-nitrotyrosine antibody. Detailed mass spectrophotomeric studies would need to be conducted to ascertain which residues are involved, and the effects of the covalent modification.

Exposure of hepatocytes to phosphatase 1A inhibitors (*e.g.*, okadaic acid) or to activators of AMPK or PKA (*e.g.*, glucagon) result in the activation of CPT1A without any change in the sensitivity to malonyl-CoA. It has been shown that this was not due to an increase in phosphorylation of CPT1A directly. Interestingly, the effects were retained when the hepatocytes were permeabilised, but were lost when mitocondria were prepared from the hepatocytes, suggesting that some link between the mitochondria and an extramitochondrial structure (*e.g.*, the cytoskeleton [200]) was essential for the occurrence/ preservation of the effect [201]. In the light of these findings, it has been shown that the enzyme responds to the AMPK-mediated phosphorylation of a protein component within the intermediate filaments of the cytoskeleton. These observations may explain the cell-volume dependence of CPT1A activity. Thus, an increase in hepatocyte volume results in the inhibition of CPT1A activity, with opposite effects of cell shrinkage [202]. These effects may

also be related to those of glucagon and insulin on the activity of the enzyme in hepatocytes, as these hormones are known to have opposite effects on cell volume.

- **Malonyl-CoA dependent regulation**

CPT1 exerts its control as the rate-limiting step in fatty acid oxidation (FAO) *via* changes in concentration of malonyl-CoA (acute or short-term control) and/or through changes in the sensitivity of CPT1 to inhibition by malonyl-CoA (long-term control). If tissue malonyl-CoA concentrations play a key role in the rapid adjustment in FAO, then the reactions producing and/or disposing of malonyl-CoA also must be subject to acute regulation.

The formation of malonyl-CoA is catalyzed by ACC, which is expressed in two isoforms (ACC1 and ACC2). ACC1 predominates in lipogenic tissues while ACC2 is the predominant form in heart and SkM [203]. There is an interesting correlation between the tissue distribution of the CPT1A and CPT1B isoforms and the 1 and 2 ACC isoforms [182]. ACC1 predominates in those tissues where CPT1A also predominates, while ACC2 is present where CPT1B is mainly expressed. Isoform expression appears to depend on the particular metabolite requirement of the different tissues. The activity of ACC isoforms is subject to acute control by rapid covalent modification of the enzyme (inactivation and activation by phosphorylation and dephosphorylation, respectively) and by feed-forward activation by citrate and feedback inhibition by LC-CoA [204]. When energy supply is scarce, the enzymes responsible for producing malonyl-CoA and synthesizing fatty acids, such as FAS, are inhibited while malonyl-CoA decarboxylase (MCD) is activated. This enzyme catalyses the conversion of malonyl-CoA to acetyl-CoA and has a critical role in the regulation of intracellular malonyl-CoA concentration [205]. One of the main regulators of this network is AMPK. This protein is the downstream element of a kinase cascade, activated by its phosphorylation in the Thr^{172} residue of the catalytic subunit [206]. In general, AMPK inhibits ATP-consuming processes, while activating catabolic pathways. Active AMPK phosphorylates and inhibits ACC and reduces the expression of FAS, thus decreasing the flux of substrates in the FAs anabolic pathway [207]. In consequence, the reduction in malonyl- CoA levels leads to an increase in CPT1 activity and FAO.

Recently, the regulation of AMPK by members of the sirtuin family of NAD^+- dependent protein deacetylases and ADP-ribosyltransferases (sirtuins) has been reported [208].

Sirtuin 1 (SIRT1) and SIRT3 stimulate AMPK by deacetylating its upstream activator, kinase LKB1 [208, 209]. In turn, the AMPK activity leads to an increase in NAD^+ levels, thereby promoting deacetylation/activation of other SIRT1 targets involved in FAO, like PGC-1α [210]. In recent years, sirtuins have emerged as critical modulators of lipid metabolism and specifically of FAO. In mammals, the seven identified members of the sirtuin family are differentially located within the cell: SIRT1, 6 and 7 are mainly located in the nucleus; SIRT3, 4 and 5 are located in the mitochondria; and SIRT2 is a cytosolic protein [211].
In specific tissues, sirtuins act on different targets promoting FAO (liver and SkM), mitochondrial respiration (BAT), lipolysis (WAT), and food intake (hypothalamus) [212].

8.5 CPT1AM: abolition of malonyl-CoA sensitivity of CPT1A

Previous studies by our group [213] identified the aminoacid residue methionine 593 (Met^{593}), which contributed to the sensitivity of CPT1 to malonyl-CoA. The site-directed mutagenesis study used to identify amino acids responsible for malonyl-CoA inhibition was based on the comparison of the sequences in a range of carnitine and choline acyltransferases, taking the positive or negative sensitivity to malonyl-CoA as a discriminatory criterion. The proposal was based on the finding that the aminoacid Met^{593} is present in malonyl-CoA- inhibitable carnitine acyltransferases (CPT1, isoforms A and B, and COT) from various organisms and absent in non-inhibitable acyltransferases (CPT2, CrAT and choline acetyltransferase (ChAT)). Mutation of the amino acid Met^{593} to its counterpart in CPT2, serine (Ser) showed that the mutation by itself, M593S, practically abolished malonyl-CoA sensitivity of CPT1A when this mutated CPT1A was expressed in yeast (80% activity at 100 µM malonyl-CoA). It is interesting that this mutant showed higher catalytic efficiency for palmitoyl-CoA as substrate than the wild type. It is proposed that the occurrence of Ser in this position has probably been evolutionary conserved in non-malonyl-CoA-sensitive carnitine acyltransferases because it prevents sensitivity to malonyl-CoA.
From now on, we named CPT1AM, the mutant form of CPT1A.

In the present study we expressed CPT1AM in 3T3-L1 CARΔ1 adipocytes and RAW 264.7 macrophages and analyzed its effects on insulin resistance and inflammation during fatty acids overload in these cells. Previous results by our group showed a beneficial effect of

CPT1AM expression on obesity and insulin resistance in several models *in vitro* [214, 215] and also *in vivo* [216], suggesting that an enhanced FAO could have the same effect in adipocytes and macrophages.

OBJECTIVES

The aim of this thesis is to study the effect of FAO increase, by CPT1AM expression, in adipose tissue during fatty acids (FAs) overload.

For this, we used **3** approaches:

1. CPT1AM expression, by adenovirus, in 3T3-L1 CARΔ1 adipocytes and analysis of its effect on inflammation, insulin resistance, ER stress and ROS damage during FAs overload.

2. CPT1AM expression, by adenovirus, in RAW 264.7 macrophages and analysis of its effect on inflammation, ER stress and ROS damage during FAs overload.

3. Analysis of CPT1A expression in human visceral and subcutaneous adipose tissue.

MATERIALS AND METHODS

1. CELL CULTURE

All solutions used for cell culture are sterilized by autoclaving at 121°C for 30 min (PBS, bd. water, etc.) or by filtering them through a 0.22 μm filter (*Millipore*) if necessary.

1.1 SOLUTIONS AND BASIC PROCEDURES IN CELL CULTURE

- **FBS inactivation**

The main role of serum in cell cultures is to provide complexes of hormones and growth factors. The serum complement has to be inactivated before used in culture. The complement is a heat-labile cascade system in the serum of all vertebrates. When activated, the complement shows a high proteolytic activity, which may affect the function of membrane proteins of cultured cells and thus cell viability. Serum bottles are stored at –20°C. To inactivate the FBS, serum is thawed in a water bath at 37°C and mixed well by inverting the bottle. FBS is inactivated by 30 min incubation in water bath at 56°C. Then, aliquots are made and kept at 4°C or stored at -20°C.

- **10X PBS**

To obtain 5 l of 10X Phosphate-Buffered Saline (PBS) 400 g of NaCl, 10 g of KCl, 72 g of Na_2HPO_4, 12 g of KH_2PO_4 are dissolved in 5 l of bd. water. Then, pH is adjusted to 7.4. For cell culture, 10X PBS is diluted to 1X, autoclaved and stored at 4°C. PBS is useful to wash and remove floating and dead cells because it provides the cells with water and inorganic ions, while maintaining physiological pH and osmotic pressure.

- **2.5 mM Palmitate/BSA (molar ratio 1:5)**

6.97 mg of sodium palmitate (*Sigma, ref. P9767-5g*) is dissolved in 1 ml of 0.1 N NaOH heating at 70°C until obtain a clear solution. At the same time, 0.325 g of FFA-BSA (*Sigma, ref. A-6003*) is dissolved in 8 ml of 0.9% NaCl by heating the solution at 35-40°C as maximum. When the palmitate is completely dissolved, it is added to BSA solution and mixed to conjugate palmitate to BSA. The final solution is filtered with a 0.45 μm filter and 1 ml aliquots are stored at -20°C.

- **Cell counting**

Cells are counted with Countess® Automated Cell Counter (*LifeTechnologies, ref. C10227*). Following the manufacturer's protocol, 10 μl of cell suspension in culture medium is added to 10 μl of 0.4% Trypan Blue Stain (*LifeTechnologies, ref. T10282*) and mixed well. Then, 10 μl of this mix is pipetted into a cell counter chamber slide (*LifeTechnologies, ref. C10228*). Finally, the slide is inserted into the instrument for cell counting. The cell counting occurs in the central location of the counting chamber and the volume counted is 0.4 μL, the same as counting four (1 mm × 1 mm) squares in a standard hemocytometer. A single sample measurement with this instrument provides, in 30 sec, the following data:

- Live and dead cell concentration/ml
- Total cell concentration/ml
- Viability (% live cells to total cells)
- Mean diameter
- Cell images
- Graphical data representation

- **Cell freezing**

First cells are detached with Trypsin-EDTA (3T3-L1 CARΔ1) or by scraping (RAW 264.7) as described above. Then, they are resuspended in 10 ml of medium, centrifuged at 1,200x *g* for 3 min and resupended in 1.5 ml plus 10% (3T3-L1 CARΔ1) or 5% DMSO (RAW 264.7) in 1.5 ml cryogenic tube. DMSO is a cryoprotector agent that physically protects the cells from the forming ice crystals, change in osmotic pressure or fast freezing. However, DMSO is toxic at 37°C, so cells must be frozen immediately at -80°C in a recipient with 100% isopropanol and stored in liquid N_2 the following day.

- **Cell thawing**

Cells stored in the cryogenic tube are thawed quickly in a 37°C water bath. Then, the 1.5 ml of cell suspension is gently transferred to a T75 flask with 12 ml of medium. At approximately 6 hours post plating the medium is replaced with fresh medium.

1.2 3T3-L1 CARΔ1 ADIPOCYTES

Despite 3T3-L1 cells are the most commonly used adipocyte cell culture lines, several studies from Dr. Orlicky lab [217] have shown that 3T3-L1 cells are inefficiently transduced by adenovirus. To overcome the inefficient transduction, they have stably introduced the gene encoding coxsackie and adenovirus receptor (CAR), which is modified by deletion of the region encoding the cytoplasmic tail, into 3T3-L1 cells. The cytoplasmic tail of CAR is not necessary for efficient transduction of adenovirus. Because the normal function of CAR is unknown, expression of a CAR allele, CARΔ1, that has the region encoding the cytoplasmic domain deleted reduces the possibility that CAR function will disrupt normal functions in cells that do not normally express CAR. 3T3-L1 CARΔ1 cells are transduced approximately 100-fold more efficiently than parental 3T3-L1 cells while having a slightly reduced level of differentiation compared to the parental cells [218]. 3T3-L1 CARΔ1 cells are kindly given by Dr. Orlicky (University of Colorado Health Science Center, CO, USA) and arrived to our lab at passage 11-14. The cells purchased from ATCC (3T3-L1; CCL 92.1 Mouse Embryo *ref. CL-173*) were designated passage 1; they were then transduced with CARΔ1 at passage 4, sorted at passage 7, and grown out. These cells continue to differentiate well until at least passage 45, but normally we used them until passage 30.

3T3-L1 CAR Δ1 preadipocytes are cultured in a humidified atmosphere containing 5% CO_2, in T75 flasks (*Corning*) and maintained in **PROLIFERATION MEDIUM** containing DMEM (*LifeTechnologies, ref. 41965-039*), 10% heat-inactivated FBS (*LifeTechnologies, ref. 10270-106*) and 1% Pen/Strep (*LifeTechnologies, ref. 15140122*). The medium is changed every 2 days. It is very important to avoid cells get confluent unless you are trying to differentiate them. Thus, we have split the cells when they are approximately 30-40% confluent and made dilutions of 1:5 – 1:8, depending on need. By doing so, cells are ready to split again after 3 days. To split the cells, medium is removed from the flask, cells washed with 1X PBS and detached with 2ml/T75 flask of pre-warmed trypsin-EDTA (*LifeTechnologies, ref. 25300-054*) for approximately 2-3 minutes at 37 °C. The trypsin is immediately neutralized by adding to the flasks 8 ml of PROLIFERATION MEDIUM.

PROLIFERATION MEDIUM	
DMEM	445 ml
10% FBS	50 ml
1% Pen/Strep	5 ml

Adipocytes differentiation is induced by treating 2-day post-confluent cultures with **DM1** containing DMEM (*LifeTechnologies, ref. 41965-039*), 10% FBS *(BioGemini, ref. GEM-100-106-S*), 1% Pen/Strep (*LifeTechnologies, ref.15140122*), 0.25 μM dexamethasone, 0.5mM IBMX (*Sigma, ref. I-7018*) and 1 μg/μl insulin (*Lilly, Humulin 100* UI/ml) for 48 h. The day of induction of differentiation is designated as Day 0. The combination of dexamethasone, IBMX and insulin, induced preadipocytes to adopt a rounded phenotype and within 5-8 days to accumulate lipids intracellularly in the form of droplets. Dexamethasone activates the transcription factor C/EBPβ. IBMX inhibits soluble cyclic nucleotide phosphodiesterases and results in increased intracellular cAMP levels. At the nuclear level, treatment with IBMX results in activation of the related transcription factor C/EBPδ. C/EBPβ and δ in turn induce transcription of C/EBPα and PPARγ. Within 3 days of exposure to inducers, the cells undergo two rounds of mitosis, termed mitotic clonal expansion, which are required for differentiation. Insulin or insulin-like growth factor-1 promotes adipocyte differentiation by activating PI3-kinase and Akt activity. Modulation of the activity of the forkhead transcription factor Foxo1 appears to be necessary for insulin to promote adipocyte differentiation. C/EBPα and PPAR direct the final phase of adipogenesis by activating expression of adipocyte-specific genes, such as fatty acid synthetase (FAS), fatty acid binding protein, leptin and adiponectin.

After 48 h, DM2 containing DMEM (*LifeTechnologies ref. 41965-039*), 10% FBS *(BioGemini, ref. GEM-100-106-S*), 1% Pen/Strep (*LifeTechnologies ref. 15140122*) and 1 μg/μl insulin (*Lilly, Humulin 100* UI/ml) is added for additional 48 h. Finally, DIFFERENTIATION MEDIUM 2 is replaced by **DM3** containing DMEM (*LifeTechnologies ref. 41965-039*), 10% FBS

(BioGemini, ref. GEM-100-106-S), 1% Pen/Strep (*LifeTechnologies ref. 15140122*) until the Day 8 (post-differentiation) when adipocyte differentiation conversion is considered complete. Mature adipocytes are used for experiments at day 8-10 post-differentiation.

DIFFERENTIATION MEDIUM 1 (DM1)	
DMEM	500ml
10% FBS	50 ml
1%Pen/Strep	5 ml
0.25μm Dexamethasone	555 μl
0.5mM IBMX	2.77 ml
1μg/μl Insulin	123 μl

DIFFERENTIATION MEDIUM 2 (DM2)	
DMEM	500 ml
10% FBS	50 ml
1% Pen/Strep	5 ml
1μg/μl Insulin	123 μl

DIFFERENTIATION MEDIUM 3 (DM3)	
DMEM	500 ml
10% FBS	50 ml
1%Pen/Strep	5 ml

- IBMX (*Sigma ref. I-7018*, 100 mg)

100mM stock : Add 0.1 g IBMX to 2.25 ml of NaOH (1ml NaOH 0.5M into 50 ml EtOH absolute), heat at 65°C and mix. Then add 2.25 ml H_2O milliQ and mix all. Filter the mixture under the hood (0.22 μm filter) and store at -20°C (several months stable). Once thawed, store IBMX at + 4°C.

- Dexametasone (*Sigma ref*. *D-4902*)

0.25mM stock: 4.9 mg in 50 ml of EtOH. Filter the mixture under the hood (0.2 μm filter), aliquot and store at +4°C for short-term storage (1 month) or at -20°C for long-term storage.

- To enhance the differentiation we also added to **DM1**, 2 μM of Rosiglitazone *(Sigma, ref. R-2408)* preparing 10 mM stock in DMSO (= 10 mg in 2.8 ml of DMSO).

1.3 RAW 264.7 MACROPHAGES

RAW 264.7 macrophages are obtained from ATCC *(ref. ATCC® TIB-71™)*. Cells are cultured in a humidified atmosphere containing 5% CO_2, in T75 flasks (Corning), and maintained in PROLIFERATION MEDIUM containing DMEM *(LifeTechnologies, ref. 41966-029),* 10% FBS *(LifeTechnologies, ref. 102070-106)* and 1% Pen/Strep *(LifeTechnologies, ref. 15140122)*. Once washed with 1X PBS, cells are split 1:8-1:10 every 2 days by scraping in fresh PROLIFERATION MEDIUM. It is very important to avoid the cells to reach 100% confluence.

1.4 HEK 293 CELLS

Human embryo kidney (HEK) 293 cells are cultured in a humidified atmosphere containing 5% CO_2, in 10 cm^2 dishes, and maintained in **MAINTENANCE MEDIUM** containing DMEM (*LifeTechnologies, ref. 41966-029*), 10% FBS (*LifeTechnologies, ref. 102070-106)* and 1% Pen/Strep (*LifeTechnologies, ref. 15140122*). The maintenance culture is passaged twice a week and the medium is changed every 2-3 days. Cells are split 1:8-1:10 every 2 days. To split the cells medium is removed from the plate (10 cm^2), cells are washed with 1X PBS and detached with 2ml/plate of pre-warmed trypsin-EDTA (*LifeTechnologies ref. 25300-054*) for approximately 2-3 minutes at 37°C. Immediately trypsin is neutralized by adding to the plate 8 ml of MAINTENANCE MEDIUM. For experiments, cells are grown until 70% of confluence.

2. ADENOVIRUS

The ability to transfer DNA rapidly and efficiently in mammalian cells has been improved by the development of a number of gene transfer vectors and techniques based on the properties of DNA viruses such as adenovirus, retrovirus, lentivirus and adenoassociated virus. Among them, we have used the adenoviruses for gene delivery because of their growth and infectivity characteristics. Adenovirus rapid and efficiently deliver DNA into a wide range of mammalian cell types. Moreover, they express relatively large DNA inserts (up to 5-7 kbp) and propagate stable high-titer viral stocks. Adenovirus integrates into genomic DNA with very low efficiency and exists predominantly in an episomal mode, therefore the expression of the transgene is transient.

2.1 ADENOVIRUS BIOLOGY

Adenoviruses (Ad) are a large family of nonenveloped, double-stranded DNA viruses. The virus is originally isolated from human adenoidal tissue in 1953. Human adenovirus serotypes 2 (Ad2) and 5 (Ad5) are the most extensively studied. For our study we chose the Ad5.The adenoviral particle consists of an icosahedral protein capsid approximately 75 nm in diameter encasing a double-stranded DNA molecule of approx. 36 kb. The most abundant viral protein is hexon, which makes up most of the outer shell of the virus. At each vertex there is a complex composed of the penton base and fiber proteins, both of which interact with cellular receptors during the process of virus infection. Ad DNA is packaged in a

complex with several viral proteins and each end of the chromosome is covalently attached to a single molecule of terminal protein (TP). TP acts as a primer for DNA synthesis and also anchors the viral chromosome to the nuclear matrix. The lytic life cycle of the wild-type virions can be divided into early and late phases, which are defined as occurring before and after the onset of viral DNA replication, respectively. Therefore the adenoviral genome could be classified into early (E1, E2, E3 and E4) genes and late genes. Strategies for adenovirus vector design are focused on deleting portions of the genome to allow packaging of relatively large DNA inserts. Wild-type adenovirus can only accommodate 2 kbp of foreign DNA, but deletion of E1 and E3 genes can allow recombinants with inserts up to 7 kbp. Deletion of the E1 gene blocks most viral gene expression as well as DNA synthesis and therefore renders Ad replication defective. E3 proteins are involved in evading the host antiviral immune response. By using a replication-defective Ad vector, cells can be infected without grossly perturbing normal functions, thus allowing analysis of the functional properties of the recombinant protein. In the case of deletion of the essential E1 gene, viral propagation is conditional because the function of the E1 gene must be provided in trans. This is achieved by growing E1-deleted recombinant virus in the HEK 293 cell line, which is originally transformed with Ad5 and contains the left 14% of the adenovirus genome integrated into cellular DNA, including the E1 region14. Although the recombinant virus cannot propagate in cells other than HEK 293 cells, if it attaches to the skin or the airway, it efficiently enters cells and expresses the target gene. Therefore, the use of security measures such as a safety hood to prevent inhalation or adhesion of the virus is strongly recommended.

2.2 ADENOVIRUS AMPLIFICATION

In this study, we used AdGFP, as control, and AdCPT1AM (expressing the permanently active mutant form of CPT1A) previously obtained in our laboratory [213, 214]. For our experiments, we needed to amplify the adenovirus stock in HEK 293 cells.

The adenovirus amplification is performed in 2 steps:

1) ***First amplification***: HEK 293 cells are cultured in 10 cm^2 dishes (final volume=10 ml for each dish). When the cells are ± 70% confluent, we removed the medium from cells, washed

the cells with 1X PBS, added 5 ml of fresh medium supplemented with 5% FBS and infected each dish with 50 μl of Adenovirus stock. After 2h, we added 5 ml of complete medium to each dish. When the cytopathic effects are complete (when the cells are completely detached), approximately 2 days after infection, we collected the culture medium containing the cells and freeze/thaw it 3 times in liquid N_2 and a water bath at 37°C. Finally, we removed cell debris by centrifugation at 3,000 rpm for 5 min at 4°C, collected the supernatant 1 and froze it at -80°C.

2) *Second amplification*: for this step also, we needed HEK 293 cells ± 70% confluent, but cultured in 150 cm^2 dishes (n=10). When the cells are ready to infect, we removed the medium, washed with 1X PBS, added 5 ml of fresh medium supplemented with 5% FBS and infected each plate with 400 μl of adenovirus amplified in the first step. After 2 h, we added 10 ml of complete medium. After 20-30 h (depending on the cellular growth speed) when cells started to detach, we collected the culture medium containing all the cells in a 50 ml tubes, pelleted the cells by centrifugation at 1,000 rpm for 5 min at room temperature (r.t.) and resuspended (all the tubes together) them in 5 ml of medium. To release the adenoviruses, which are inside the cells, we subjected the suspension to 3 freeze-thaw cycles. Finally, we removed cell debris by centrifugation at 3,000 rpm for 5 min at 4°C, collected the supernatant and froze it at -80°C.

2.3 ADENOVIRUS TITRATION

Quantification of adenoviral stocks, *i.e.* the determination of the viral **plaque forming units (pfu)** per ml, is important to ensure consistency between samples and to achieve the right level of transient expression. Careful titration is performed using the **Adeno-X™ Rapid Titer Kit** (*Clontech, ref. 632250*). Also when producing viral stocks, it's important to know the titer of infectious particles for successful virus production. This method takes advantage of production of viral hexon proteins for the quantification of viral stocks. Dilutions of the viral stock are used to infect HEK 293 cells. Just 48 h later, these cells are fixed and stained with the antibody specific to the adenovirus hexon protein. Signal is detected after a secondary antibody conjugated with horseradish peroxidase (HRP) amplifies the signal of the antihexon antibody. Subsequent exposure to metal-enhanced 3,3'-diaminobenzidine (DAB) peroxidase substrate turns only the infected cells dark brown. Then the titer of the stock can be

determined by counting the number of brown cells in a given area. Each stained cell corresponds to a single infectious unit (ifu).

The titration procedure is as follows:
1 ml of healthy, log-phase HEK 293 cells (5 x 10^5 cells/ml) is seeded in each well of a 12-well plate. Using medium as diluent, 10-fold serial dilutions (duplicate) from 10^{-2} to 10^{-7} of the viral stock are prepared and 100 µl of each one is added to each well. After 48 h of incubation at 37°C in 5% CO_2, medium is aspirated and cells are allowed to dry in the hood for 5 min, avoiding over dry. Then, cells are fixed by adding very gently without dislodging the cell monolayer, 1 ml of ice-cold 100% methanol to each well. After keeping them at -20°C for 10 min they are gently rinsed three times with 1 ml PBS + 1% BSA (*Sigma, A-6003*). Cells are then incubated for 1 h at 37°C with 0.5 ml/well of Anti-Hexon Antibody diluted 1/3,000 in PBS + 1% BSA. Next, cells are gently rinsed three times with 1 ml PBS + 1% BSA and incubated for 1 h at 37°C with 0.5 ml/well of Rat Anti-Mouse Antibody (HRP conjugate) diluted 1/500 in PBS + 1% BSA. The rinsing steps are repeated as before and then cells are finally incubated at r.t. for 10 min with 500 µl/well of the DAB substrate. To calculate the titer of the viral stock the DAB substrate is aspirated, 1 ml PBS is added to each well and at least three fields of brown/black positive cells are counted on a microscope with a 20X objective. The pfu/ml is calculated from the resulting average number of positive cells/unit dilution as follows:

Adenovirus titer (pfu/ml) = [(infected cells/field) x 573] / [0.1 x dilution factor]

Where **573** is the number of fields/well in a 20X objective and **0.1** is the volume of viral dilution used in ml.

2.4 ADENOVIRUS INFECTION

For 3T3-L1CARΔ1 ADIPOCYTES, the infection protocol is as follows:

1) At day 8 post-differentiation, as described above, adipocytes are mature and ready to be infected. The final concentration of cells/ml in each well, in a 12-well plate, is 400,000 cells/well approximately. One well/plate is used for cell count to calculate the required amount of virus/cell. Cells are then infected with the same m.o.i. = **100** of AdGFP and

AdCPT1AM at 37°C for 24 h. The required amount of each adenovirus is mixed with **INFECTION MEDIUM.** Infection is performed in 1 ml of medium for each well.

3T3-L1CARΔ1 INFECTION MEDIUM	
DMEM *(Lifetechnologies, ref. 41965-039)*	500 ml
1% Pen/Strep	5 ml

2) After this time, **at day 9 post-differentiation**, INFECTION MEDIUM is removed, cells are washed with 1X PBS and 1ml of **DM3** is added to each well. Infected adipocytes are maintained in this medium for further 24 h and then collected for desired experiments.

For RAW 264.7 macrophages, the infection protocol is as follows**:**

1) Cells are homogeneously seeded in 12-well plates (70,000 cells/ml), further cultured for 3 days before infection.

2) The day of the infection, one well/plate is used for cell count to calculate the required amount of virus/cell. The final concentration of cells/ml in each well is $1x10^6$ cells/well approximately. Cells are then infected with the same m.o.i.= **100** of AdGFP and AdCPT1AM at 37°C for 24 h. The required amount of each adenovirus is mixed with **INFECTION MEDIUM.** Infection is performed one in approx. 1/4 volume of the total volume of the well or dish, *i.e.* in 200 μl of medium for 12-well plates. Therefore, proximity of the virus to the cells is enhanced. Cells are incubated with the different adenoviruses at 37°C for 2h. After this time, 800 μl of **PROLIFERATION MEDIUM** are added to each well. Infected macrophages are maintained in this medium for 24 h.

RAW 264.7 INFECTION MEDIUM	
DMEM (*LifeTechnologies ref. 41966-029)*	500 ml
1% Pen/Strep	5 ml

3) After this time, medium is removed, cells are washed with 1X PBS and 1 ml of fresh **PROLIFERATION MEDIUM** is added to each well. Cells are maintained in this medium for additional 48 h and then collected for desired experiments.

3. PROTEIN ANALYSIS

3.1 TOTAL PROTEIN EXTRACTION FROM CELL CULTURE

Cells are cultured, differentiated (in case of adipocytes) and infected as described above. The day of extraction, medium is removed, cells are washed with 1 ml of cold 1X PBS (x3) and plates are put on ice. 100 μl of cold Lysis Buffer is added to each well and plates left on ice, for 5 min, shaking every minute, more or less. Cells are then detached by scraping, homogenized and the lysate collected in 1.5 ml tube. Cell lysates are left on ice for 10 min, vortexing a little every 3 min. Finally, lysates are centrifuged for 10 min at 4°C, maximum speed. After this time, supernatants are collected, discarding the pellet, and stored at -20°C until quantitation.

LYSIS BUFFER (50 ml)	
HEPES-NaCl	40 ml
100% Glycerol	5 ml
20% Triton X-100	2.5 ml
10% Deoxycolate (DOC)	2.5 ml
50X Protease Inhibitor	1 tablet
100X Phosphatase Inhibitor	1X [When necessary (*e.g*. pAkt detection)]

- 10% DOC: 5 g DOC in 50 ml H_2O (stored at 4°C, protected from light)
- 20% Triton X-100: 10 ml X-100 Triton + 40 ml H_2O

HEPES-NaCl mix: 30 mM HEPES, pH 7.4, 150 mM NaCl (aliquots stored at - 20°C)

3.2 BCA PROTEIN QUANTITATION

BCA Protein Assay is a detergent-compatible formulation based on bicinchoninic acid (BCA) for the colorimetric detection and quantitation of total protein. This method combines the

well-known reduction of Cu^{+2} to Cu^{+1} by protein in an alkaline medium (the biuret reaction) with the highly sensitive and selective colorimetric detection of the cuprous cation (Cu^{+1}) using a unique reagent containing bicinchoninic acid. The purple-colored reaction product of this assay is formed by the chelation of two molecules of BCA with one cuprous ion. This water-soluble complex exhibits a strong absorbance at 562 nm that is nearly linear with increasing protein concentrations over a broad working range (20-2000 μg/ml). The BCA method is not a true end-point method; that is, the final color continues to develop. However, following incubation, the rate of continued color development is sufficiently slow to allow large numbers of samples to be assayed together. Protein concentration is measured according to the manufacturer's instructions (*Thermoscientific, Pierce ® BCA Protein Assay kit, ref. 23225*), using BSA as a protein standard (stock solution: 2mg/ml). BCA Working Reagent (WR) is prepared by mixing 50 parts of BCA Reagent A with 1 part of BCA Reagent B (50:1, Reagent A: B). BSA standards and samples are added, in duplicate, to 96-well plate. Then, 200 μl of WR are added to each well with a multichannel pipette and the solution is mixed by pipetting up and down several times. Finally, the absorbance is measured at or near 562 nm on a plate reader.

	BSA stock	**H_2O**	**BCA WR**
Blank	-	20 μl	200 μl
BSA 0.018 μg/μl	2 μl	18 μl	200 μl
BSA 0.0368 μg/μl	4 μl	16 μl	200 μl
BSA 0.072 μg/μl	8 μl	12 μl	200 μl
BSA 0.145 μg/μl	16 μl	4 μl	200 μl
BSA 0.181 μg/μl	20 μl	-	200 μl
Samples	2-5 μl	Up to 20 μl	200 μl

3.3 WESTERN BLOT (WB)

The Western Blot (WB) technique detects, with a specific antibody, a protein between a sample of proteins that have been separated by electrophoresis and transferred to a nitrocellulose/PVDF membrane. Western blot is applied for the analysis of CPT1A, pAkt and

Akt proteins levels in whole cell lysates. The procedure has the following steps:

1) Samples preparation

2) Electrophoresis

3) Transfer

4) Antibody incubation and detection

1) SAMPLES PREPARATION

Equal amounts of protein from whole cell lysates, previously quantified by BCA method, are prepared to load into the gel, adding to each sample **4X LOADING BUFFER** to a final concentration of 1X. This loading buffer contains the denaturalizing agent SDS and DTT that reduces disulphide bonds. Samples are then heated at 95°C for 5 min, briefly centrifuged and placed on ice before loading onto the gel. Samples could be stored in loading buffer at -20°C for 4-6 months. However, after several freeze-thaw cycles proteins will begin to degrade and fail to give sharp bands.

4X LOADING BUFFER
200 mM Tris-HCl (pH 6.8)
8% SDS
40-50% Glycerol
400 mM DTT
0,4% Bromophenol Blue
H_2O up to total volume

⇒ Aliquots of 4X LOADING BUFFER are prepared and stored at -20°C.

2) ELECTROPHORESIS (SDS-PAGE)

- *Gel preparation:* 8% separating gel is prepared.
- Separating gel is prepared by adding the polymerizing agents TEMED and ammonium persulphate (prepared the day of the experiment) at the end. For the electrophoresis, we used two systems, Mini-PROTEAN® and CRITERION ® (Sigma),

following the manufacturer's instructions. Some drops of isopropanol are added on the top to achieve a straight edge of the gel. Once the gel is polymerized isopropanol is removed. Then, stacking gel is prepared and cast and a 1.5 mm comb is adjusted between the two glasses. Both the separating and stacking gel take approximately 30 min to polymerize. Bubbles must be avoided during all the process.

- *Electrophoresis performance*: To run the electrophoresis, the 1.5 mm comb is removed and **1X RUNNING BUFFER** is added on to the electrophoresis chamber and on to the sample loading wells. Samples and protein marker (*GEHealthcare, ref. RPN800E*) are loaded onto the gel and electrophoresis is performed at a constant current of 25 mA for 1 h approximately. Electrophoresis is stopped when bromophenol blue is just off the bottom of the gel.

10X RUNNING BUFFER (1 l)	
Tris-HCl	25 mM
Glycine	192 mM
SDS	0,1 %
H_2O	Up to 1 l
pH 8.8	

⇒ For each electrophoresis, 1X RUNNING BUFFER, stored at RT, is prepared fresh from 10X stock.

8% SEPARATING GEL (1.5mm)	
bd H_2O	5.9 ml
40% Acrilamide (29:1)	2 ml
1.875 M Tris HCL (pH 8.8)	2 ml
10% SDS	100 μl
10% Ammonium Persulphate	66.6 μl
TEMED	10 μl

5% STACKING GEL (1.5mm)	
bd H_2O	3.02 ml
40% Acrilamide (29:1)	0.5 ml
1.875 M Tris HCl (pH 8.8)	0.4 ml
10% SDS	40 µl
10% Ammonium Persulphate	27.2 µl
TEMED	8 µl

3) TRANSFER

Once electrophoresis is finished, stacking gel is removed and proteins in the separating gel are transferred to a Hybond PVDF membrane (*GEHealthcare, ref. RPN303F)* for its later antibody incubation. For the transfer, we used two systems, Mini-Transblot Electrophoretic Transfer Cell ® or Criterion Blotter With Wire Electrodes ® *(Sigma*). The transfer sandwich contains, in the following order from the negative to the positive pole: a sponge, 2 Whatman papers, the gel, the PVDF membrane, 2 Whatman papers and another sponge. All must be submersed in **1X TRANSFER BUFFER** avoiding bubbles. Whatman papers and the PVDF membrane must have the same size as the gel (approximately). The side of the membrane in contact with the gel is marked to identify the side where proteins are, for later antibody incubation and detection. The transfer is performed at 4°C for 1 h at 250 mA or for 2 h at 125 mA. Once it is finished, membrane is washed in water and effectiveness of the transfer is checked by Ponceau S solution (*Sigma, ref. P-7170)* staining of the protein bands. To remove the red staining, membrane is washed in 0,1% PBS-Tween for a few minutes.

- Before performing the transfer, it is necessary to activate the Hybond PVDF membrane as follow: 5 min in Methanol +5 min in H_2O+ 10 min in 1X TRANSFER BUFFER.

⇒ For each electrophoresis, 1X TRANSFER BUFFER is prepared fresh from 10X stock as follow: 80 ml 10X stock + 160 ml Methanol + H_2O (up to 800 ml). It is stored at + 4°C until use.

⇒ **0,1% PBS-Tween (PBS-T)**: 1 ml of Tween-20 is diluted in 1 l of 1X PBS. It is stored at room temperature (r.t.).

10X TRANSFER BUFFER (1 l)	
Tris-HCl	20 mM
Glycine	150 mM
H_2O	Up to 1 l
pH 8.5	

4) ANTIBODY INCUBATION

Immunoblotting is carried out with the enhanced chemifluorescence (ECL) immunoblotting detection system (*GE Healthcare, ref. RPN2235)* and the results are quantitatively analysed using Image Quant LAS4000 Mini (GE Healthcare). For CPT1A detection, membranes are incubated. According to the manufacturer's instructions the protocol is as follows:

- *Blocking the membrane*: Non-specific binding sites are blocked by immersing the membrane in blocking solution for 1 h on an orbital shaker at r.t.. After this time, membrane is rinsed and washed once for 15 min and twice for 5 min in PBS-T on an orbital shaker.

  ⇒ Blocking solution: 5% w/v of nonfat dry milk in PBS-T.

- *First antibody incubation*: We used the following primary antibodies diluted as described below:

CPT1A (from rabbit) [214]	1:6,000 in PBS-T + 5% nonfat dry milk
I-19 Actin (from rabbit) *Santa Cruz, Biotechnology, ref. sc-1616-HRP*	1:4,000 in PBS-T
pAkt (Ser473) (from mouse) *Cell Signalling, ref. 4051*	1:1,000 in PBS-T + 5% nonfat dry milk
Akt (from rabbit) *Cell Signalling, ref. 9272*	1:1,000 in PBS-T + 5% BSA

For CPT1A and β-actin primary antibodies, incubation is performed over 1h, at r.t. an orbital shaker, or overnight (O/N) at 4°C, for pAkt and Akt.
After this time, membrane is rinsed and washed once for 15 min and twice for 5 min in PBS-T on an orbital shaker. The first antibodies could be reused by storing them at -20°C.

- *Second antibody incubation*: The second antibody is diluted 1:10,000 (anti-rabbit) or 1:6,000 (anti-mouse) in PBS-T. Incubation is performed over 1 h at r.t. on an orbital shaker. After this time, membrane is rinsed and washed once for 15 min and twice for 5 min in PBS-T on an orbital shaker.
- *Detection***:** After washing, membrane is dried and incubated for 2 min with the ECL substrate. The volume of ECL should be enough to cover the membrane surface. After this time, the membrane is drained and placed in a plastic directly on to the sample holder of detection instrument and intensity of the bands is quantified with ImageQuant software.
  √ ECL Anti-Rabbit HRP (from donkey): *GEHealthcare, ref. NA934V-1ml*
  √ ECL Anti-Mouse HRP (from goat): *GEHealthcare, ref. NA913V-1ml*

4. PROTEIN CARBONYL CONTENT ANALYSIS (OXYBLOT)

Oxidative modification of proteins by oxygen free radicals and other reactive species occurs in physiologic and pathologic processes. Proteins are one of the major targets of oxygen free radicals and other reactive species. Oxidative modification of proteins modifies the side chains of methionine, histidine, and tyrosine and forms cysteine disulphide bonds. Metal catalyzed oxidation of proteins introduces carbonyl groups (aldehydes and ketones) at lysine, arginine, proline or threonine residues in a site-specific manner. The **OxyBlotTM Kit** (*Millipore, ref. S7150*) provides reagents for simple and sensitive immunodetection of these carbonyl groups, which is a hallmark of the oxidation status of proteins. The carbonyl groups in the protein side chains are derivatized to 2,4-dinitrophenylhydrazone (DNPhydrazone) by reaction with 2,4-dinitrophenylhydrazine (DNPH). The DNP-derivatized protein samples are separated by polyacrylamide gel electrophoresis followed by Western blotting, performed as described in section **4.** Individual oxidized proteins are separated and identified from a complex mixture by SDS-PAGE. The oxidative status of each protein can be analyzed

quantitatively by comparison of the signal intensity of the same protein in different lanes on the same or different gels. In our case, 8-10 μg of total protein are used for Oxyblot.

5. CPT1 ACTIVITY ANALYSIS

CPT1 activity assays are performed with mitochondrion-enriched fractions from cell culture. Fresh mitochondria are used for the CPT1 activity assay or stored at - 80°C. For this assay, cells are cultured and differentiated in 100 cm^2 plates.

5.1 MITOCHONDRIA ISOLATION FROM CELL CULTURE

To obtain the mitochondrion-enriched fractions, cells are washed with cold 1X PBS and resuspended in 2 ml of the same solution. All the process is performed at 4°C. Cells are centrifuged for 5 min at 1,200x *g*, surnatant is removed and pellet is resuspended in 1 ml of **HOMOGENIZATION BUFFER**. After resuspension, cells are broken with a glass homogenizer fitted with a loose and a tight pestle. 20 cycles are done with each one. Further centrifugation is performed for 3 min at 2,000x *g* to remove cell nucleus and membranes. Supernatant is centrifuged at 16,000x *g* for 30 min and mitochondria are resuspended in 25 μl of HOMOGENIZATION BUFFER. Mitochondria concentration is quantified by the BCA assay, and 25 (3T3-L1 CARΔ1 adipocytes) or 30 μg (RAW 264.7 macrophages) are used for the CPT1 activity assay.

HOMOGENIZATION BUFFER (stored at 4°C)	
Mannitol	210 mM
Sucrose	70 mM
EDTA	1 mM
HEPES pH 7.4	10 mM
Protease Inhibitors	1X

5.2 CPT1 ACTIVITY ASSAY

CPT1 activity is determined by the radiometric method as previously described [219] with minor modifications. CPT1 is assayed with the mitochondrion-enriched fractions obtained as described above where the mitochondria remain largely intact. When mitochondria are

frozen, membranes could be broken, allowing CPT2 to contribute to the measured activity. To avoid CPT2 interferences freshly obtained mitochondria are used for each experiment.

The substrates for the CPT1 activity assay are L- [methyl-^{3}H] carnitine hydrochloride (*PerkinElmer, ref. NET1181250UC*) and palmitoyl-CoA and the reaction is done in the following direction:

$$^{3}\text{H-carnitine} + \text{palmitoyl-CoA} \rightarrow \text{palmitoyl-}^{3}\text{H-carnitine} + \text{CoA-SH}$$

The procedure takes advantage of the fact that the product of the reaction, palmitoyl-^{3}H-carnitine, is soluble in an organic medium. Therefore, it could be separated by extraction from the radioactive substrate, ^{3}H-carnitine, that has not been reacted and which will remain in the aqueous phase.

Deacylases convert the substrate acyl-CoA in acyl plus CoA-SH, generating ATP. This process will reduce the availability of the substrate palmitoyl-CoA in the reaction. Therefore, ATP is added to the reaction mix to minimize this process, by inverting the equilibrium of the deacylase reaction and by stimulating the reaction of the acyl-CoA synthetases and thus regenerating the substrate palmitoyl-CoA. KCN is added to avoid mitochondrial oxidation. Glutathione (GSH, reduced form) is used as a reduction agent instead of dithiothreitol (DTT) or dithioeritrol (DTE) because DTT and DTE have been shown to reduce malonyl-CoA sensitivity. Defatted BSA is added to protect mitochondria from the detergent effect of fatty acids. However, BSA concentration must not be higher than 0.1% because this could give a sigmoidal effect in the enzyme *vs* acyl-CoA kinetic. Finally, KCl is added because it increases enzyme activity.

Since activity and sensitivity to malonyl-CoA depend on pH, we chose pH 7.2, the optimum for both conditions. The temperature for the assay is 30°C to compensate a good enzymatic activity, which increases with the temperature, with a convenient inhibition, which decreases with the temperature.

The procedure for the CPT1 activity assay is as follows:

The reaction mix is prepared in a 15 ml tube kept on ice. GSH is prepared by dissolving it in water on the day of the experiment. Samples are done in duplicate. The following amounts are per point:

CPT1 reaction mix/point	
bd H_2O	92.33 μl
4X CPT1 buffer	40 μl
1mM Palmitoyl-CoA	10 μl
80mM ATP	10 μl
30% BSA	0.67 μl
25mM GSH	2 μl
16mM ^{3}H-Carnitine	5 μl
Total volume	160 μl

Protein samples are prepared on ice in 1.5 ml tubes by diluting the protein in **4X CPT1 BUFFER** and by adjusting the volume with bd. water up to 40 μl. The blank contained bd. water instead of protein.

Protein samples	
Protein	20-30 μg
4X CPT1 BUFFER	10 μl
bd H_2O	Up to 40 μl

One by one, 160 μl of the reaction mix is added to each protein sample. Samples are vortex-mixed and placed on a water bath at 30°C for exactly 5 min. Reaction is stopped with the addition of 200 μl of 1.2 M HCl. Samples are vortex-mixed and placed on ice. Extractions of the product of the reaction, palmitoyl-^{3}H-carnitine, are done by adding 600 μl of water-saturated butanol. Samples are vortex-mixed and centrifuged for 2 min at 13,000 rpm in a microcentrifuge. 400 μl of the upper phase is added to another 1.5 ml tube with 200 μl of bd. water. Samples are vortex-mixed and centrifuged for 2 min at 13,000 rpm. 250 μl of the upper phase is counted in plastic scintillation vials with 5 ml of scintillation liquid (Ecolite, ICN). ^{3}H radioactivity is counted in a RackBeta apparatus.

Specific activity of the enzyme is calculated as follows:

S.A. (nmol/mg prot/min)= (cpm x 600 µl) / (S.R. x mg prot. x min x 250 µl)

Where cpm are the counts per minute, S.R. is the ^{3}H-carnitine specific radioactivity (approx. 3000 cpm/nmol) and 600 µl/250 µl is the dilution factor.

4X CPT1 BUFFER (stored at 4°C)	
Tris-HCl pH 7.2	420 mM
KCN	8 mM
$MgCl_2$	16 mM
KCl	60 mM

⇒ **16 mM ^{3}H-carnitine**: 6.6 mg of cold carnitine is dissolved in 982.3 µl of 95% ethanol plus 982.3 µl of bd water and 125 µl of L- [*methyl*-^{3}H] carnitine hydrochloride (80 Ci/mmol) is added. Aliquots of 125 µl are stored at -80°C.

5.3 MALONYL-CoA INHIBITION ASSAY

For malonyl-CoA inhibition assays, the different amounts of malonyl-CoA are added to the protein samples adjusting the final volume up to 40 µl. The stock of 2 mM malonyl-CoA used is prepared in 1 mM sodium acetate pH 5.9 and stored at -20°C. Samples are vortex-mixed and preincubated for 1 min at 30°C prior to the addition of the reaction mix. It has been described [220] that this preincubation increases the inhibition level. CPT1 activity assay is performed as described above.

6. CELLULAR METABOLISM ANALYSIS

6.1 OLEATE OXIDATION

Oleate oxidation assay is done with attached cells and allows studying the capacity of the cells to oxidize oleate. Cells are incubated with [1-^{14}C] oleate and the $^{14}CO2$ released and the acid-soluble products (ASP) are measured. Total oleate oxidation will be the sum of both. Oleate oxidation assay is performed in T25 flasks.

This method has been described by Roduit *et al*. [221] and utilizes T25 flasks in which the $^{14}CO_2$ released is also trapped in a KOH soaked Whatman paper. The reaction is stopped by the addition to the cells of perchloric acid. The system, still closed, is left o/n and therefore all the $^{14}CO_2$ in the atmosphere of the flask is captured by the Whatman paper. Oleate oxidation in 25-cm_2 flasks allows time for the $^{14}CO_2$ to be taken up into the Whatman paper in a closed system giving slightly higher oxidation rates.

The procedure is as follows:

Cells are seeded in T25 flasks, infected and treated as described above. The day of the assay, solutions A and B are prepared and warmed in a waterbath at 37°C. Cells are first ished three times with 3ml/flask of **Solution A** and then incubated with 2ml/flask of **Solution B** for 30 min at 37°C. After this time, **Solution B** is removed and 2 ml of the **Reaction Mix** is added to each flask. Blanks are flasks without cells. The T25 flasks are sealed at the beginning of the incubation with a rubber stopper (size 14.5, *Fisher, ref.14-126BB*) supporting a 3 cm length of PVC tubing (I.D. 4.7 mm, *Fisher, ref. 14-169-7B*) containing a piece of Whatman paper soaked in 0.1 N KOH. One end of the PVC tubing is wrapped in parafilm without covering the lumen, so that tubing will fit firmly into the under-side of the stopper. The Whatman paper inside the tubing must be well clear to the opening. Flasks are then incubated at 37°C for 3 h (3T3-L1 CARΔ adipocytes) or 2 h (RAW 264.7 macrophages). At the end of the incubation period, 0.2 ml of 40% (v/v) perchloric acid is injected into each flask *via* a needle through the rubber stopper to acidify the medium, liberate $^{14}CO_2$ and stop oleate oxidation. Perchloric acid must be well mixed. After o/n isotopic equilibration at RT, Whatman papers are removed and the trapped $^{14}CO_2$ is measured by liquid scintillation counting after o/n equilibration in 5 ml of the scintillation fluid. It is left o/n because it takes more than 12 h to $^{14}CO_2$ to leach out of Whatman paper into scintillation fluid. The addition of perchloric acid generates a precipitate, therefore for the Bradford protein assay cells from parallel flasks, without perchloric acid, are removed with 1 ml of KRBH. The scintillation values are normalized to protein content of each flask.

Results are expressed as:

nmol of oleate.mg^{-1} prot.h^{-1} = (cpm-blank cpm) x 600 / (total cpm x mg prot x h)

Where **600** is the total nmol of oleate per flask, **total cpm** are the counts resulting from directly counting on the scintillation liquid the amount of 3 mM [1- ^{14}C] oleate used per flask

and **h** is the time of incubation.

6.2 OLEATE OXIDATION TO ACID-SOLUBLE PRODUCTS (ASP)

Fatty acid oxidation into acid-soluble products (ASP) is measured from the perchloric acid treated medium. The perchloric acid injected into the media precipitates the fatty acid tracer bound to proteins leaving the ASPs in solution. In case of the oleate oxidation assay performed in T25 flasks, 1 ml of the incubation media already treated with perchloric acid is taken and centrifuged at 14,000 rpm for 10 min in a microcentrifuge. 800 µl of the supernatant is counted on a scintillation vial with 5 ml of scintillation fluid.

Results are expressed as:

$$\textbf{nmol of oleate.mg}^{-1}\textbf{ prot.h}^{-1}\textbf{ = (cpm-blank cpm) x 600 x (2.200/800) / (total cpm x mg prot x h)}$$

Where **600** is the total nmol of oleate per flask, total cpm are the counts resulting from directly counting on the scintillation liquid the amount of 3 mM [1- ^{14}C] oleate used per flask, **2.000/800** is the dilution factor and **h i**s the time of incubation.

5X KRB (stored at 4°C)	
135 mM NaCl	19.72 g
3.6 mM KCl	0.670 g
0.5 mM NaH_2PO_4	0.17 g
0.5 mM $MgSO_4$	0.25 g
1.5 mM $CaCl_2$	0.55 g
bd H_2O	Up to 500 ml

⇒ $CaCl_2$ can be dissolved separately from the rest because it precipitates.

KRBH (100 ml) (stored at 4°C)	
5X KRB	20 ml
100 mM $NaHCO_3$	2 ml
1M HEPES pH 7.4	1 ml
bd H_2O	Up to 100 ml

- **Solution A:** 0.1 % BSA in KRBH
- **Solution B:** 1% BSA in KRBH

Reaction mix (2 ml for each flask)	
3 mM [1-^{14}C] oleate	200 μM
1M glucose	11 mM
8 mM carnitine	800 μM
KRBH	Up to total mix volume

⇒ Whatman Paper: cut the papers into pieces with 2cm^2 dimension/well and 100 μl of KOH with the pipette.

- **3 mM [1-^{14}C]oleate bound to BSA**

To prepare the labelled oleate bound to BSA, 500 μl of [1-^{14}C] oleic acid (*Perkin Elmer, ref. NEC317050UC, 50μCi)* is placed on a glass vial under the hood to evaporate the ethanol solution O/N. 4.567 mg of cold sodium oleate (*Sigma, ref. O7501-250MG*) are dissolved in 500 μl of 0.1 N NaOH in an 1,5 ml tube and heated in a heat block at 80-100°C. The solution is immediately added into the glass vial containing [1-^{14}C] oleic acid, stirred and heated at 80-100ºC until the solution is clear. On a beaker, 0.5 g of defatted BSA (*Sigma, ref. A-6003*) is dissolved in 4.5 ml of 0.9% NaCl by stirring and heating it in a water bath to 50°C maximum (better 30°C). Heating to more than 55ºC will turn the BSA solution into a gel. Oleate solution is added rapidly drop by drop onto the BSA solution. The resulting solution is filtered through a 0.45 μm filter and 1 ml aliquots are stored at -20°C.

Final concentration: 0.3mM [1-^{14}C] oleate, 1% BSA and 1μCi/ml.

6.3 TRYGLICERIDES (TG) CONTENT ANALYSIS

Cells are grown, differentiated and infected as described above. After 24 h (3T3-L1 CARΔ1 adipocytes) or 18 h (RAW 264.7 macrophages) of palmitate (PA) treatment, cells are collected for lipid extraction following *Gesta et al*. [222] with minor modifications: after cell lysis with 0.1% SDS, 1/2/0.12 (v/v/v) Methanol/Chloroform/0.5 M KCl solution is added, the two phases are separated by centrifugation and the upper phase is dried with nitrogen. Finally, lipids are resuspended in 200 μl of 100% isopropanol and 10 μl of TG suspension are quantified using TG Triglyceride kit (*Sigma, ref. TR0100*), according to the manufacturer's instructions. Protein concentrations are used to normalize sample values.

6.4 OIL RED O STAINING

Triglycerides content content is also analysed by Oil Red O staining. Oil Red O (*Sigma, ref. O-0625*) is a lysochrome (fat-soluble dye) used for staining of neutral triglycerides and lipids. For cultured cells, the staining protocol is as follow: cells are grown, differentiated and infected as described above. After 24 h (3T3-L1 CARΔ1 adipocytes) or 18 h (RAW 264.7 macrophages) of FFAs treatment medium is removed and cells washed with 1X PBS. PBS is removed and 1 ml of 10 % Formalin (*Sigma, ref. HT5014)* is added to each well (12-well plate) and incubated for 10 min at r.t. After this time, formalin is discarded and 1 ml of fresh formalin is added to each well and incubated for at least 1 hour at r.t. Cells can be kept in formalin for a couple of days before staining; in this case, it is necessary to wrap with parafilm and cover with aluminium foil to prevent cells from drying. Then, formalin is removed, cells are washed with 2 ml of bd H_2O twice. 1 ml of 60% isopropanol is added to each well and leaved for 5 min at r.t. Isopropanol is removed and cells are left to dry completely at r.t. Finally, 500 μl of Oil Red O Working solution is added to each well and incubated for 10 min at r.t. After this time, Oil Red O solution is removed and bd H_2O is immediately added to each well. To remove Oil Red O excess, cells are washed with bd H_2O times and then images are acquired under the microscope for analysis. H_2O is removed and wells are leaved to dry. Oil Red O is eluted in 100% Isopropanol by adding 500 μl of 100% isopropanol, incubating for 10 min with gently shaking. When the solution is red, it is transferred to a 1.5ml tube and O.D. is measured at 500 nm using 100% isopropanol as blank. Protein concentrations or live cells/well are used to normalize O.D. sample values.

- **Oil Red O Stock**: 0.35 g Oil Red O (*Sigma, ref. O0625*) are dissolved in 100 ml of

isopropanol. The solution is stirred O/N, filtered (0.22µm filter) and stored at 4°C.

- **Oil Red O Working Solution**: the day of the assay, 6 ml of Oil Red O stock solution is mixed with 4 ml of bd H_2O. The solution is leaved for 20 min at r.t., followed by filtering (0.2 µm filter).

6.5 NILE RED STAINING

TG content is also analysed by Nile Red staining. Nile Red (*Sigma, ref. 72485*) is an excellent vital stain for the detection of intracellular lipid droplets by fluorescence microscopy. To perform a Nile Red Staining for microscopy analysis, it´s necessary to seed cells on coverslips and to allow them to adhere for 24 h in complete medium. Then, cells are grown, differentiated and infected as described above. After 24 h (3T3-L1 CARΔ1 adipocytes) or 18 h (RAW 264.7 macrophages) of FFAs treatment medium is removed, cells washed with 1X PBS and fixed with 1% paraformaldehyde in PBS for 10 min at r.t. After this time, paraformaldehyde is carefully removed cells are washed 3 times with 1X PBS. 1mg/ml in acetone of Nile Red stock is prepared. The day of the experiment**,** Nile Red staining solution is prepared in 1X PBS with a final concentration of 1 µg/ml. The concentration used for cell staining is 100 ng/µl. 1 ml of staining solution is added to each well for 30 min. After this time, staining solution is removed and cells are washed with 1X PBS (X3), 5 min. For nuclear counterstaining, we used DAPI *(Lifetechnologies, ref. D3571).* 5 mg/ml in H_2O of DAPI stock is prepared and for cells staining, we used a final concentration of 300 nM. 1ml of the staining solution in PBS is added to each well for 5 min. After this time, cells are washed with PBS (X3), 5 min. Cells are kept in PBS to remove easier the coverslips. Coverslips with stained cells are then mounted with an antifade solution (Immumount) *(Thermoscientific, ref. 9990402)* and analyzed by fluorescence microscopy.

Before seeding the cells on coverslips, it's important to treat the plates and coverslips with poly-L-lysine *(Sigma, ref. P4707)*, the day before the staining; to ensure optimal conditions for cell attachment. Therefore, coverslips are sterilized by alcohol/UV treatment O/N. Then, one round coverslip is placed in each well (12-well plate) and add 1ml of poly-Lysine solution is added to coat the whole surface. Poly-L-Lysine is left O/N, r.t. (for short-term) or at +4°C (for long term). Before plating the cells, poly-L-lysine is removed from each well and washed with 1X PBS several times.

7. RNA ANALYSIS

7.1 TOTAL RNA EXTRACTION

Total RNA is extracted from cultured cells using Illustra MiniRNA Spin kit (*GE Healthcare, ref. 25-0500-71*) following the manufacturer's instruction with minor modifications: **a)** cultured cells are lysed directly adding 350 μl of RA1 buffer + 3.5 μl of β–mercaptoethanol to each well; **b)** pure RNA is eluted in 30 μl of RNase free H_2O. RNA concentration and quality ($O.D._{260}/O.D._{280}$) are determined by Nanodrop® (ND-100), using 1 μl of each sample. All samples showed a $O.D._{260}/O.D._{280}$ =1.8-2 that indicates a pure RNA.

7.2 RT-PCR (REVERSE TRANSCRIPTASE PCR)

cDNA is obtained using Transcriptor First Strand cDNA Synthesis kit (*Roche,ref. 04379012001*), from 1 μg of total RNA, as detailed in manufacturer's instructions.

7.3 qRT-PCR (Quantitative REAL TIME PCR)

Quantitative real-time PCR is performed using SYBR Green PCR Master Mix Reagent Kit (*Life Technologies, ref.4360706*) and LightCycler® 480 instrument (*Roche*) using 2.5 ng/μl of cDNA of each sample. Levels of mRNA are normalized to those of β-actin and expressed as fold change.

Primers sequence is detailed in the next table:

qRT-PCR PRIMERS SEQUENCE

	Forward	Reverse
β-actin	5'- AAGTCCCTCACCCTCCCAAAG- 3’	5'- AAGCAATGCTGTCACCTTCCC-3’
Atf-4	5'-CCTTCGACCAGTCGGGTTTG- 3’	5'-CTGTCCCGGAAAAGGCATCC- 3’
Chop	5´-CCCTGCCTTTCACCTTGG- 3’	5´-CCGCTCGTTCTCCTGCTC- 3’
*Cpt1a**	5'- GCAGCAGATGCAGCAGATCC- 3’	5'- TCAGGATCCTCCTCTCTGTATCCC-3’
Edem	5'-AAGCCCTCTGGAACTTGCG- 3’	5'-AACCCAATGGCCTGTCTGG- 3’
Grp78	5´-ACTTGGGGACCACCTATTCCT- 3’	5´-ATCGCCAATCAGACGCTCC- 3’
Il-β	5'- GCCCATCCTCTGTGACTCAT- 3’	5'- AGGCCACAGGTATTTTGTCG- 3’
Ifn-γ	5'- ATCTGGAGGAACTGGCAAAA- 3’	5'-TTCAAGACTTCAAAGAGTCTGAGGTA- 3’
Mcp-1	5'- TCCCAATGAGTAGGCTGGAG-3’	5'- AAGTGCTTGAGGTGGTTGTG- 3’
Pdi	5'-ACCTGCTGGTGGAGTTCTATG- 3’	5'-CGGCAGCTTTGGCATACT- 3’
Tlr-4	5'- GGACTCTGATCATGGCACTG- 3’	5'- CTGATCCATGCATTGGTAGGT- 3’
Tnf-α	5'-ACGGCATGGATCTCAAAAGAC-3’	5'-AGATAGCAAATCGGCTGAACG- 3’

*Recognizes both CPT1A and CPT1AM

8. ANALYSIS OF CPT1A EXPRESSION IN HUMAN ADIPOSE TISSUE

In collaboration with Dr. Joan Vendrell’s group of the University Hospital Joan XXIII (Tarragona, Spain), we analysed CPT1A expression in human adipose tissue.

8.1 SELECTION OF PATIENTS

Adipose tissue, serum and plasma samples are selected from an adipose tissue biobank collection of the University Hospital Joan XXII.

Subjects are recruited by the endocrinology and surgery departments at the University Hospital Joan XXIII (Tarragona, Spain). All subjects are of Caucasian origin and reported that their body weight had been stable for at least 3 months before the study. They had no systemic disease other than obesity or T2DM and all had been free of any infections in the previous month before the study. Liver and renal diseases are specifically excluded by

biochemical work-up.

Appropriate Institutional Review Board approval and adequate biobank informed consent is obtained from all participants. Bio-banking samples included total and fractionated adipose tissue from subcutaneous and visceral origin, serum, plasma and DNA.

Samples are selected according stratification by age, gender and body mass index (BMI) and grouped into two cohorts:

Obesity cohort. Subjects are classified by BMI according to the World Health Organization criteria (WHO, 2000). The study included 19 lean, 28 overweight, and 15 obese non-diabetic subjects, matched for age and gender.

Type 2 diabetes cohort. Patients are classified as having T2DM according to the American Diabetes Association criteria (1997). Variability in metabolic control is assessed by stable glycated hemoglobin A1c (HbA1c) values during the previous 6 months. Gathering these criteria, there are 11 T2D subjects. As a control group, we selected 36 subjects without diabetes from the obesity cohort, matched for age, BMI and gender. No patients are being treated with thiazolidinedione. Pharmacological treatment of the patients with T2D is as follows: insulin, 9.1%; oral hypoglycemic agents, 54.5%; statins, 63.6%; blood-pressure-lowering agents, 54.5%.

8.2 ANTHROPOMETRIC MEASUREMENTS

Height is measured to the nearest 0.5 cm and body weight to the nearest 0.1 kg. BMI is calculated as weight (kilograms) divided by height (meters) squared. Waist circumference is measured midway between the lowest rib margin and the iliac crest.

8.3 COLLECTIONS AND PROCESSING OF HUMAN SAMPLES

Samples from VAT (omental) and SAT (anterior abdominal wall) from the same individual are obtained during abdominal elective surgical procedures (cholecystectomy or surgery for abdominal hernia). All patients had fasted overnight, at least 12 hours before surgical procedure. Blood samples are collected before the surgical procedure from the antecubital vein, 20 ml of blood with EDTA (1 mg/ml) and 10 ml of blood in silicone tubes. 15 ml of collected blood is used for the separation of plasma. Plasma and serum samples are stored at -80°C until analytical measurements are performed. 5ml of blood with EDTA is used for

the determination of HbA1c. Adipose tissue samples are collected, washed in 1X PBS, immediately frozen in liquid N_2 and stored at -80°C.

8.4 ADIPOSE TISSUE FRACTIONATION

Adipose tissue biopsies are immediately processed. The adipose tissue is finely diced into small pieces (10-30 mg), washed in 1X PBS and incubated in Medium 199 *(Lifetechnologies)* supplemented with 4% BSA plus 2 mg/mL of collagenase Type I *(Sigma)* for 1 h in a shaking waterbath at 37°C. After digestion, mature adipocytes (ADI) are separated from tissue matrix by filtration through a 200mm mesh fabric *(Spectrum Laboratories*, *Rancho Domínguez, CA, USA).* The filtrated solution is centrifuged for 5 min at 1500*x g*. The mature adipocytes are removed from the top layer and the SVF cells remained at the pellet. Cells are washed 4 times in 1X PBS and processed for RNA and protein extraction.

8.5 ANALYTICAL METHODS

Glucose, cholesterol and triglyceride plasma levels are determined in an auto-analyzer *(Hitachi 737, Boehringer Mannheim, Marburg, Germany)* using the standard enzyme methods. High-density lipoprotein (HDL) cholesterol is quantified after precipitation with polyethylene glycol (PEG-6000) at r.t. Plasma insulin is determined by radioimmunoassay *(Coat-A-Count insulin; Diagnostic Products Corp., Los Angeles, CA)* in all subjects of study, except in insulin-treated T2D patients. Non-esterified Free Fat Acid (NEFA) serum levels are determined in an autoanalyzer *(Advia 1200, Siemens AG, Munich, Germany)* using an enzymatic method developed by Wako Chemicals (Neuss, Germany). Plasma glycerol levels are analyzed by using a free glycerol determination kit, a quantitative enzymatic determination assay *(Sigma-Aldrich Corp., St. Louis, MO*). Intra- and interassay CV are less than 6% and less than 9.1%, respectively. The degree of insulin resistance is determined by the homeostasis model assessment (HOMA), as [glucose (mmol/L) x insulin (mIU/L)]/22.5] [223].

8.6 WESTERN BLOT

Human fat tissue is homogenized in radioimmunoprecipitation assay (RIPA) buffer as described before [224]. Protein extracts (10 µg) are loaded, resolved on 10% SDS-PAGE and

transferred to Hybond ECL nitrocellulose membranes by conventional procedures. Membranes are stained with 0.15% Ponceau red *(Sigma-Aldrich, St Louis, MO, USA)* to ensure equal loading after transfer and then blocked with 5% (w/v) BSA in TBS buffer with 0.1% Tween 20. Immunoblotting is performed with 1:2000 goat anti-human CPT1A (*Abcam, ref. ab53532).* Blots are incubated with the appropriate IgG-HRP-conjugated secondary antibody. Immunoreactive bands are visualized with an enhanced-chemiluminescence (ECL-plus) reagent kit *(GE Healthcare).* Optical densities of the immunoreactive bands are measured using Image J analysis software.

8.7 IMMUNOHISTOCHEMISTRY

Five-micron sections of formalin-fixed paraffin-embedded adipose tissue are deparaffinised and rehydrated prior to antigen unmasking by boiling in 1 mM EDTA, pH 8. Sections are blocked in normal serum and incubated overnight with rabbit anti-CPT1A *(Sigma-Aldrich, ref. HPA008835)* at 1:50 dilution. Secondary antibody staining is performed using the VECTASTAIN ABC kit *(Vector Laboratories, Inc. Burlingame, CA*) and detected with diaminobenzidine (DAB, Vector Laboratories, Inc.). Sections are counterstained with hematoxylin prior to dehydration and coverslip placement, and examined under a Nikon Eclipse 90i microscope (Heidelberg, Germany). As a negative control, the procedure is performed in the absence of primary antibody.

8.8 IMMUNOFLUORESCENCE

Five-micron sections of formalin-fixed paraffin-embedded adipose tissue are blocked in normal serum and incubated overnight with rabbit anti-CPT1A antibody *(Sigma-Aldrich, ref. HPA008835)* at 1:50 dilution, and with mouse anti-CD68 *(Santa Cruz Biotechnology, Inc.,ref. sc-59104)* at 1:50 dilution, washed, and visualized using Alexa Fluor 546 goat anti-rabbit, and Alexa Fluor 488 goat anti-mouse antibodies, respectively (1:500; *Molecular Probes Inc, OR, USA*). The slides are counterstained with DAPI (4,6-diamidino-2-phenylindole) to reveal nuclei and are examined under a Nikon Eclipse 90i fluorescent microscope. As a negative control, the assay is performed in the absence of primary antibody.

8.9 RNA ANALYSIS

400–500mg frozen human adipose tissue was homogenized with an Ultra-Turrax 8 *(Ika, Staufen, Germany)*. Total RNA from adipose biopsies, stromal-vascular fractions (SVF) and isolated adipocytes were extracted by using RNeasy Lipid Tissue Midi *Kit (QIAGEN Science, Hilden, Germany)* following the manufacturer's instructions and total RNA was treated with 55 U RNase-free DNase *(QIAGEN)* to avoid contamination with genomic DNA. Between 0.2 and 1 µg of total RNA was reverse-transcribed to cDNA using TaqMan Reverse Transcription reagents *(Applied Biosystems, Foster City, CA, USA),* and subsequently diluted with nuclease-free water *(Sigma)* to 20 ng/µl cDNA. Real-time quantitative PCR was performed, with duplicates, on a 7900HT Fast Real-Time PCR System using commercial Taqman Assays *(Applied Biosystems)* and the following primers from Life Technologies: Hs00912671_m1 (CPT1A) and Hs99999904_m1 (PPIA-cyclophilin as reference gene). SDS software 2.3 and RQ Manager 1.2 (Applied Biosystems) were used to analyze the results with the comparative threshold cycle (Ct) method ($2^{\Delta\Delta Ct}$). C_t values for each sample were normalized with an optimal reference gene (cyclophilin), after testing three additional housekeeping genes: β-actin and RNA 18s.

9. STATISTICAL ANALYSIS

For *in vitro* experiments, data are expressed as the mean ± SEM. Statistical analysis is performed by Student's *t*-test (column analysis) or two-way ANOVA test (grouped analysis). All figures are generated using GraphPad Prism 6.0 (*GraphPad Software, San Diego, CA, USA)*. *P<* 0.05 is considered statistically significant.

For human data, statistical analyses are performed with SPSS 12.0 (SPSS, Chicago, IL). For uniformity, results are expressed as mean ± SD. The non-normally distributed variables are represented as the median (interquartile range). Categorical variables are reported by number (percentages). Student's t test analysis is used to compare the mean value of normally distributed continuous variables. Variables with a non-Gaussian distribution are analysed by using non-parametric test (Kruskal-Wallis or Mann-Whitney test when appropriated). Associations between continuous variables are sought by correlation analyses. Finally a stepwise multiple linear regression analysis is performed to determine independent variables associated with CPT1A gene expression levels in SAT and VAT depot.

Results are expressed as unstandardized coefficient (B), and 95% confidence interval for B (95%CI(B)). Statistical significance occurred if a computed two-tailed probability value (*P*) is < 0.05.

RESULTS

Obesity and T2DM are associated with adipocyte dysfunction, macrophage infiltration, inflammation and decreased fatty acid oxidation (FAO) levels. In this work, we propose that an increase in adipocytes and macrophages FAO rate could protect from obesity and insulin resistance by a decrease in the lipid content and inflammatory levels. So, taking into account that CPT1A is the key enzyme in fatty acid catabolism, we increased the β-oxidation in adipocytes and macrophages by the expression of the mutant but active form of CPT1A (CPT1AM), insensitive to its physiological inhibitor malonyl-CoA and analysed its beneficial effects on crucial pathways affected in metabolic disorders.

1. EFFECT OF CPT1AM EXPRESSION IN 3T3-L1 CARΔ1 ADIPOCYTES ON LIPID METABOLISM, INSULIN RESISTANCE, INFLAMMATION AND ROS DAMAGE DURING FATTY ACIDS OVERLOAD

1.1 Adenovirus infection of 3T3-L1 CARΔ1 adipocytes

As described in Materials and Methods (section 2.4), the increase in FAO was achieved by the use of adenoviruses carrying the gene of CPT1AM (AdCPT1AM) and GFP (AdGFP), used as control of the infection in all the experiments, to infect fully differentiated adipocytes. Adenovirus stocks were obtained as described in Materials and Methods, section 2.2. The title obtained for the viruses was $3.7x10^{11}$ pfu/ml for AdGFP and $6x10^{10}$ pfu/ml for AdCPT1AM.

1.2 Analysis of CPT1A mRNA, protein and activity level

To optimize the efficiency of adenovirus infection, at day 8 post-differentiation, 3T3-L1 CARΔ1 adipocytes were infected for 48 h (as described in Materials and Methods, section 2.4) with different amounts of AdGFP (10, 50, 70, 100 m.o.i.). After this time, GFP signal was analysed by fluorescence microscopy. In the **Fig.1A**, 3T3-L1 adipocytes infected with 100 m.o.i of AdGFP showed a 50% of infection. At the same time, we infected the cells with different amounts of AdCPT1AM (10, 50, 70, 100 m.o.i.) for 48 h. After this time, we collected the cells and analysed CPT1A protein level by WB in whole cell lysates. CPT1A protein levels were normalized to those of β–actin. As shown in **Fig.1B**, a gradual increase of

CPT1A protein level was observed in CPT1AM-expressing adipocytes compared to GFP control cells.

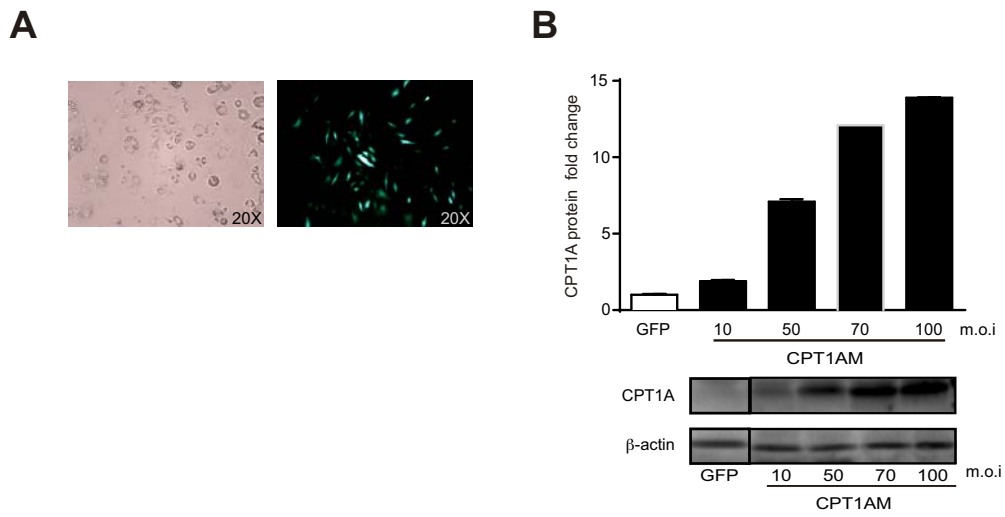

Fig.1 Analysis of CPT1A expression in 3T3-L1 CARΔ1 adipocytes infected with different amounts of AdGFP and AdCPT1AM.
A. 3T3-L1 CARΔ1 adipocytes were infected with different amounts of AdGFP (10, 50, 70, 100 m.o.i.) for 48 h to check the efficiency of infection. After this time, GFP signal was analysed by fluorescence microscopy. In the picture, 3T3-L1 adipocytes infected with 100 m.o.i of AdGFP showed a 50% of infection. **B.** 3T3-L1 CARΔ1 adipocytes were infected different amounts of AdCPT1AM (10, 50, 70, 100 m.o.i.) for 48 h. 20 μg of total protein were analyzed by WB. CPT1A protein levels were expressed as fold change. CPT1A protein levels were normalized to those of β–actin. Data are representative of three independent experiments and presented as mean±SEM, n=3, *P*<0.05.

Finally, we choose **100 m.o.i.** for both viruses as the final virus amount for the following experiments to obtain a significant increase of CPT1A protein level (9.4-fold change, P<0.05) respect to control, but at the same time to avoid prejudicial effects of an excessive virus amount on cell viability.

Then, we analysed CPT1A mRNA and activity level by qRT-PCR and radiometric assay, respectively, to confirm WB results. For qRT-PCR we used 2.5 μg/μl of cDNA and normalized the CPT1A levels to those of β-actin; whereas CPT1 activity was performed with 20 μg of mitochondrion-enriched cell fractions incubated with or without 100 μM of malonyl-CoA. As shown in **Fig.2A,** we observed a significant increase of CPT1A mRNA levels (14.5-fold change, P<0.05) in CPT1A-expressing adipocytes. For CPT1A detection 20 μg of total protein were

used and CPT1A protein levels were normalized to those of β-actin **(Fig.2B).** Importantly, we proved, for the first time, that CPT1AM-expressing adipocytes retained most of their CPT1 activity after incubation with the CPT1 inhibitor malonyl-CoA, compared to GFP-expressing controls **(Fig.2C).**

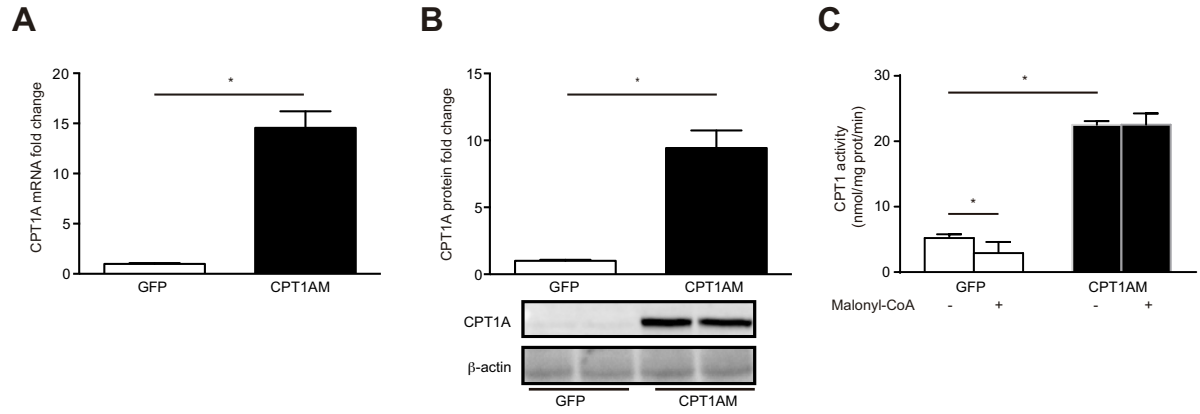

Fig.2 Analysis of CPT1A mRNA, protein and activity levels in CPT1AM-expressing 3T3-L1 CARΔ1 adipocytes.

A. Fully differentiated 3T3-L1 CARΔ1 adipocytes (day 8 post-differentiation) were Ad-infected (100 m.o.i.) and after 48 h, CPT1A mRNA levels were analyzed by qRT-PCR and normalized to those of β–actin CPT1A protein levels were analyzed by WB. **B.** CPT1A protein levels of CPT1AM-expressing 3T3-L1 CARΔ1 adipocytes were analyzed by WB. **C.** CPT1 activity of CPT1AM-expressing 3T3-L1 CARΔ1 adipocytes, incubated with or without 100 μM of malonyl-CoA, was analyzed by radiometric assay as detailed in Materials and Methods, section 6.2. Data shown are representative of three independent experiments and presented as mean±SEM, n=3-6, *P*<0.05.

1.3 Analysis of fatty acid oxidation (FAO) rate

To examine whether the increase in CPT1 protein and activity level seen before was correlated with an increase in FAO, we assessed a fatty acid oxidation assay in Ad-infected 3T3-L1 adipocytes, using a monounsaturated long chain fatty acid, oleate, as substrate. FAO rate was measured as total oleate oxidation *i.e.* sum of CO_2 (indicating the complete oxidation of fatty acid molecule) and ASP production (Acid-Soluble Products). Fatty acid oxidation to CO_2 and to ASP was measured as detailed in Materials and Methods, section 6.1-6.2. Interestingly, as shown in **Fig.3,** total oxidation was concordantly enhanced (1.7-fold increase, P<0.05) in CPT1AM-expressing adipocytes compared to GFP control cells.

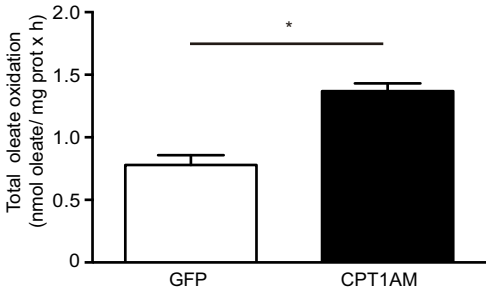

Fig.3 Analysis of total oleate oxidation in CPT1AM-expressing 3T3-L1 CARΔ1 adipocytes. Fully differentiated 3T3-L1 CARΔ1 adipocytes (day 8 post-differentiation), cultured and differentiated in 25 cm^2 flasks, were Ad-infected, as described in Materials and Methods section 3.4. After 48 h, cells were incubated with Reaction Mix containing 200 μM [1-^{14}C] oleate, 11 mM glucose and 8 μM of carnitine at 37°C for 3 h. Fatty acid oxidation to CO_2 and to ASP was measured as detailed in Materials and Methods, section 6.1-6.2. Data shown are representative of three independent experiments and presented as mean±SEM, n=3-5, *P*<0.05.

1.4 Analysis of triglycerides (TG) content

As explained above, we expected that an increase in lipid oxidation could decrease excess of lipid storage in adipocytes during obesity. Therefore, 24 h post-infection, we incubated adipocytes with 1 mM palmitate (PA) or BSA, prepared as described in Materials and Methods, section 1.1., for additional 24 h to simulate an obese state *in vitro*. After this time, we extracted intracellular lipids and cellular TG content was measured as described in Materials and Methods, section 6.3. Fatty Acids (FAs) incubation induced a significant increment (1.2 fold increase, P<0.05) of intracellular TG in GFP infected cells. Whereas, we observed that CPT1AM expression was able to restore PA-induced increase in TG content **(Fig.4)**. These results clearly indicate the relevance of CPT1A in the regulation of lipid metabolism in adipocytes.

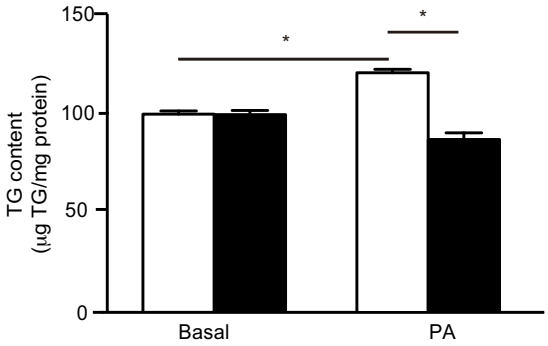

Fig.4 Analysis of TG content in CPT1AM-expressing 3T3-L1 CARΔ1 adipocytes.
Fully differentiated 3T3-L1 CARΔ1 adipocytes (day 8 post-differentiation) were Ad- infected and after 24 h, incubated with 1 mM PA or BSA for additional 24 h. After this time intracellular TG content was measured as described in Materials and Methods, section 6.3. Data shown are representative of three independent experiments and presented as mean±SEM, n=3-5, *P*<0.05.

1.5 Analysis of insulin sensitivity

Free Fatty Acids (FFAs) have a well-established role as a principal mediator of adipocytes dysfunction in obesity including insulin resistance and activation of inflammatory response [8]. In line with our finding that CPT1AM promoted a decrease of intracellular TG, it is highly possible that expression of CPT1AM in adipocytes may improve FFAs-induced insulin resistance. Therefore, we investigated the effect of increased FAO on insulin sensitivity in 3T3-L1 CARΔ1 adipocytes infected with AdCPT1AM.

We evaluated basal and insulin-stimulated Akt phosphorylation of adipocytes incubated with or without 0.3 mM PA for 24 h. pAkt/Akt levels were analysed by WB in whole cell lysates. Under normal conditions, there were no significant differences of pAKt levels in both basal (BSA) and PA treated cells. After 15 min of 100 nM insulin stimulation, Akt signalling was activated but FA incubation significantly decreased Akt activation in GFP control cells. However, we observed that expression of CPT1AM rendered cells resistant to the impairment of Akt phosphorylation caused by FA treatment (**Fig.5A and B)**. These data demonstrated that enhancing CPT1 activity and FAO in adipocytes is able to ameliorate FFA-induced insulin resistance.

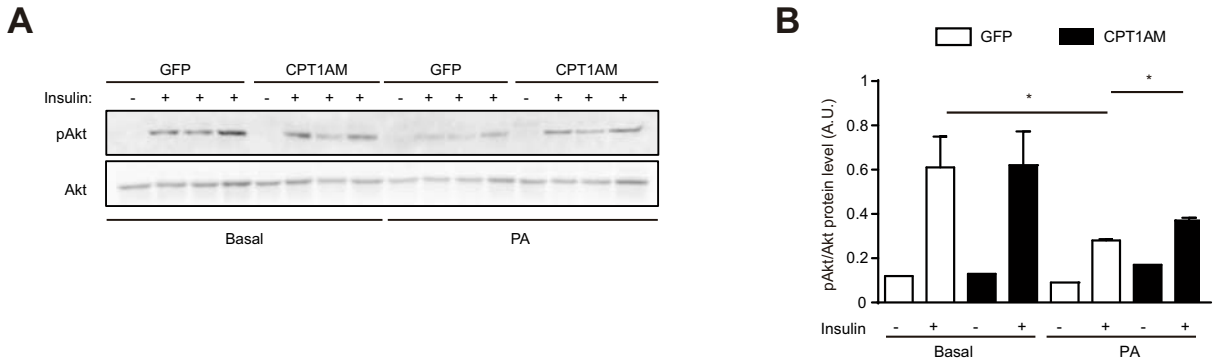

Fig.5 Analysis of insulin sensitivity in CPT1AM-expressing 3T3-L1 CARΔ1 adipocytes.
A. Fully differentiated 3T3-L1 CARΔ1 adipocytes (day 8 post-differentiation) were Ad-infected and after. 24 h, cells were incubated with 0.3 mM PA or BSA for additional 24 h. After this time, 100 nM insulin were added to stimulate Akt phosphorylation (Ser 473). $pAkt^{Ser\ 473}$ and total Akt levels were analysed by WB. **B.** pAkt/Akt WB quantitation. pAkt/AKt level was expressed as A.U. Data are representative of three independent experiments and presented as mean±SEM, n=3-5, $P<0.05$.

1.6 Analysis of inflammatory cytokines levels

We next examined whether manipulation of CPT1A expression in adipocytes could decrease the inflammatory cytokines levels. To address this question, we incubated Ad-infected 3T3-L1 CARΔ1 with 1 mM PA or BSA for 24 h. After this time, mRNA of several proinflammatory cytokines levels was analysed by qRT-PCR. 1mM PA incubation during 24 h induced a significant increase of mRNA level of MCP-1 and IL-1β in GFP control cells, but this up-regulation was nicely blunted in CPT1AM-expressing adipocytes **(Fig.6).**

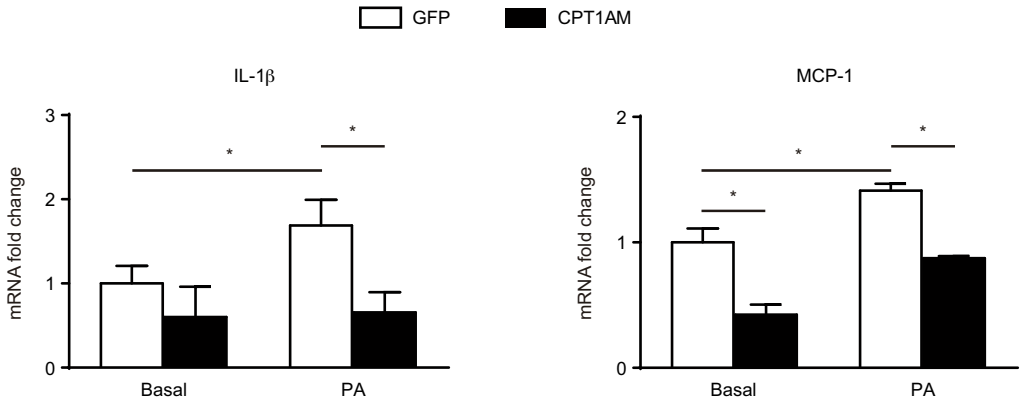

Fig.6 Analysis of inflammatory cytokines levels in CPT1AM-expressing 3T3-L1 CARΔ1 adipocytes.

Fully differentiated 3T3-L1 CARΔ1 adipocytes (day 8 post-differentiation) were Ad-infected and after 24 h, incubated with 1 mM PA or BSA for additional 24 h. After this time, mRNA level of proinflammatory cytokines was analyzed by qRT-PCR. Levels of mRNA are normalized to those of β-actin and expressed as fold change. Data are representative of three independent experiments and presented as mean±SEM, n=3-6, $P<0.05$.

1.7 Analysis of endoplasmic reticulum (ER) stress

Given that CPT1AM expression decreased PA-induced inflammation in 3T3-L1 CARΔ1 adipocytes, we next examined the role of increased FAO in controlling and alleviating FFA-induced ER stress. Therefore, we infected adipocytes as described in Materials and Methods, section 2.4, and after 24 h, we incubated the cells with 1 mM PA or BSA for additional 24 h. After this time, cells were collected and mRNA level of several ER stress markers was analysed by qRT-PCR. Following FA treatment, only CHOP and GRP78 expression was significantly elevated in GFP control cells, whereas we didn't observe any change in other markers (PDI, EDEM). PA-induced increase in ER stress was not restored in in CPT1AM-expressing adipocytes **(Fig.7)**. These data suggest that an enhanced mitochondrial FAO does not affect FA-induced ER stress in adipocytes.

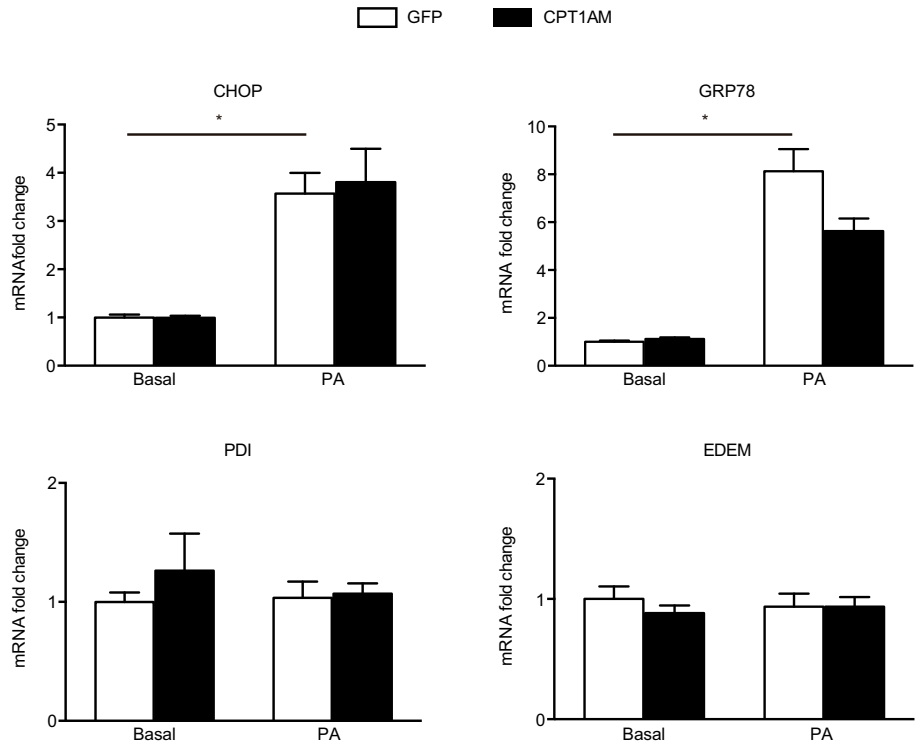

Fig.7 Analysis of ER stress markers levels in CPT1AM-expressing 3T3-L1 CARΔ1 adipocytes.

Fully differentiated 3T3-L1 CARΔ1 adipocytes (day 8 post-differentiation) were Ad-infected and after 24 h, incubated with 1 mM PA or BSA for additional 24 h. After this time, mRNA level of ER stress markers was analysed by qRT-PCR. Levels of mRNA are normalized to those of β-actin and expressed as fold change. Data are representative of three independent experiments and presented as mean±SEM, n=3-6, *P*<0.05.

1.8 Analysis of ROS damage

In obesity, the excess of FFAs increases ROS generation contributing to the development of insulin resistance. It is also well-known that FAO contributes to ROS production [225]. To evaluate the potential benefit of an enhanced and efficient FAO on FA-treated adipocytes, protein carbonyl content was analysed by Oxyblot in total protein extracts. In our conditions, we didn't observe any difference in protein carbonyl content after PA incubation so we could not prove the beneficial effect of CPT1AM expression on ROS damage **(Fig.8).**

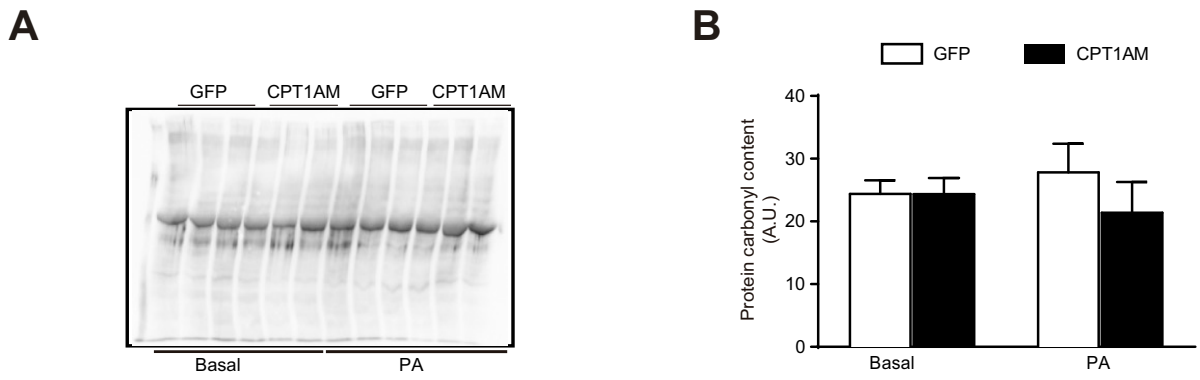

Fig.8 Analysis of protein carbonyl content in CPT1AM-expressing 3T3-L1 CARΔ1 adipocytes.
A. Fully differentiated 3T3-L1 CARΔ1 adipocytes (day 8 post-differentiation) were Ad-infected and after 24 h, incubated with 1 mM PA or BSA for additional 24 h. After this time, cells were collected and protein carbonyl content was analyzed in total protein extracts by Oxyblot, as described in Materials and Methods, section 4. **B.** Oxyblot quantiation. Protein carbonyl content was expressed as A.U. (Arbitrary Units). Data are representative of three independent experiments and presented as mean±SEM, n=3, *P*<0.05.

2. EFFECT OF CPT1AM EXPRESSION IN RAW 264.7 MACROPHAGES ON LIPID METABOLISM, INFLAMMATION AND ROS DAMAGE DURING FATTY ACIDS OVERLOAD

The pathophysiology of obesity-induced insulin resistance has also been correlated with an increased infiltration of immune cells, such as macrophages, in the hypertrophied adipocytes

that are activated and secrete a variety of proinflammatory cytokines that contributes to chronic low-grade inflammatory milieu of adipose tissue [226].

2.1 Adenovirus infection of RAW 264.7 macrophages

As described above for 3T3-L1 CARΔ1 adipocytes, the increase in FAO in RAW 264.7 macrophages was achieved by the use of adenoviruses carrying CPT1AM gene (AdCPT1AM) or GFP (AdGFP), used as control of the infection in all the experiments. Adenovirus stocks were obtained as described in Materials and Methods, section 2.2. The title obtained for the viruses was $3.7x10^{11}$ pfu/ml for AdGFP and $6x10^{10}$ pfu/ml for AdCPT1AM.

2.2 Effect of adenovirus infection on RAW 264.7 macrophages

Adenovirus can trigger an inflammatory response in macrophages. Therefore, we infected RAW 264.7 macrophages for 72 h with AdGFP (as described in Materials and Methods, section 2.4), using no infected cells as control. After infection, mRNA level of some proinflammatory cytokines was analysed by qRT-PCR and we observed a significant increase only for TNF-α (2.4-fold increase, P<0.05) in AdGFP-infected cells compared to controls **(Fig.9)**. From now on, we infected the cells with the same amount of AdGFP and AdCPT1AM, accounting the same basal level of inflammation in both cells.

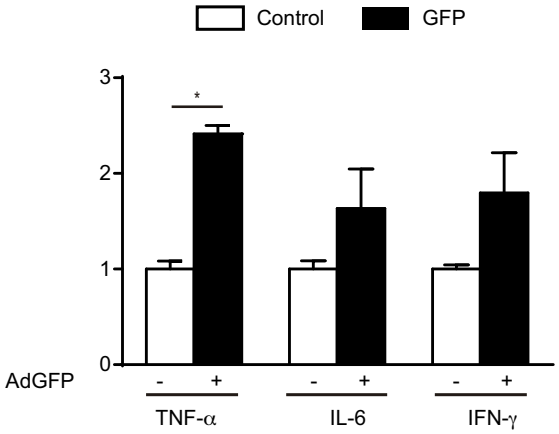

Fig.9 Analysis of adenovirus infection of RAW 264.7 macrophages
RAW 264.7 macrophages were infected with AdGFP for 72 h. After this time, mRNA level of proinflammatory cytokines levels was analysed by qRT-PCR. Levels of mRNA are normalized to those of β-actin and expressed as fold change. Data are representative of three independent experiments and presented as mean±SEM, n=3, *P*<0.05.

2.3 Analysis of CPT1A mRNA, protein level and CPT1A activity

To optimize the efficiency of adenovirus infection, RAW 264.7 macrophages were infected for 72 h (as described in Materials and Methods, section 2.4) with different amounts of AdGFP (25, 50, 75, 100 and 150 m.o.i.). After this time, GFP signal was analysed by fluorescence microscopy. In the **Fig.10A**, 3T3-L1 adipocytes infected with 100 m.o.i of AdGFP showed a 70% of infection. At the same time, we infected the cells with different amounts of AdCPT1AM (25, 50, 75, 100 and 150 m.o.i.) for 72 h. After this time, we collected the cells and analysed CPT1A protein level by WB in whole cell lysates. CPT1A protein levels were normalized to those of β–actin. As shown in **Fig.10B**, a gradual increase of CPT1A protein level was observed in CPT1AM-expressing adipocytes compared to GFP control cells.

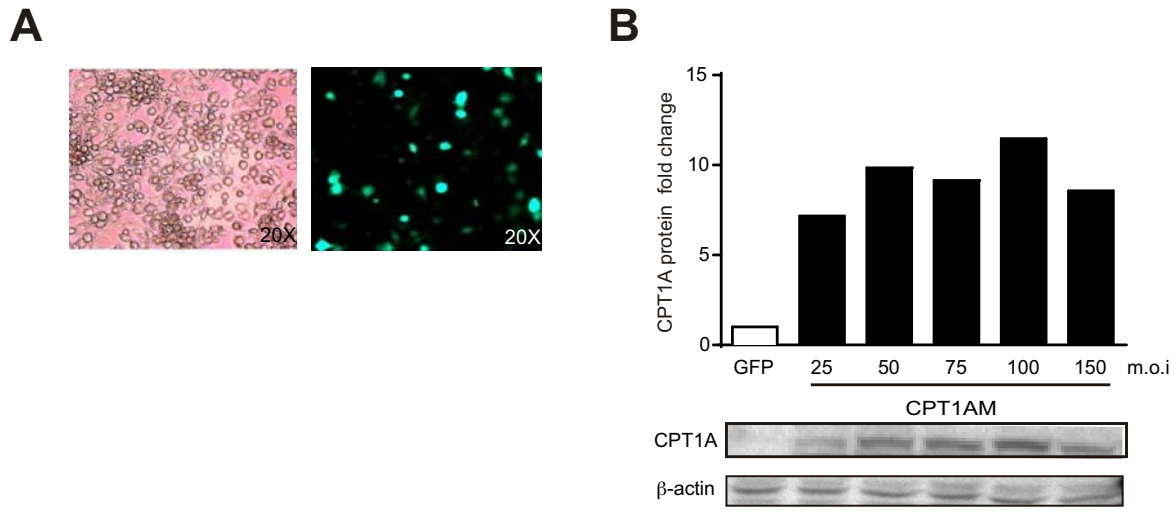

Fig.10 Analysis of CPT1A expression in RAW 264.7 macrophages infected with different amounts of AdGFP and AdCPT1AM.
A. RAW 264.7 macrophages were infected with different amounts (25, 50, 75, 100 and 150 m.o.i) of AdGFP for 72 h. After this time, to check the efficiency of infection, GFP signal was analysed by fluorescence microscopy. In the picture, RAW 264.7 macrophages infected with 100 m.o.i showed 70 % of infection. CPT1A protein levels were expressed as fold change. **B.** RAW 264.7 macrophages were infected with different amounts of AdCPT1AM (25, 50, 75, 100 and 150 m.o.i) for 72 h. 20 μg of total protein were analyzed by WB. CPT1A protein levels were expressed as fold change. CPT1A protein levels were normalized to those of β–actin. Data are representative of three independent experiments and presented as mean±SEM, n=3, $P<0.05$.

We choose **100 m.o.i.** of both viruses as final virus amount for the following experiments to obtain a significant increase of CPT1A protein levels (6.6- fold change, $P<0.05$) respect to

control **(Fig.11B)**, but at the same time to avoid prejudicial effects of an excessive virus amount on cell viability. Then, we analysed CPT1A mRNA and activity level by qRT-PCR and radiometric assay, respectively, to confirm the results of WB. As shown in **Fig.11A,** we observed a significant increase of CPT1A mRNA (2.4-fold change, P<0.05) in CPT1A-expressing macrophages compared to GFP control cells. In addition, we proved, for the first time, that malonyl-CoA was unable to inhibit CPT1A activity in CPT1AM-expressing macrophages as it does in GFP control cells **(Fig.11C).**

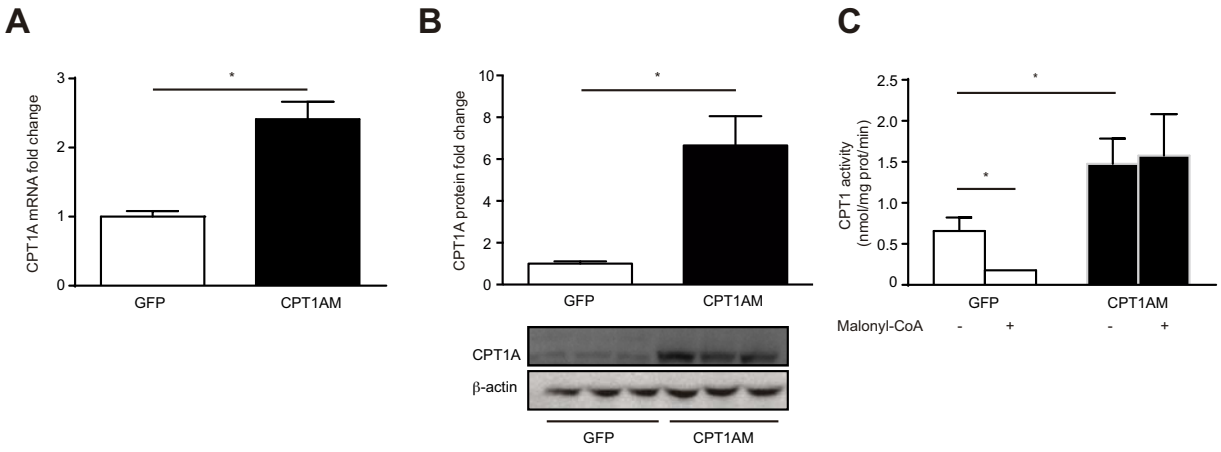

Fig.11 Analysis of CPT1A mRNA, protein and activity levels in CPT1AM-expressing RAW 264.7 macrophages.
A. RAW 264.7 macrophages were Ad-infected (100 m.o.i.) and after 72 h, CPT1A mRNA levels were analyzed by qRT-PCR and normalized to those of β–actin. **B.** CPT1A protein of CPT1AM-expressing RAW 264.7 macrophages were analyzed by WB. **C.** CPT1 activity of CPT1AM-expressing RAW 264.7 macrophages, incubated with or without 100 μM of malonylCoA, was analyzed by radiometric assay as detailed in Materials and Methods, section 6.2. Data shown are representative of three independent experiments and presented as mean±SEM, n=3-6, *P*<0.05.

2.4 Analysis of fatty acid oxidation (FAO) rate

To examine whether the increase in CPT1 protein and activity level seen before was correlated with an increase in FAO, we assessed a fatty acid oxidation assay in Ad-infected RAW 264.7 macrophages, using a monounsaturated long chain fatty acid, oleate, as substrate. FAO rate was measured as total oleate oxidation *i.e.* sum of CO_2 (indicating the complete oxidation of fatty acid molecule) and ASP production (Acid-Soluble Products). Fatty acid oxidation to CO_2 and to ASP was measured as detailed in Materials and Methods,

section 6.1-6.2. CPT1AM-expressing macrophages showed a 1.5-fold increase in FAO rate compared to GFP control cells **(Fig.12).**

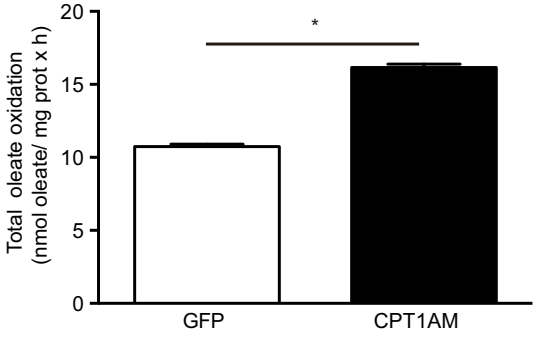

Fig.12 Analysis of total oleate oxidation in CPT1AM-expressing RAW 264.7 macrophages. RAW 264.7 macrophages, cultured in 25 cm^2 flasks, were Ad-infected and after 72 h incubated with Reaction Mix containing 200 μM [1-^{14}C] oleate, 11 mM glucose and 8 μM of carnitine at 37°C for 2 h. Fatty acid oxidation to CO_2 and to ASP was measured as detailed in Materials and Methods, section 6.1-6.2. Data shown are representative of three independent experiments and presented as mean±SEM, n=3-5, P<0.05.

2.5 Analysis of triglycerides (TG) content

To investigate the role of β-oxidation in macrophages and its effect on TG content, RAW 264.7 macrophages were infected, as described before, and incubated with 0.75 mM palmitate (PA) or BSA, prepared as described in Materials and Methods, section 1.1., for 18 h. After this time, cellular TG content was measured as described in Materials and Methods, section 6.3. Fatty Acids (FAs) incubation led to a significant increment (6.2-fold increase, P<0.05) of intracellular TG in GFP-infected cells. Interestingly, CPT1AM expression was able to completely restore PA-induced increase in TG content **(Fig.13)**.

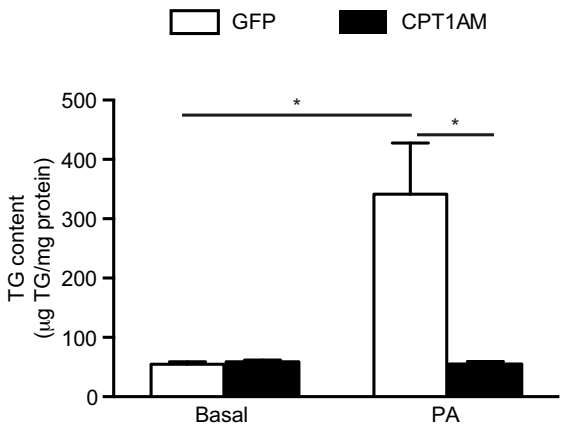

Fig.13 Analysis of TG content in CPT1AM-expressing RAW 264.7 macrophages.
RAW 264.7 macrophages were Ad- infected and after 48 h, incubated with 0.75 mM PA or BSA for additional 18 h. After this time, intracellular TG content was measured as described in Materials and Methods, section 6.3. Data shown are representative of three independent experiments and presented ad mean±SEM, n=3-5, P<0.05.

2.6 Analysis of inflammatory cytokines levels

We addressed the question whether increasing FAO could reduce inflammation in FA-treated macrophages. Therefore, we infected RAW 264.7 macrophages as described before and after 48 h we incubated the cells with 0.3 mM PA for additional 24 h or with 0.5 mM PA for additional 8 h. After this time, mRNA level of several proinflammatory citokynes was analysed by qRT-PCR. Following FA treatment, IL-1β and MCP-1 expression was significantly elevated in GFP control cells. Unlike adipocytes, we observed also a significant increase of TLR-4 and TNF-α levels, after FA incubation in GFP control cells. PA-induced inflammatory response was significantly blunted in CPT1AM-expressing macrophages **(Fig.14).**

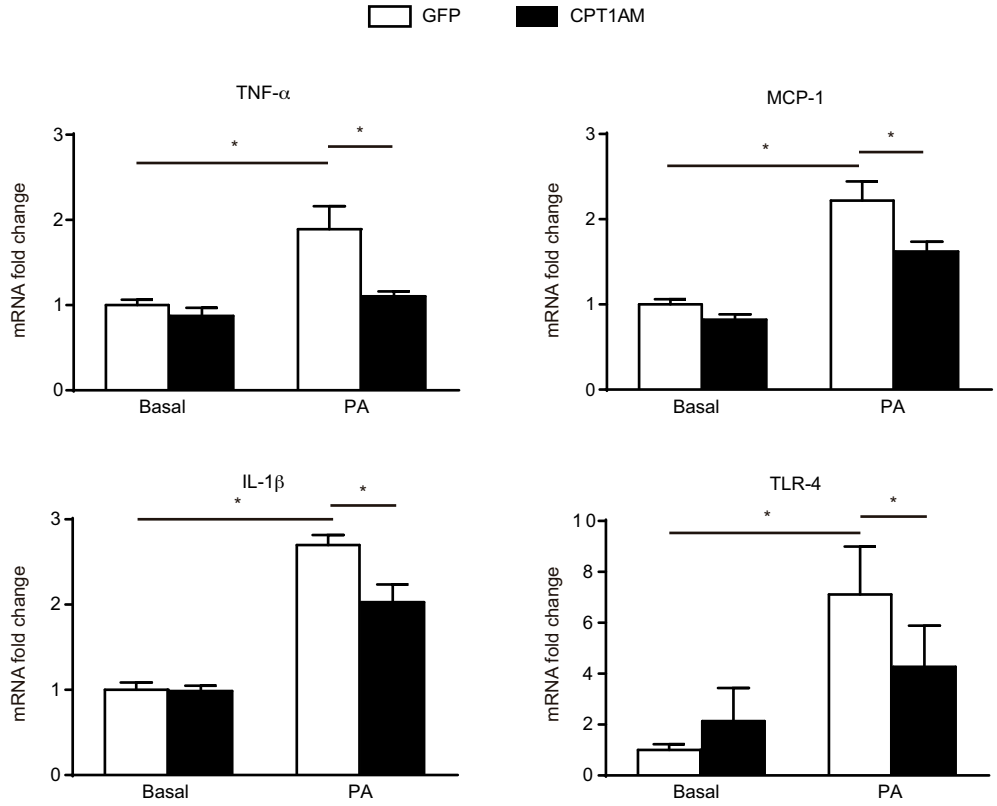

Fig.14 Analysis of inflammatory cytokines levels in CPT1AM-expressing RAW 264.7 macrophages.
RAW 264.7 macrophages were Ad-infected and after 48 h, incubated with 0.3 mM PA for additional 24 h (TLR-4 and IL-1β) or 0.5 mM for 8 h (TNF-α and MCP-1). After this time, mRNA level of proinflammatory cytokines levels was analysed by qRT-PCR. Levels of mRNA are normalized to those of β-actin and expressed as fold change. Data shown are representative of three independent experiments and presented ad mean±SEM, n=3-6, $P<0.05$.

These data suggest a beneficial impact of mitochondrial FAO in the context of FA-induced inflammation in macrophages.

2.7 Analysis of Endoplasmic Reticulum (ER) stress

Given that CPT1AM expression decreased PA-induced inflammation in RAW 264.7 macrophages, we also questioned the role of increased FAO in controlling and alleviating FFA-induced ER stress. Therefore, we infected macrophages as described in Materials and Methods, section 2.4, and after 48 h, we incubated the cells with 0.3 mM PA or BSA for additional 24 h. After this time, mRNA level of several ER stress markers was analysed by qRT-PCR. Levels of mRNA are normalized to those of β-actin and expressed as fold change. Following FA treatment, CHOP, GRP78, PDI and EDEM expression were significantly elevated in GFP control cells. PA-induced increase in ER stress was blunted in CPT1AM-expressing macrophages **(Fig.15)**.

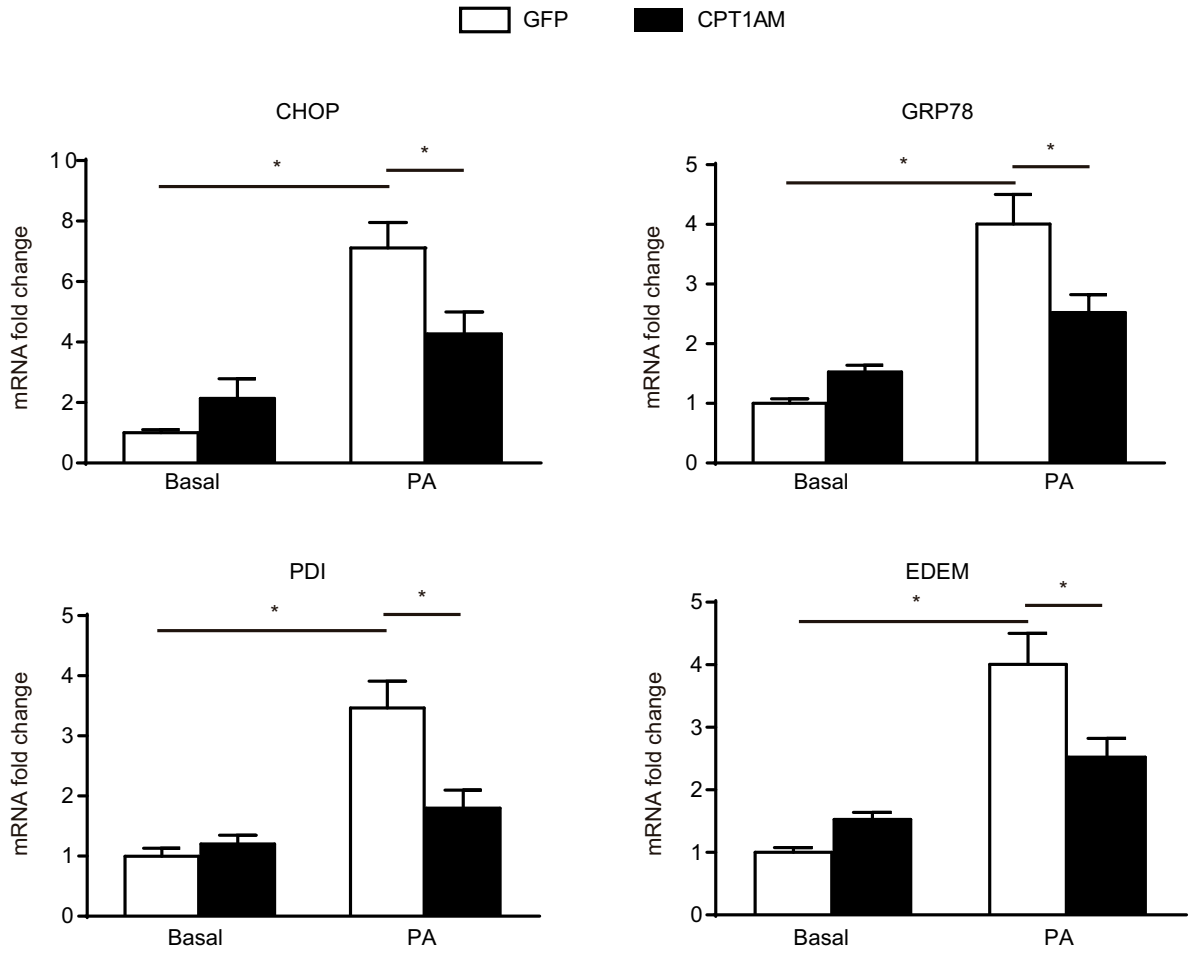

Fig.15 Analysis of ER stress markers levels in CPT1AM-expressing RAW 264.7 macrophages. RAW 264.7 macrophages were Ad-infected and after 48 h, cells were incubated with 0.3 mM PA or BSA for additional 24 h. After this time, mRNA level of several ER stress markers levels was analysed by qRT-PCR. Levels of mRNA are normalized to those of β-actin and expressed as fold change. Data shown are representative of three independent experiments and presented ad mean±SEM, n=3-6, $P<0.05$

These data suggest a beneficial impact of mitochondrial FAO in the context of FA-induced ER stress.

2.8 Analysis of ROS damage

To evaluate the potential benefit of an enhanced and efficient FAO on FA-induced ROS damage, RAW 264.7 macrophages were infected as described before and incubated with 0.75 mM PA or BSA for 18 h. After this time, we collected the cells and analysed protein carbonyl content by Oxyblot in total protein extracts. PA incubation caused a strong ROS

damage in GFP control cells, but CPT1AM expression allowed a significant attenuation of FA effect **(Fig.16A and B).**

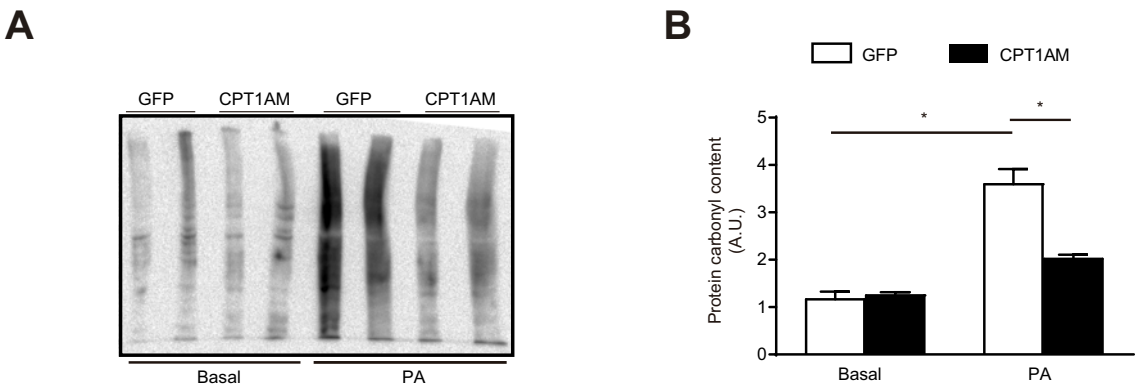

Fig.16 Analysis of protein carbonyl content in CPT1AM-expressing RAW 264.7 macrophages.
A. RAW 264.7 macrophages were Ad-infected and after. 48 h, incubated with 0.75 mM PA or BSA for additional 18 h. After this time, protein carbonyl content was analyzed in total protein extracts by Oxyblot, as described in Materials and Methods, section 4. **B.** Oxyblot quantitation. Protein carbonyl content was expressed as A.U. Data shown are representative of three independent experiments and presented ad mean±SEM, n=3-6,*P*<0.05.

3. CPT1A EXPRESSION IN HUMAN ADIPOSE TISSUE

In collaboration with Dr. Joan Vendrell's group at the University Hospital Joan XXIII (Tarragona, Spain), we analysed CPT1A expression in human adipose tissue.

3.1 Analysis of CPT1A expression during differentiation of human adipocytes

To evaluate the expression of CPT1A during differentiation of adipocytes, we performed performed qRT-PCR analysis of human SGBS preadipocytes from day 0 to day 14 of differentiation. Interestingly, we observed that CPT1A decreased along differentiation **(Fig. 17).**

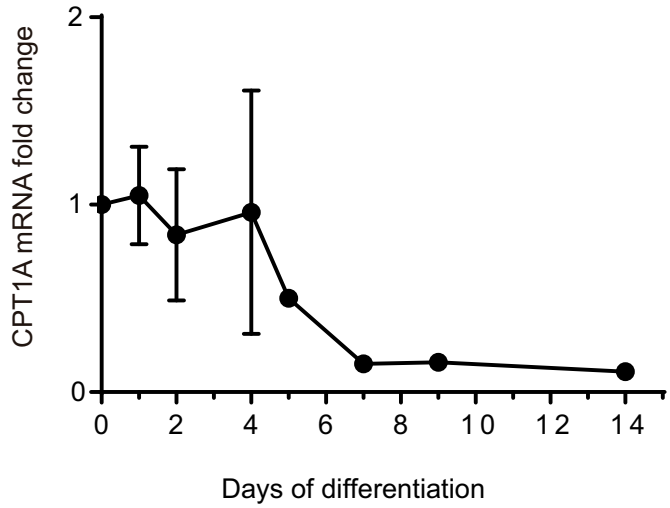

Fig. 17 Analysis of CPT1A expression during differentiation of human adipocytes.
CPT1A mRNA levels of SGBS human adipocytes during differentiation. Levels of CPT1A mRNA are normalized to those of cyclophilin and expressed as fold change. *P*< 0.05.

3.2 Analysis of CPT1A expression in human adipose tissue macrophages

To determine the cellular distribution of CPT1A protein in human adipose tissue biopsies, we performed qRT-PCR and immunostaining analysis on both adipose (AD) and stromal vascular fraction (SVF) as described in Materials and Methods, section 8. CPT1A was mostly detected in the SVF cells of both human subcutaneous adipose tissue (SAT) and visceral adipose tissue (VAT) **(Fig.18A)**. Immunohistochemical staining detected CPT1A (brown) in human overweight SAT **(Fig.18B).** Immunofluorescence detection on human overweight SAT showed a bright staining pattern in cells resembling adipose tissue macrophages. In fact, co-staining analysis using CPT1A and CD68 (a macrophage marker) antibodies confirmed co-localization of CPT1A (red) and CD68 (green) proteins in most of the cells **(Fig.18C).** Macrophages seem to localize forming the so-called “crown-like structures” surrounding the adipocytes.

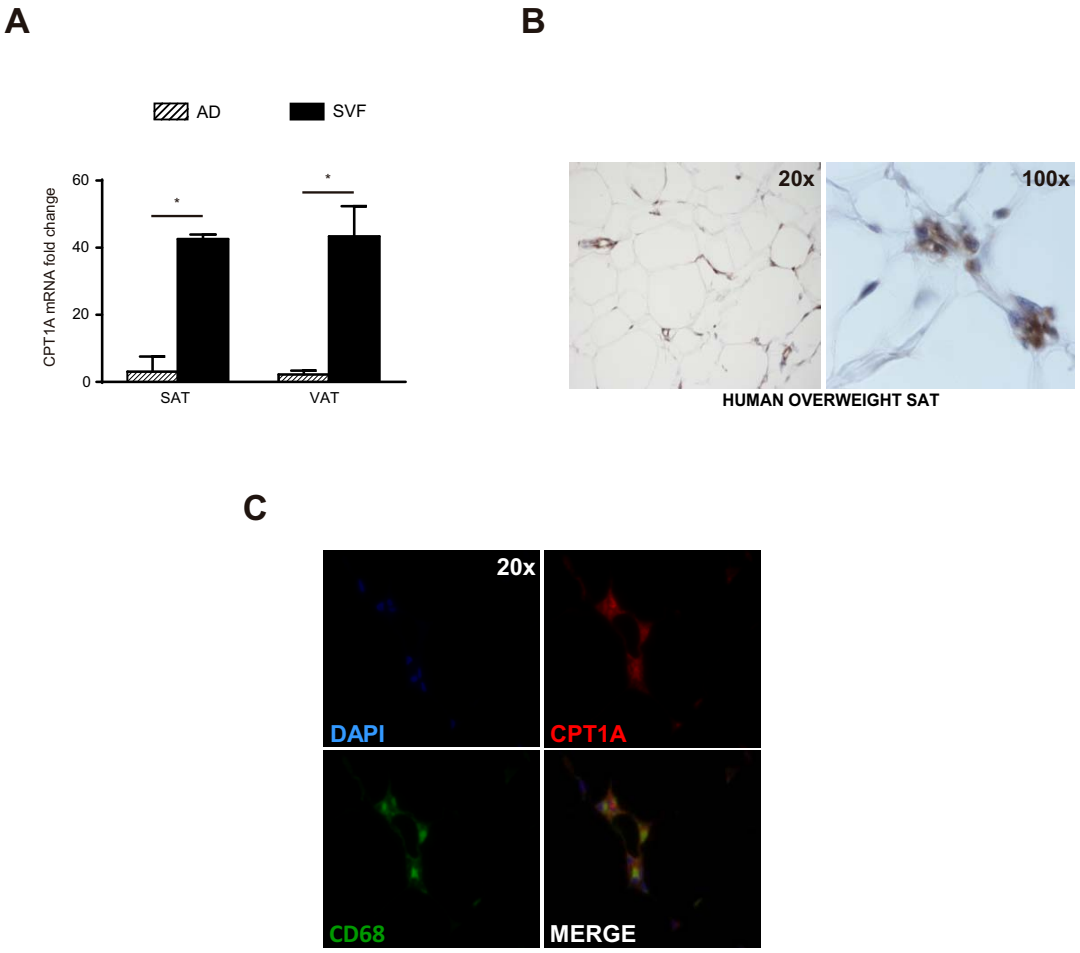

Fig.18 Analysis of CPT1A expression in human adipose tissue macrophages.
A. CPT1A mRNA levels in both adipose (AD) and stromal vascular fraction (SVF) of human subcutaneous adipose tissue (SAT) and visceral adipose tissue (VAT). Levels of CPT1A mRNA are normalized to those of cyclophilin and expressed as fold change. n=4. **B.** Immunohistochemical detection of CPT1A (brown) in human overweight SAT. **C.** Immunofluorescence co-localization of CPT1A (red) and CD68 (green) proteins in human overweight SAT. The counterstaining of nuclei (DAPI) is shown in blue. Images are representative of adipose tissue preparations collected from three subjects. $P< 0.05$.

3.3 Analysis of CPT1A expression in human adipose tissue from obesity cohort

Visceral (VAT) and subcutaneous (SAT) adipose tissue was analyzed from an obesity cohort including lean, overweight and non-diabetic obese patients as described in Materials and Methods, section 8.1. **Fig.19** shows the main phenotypic and metabolic characteristics of the studied subjects at the obesity cohort. Overweight and obese subjects had significant higher fasting glucose levels and subjects with obesity had increased HOMA index, plasma insulin, soluble IL-6 (sIL-6) levels and diastolic and systolic blood pressure.

Clinical, analytical and CPT1A gene expression analysis of the obesity cohort.

	Lean **BMI<25** (13 male; 6 female)	**Overweight** **25=<BMI<30** (16 male; 12 female)	**Obese** **BMI>=30** (9 male; 6 female)
Age (years)	51.7 ± 16.0	57.1 ± 15.0	57.4 ± 12.8
BMI (kg/m^2)	23.6 (22.1-24.2)	27.2 (26.5-27.9)*	32.1 (30.8-33.6)*$^{\#}$
Waist (cm)	83.0 (79.0-90.0)	97.0 (90.5-100.0)*	107.0 (100.0-117.2)*$^{\#}$
Cholesterol (mM)	5.2 ± 1.2	4.9 ± 1.0	5.2 ± 0.8
HDL-chol (mM)	1.5 ± 0.5	1.3 ± 0.3	1.4 ± 0.3
Triglycerides (mM)	1.0 (0.7-1.6)	1.1 (0.8-1.5)	1.0 (0.7-1.3)
Glucose (mM)	4.8 ± 0.7	5.5 ± 0.5*	5.6 ± 0.5*
Insulin (μIU/ml)	3.4 (2.1-6.7)	4.0 (2.8-7.2)	6.6 (4.5-16.5)¶
HOMA-IR	0.75 (0.54-1.83)	1.01 (0.52-2.09)	1.60 (1.19-4.79) ¶
sIL-6 (pg/ml)	1.4 (1.1-2.5)	1.0 (0.7-2.2)	2.5 (1.4-5.2) §
SBP (mmHg)	120 (120-127)	130 (121-140)	145 (130-160)*§
DBP (mmHg)	70 (60-80)	70 (70-80)	80 (78-90)¶

Fig.19 Phenotypic and metabolic characteristics of obesity cohort.
Values are expressed as mean±SD or median (interquartile range) for a non-Gaussian distributed variables. Differences *vs* Lean: * *P*< 0.001; ¶ *P*< 0.05. Differences *vs* Overweight: $^{\#}$ *P*< 0.001; §*P*< 0.05.
BMI: Body Mass Index; sIL-6: soluble Interleukine-6; SBP: systolic blood pressure; DBP: diastolic blood pressure.

Interestingly, when comparing SAT and VAT in obesity cohort, there was a significantly higher CPT1A mRNA levels in VAT compared to SAT in lean and overweight patients, but this difference was lost in obese patients **(Fig.20).**

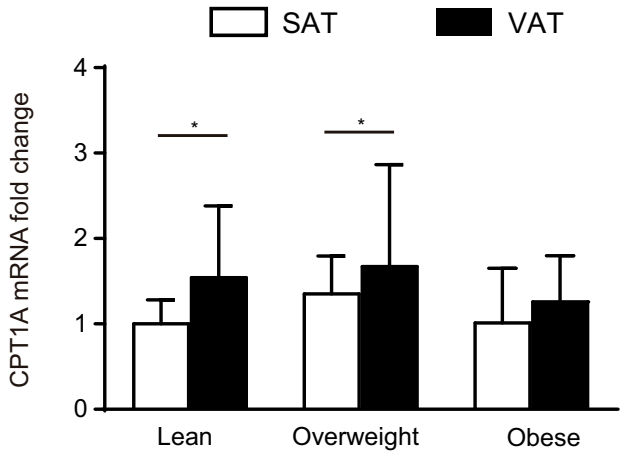

Fig.20 CPT1A mRNA levels in human visceral (VAT) and subcutaneous adipose tissue (SAT) of obesity cohort

CPT1A mRNA levels in human visceral (VAT) and subcutaneous adipose tissue (SAT) quantified by qRT-PCR. Levels of CPT1A mRNA are normalized to those of cyclophilin and expressed as fold change n=14. *P*< 0.05.

The results from qRT-PCR were corroborated by WB with human adipose tissue of overweight individuals showing the higher CPT1A expression levels in VAT *vs* SAT **(Fig.21A and B).**

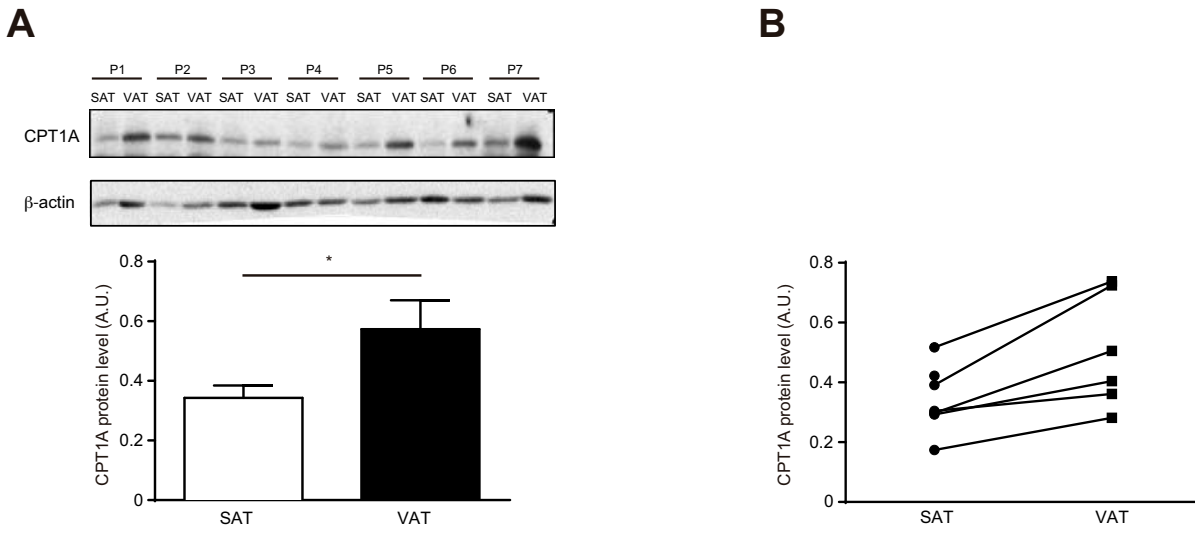

Fig.21 CPT1A protein expression levels in human VAT and SAT.

A. Representative WB analysis of CPT1A protein of VAT and SAT of overweight individuals. **B.** Paired relative intensity values from band densitometry in visceral and subcutaneous fat samples from the same individual are represented. *P*< 0.05.

3.4 Analysis of CPT1A expression in human adipose tissue from T2D cohort

VAT and SAT were also analyzed from a T2DM cohort including control and T2D patients as described in Materials and Methods, section 8.1. The main clinical and metabolic characteristics of the T2D cohort are shown in **Fig.22**. Subjects with diabetes had significantly higher fasting triglycerides, glucose and glycerol plasma levels and HOMA index.

Clinical, analytical and CPT1 gene expression analysis in type 2 diabetes cohort.

	Control (21 male, 15 female)	**Type2 Diabetes** (5 male, 6 female)
Age (years)	61.6 ± 10.6	66.1± 8.6
BMI (kg/m^2)	28.6 (27.0-31.5)	28.7 (26.9-30.4)
Waist (cm)	100.0 (94.0-107.0)	97.0 (94.0-102.0)
Cholesterol (mM)	5.1 ± 0.9	4.7 ± 1.2
HDL-chol (mM)	1.4 (1.2-1.6)	1.2 (1.0-1.9)
Triglycerides (mM)	1.0 (0.7-1.5)	1.7 (1.2-2.3) ¶
NEFA (μM)	775.5 ± 275.1	926.4 ± 412.3
Glycerol (μM)	135.2 (117.2-222.3)	301.6 (209.6-465.3)¶
Glucose (mM)	5.6 (5.3-5.8)	8.3 (7.0-10.1)*
Insulin (μIU/ml)	4.5 (3.5-7.7)	10.2 (3.5-21.4)
HOMA-IR	1.22 (0.89-2.10)	3.66 (1.71-23.66) ¶
sIL-6 (pg/ml)	1.4 (1.0-2.6)	1.5 (1.0-2.4)
SBP (mmHg)	140 (130-150)	140 (124-156)
DBP (mmHg)	80 (70-80)	80(63-83)

Fig.22 Phenotypic and metabolic characteristics of T2DM cohort.
Values are expressed as mean±SD or median (interquartile range) for a non-Gaussian distributed variables. Differences *vs* Controls: * *P*< 0.001; ¶ *P*< 0.05.
BMI: Body Mass Index; sIL-6: soluble Interleukine-6; SBP: systolic blood pressure; DBP: diastolic blood pressure.

Significant increase of CPT1A gene expression in VAT *vs* SAT was observed in control patients, but this difference was lost in diabetic counterparts **(Fig.23).**

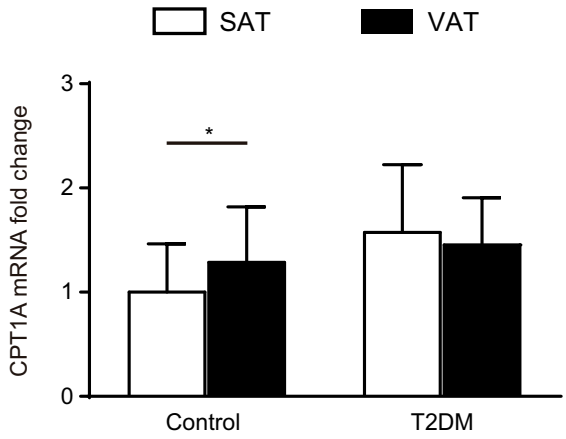

Fig.23 CPT1A mRNA levels in human visceral (VAT) and subcutaneous adipose tissue (SAT) of T2DM cohort.

CPT1A mRNA levels in human visceral (VAT) and subcutaneous adipose tissue (SAT) of T2DM cohort quantified by qRT-PCR. Levels of CPT1A mRNA are normalized to those of cyclophilin and expressed as fold change n=14.

P = 0.03.

3.5 Bivariate correlation and multiple regression analysis for human adipose tissue CPT1A expression in the obesity cohort

Bivariate correlation analysis of CPT1A gene expression levels with selected genes in SAT and VAT depots of obese patients was performed**.** Statistical significance occurred if a computed two-tailed probability value was <0.05. In our case, *P*<0.001. This analysis showed that CPT1A mRNA expression is negatively correlated with PPARγ mRNA expression in SAT depots of obese patients, and positively correlated with AGPAT5, SREBF-1, BCL-2 and CD163 mRNA expression in SAT depots of obese patients. In VAT depots of obese patients, CPT1A mRNA expression is positively correlated with AGPAT5, SREBF-1, BCL-2 and CD163 **(Fig.24).**

	CPT1A	
	SAT	VAT
	R	**R**
PPARγ	-0.382	
AGPAT5	0.639	0.714
SREBF1	0.525	0.757
BCL2	0.639	0.580
CD163	0.731	0.716

Fig.24 Bivariate correlation analysis of CPT1A gene expression level with selected genes of SAT and VAT depots of obese patients.
AGPAT5**:** 1-Acylglycerol-3-Phosphate-O-Acyltransferase 5; SREBF1: Sterol Regulatory Element-Binding Factor 1; BCL2: B-cell lymphoma 2; CD163: Cluster of Differentiation 163; R: Correlation coefficient. *P*<0.001.

A stepwise multiple linear regression analysis was also performed to determine independent variables associated with CPT1A gene expression (dependent variable) levels in SAT and VAT depots of the obesity cohort. This analysis showed that on the one hand, CPT1A mRNA expression in VAT decreases with PPARγ and age, whereas it increases with CD163 and SREBF1. On the other hand, in SAT, CPT1A mRNA expression increases with CD163, AGPAT5 and SREBF1. Results are expressed as unstandardized coefficient (B), and 95% confidence interval for B (95%CI (B)). Statistical significance occurred if a computed two-tailed probability value *(P)* was <0.05. **(Fig.25).**

SAT

R^2 of the model: 0.71

Independent variables	B (95% CI)	β st	*P*
AGPAT5	0.64 (0.33 – 0.95)	0.345	<0.0001
SREBF1	0.19 (0.06 – 0.33)	0.245	0.006
CD163	0.34 (0.20 – 0.49)	0.446	<0.0001

VAT

R^2 of the model: 0.70

Independent variables	B (95% CI)	β st	*P*
PPARγ	-0.29 (-0.53 – -0.05)	-0.19	0.017
SREBF1	0.413 (0.13 – 0.69)	0.323	0.005
CD163	0.34 (0.21 – 0.48)	0.569	<0.0001
Age	-0.15 (-0-025 – -0.004)	-0.22	0.006

Fig.25 Multiple linear regression analysis for CPT1A as dependent variable in SAT and VAT depots of obesity cohort.

Independent variables included in the model: age, gender, BMI, PPARγ, PPARα, AGPAD5, SREBF1, BCL2 and CD163 gene expression levels.

R^2 (R squared): coefficient of determination; **β st**: standardized β coefficient, **95%CI (B):** CI confidence interval for B.

DISCUSSION

Since an excess of lipids is found in obesity and associated pathologies, a lot of research studies how to eliminate them through an increase in fatty acid oxidation (FAO). Beneficial effects of an increase in energy expenditure in obesity have been described in several tissues, including liver, muscle, white adipose tissue (WAT), and more recently brown adipose tissue (BAT). On the contrary, FAO therapeutic inhibition in hypothalamus seems to reduce food intake. Whether or not FAO should be modulated in the above-mentioned tissues to improve insulin resistance or to lose weight is still a subject of debate. Therefore, CPT1, as rate-limiting step in mitochondrial oxidation of free fatty acids (FFAs), seems to be a good molecular target for FAO modulation. Although experimental data suggest a beneficial impact of mitochondrial FAO in the context of fatty acid-induced inflammation, the role of FAO in the development of insulin resistance is controversially discussed [227]. However, the results presented here support the notion that increased flux of fatty acids (FAs) in mitochondria of 3T3-L1 CARΔ1 adipocytes and RAW 264.7 macrophages by chronic overexpression of the β-oxidation key enzyme, CPT1A, improves obesity-induced inflammation and insulin resistance. The beneficial effects of CPT1AM gene transfer reported here were mainly the consequence of two key factors. First, the choice of white adipocytes as a target, because its relevance in Metabolic Syndrome. And second, the use of a mutant but active form of CPT1A (CPT1AM), which is insensitive to its physiological inhibitor, malonyl-CoA. Previous studies have shown that expression of CPT1AM leads to a permanent rise in the rate of FAO, independently of the glucose-derived malonyl-CoA levels [214-216, 228].

EFFECT OF CPT1AM EXPRESSION IN 3T3-L1 CAR ADIPOCYTES ON LIPID METABOLISM, INSULIN RESISTANCE, INFLAMMATION AND ROS DAMAGE DURING FATTY ACIDS OVERLOAD.

As a consequence of increased fatty acids flux through mitochondria, CPT1AM-expressing adipocytes showed a decreased lipid accumulation. Enhanced adipocyte FAO also reduced inflammation and improved insulin sensitivity in FAs-treated adipocytes. These results are concordant with previous studies [229] reporting that direct CPT1A overexpression in 3T3-L1 adipocytes decreased intracellular TG after FAs treatment, rescued FAs acid-induced insulin resistance and finally reduced pro-inflammatory cytokines expression and secretion via

suppression of JNK signalling in these cells. In the same study, knocking-down of CPT1A and pharmacological inhibition of CPT1A by etomoxir deteriorated insulin resistance and inflammation through activation of JNK. Likewise, our strategy directly increases FAO in adipocytes but this rise in lipid utilization is chronic by the permanently active expression of CPT1AM. In addition, our experiments were performed under a higher palmitate concentration and longer incubation times. Recently, Vernochet *et al*. [230] showed that increasing mitochondrial oxidation in fat by adipose-specific deletion of mitochondrial transcription factor A (TFAM) had positive metabolic effects by protecting mice from obesity and insulin resistance. In the latest findings by Laurent *et al.* [231] mice lacking SIRT4 displayed elevated malonyl-CoA decarboxylase (MCD) activity and decreased malonyl-CoA levels in SkM and WAT. Consequently, SIRT4 KO mice under HFD have a significant increase in energy expenditure and are resistant to diet-induced obesity. However, Kusminski *et al.* [232] demonstrated that overexpression of mitoNEET in adipocytes, during high caloric intake, compromised mitochondrial function disrupting the cellular energy balance and driving a decline in β-oxidation but finally, resulted in system-wide improvements in insulin sensitivity. Thus, taking into account these controversial data, further research is needed to gain insight into the potential beneficial effect of an increase in FAO in obesity-induced insulin resistance.

EFFECT OF CPT1AM EXPRESSION IN RAW 264.7 MACROPHAGES ON LIPID METABOLISM, INSULIN RESISTANCE, INFLAMMATION AND ROS DAMAGE DURING FATTY ACIDS OVERLOAD.

Saturated fatty acids (SFAs), commonly elevated in obese humans [26, 233, 234], mediated in part M1 activation of macrophages, rendering them inflammatory. In addition, total macrophage lipid content is increased in obese rodents fed HFD, and this is associated with M1 activation. It was shown that increasing FAs conversion to TG through overexpression of diacylglycerol acyltransferase 1 (DGAT1) reduced macrophage inflammatory activation by SFAs [235]. Also genetic deletion of the AMPKβ1 subunit drastically reduces macrophages AMPKα1 activity, suppressing the expression of mitochondrial enzymes and ACC phosphorylation, which results in increased macrophage lipid accumulation and inflammation [236]. However, the impact of FAO on macrophage inflammation is less clear

and there is no direct evidence proving a regulatory role of FAO in macrophages. Interestingly, our data showed, for the first time, that an enhanced β-oxidation counteracts inflammation and ER stress associated with the increased uptake of FFAs in macrophages. Indeed, CPT1AM-expressing macrophages showed reduced inflammatory and ER stress levels induced by palmitate (PA) treatment. These findings suggest that, similar to observations made in other cellular systems, an increased flux of FAs towards FAO alleviates cell dysfunction associated with FFAs overload [216, 237-240]. FAO supports the formation of reactive oxygen species (ROS) in isolated mitochondria [241] and mitochondrial ROS are heavily implicated in the development of insulin resistance [242]. In adipocytes, there is still no evidence that increasing adipose tissue FAO would decrease FFAs-induced ROS production. In our conditions PA was not able to induce ROS damage in adipocytes, so we could not prove the beneficial effect of CPT1AM expression. On the other hand, in macrophages PA-induced oxidative stress appears to be antagonized by efficient FAO. We observed that PA incubation caused a robust increase of ROS damage that was significantly attenuated in CPT1AM-expressing macrophages. Decreased TG content in PA-treated macrophages after FAO stimulation may also contribute to attenuate ER stress and inflammatory responses. Accordingly, previous findings showed that mice deficient in regulators of FAO and mitochondrial capacity including PPARγ [243, 244], PPARδ [245, 246], and PGC1-β [247] have an increased propensity for developing lipid-induced inflammation and insulin resistance. Similarly, deletion of the FAs-binding protein aP2 or aP2 inhibitor protects mice against the development of obesity-related inflammation, insulin resistance, and atherosclerosis [248, 249].

COMPARISON OF CPT1AM EXPRESSION IN 3T3-L1 CARΔ1 ADIPOCYTES AND RAW 264.7 MACROPHAGES

The comparison between our results in 3T3-L1 CARΔ1 adipocytes and RAW 264.7 macrophages, as summarized in the next table, helped us to show important remarks. CPT1AM expression was stronger in adipocytes than macrophages, when analysing CPT1A protein, activity and FAO rate. This may be due to the low basal CPT1A expression in adipocytes compared to macrophages. However, the higher CPT1AM expression achieved by adenovirus infection in adipocytes compared to macrophages was not translated into higher beneficial effects on other measurements such as TG content, inflammation, ER stress and

ROS levels, who were higher in CPT1AM-expressing macrophages than in adipocytes. Probably, 3T3-L1 CARΔ1 adipocytes are more sensitive to any challenge (*e.g.* adenovirus infection, fatty acid treatment) than macrophages. Thus, taking into account all of our observations, we propose macrophages as a good target for future anti-obesity therapies.

	3T3-L1 CAR adipocytes	RAW 264.7 macrophages
Infection	50 %	70 %
	Fold increase	Fold increase
CPT1A mRNA	14.5	2.4
CPT1A protein	9.4	6.6
CPT1A activity	4.3	2.2
FAO rate	1.7	1.5

CPT1A EXPRESSION IN HUMAN ADIPOSE TISSUE

Recent studies in humans [224], employing a proteomic approach, have analysed VAT biopsies from non-obese and morbidly obese individuals, to uncover differences in protein expression in these two sets of subjects. They reported the down-regulation of proteins related to lipid metabolism suggesting a reduction of metabolic activity in the obese VAT. These findings are in agreement with previous microarray analysis revealing a coordinated down-regulation of catabolic pathways operating in the mitochondria such as: FAO, TCA cycle and ETC [250]. Krishnan *et al.* [163] also have analysed the expression of FAO regulators (such as PGC-1α) and CPT1 in VAT biopsies of obese human subjects and lean subjects. Lean subjects were generally characterized by high CPT1 protein levels, while the inverse was observed in biopsies of obese subjects. Moreover, an overall decrease in the expression of FAO regulators (*e.g*. PGC-1α), mitochondrial biogenesis markers (*e.g.* TFAM) and components of ETC (*e.g.* MTND1), was noted in AT of obese *vs* lean subjects. Despite these evidences, we found no decrease in CPT1A expression of obese subjects compared to

lean counterparts. However, we cannot rule out that some metabolic genes, such as CPT1A, are expressed at significant levels in other AT cell types. Indeed, in our obesity cohort, we analysed CPT1A expression in both adipocytes and SVF, enriched in macrophages. CPT1A was highly expressed in SVF compared with adipocyte fraction. Thus, probably the increased number of macrophage infiltration in the obese adipose tissue (AT) led to similar levels of CPT1A expression between lean and obese AT. More investigation is required to confirm this hypothesis. Of note, our results showed that CPT1A mRNA expression in VAT decreases with PPARγ, suggesting that stimulating FAO might enhance hyperplastic growth and adipocyte differentiation in these subjects. Interestingly, the differentiation state of obese adipocytes is altered and the expression of adipogenic genes is decreased in obesity [251, 252]. Strikingly, regression analysis also showed a decrease of CPT1A expression with age in visceral adipose tissue (VAT) of obese subjects. Considering that VAT accretion is a hallmark of aging and especially, it is a stronger risk factor for co-morbities and mortality [253], we speculate a favourable role of enhanced CPT1A expression on age metabolic decline and related pathological conditions.

However, several questions still need to be answered before FAO can become an obesity therapy. First, it is not known whether a long-term increase in energy expenditure would cause an enhancement of appetite as a compensatory mechanism. Second, an increase in FAO could induce pathological levels of ROS and/or other incomplete oxidation products. Third, it is not known whether FAO enhancement might reach a limit in a specific tissue, such as in BAT, in which thermogenesis is tightly adjusted to the environmental temperature. Finally, since increasing flux through β-oxidation would only make sense together with a corresponding enhancement in energy demand [254], the physiological relevance of improved mitochondrial FAO might be questioned if the individual remains sedentary (muscle, WAT, or liver) or warm (BAT). Potential mechanisms to explain the beneficial effects of targeting mitochondrial FAO could be the concomitant enhancement of hepatic ketone bodies, CO_2, acid soluble products, ATP production, and endergonic processes (*e.g.*, gluconeogenesis) seen in previous publications [216, 255, 256]. Increased FAO may also decrease glucose oxidation to maintain energy homeostasis, augment mitochondrial burning capacity through an increase in the number of mitochondria and/or the increased

expression of UCPs, and thus dissipate the excess of energy as heat and ATP. All of these could well alleviate the mitochondrial pressure found in lipid overload states.

Regarding our results, it would be interesting to analyse the expression of CPT1B in our model, given that it is the main isoform expressed by mature human adipocytes.

Overall, the present study uncovers a favourable role for enhanced and permanent CPT1A expression in adipocytes and macrophages during fatty acids overload.

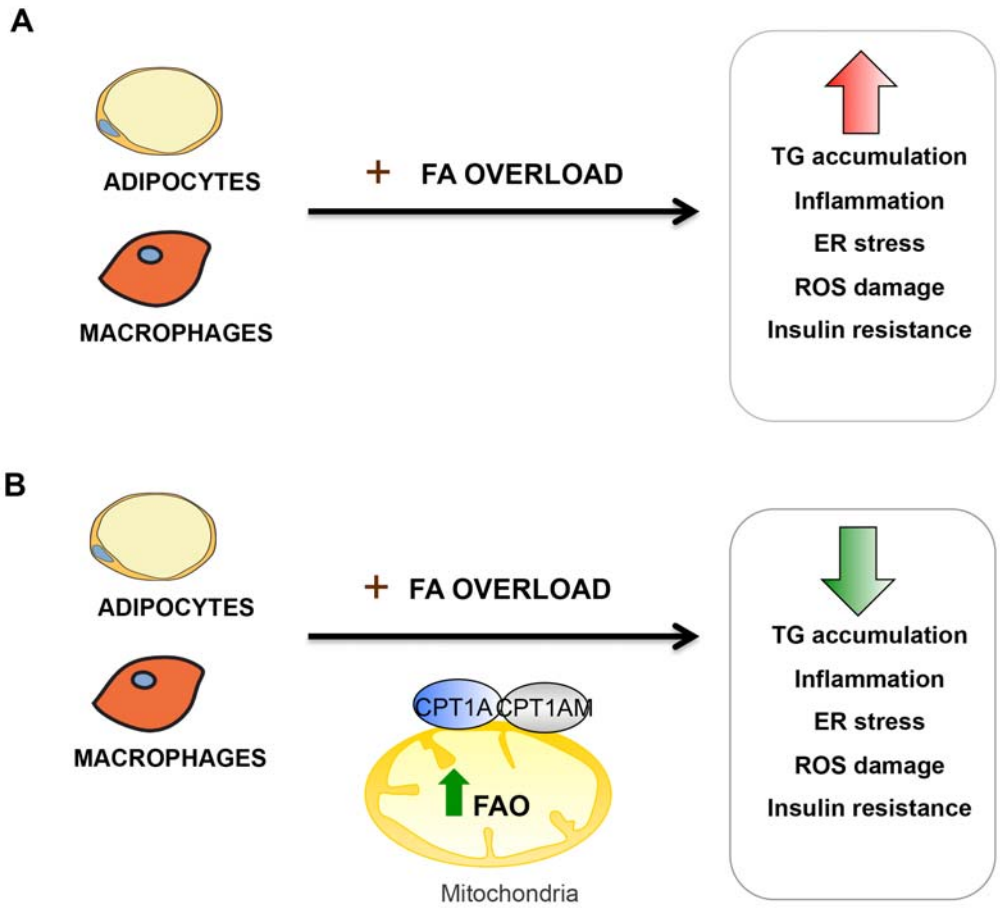

Enhanced FAO on adipocytes and macrophages during fatty acids overload.
A. Fatty acids overload increases TG accumulation, inflammation, ER and oxidative stress that contribute to insulin resistance in adipocytes and macrophages. **B.** Enhanced FAO by CPT1AM expression in adipocytes and macrophages decreases TG content, inflammation, ER stress and ROS damage and improves insulin sensitivity.

FUTURE PERSPECTIVES

In the future, it would be very interesting to analyse the effect of CPT1AM expression on mitochondrial respiratory capacity during obesity. In addition, co-culture of adipocytes and macrophages after CPT1A expression could be fascinating to elucidate the cross-talk mechanisms occurring during obesity. Finally, it would be very exciting to explore *in vivo* the impact of chronic enhanced FAO in obese adipose tissue on the whole body.

Although more research is needed, our results *in vitro* and *in vivo*, together with those cited herein, highlight how targeting FAO and cell energy expenditure could be a potential new therapy to treat obesity and its associated severe diseases.

CONCLUSIONS

- **CPT1AM EXPRESSION IN 3T3-L1 CARΔ1 ADIPOCYTES BY ADENOVIRUS**

1. CPT1AM expression in 3T3-L1 CARΔ1 adipocytes increases CPT1A mRNA and protein levels and CPT1 activity compared to GFP-expressing controls.
2. CPT1AM-expressing adipocytes retain most of their CPT1 activity after incubation with the CPT1 inhibitor malonyl-CoA, compared to GFP-expressing controls.
3. Total fatty acid oxidation is enhanced in CPT1AM-expressing adipocytes compared to GFP-expressing controls.
4. CPT1AM expression in 3T3-L1 CARΔ1 adipocytes is able to restore PA-induced increase in TG content compared to GFP-expressing controls.
5. CPT1AM expression in 3T3-L1 CARΔ1 adipocytes restores PA-induced impairment in Akt phosphorylation compared to GFP-expressing controls.
6. FA-induced increase in inflammation is blunted in CPT1AM-expressing adipocytes compared to GFP-expressing controls.
7. Following PA treatment, only CHOP and GRP78 expression was significantly elevated in GFP control cells, whereas we doesn't observe any change in other markers (PDI, EDEM). PA-induced increase in ER stress is not restored in in CPT1AM-expressing adipocytes.
8. Following PA treatment, we doesn't observed any change in protein carbonyl content of adipocytes.

- **CPT1AM EXPRESSION IN RAW 264.7 MACROPHAGES BY ADENOVIRUS**

9. After AdGFP infection, RAW 264.7 macrophages show an increase of TNF-α mRNA, compared to no infected cells.
10. CPT1AM expression in RAW 264.7 macrophages increases CPT1A mRNA and protein levels and CPT1 activity compared to GFP-expressing controls.
11. CPT1AM-expressing macrophages retain most of their CPT1 activity after incubation with the CPT1 inhibitor malonyl-CoA, compared to GFP-expressing controls.
12. Total oxidation is enhanced in CPT1AM-expressing macrophages compared to GFP control cells.

13. CPT1AM expression in RAW 264.7 macrophages is able to restore PA-induced increase in TG content compared to GFP-expressing controls.

14. FA-induced increase in inflammation is blunted in CPT1AM-expressing macrophages compared to GFP controls.

15. FA-induced increase in ER stress is decreased in CPT1AM-expressing macrophages compared to GFP-expressing controls.

16. FA-induced ROS damage is decreased in CPT1AM-expressing macrophages compared to GFP- control cells.

- **CPT1A EXPRESSION IN HUMAN ADIPOSE TISSUE**

17. CPT1A mRNA levels decrease along human adipocytes differentiation.

18. qRT-PCR and immunohistochemistry analysis on both adipose and SVF of human SAT show that CPT1A is mostly present in the SVF cells.

19. Immunofluorescence detection shows co-localization of CPT1A and macrophages in human overweight SAT.

20. CPT1A mRNA levels are higher in VAT compared to SAT in both lean and overweight patients. However, this difference is lost in the obese patients.

21. Bivariate correlation analyses show that CPT1A mRNA expression is negatively correlated with PPAR-γ mRNA expression in SAT depots of obese patients, and positively correlated with AGPAT-5, SREBF-1, BCL-2 and CD163. In VAT depots of obese patients, CPT1A mRNA expression is positively correlated AGPAT-5, SREBF-1, BCL-2 and CD163.

22. A stepwise multiple regression analysis of VAT and SAT depots of obesity cohort shows that on one hand, CPT1A mRNA expression in VAT decreases with PPAR-γ and age, whereas it increases with CD163. On other hand, in SAT, CPT1A mRNA expression increases with CD163 and AGPAT5.

REFERENCES

1. Flegal, K.M., et al., *Prevalence and trends in obesity among US adults, 1999-2008.* JAMA, 2010. 303(3): p. 235-41.

2. *Obesity: preventing and managing the global epidemic. Report of a WHO consultation.* World Health Organ Tech Rep Ser, 2000. 894: p. i-xii, 1-253.

3. Taubes, G., *Insulin resistance. Prosperity's plague.* Science, 2009. 325(5938): p. 256-60.

4. Ahima, R.S., *Digging deeper into obesity.* J Clin Invest, 2011. 121(6): p. 2076-9.

5. Reaven, G.M., *Role of insulin resistance in human disease (syndrome X): an expanded definition.* Annu Rev Med, 1993. 44: p. 121-31.

6. Moller, D.E. and K.D. Kaufman, *Metabolic syndrome: a clinical and molecular perspective.* Annu Rev Med, 2005. 56: p. 45-62.

7. Virtue, S. and A. Vidal-Puig, *Adipose tissue expandability, lipotoxicity and the Metabolic Syndrome--an allostatic perspective.* Biochim Biophys Acta, 2010. 1801(3): p. 338-49.

8. Johnson, A.M. and J.M. Olefsky, *The origins and drivers of insulin resistance.* Cell, 2013. 152(4): p. 673-84.

9. Saltiel, A.R. and C.R. Kahn, *Insulin signalling and the regulation of glucose and lipid metabolism.* Nature, 2001. 414(6865): p. 799-806.

10. Samuel, V.T. and G.I. Shulman, *Mechanisms for insulin resistance: common threads and missing links.* Cell, 2012. 148(5): p. 852-71.

11. Pessin, J.E. and A.R. Saltiel, *Signaling pathways in insulin action: molecular targets of insulin resistance.* J Clin Invest, 2000. 106(2): p. 165-9.

12. Murrow, B.A. and K.L. Hoehn, *Mitochondrial regulation of insulin action.* Int J Biochem Cell Biol, 2010. 42(12): p. 1936-9.

13. Schaffer, J.E., *Lipotoxicity: when tissues overeat.* Curr Opin Lipidol, 2003. 14(3): p. 281-7.

14. Unger, R.H., *Lipid overload and overflow: metabolic trauma and the metabolic syndrome.* Trends Endocrinol Metab, 2003. 14(9): p. 398-403.

15. Mittendorfer, B., *Origins of metabolic complications in obesity: adipose tissue and free fatty acid trafficking.* Curr Opin Clin Nutr Metab Care, 2011. 14(6): p. 535-41.

16. Sathyanarayana, P., et al., *Activation of the Drosophila MLK by ceramide reveals TNF-alpha and ceramide as agonists of mammalian MLK3.* Mol Cell, 2002. 10(6): p. 1527-33.

17. Wang, X., et al., *Signaling functions of phosphatidic acid.* Prog Lipid Res, 2006. 45(3): p. 250-78.

18. Jean-Baptiste, G., et al., *Lysophosphatidic acid mediates pleiotropic responses in skeletal muscle cells.* Biochem Biophys Res Commun, 2005. 335(4): p. 1155-62.

19. Sampson, S.R. and D.R. Cooper, *Specific protein kinase C isoforms as transducers and modulators of insulin signaling.* Mol Genet Metab, 2006. 89(1-2): p. 32-47.

20. Hotamisligil, G.S., N.S. Shargill, and B.M. Spiegelman, *Adipose expression of tumor necrosis factor-alpha: direct role in obesity-linked insulin resistance.* Science, 1993. 259(5091): p. 87-91.

21. Hotamisligil, G.S., et al., *Increased adipose tissue expression of tumor necrosis factor-alpha in human obesity and insulin resistance.* J Clin Invest, 1995. 95(5): p. 2409-15.

22. Hotamisligil, G.S., et al., *IRS-1-mediated inhibition of insulin receptor tyrosine kinase activity in TNF-alpha- and obesity-induced insulin resistance.* Science, 1996. 271(5249): p. 665-8.

23. Weisberg, S.P., et al., *Obesity is associated with macrophage accumulation in adipose tissue.* J Clin Invest, 2003. 112(12): p. 1796-808.

24. Xu, H., et al., *Chronic inflammation in fat plays a crucial role in the development of obesity-related insulin resistance.* J Clin Invest, 2003. 112(12): p. 1821-30.

25. Lumeng, C.N., J.L. Bodzin, and A.R. Saltiel, *Obesity induces a phenotypic switch in adipose tissue macrophage polarization.* J Clin Invest, 2007. 117(1): p. 175-84.

26. Nguyen, M.T., et al., *A subpopulation of macrophages infiltrates hypertrophic adipose tissue and is activated by free fatty acids via Toll-like receptors 2 and 4 and JNK-dependent pathways.* J Biol Chem, 2007. 282(48): p. 35279-92.

27. Peraldi, P., et al., *Tumor necrosis factor (TNF)-alpha inhibits insulin signaling through stimulation of the p55 TNF receptor and activation of sphingomyelinase.* J Biol Chem, 1996. 271(22): p. 13018-22.

28. Osborn, O. and J.M. Olefsky, *The cellular and signaling networks linking the immune system and metabolism in disease.* Nat Med, 2012. 18(3): p. 363-74.

29. Gregor, M.F. and G.S. Hotamisligil, *Inflammatory mechanisms in obesity.* Annu Rev Immunol, 2011. 29: p. 415-45.

30. Obstfeld, A.E., et al., *C-C chemokine receptor 2 (CCR2) regulates the hepatic recruitment of myeloid cells that promote obesity-induced hepatic steatosis.* Diabetes, 2010. 59(4): p. 916-25.

31. De Souza, C.T., et al., *Consumption of a fat-rich diet activates a proinflammatory response and induces insulin resistance in the hypothalamus.* Endocrinology, 2005. 146(10): p. 4192-9.

32. Milanski, M., et al., *Inhibition of hypothalamic inflammation reverses diet-induced insulin resistance in the liver.* Diabetes, 2012. 61(6): p. 1455-62.

33. Ehses, J.A., et al., *Increased number of islet-associated macrophages in type 2 diabetes.* Diabetes, 2007. 56(9): p. 2356-70.

34. Carey, A.L., et al., *Interleukin-6 and tumor necrosis factor-alpha are not increased in patients with Type 2 diabetes: evidence that plasma interleukin-6 is related to fat mass and not insulin responsiveness.* Diabetologia, 2004. 47(6): p. 1029-37.

35. Febbraio, M.A., et al., *Skeletal muscle interleukin-6 and tumor necrosis factor-alpha release in healthy subjects and patients with type 2 diabetes at rest and during exercise.* Metabolism, 2003. 52(7): p. 939-44.

36. Mosser, D.M. and J.P. Edwards, *Exploring the full spectrum of macrophage activation.* Nat Rev Immunol, 2008. 8(12): p. 958-69.

37. Talukdar, S., et al., *Neutrophils mediate insulin resistance in mice fed a high-fat diet through secreted elastase.* Nat Med, 2012. 18(9): p. 1407-12.

38. Liu, J., et al., *Genetic deficiency and pharmacological stabilization of mast cells reduce diet-induced obesity and diabetes in mice.* Nat Med, 2009. 15(8): p. 940-5.

39. Winer, D.A., et al., *B cells promote insulin resistance through modulation of T cells and production of pathogenic IgG antibodies.* Nat Med, 2011. 17(5): p. 610-7.

40. Nishimura, S., et al., *CD8+ effector T cells contribute to macrophage recruitment and adipose tissue inflammation in obesity.* Nat Med, 2009. 15(8): p. 914-20.

41. Winer, S., et al., *Normalization of obesity-associated insulin resistance through immunotherapy.* Nat Med, 2009. 15(8): p. 921-9.

42. Cipolletta, D., et al., *PPAR-gamma is a major driver of the accumulation and phenotype of adipose tissue Treg cells.* Nature, 2012. 486(7404): p. 549-53.

43. Feuerer, M., et al., *Lean, but not obese, fat is enriched for a unique population of regulatory T cells that affect metabolic parameters.* Nat Med, 2009. 15(8): p. 930-9.

44. Wu, D., et al., *Eosinophils sustain adipose alternatively activated macrophages associated with glucose homeostasis.* Science, 2011. 332(6026): p. 243-7.

45. Lee, J.Y., et al., *Saturated fatty acids, but not unsaturated fatty acids, induce the expression of cyclooxygenase-2 mediated through Toll-like receptor 4.* J Biol Chem, 2001. 276(20): p. 16683-9.

46. Shi, H., et al., *TLR4 links innate immunity and fatty acid-induced insulin resistance.* J Clin Invest, 2006. 116(11): p. 3015-25.

47. Glass, C.K. and J.M. Olefsky, *Inflammation and lipid signaling in the etiology of insulin resistance.* Cell Metab, 2012. 15(5): p. 635-45.

48. Wen, H., J.P. Ting, and L.A. O'Neill, *A role for the NLRP3 inflammasome in metabolic diseases--did Warburg miss inflammation?* Nat Immunol, 2012. 13(4): p. 352-7.

49. Holzer, R.G., et al., *Saturated fatty acids induce c-Src clustering within membrane subdomains, leading to JNK activation.* Cell, 2011. 147(1): p. 173-84.

50. Wong, S.W., et al., *Fatty acids modulate Toll-like receptor 4 activation through regulation of receptor dimerization and recruitment into lipid rafts in a reactive oxygen species-dependent manner.* J Biol Chem, 2009. 284(40): p. 27384-92.

51. Solinas, G. and M. Karin, *JNK1 and IKKbeta: molecular links between obesity and metabolic dysfunction.* FASEB J, 2010. 24(8): p. 2596-611.

52. Lumeng, C.N. and A.R. Saltiel, *Inflammatory links between obesity and metabolic disease.* J Clin Invest, 2011. 121(6): p. 2111-7.

53. Cnop, M., F. Foufelle, and L.A. Velloso, *Endoplasmic reticulum stress, obesity and diabetes.* Trends Mol Med, 2012. 18(1): p. 59-68.

54. Flamment, M., et al., *New insights into ER stress-induced insulin resistance.* Trends Endocrinol Metab, 2012. 23(8): p. 381-90.

55. Sharma, N.K., et al., *Endoplasmic reticulum stress markers are associated with obesity in nondiabetic subjects.* J Clin Endocrinol Metab, 2008. 93(11): p. 4532-41.

56. Boden, G., et al., *Increase in endoplasmic reticulum stress-related proteins and genes in adipose tissue of obese, insulin-resistant individuals.* Diabetes, 2008. 57(9): p. 2438-44.

57. Vendrell, J., et al., *Tumor necrosis-like weak inducer of apoptosis as a proinflammatory cytokine in human adipocyte cells: up-regulation in severe obesity is mediated by inflammation but not hypoxia.* J Clin Endocrinol Metab, 2010. 95(6): p. 2983-92.

58. Xu, L., G.A. Spinas, and M. Niessen, *ER stress in adipocytes inhibits insulin signaling, represses lipolysis, and alters the secretion of adipokines without inhibiting glucose transport.* Horm Metab Res, 2010. 42(9): p. 643-51.

59. Zhou, Q.G., et al., *Asymmetrical dimethylarginine triggers lipolysis and inflammatory response via induction of endoplasmic reticulum stress in cultured adipocytes.* Am J Physiol Endocrinol Metab, 2009. 296(4): p. E869-78.

60. Liu, M., et al., *A disulfide-bond A oxidoreductase-like protein (DsbA-L) regulates adiponectin multimerization.* Proc Natl Acad Sci U S A, 2008. 105(47): p. 18302-7.

61. Zhou, L., et al., *DsbA-L alleviates endoplasmic reticulum stress-induced adiponectin downregulation.* Diabetes, 2010. 59(11): p. 2809-16.

62. Lefterova, M.I., et al., *Endoplasmic reticulum stress regulates adipocyte resistin expression.* Diabetes, 2009. 58(8): p. 1879-86.

63. Kau, A.L., et al., *Human nutrition, the gut microbiome and the immune system.* Nature, 2011. 474(7351): p. 327-36.

64. Blumberg, R. and F. Powrie, *Microbiota, disease, and back to health: a metastable journey.* Sci Transl Med, 2012. 4(137): p. 137rv7.

65. Hildebrandt, M.A., et al., *High-fat diet determines the composition of the murine gut microbiome independently of obesity.* Gastroenterology, 2009. 137(5): p. 1716-24 e1-2.

66. Ley, R.E., et al., *Obesity alters gut microbial ecology.* Proc Natl Acad Sci U S A, 2005. 102(31): p. 11070-5.

67. Turnbaugh, P.J., et al., *Diet-induced obesity is linked to marked but reversible alterations in the mouse distal gut microbiome.* Cell Host Microbe, 2008. 3(4): p. 213-23.

68. Burcelin, R., L. Garidou, and C. Pomie, *Immuno-microbiota cross and talk: the new paradigm of metabolic diseases.* Semin Immunol, 2012. 24(1): p. 67-74.

69. Rosen, E.D. and B.M. Spiegelman, *Adipocytes as regulators of energy balance and glucose homeostasis.* Nature, 2006. 444(7121): p. 847-53.

70. Rigamonti, A., et al., *Rapid cellular turnover in adipose tissue.* PLoS One, 2011. 6(3): p. e17637.

71. Spalding, K.L., et al., *Dynamics of fat cell turnover in humans.* Nature, 2008. 453(7196): p. 783-7.

72. Gesta, S., Y.H. Tseng, and C.R. Kahn, *Developmental origin of fat: tracking obesity to its source.* Cell, 2007. 131(2): p. 242-56.

73. Bijland, S., S.J. Mancini, and I.P. Salt, *Role of AMP-activated protein kinase in adipose tissue metabolism and inflammation.* Clin Sci (Lond), 2013. 124(8): p. 491-507.

74. Ducharme, N.A. and P.E. Bickel, *Lipid droplets in lipogenesis and lipolysis.* Endocrinology, 2008. 149(3): p. 942-9.

75. Berggreen, C., et al., *Protein kinase B activity is required for the effects of insulin on lipid metabolism in adipocytes.* Am J Physiol Endocrinol Metab, 2009. 296(4): p. E635-46.

76. Nye, C., et al., *Reassessing triglyceride synthesis in adipose tissue.* Trends Endocrinol Metab, 2008. 19(10): p. 356-61.

77. Cadoudal, T., et al., *Pyruvate dehydrogenase kinase 4: regulation by thiazolidinediones and implication in glyceroneogenesis in adipose tissue.* Diabetes, 2008. 57(9): p. 2272-9.

78. Daval, M., F. Foufelle, and P. Ferre, *Functions of AMP-activated protein kinase in adipose tissue.* J Physiol, 2006. 574(Pt 1): p. 55-62.

79. Chaves, V.E., D. Frasson, and N.H. Kawashita, *Several agents and pathways regulate lipolysis in adipocytes.* Biochimie, 2011. 93(10): p. 1631-40.

80. Marin, P., et al., *The morphology and metabolism of intraabdominal adipose tissue in men.* Metabolism, 1992. 41(11): p. 1242-8.

81. Tang, Q.Q. and M.D. Lane, *Adipogenesis: from stem cell to adipocyte.* Annu Rev Biochem, 2012. 81: p. 715-36.

82. Feng, B., T. Zhang, and H. Xu, *Human adipose dynamics and metabolic health.* Ann N Y Acad Sci, 2013. 1281: p. 160-77.

83. Tontonoz, P. and B.M. Spiegelman, *Fat and beyond: the diverse biology of PPARgamma.* Annu Rev Biochem, 2008. 77: p. 289-312.

84. Ouchi, N., et al., *Adipokines in inflammation and metabolic disease.* Nat Rev Immunol, 2011. 11(2): p. 85-97.

85. Zhang, Y., et al., *Positional cloning of the mouse obese gene and its human homologue.* Nature, 1994. 372(6505): p. 425-32.

86. Piya, M.K., P.G. McTernan, and S. Kumar, *Adipokine inflammation and insulin resistance: the role of glucose, lipids and endotoxin.* J Endocrinol, 2013. 216(1): p. T1-T15.

87. Fain, J.N., et al., *Comparison of the release of adipokines by adipose tissue, adipose tissue matrix, and adipocytes from visceral and subcutaneous abdominal adipose tissues of obese humans.* Endocrinology, 2004. 145(5): p. 2273-82.

88. Fernandez-Sanchez, A., et al., *Inflammation, oxidative stress, and obesity.* Int J Mol Sci, 2011. 12(5): p. 3117-32.

89. Friedman, J.M. and J.L. Halaas, *Leptin and the regulation of body weight in mammals.* Nature, 1998. 395(6704): p. 763-70.

90. Santos-Alvarez, J., R. Goberna, and V. Sanchez-Margalet, *Human leptin stimulates proliferation and activation of human circulating monocytes.* Cell Immunol, 1999. 194(1): p. 6-11.

91. Kiguchi, N., et al., *Leptin enhances CC-chemokine ligand expression in cultured murine macrophage.* Biochem Biophys Res Commun, 2009. 384(3): p. 311-5.

92. Zarkesh-Esfahani, H., et al., *Leptin indirectly activates human neutrophils via induction of TNF-alpha.* J Immunol, 2004. 172(3): p. 1809-14.

93. Grunfeld, C., et al., *Endotoxin and cytokines induce expression of leptin, the ob gene product, in hamsters.* J Clin Invest, 1996. 97(9): p. 2152-7.

94. Lord, G.M., et al., *Leptin modulates the T-cell immune response and reverses starvation-induced immunosuppression.* Nature, 1998. 394(6696): p. 897-901.

95. Ouchi, N., et al., *Obesity, adiponectin and vascular inflammatory disease.* Curr Opin Lipidol, 2003. 14(6): p. 561-6.

96. Ryo, M., et al., *Adiponectin as a biomarker of the metabolic syndrome.* Circ J, 2004. 68(11): p. 975-81.

97. Hosogai, N., et al., *Adipose tissue hypoxia in obesity and its impact on adipocytokine dysregulation.* Diabetes, 2007. 56(4): p. 901-11.

98. Sikaris, K.A., *The clinical biochemistry of obesity.* Clin Biochem Rev, 2004. 25(3): p. 165-81.

99. Lastra, G., C.M. Manrique, and M.R. Hayden, *The role of beta-cell dysfunction in the cardiometabolic syndrome.* J Cardiometab Syndr, 2006. 1(1): p. 41-6.

100. Yokota, T., et al., *Adiponectin, a new member of the family of soluble defense collagens, negatively regulates the growth of myelomonocytic progenitors and the functions of macrophages.* Blood, 2000. 96(5): p. 1723-32.

101. Yamaguchi, N., et al., *Adiponectin inhibits Toll-like receptor family-induced signaling.* FEBS Lett, 2005. 579(30): p. 6821-6.

102. Kumada, M., et al., *Adiponectin specifically increased tissue inhibitor of metalloproteinase-1 through interleukin-10 expression in human macrophages.* Circulation, 2004. 109(17): p. 2046-9.

103. Hotamisligil, G.S., et al., *Reduced tyrosine kinase activity of the insulin receptor in obesity-diabetes. Central role of tumor necrosis factor-alpha.* J Clin Invest, 1994. 94(4): p. 1543-9.

104. Uysal, K.T., et al., *Protection from obesity-induced insulin resistance in mice lacking TNF-alpha function.* Nature, 1997. 389(6651): p. 610-4.

105. Kern, P.A., et al., *The expression of tumor necrosis factor in human adipose tissue. Regulation by obesity, weight loss, and relationship to lipoprotein lipase.* J Clin Invest, 1995. 95(5): p. 2111-9.

106. Starkie, R., et al., *Exercise and IL-6 infusion inhibit endotoxin-induced TNF-alpha production in humans.* FASEB J, 2003. 17(8): p. 884-6.

107. Kelly, M., et al., *AMPK activity is diminished in tissues of IL-6 knockout mice: the effect of exercise.* Biochem Biophys Res Commun, 2004. 320(2): p. 449-54.

108. Senn, J.J., et al., *Interleukin-6 induces cellular insulin resistance in hepatocytes.* Diabetes, 2002. 51(12): p. 3391-9.

109. Senn, J.J., et al., *Suppressor of cytokine signaling-3 (SOCS-3), a potential mediator of interleukin-6-dependent insulin resistance in hepatocytes.* J Biol Chem, 2003. 278(16): p. 13740-6.

110. Rotter, V., I. Nagaev, and U. Smith, *Interleukin-6 (IL-6) induces insulin resistance in 3T3-L1 adipocytes and is, like IL-8 and tumor necrosis factor-alpha, overexpressed in human fat cells from insulin-resistant subjects.* J Biol Chem, 2003. 278(46): p. 45777-84.

111. Matthews, V.B., et al., *Interleukin-6-deficient mice develop hepatic inflammation and systemic insulin resistance.* Diabetologia, 2010. 53(11): p. 2431-41.

112. Sabio, G., et al., *A stress signaling pathway in adipose tissue regulates hepatic insulin resistance.* Science, 2008. 322(5907): p. 1539-43.

113. Pou, K.M., et al., *Visceral and subcutaneous adipose tissue volumes are cross-sectionally related to markers of inflammation and oxidative stress: the Framingham Heart Study.* Circulation, 2007. 116(11): p. 1234-41.

114. Kanda, H., et al., *MCP-1 contributes to macrophage infiltration into adipose tissue, insulin resistance, and hepatic steatosis in obesity.* J Clin Invest, 2006. 116(6): p. 1494-505.

115. Sartipy, P. and D.J. Loskutoff, *Monocyte chemoattractant protein 1 in obesity and insulin resistance.* Proc Natl Acad Sci U S A, 2003. 100(12): p. 7265-70.

116. Cannon, B. and J. Nedergaard, *Brown adipose tissue: function and physiological significance.* Physiol Rev, 2004. 84(1): p. 277-359.

117. Virtanen, K.A., et al., *Functional brown adipose tissue in healthy adults.* N Engl J Med, 2009. 360(15): p. 1518-25.

118. Cypess, A.M., et al., *Identification and importance of brown adipose tissue in adult humans.* N Engl J Med, 2009. 360(15): p. 1509-17.

119. van Marken Lichtenbelt, W.D., et al., *Cold-activated brown adipose tissue in healthy men.* N Engl J Med, 2009. 360(15): p. 1500-8.

120. Frontini, A. and S. Cinti, *Distribution and development of brown adipocytes in the murine and human adipose organ.* Cell Metab, 2010. 11(4): p. 253-6.

121. Enerback, S., et al., *Mice lacking mitochondrial uncoupling protein are cold-sensitive but not obese.* Nature, 1997. 387(6628): p. 90-4.

122. Feldmann, H.M., et al., *UCP1 ablation induces obesity and abolishes diet-induced thermogenesis in mice exempt from thermal stress by living at thermoneutrality.* Cell Metab, 2009. 9(2): p. 203-9.

123. Kontani, Y., et al., *UCP1 deficiency increases susceptibility to diet-induced obesity with age.* Aging Cell, 2005. 4(3): p. 147-55.

124. Kopecky, J., et al., *Expression of the mitochondrial uncoupling protein gene from the aP2 gene promoter prevents genetic obesity.* J Clin Invest, 1995. 96(6): p. 2914-23.

125. Bargmann, W., G. von Hehn, and E. Lindner, *[On the cells of the brown fatty tissue and their innervation].* Z Zellforsch Mikrosk Anat, 1968. 85(4): p. 601-13.

126. Merklin, R.J., *Growth and distribution of human fetal brown fat.* Anat Rec, 1974. 178(3): p. 637-45.

127. Carter, B.W. and W.G. Schucany, *Brown adipose tissue in a newborn.* Proc (Bayl Univ Med Cent), 2008. 21(3): p. 328-30.

128. Enerback, S., *Brown adipose tissue in humans.* Int J Obes (Lond), 2010. 34 Suppl 1: p. S43-6.

129. Wu, J., et al., *Beige adipocytes are a distinct type of thermogenic fat cell in mouse and human.* Cell, 2012. 150(2): p. 366-76.

130. Tseng, Y.H., et al., *New role of bone morphogenetic protein 7 in brown adipogenesis and energy expenditure.* Nature, 2008. 454(7207): p. 1000-4.

131. Seale, P., et al., *Transcriptional control of brown fat determination by PRDM16.* Cell Metab, 2007. 6(1): p. 38-54.

132. Uldry, M., et al., *Complementary action of the PGC-1 coactivators in mitochondrial biogenesis and brown fat differentiation.* Cell Metab, 2006. 3(5): p. 333-41.

133. Ortega, F.J., et al., *Type I iodothyronine 5'-deiodinase mRNA and activity is increased in adipose tissue of obese subjects.* Int J Obes (Lond), 2012. 36(2): p. 320-4.

134. Hondares, E., et al., *Hepatic FGF21 expression is induced at birth via PPARalpha in response to milk intake and contributes to thermogenic activation of neonatal brown fat.* Cell Metab, 2010. 11(3): p. 206-12.

135. Bordicchia, M., et al., *Cardiac natriuretic peptides act via p38 MAPK to induce the brown fat thermogenic program in mouse and human adipocytes.* J Clin Invest, 2012. 122(3): p. 1022-36.

136. Bostrom, P., et al., *A PGC1-alpha-dependent myokine that drives brown-fat-like development of white fat and thermogenesis.* Nature, 2012. 481(7382): p. 463-8.

137. Nguyen, K.D., et al., *Alternatively activated macrophages produce catecholamines to sustain adaptive thermogenesis.* Nature, 2011. 480(7375): p. 104-8.

138. Whittle, A.J., et al., *BMP8B increases brown adipose tissue thermogenesis through both central and peripheral actions.* Cell, 2012. 149(4): p. 871-85.

139. Sun, K., C.M. Kusminski, and P.E. Scherer, *Adipose tissue remodeling and obesity.* J Clin Invest, 2011. 121(6): p. 2094-101.

140. Cinti, S., et al., *Adipocyte death defines macrophage localization and function in adipose tissue of obese mice and humans.* J Lipid Res, 2005. 46(11): p. 2347-55.

141. Stienstra, R., et al., *The inflammasome puts obesity in the danger zone.* Cell Metab, 2012. 15(1): p. 10-8.

142. Freedland, E.S., *Role of a critical visceral adipose tissue threshold (CVATT) in metabolic syndrome: implications for controlling dietary carbohydrates: a review.* Nutr Metab (Lond), 2004. 1(1): p. 12.

143. Ibrahim, M.M., *Subcutaneous and visceral adipose tissue: structural and functional differences.* Obes Rev, 2010. 11(1): p. 11-8.

144. Capurso, C. and A. Capurso, *From excess adiposity to insulin resistance: the role of free fatty acids.* Vascul Pharmacol, 2012. 57(2-4): p. 91-7.

145. Sica, A. and A. Mantovani, *Macrophage plasticity and polarization: in vivo veritas.* J Clin Invest, 2012. 122(3): p. 787-95.

146. Johnson, A.R., J.J. Milner, and L. Makowski, *The inflammation highway: metabolism accelerates inflammatory traffic in obesity.* Immunol Rev, 2012. 249(1): p. 218-38.

147. Prieur, X., et al., *Differential lipid partitioning between adipocytes and tissue macrophages modulates macrophage lipotoxicity and M2/M1 polarization in obese mice.* Diabetes, 2011. 60(3): p. 797-809.

148. Lumeng, C.N., et al., *Increased inflammatory properties of adipose tissue macrophages recruited during diet-induced obesity.* Diabetes, 2007. 56(1): p. 16-23.

149. Tseng, Y.H., A.M. Cypess, and C.R. Kahn, *Cellular bioenergetics as a target for obesity therapy.* Nat Rev Drug Discov, 2010. 9(6): p. 465-82.

150. Mailloux, R.J. and M.E. Harper, *Mitochondrial proticity and ROS signaling: lessons from the uncoupling proteins.* Trends Endocrinol Metab, 2012. 23(9): p. 451-8.

151. Leloup, C., et al., *Balancing mitochondrial redox signaling: a key point in metabolic regulation.* Antioxid Redox Signal, 2011. 14(3): p. 519-30.

152. Mailloux, R.J. and M.E. Harper, *Uncoupling proteins and the control of mitochondrial reactive oxygen species production.* Free Radic Biol Med, 2011. 51(6): p. 1106-15.

153. Rains, J.L. and S.K. Jain, *Oxidative stress, insulin signaling, and diabetes.* Free Radic Biol Med, 2011. 50(5): p. 567-75.

154. Kusminski, C.M. and P.E. Scherer, *Mitochondrial dysfunction in white adipose tissue.* Trends Endocrinol Metab, 2012. 23(9): p. 435-43.

155. Zhang, K. and R.J. Kaufman, *From endoplasmic-reticulum stress to the inflammatory response.* Nature, 2008. 454(7203): p. 455-62.

156. Wilson-Fritch, L., et al., *Mitochondrial biogenesis and remodeling during adipogenesis and in response to the insulin sensitizer rosiglitazone.* Mol Cell Biol, 2003. 23(3): p. 1085-94.

157. Tormos, K.V., et al., *Mitochondrial complex III ROS regulate adipocyte differentiation.* Cell Metab, 2011. 14(4): p. 537-44.

158. Gao, C.L., et al., *Mitochondrial dysfunction is induced by high levels of glucose and free fatty acids in 3T3-L1 adipocytes.* Mol Cell Endocrinol, 2010. 320(1-2): p. 25-33.

159. Wilson-Fritch, L., et al., *Mitochondrial remodeling in adipose tissue associated with obesity and treatment with rosiglitazone.* J Clin Invest, 2004. 114(9): p. 1281-9.

160. Choo, H.J., et al., *Mitochondria are impaired in the adipocytes of type 2 diabetic mice.* Diabetologia, 2006. 49(4): p. 784-91.

161. Keller, M.P. and A.D. Attie, *Physiological insights gained from gene expression analysis in obesity and diabetes.* Annu Rev Nutr, 2010. 30: p. 341-64.

162. Devarakonda, S., et al., *Disorder-to-order transition underlies the structural basis for the assembly of a transcriptionally active PGC-1alpha/ERRgamma complex.* Proc Natl Acad Sci U S A, 2011. 108(46): p. 18678-83.

163. Krishnan, J., et al., *Dietary obesity-associated Hif1alpha activation in adipocytes restricts fatty acid oxidation and energy expenditure via suppression of the Sirt2-NAD+ system.* Genes Dev, 2012. 26(3): p. 259-70.

164. Bogacka, I., et al., *Structural and functional consequences of mitochondrial biogenesis in human adipocytes in vitro.* J Clin Endocrinol Metab, 2005. 90(12): p. 6650-6.

165. Lin, Y., et al., *The hyperglycemia-induced inflammatory response in adipocytes: the role of reactive oxygen species.* J Biol Chem, 2005. 280(6): p. 4617-26.

166. Chen, X.H., et al., *TNF-alpha induces mitochondrial dysfunction in 3T3-L1 adipocytes.* Mol Cell Endocrinol, 2010. 328(1-2): p. 63-9.

167. Houstis, N., E.D. Rosen, and E.S. Lander, *Reactive oxygen species have a causal role in multiple forms of insulin resistance.* Nature, 2006. 440(7086): p. 944-8.

168. Furukawa, S., et al., *Increased oxidative stress in obesity and its impact on metabolic syndrome.* J Clin Invest, 2004. 114(12): p. 1752-61.

169. De Pauw, A., et al., *Mild mitochondrial uncoupling does not affect mitochondrial biogenesis but downregulates pyruvate carboxylase in adipocytes: role for triglyceride content reduction.* Am J Physiol Endocrinol Metab, 2012. 302(9): p. E1123-41.

170. Curtis, J.M., et al., *Downregulation of adipose glutathione S-transferase A4 leads to increased protein carbonylation, oxidative stress, and mitochondrial dysfunction.* Diabetes, 2010. 59(5): p. 1132-42.

171. Van Nieuwenhoven, F.A., G.J. Van der Vusse, and J.F. Glatz, *Membrane-associated and cytoplasmic fatty acid-binding proteins.* Lipids, 1996. 31 Suppl: p. S223-7.

172. Bernlohr, D.A., et al., *Intracellular lipid-binding proteins and their genes.* Annu Rev Nutr, 1997. 17: p. 277-303.

173. Eaton, S., K. Bartlett, and M. Pourfarzam, *Mammalian mitochondrial beta-oxidation.* Biochem J, 1996. 320 (Pt 2): p. 345-57.

174. Watkins, P.A., *Fatty acid activation.* Prog Lipid Res, 1997. 36(1): p. 55-83.

175. Hesler, C.B., C. Olymbios, and D. Haldar, *Transverse-plane topography of long-chain acyl-CoA synthetase in the mitochondrial outer membrane.* J Biol Chem, 1990. 265(12): p. 6600-5.

176. Zammit, V.A., *Carnitine acyltransferases: functional significance of subcellular distribution and membrane topology.* Prog Lipid Res, 1999. 38(3): p. 199-224.

177. Bieber, L.L., *Carnitine.* Annu Rev Biochem, 1988. 57: p. 261-83.

178. Ferdinandusse, S., et al., *Molecular cloning and expression of human carnitine octanoyltransferase: evidence for its role in the peroxisomal beta-oxidation of branched-chain fatty acids.* Biochem Biophys Res Commun, 1999. 263(1): p. 213-8.

179. McGarry, J.D. and N.F. Brown, *The mitochondrial carnitine palmitoyltransferase system. From concept to molecular analysis.* Eur J Biochem, 1997. 244(1): p. 1-14.

180. Kerner, J. and C. Hoppel, *Fatty acid import into mitochondria.* Biochim Biophys Acta, 2000. 1486(1): p. 1-17.

181. McGarry, J.D. and D.W. Foster, *Regulation of hepatic fatty acid oxidation and ketone body production.* Annu Rev Biochem, 1980. 49: p. 395-420.

182. Zammit, V.A., *The malonyl-CoA-long-chain acyl-CoA axis in the maintenance of mammalian cell function.* Biochem J, 1999. 343 Pt 3: p. 505-15.

183. Ruderman, N.B., et al., *Malonyl-CoA, fuel sensing, and insulin resistance.* Am J Physiol, 1999. 276(1 Pt 1): p. E1-E18.

184. Brown, N.F., et al., *Mouse white adipocytes and 3T3-L1 cells display an anomalous pattern of carnitine palmitoyltransferase (CPT) I isoform expression during differentiation. Inter-tissue and inter-species expression of CPT I and CPT II enzymes.* Biochem J, 1997. 327 (Pt 1): p. 225-31.

185. Nyman, L.R., et al., *Homozygous carnitine palmitoyltransferase 1a (liver isoform) deficiency is lethal in the mouse.* Mol Genet Metab, 2005. 86(1-2): p. 179-87.

186. Adams, S.H., et al., *Expression and possible role of muscle-type carnitine palmitoyltransferase I during sperm development in the rat.* Biol Reprod, 1998. 59(6): p. 1399-405.

187. Esser, V., et al., *Expression of a cDNA isolated from rat brown adipose tissue and heart identifies the product as the muscle isoform of carnitine palmitoyltransferase I (M-CPT I). M-CPT I is the predominant CPT I isoform expressed in both white (epididymal) and brown adipocytes.* J Biol Chem, 1996. 271(12): p. 6972-7.

188. Yamazaki, N., et al., *High expression of a novel carnitine palmitoyltransferase I like protein in rat brown adipose tissue and heart: isolation and characterization of its cDNA clone.* FEBS Lett, 1995. 363(1-2): p. 41-5.

189. Price, N., et al., *A novel brain-expressed protein related to carnitine palmitoyltransferase I.* Genomics, 2002. 80(4): p. 433-42.

190. Britton, C.H., et al., *Fine chromosome mapping of the genes for human liver and muscle carnitine palmitoyltransferase I (CPT1A and CPT1B).* Genomics, 1997. 40(1): p. 209-11.

191. Sorensen, A., et al., *Localization of messenger RNAs encoding enzymes associated with malonyl-CoA metabolism in mouse brain.* Brain Res Gene Expr Patterns, 2002. 1(3-4): p. 167-73.

192. Sierra, A.Y., et al., *CPT1c is localized in endoplasmic reticulum of neurons and has carnitine palmitoyltransferase activity.* J Biol Chem, 2008. 283(11): p. 6878-85.

193. Dai, Y., et al., *Localization and effect of ectopic expression of CPT1c in CNS feeding centers.* Biochem Biophys Res Commun, 2007. 359(3): p. 469-74.

194. Gao, S., et al., *Important roles of brain-specific carnitine palmitoyltransferase and ceramide metabolism in leptin hypothalamic control of feeding.* Proc Natl Acad Sci U S A, 2011. 108(23): p. 9691-6.

195. Ramirez, S., et al., *Hypothalamic Ceramide Levels Regulated by CPT1C Mediate the Orexigenic Effect of Ghrelin.* Diabetes, 2013. 62(7): p. 2329-2337.

196. Curran, A.R. and D.M. Engelman, *Sequence motifs, polar interactions and conformational changes in helical membrane proteins.* Curr Opin Struct Biol, 2003. 13(4): p. 412-7.

197. Brandt, J.M., F. Djouadi, and D.P. Kelly, *Fatty acids activate transcription of the muscle carnitine palmitoyltransferase I gene in cardiac myocytes via the peroxisome proliferator-activated receptor alpha.* J Biol Chem, 1998. 273(37): p. 23786-92.

198. Eaton, S., et al., *Myocardial carnitine palmitoyltransferase I as a target for oxidative modification in inflammation and sepsis.* Biochem Soc Trans, 2003. 31(Pt 6): p. 1133-6.

199. Fukumoto, K., et al., *Tyrosine nitration of carnitine palmitoyl transferase I during endotoxaemia in suckling rats.* Biochim Biophys Acta, 2004. 1683(1-3): p. 1-6.

200. Leterrier, J.F., et al., *Interactions between brain mitochondria and cytoskeleton: evidence for specialized outer membrane domains involved in the association of cytoskeleton-associated proteins to mitochondria in situ and in vitro.* Microsc Res Tech, 1994. 27(3): p. 233-61.

201. Guzman, M., et al., *Evidence against direct involvement of phosphorylation in the activation of carnitine palmitoyltransferase by okadaic acid in rat hepatocytes.* Biochem J, 1994. 300 (Pt 3): p. 693-9.

202. Guzman, M., et al., *Inhibition of carnitine palmitoyltransferase I by hepatocyte swelling.* FEBS Lett, 1994. 344(2-3): p. 239-41.

203. Brownsey, R.W., R. Zhande, and A.N. Boone, *Isoforms of acetyl-CoA carboxylase: structures, regulatory properties and metabolic functions.* Biochem Soc Trans, 1997. 25(4): p. 1232-8.

204. Allred, J.B. and K.E. Reilly, *Short-term regulation of acetyl CoA carboxylase in tissues of higher animals.* Prog Lipid Res, 1996. 35(4): p. 371-85.

205. Dyck, J.R., et al., *Characterization of rat liver malonyl-CoA decarboxylase and the study of its role in regulating fatty acid metabolism.* Biochem J, 2000. 350 Pt 2: p. 599-608.

206. Woods, A., et al., *LKB1 is the upstream kinase in the AMP-activated protein kinase cascade.* Curr Biol, 2003. 13(22): p. 2004-8.

207. Yeh, L.A., K.H. Lee, and K.H. Kim, *Regulation of rat liver acetyl-CoA carboxylase. Regulation of phosphorylation and inactivation of acetyl-CoA carboxylase by the adenylate energy charge.* J Biol Chem, 1980. 255(6): p. 2308-14.

208. Lan, F., et al., *SIRT1 modulation of the acetylation status, cytosolic localization, and activity of LKB1. Possible role in AMP-activated protein kinase activation.* J Biol Chem, 2008. 283(41): p. 27628-35.

209. Pillai, V.B., et al., *Exogenous NAD blocks cardiac hypertrophic response via activation of the SIRT3-LKB1-AMP-activated kinase pathway.* J Biol Chem, 2010. 285(5): p. 3133-44.

210. Canto, C., et al., *AMPK regulates energy expenditure by modulating NAD+ metabolism and SIRT1 activity.* Nature, 2009. 458(7241): p. 1056-60.

211. Michan, S. and D. Sinclair, *Sirtuins in mammals: insights into their biological function.* Biochem J, 2007. 404(1): p. 1-13.

212. Schug, T.T. and X. Li, *Sirtuin 1 in lipid metabolism and obesity.* Ann Med, 2011. 43(3): p. 198-211.

213. Morillas, M., et al., *Identification of conserved amino acid residues in rat liver carnitine palmitoyltransferase I critical for malonyl-CoA inhibition. Mutation of methionine 593 abolishes malonyl-CoA inhibition.* J Biol Chem, 2003. 278(11): p. 9058-63.

214. Herrero, L., et al., *Alteration of the malonyl-CoA/carnitine palmitoyltransferase I interaction in the beta-cell impairs glucose-induced insulin secretion.* Diabetes, 2005. 54(2): p. 462-71.

215. Sebastian, D., et al., *CPT I overexpression protects L6E9 muscle cells from fatty acid-induced insulin resistance.* Am J Physiol Endocrinol Metab, 2007. 292(3): p. E677-86.

216. Orellana-Gavalda, J.M., et al., *Molecular therapy for obesity and diabetes based on a long-term increase in hepatic fatty-acid oxidation.* Hepatology, 2011. 53(3): p. 821-32.

217. Orlicky, D.J. and J. Schaack, *Adenovirus transduction of 3T3-L1 cells.* J Lipid Res, 2001. 42(3): p. 460-6.

218. Orlicky, D.J., J. DeGregori, and J. Schaack, *Construction of stable coxsackievirus and adenovirus receptor-expressing 3T3-L1 cells.* J Lipid Res, 2001. 42(6): p. 910-5.

219. Morillas, M., et al., *Identification of the two histidine residues responsible for the inhibition by malonyl-CoA in peroxisomal carnitine octanoyltransferase from rat liver.* FEBS Lett, 2000. 466(1): p. 183-6.

220. Zammit, V.A., *Time-dependence of inhibition of carnitine palmitoyltransferase I by malonyl-CoA in mitochondria isolated from livers of fed or starved rats. Evidence for transition of the enzyme between states of low and high affinity for malonyl-CoA.* Biochem J, 1984. 218(2): p. 379-86.

221. Roduit, R., et al., *A role for hormone-sensitive lipase in glucose-stimulated insulin secretion: a study in hormone-sensitive lipase-deficient mice.* Diabetes, 2001. 50(9): p. 1970-5.

222. Gesta, S., et al., *Mesodermal developmental gene Tbx15 impairs adipocyte differentiation and mitochondrial respiration.* Proc Natl Acad Sci U S A, 2011. 108(7): p. 2771-6.

223. Matthews, D.R., et al., *Homeostasis model assessment: insulin resistance and beta-cell function from fasting plasma glucose and insulin concentrations in man.* Diabetologia, 1985. 28(7): p. 412-9.

224. Perez-Perez, R., et al., *Attenuated metabolism is a hallmark of obesity as revealed by comparative proteomic analysis of human omental adipose tissue.* J Proteomics, 2012. 75(3): p. 783-95.

225. Serra, D., et al., *Mitochondrial Fatty Acid Oxidation in Obesity.* Antioxid Redox Signal, 2012.

226. Mathis, D., *Immunological Goings-on in Visceral Adipose Tissue.* Cell Metab, 2013. 17(6): p. 851-9.

227. Muoio, D.M. and P.D. Neufer, *Lipid-induced mitochondrial stress and insulin action in muscle.* Cell metabolism, 2012. 15(5): p. 595-605.

228. Akkaoui, M., et al., *Modulation of the hepatic malonyl-CoA-carnitine palmitoyltransferase 1A partnership creates a metabolic switch allowing oxidation of de novo fatty acids.* Biochem J, 2009. 420(3): p. 429-38.

229. Gao, X., et al., *Carnitine palmitoyltransferase 1A prevents fatty acid-induced adipocyte dysfunction through suppression of c-Jun N-terminal kinase.* Biochem J, 2011. 435(3): p. 723-32.

230. Vernochet, C., et al., *Adipose-specific deletion of TFAM increases mitochondrial oxidation and protects mice against obesity and insulin resistance.* Cell Metab, 2012. 16(6): p. 765-76.

231. Laurent, G., et al., *SIRT4 Coordinates the Balance between Lipid Synthesis and Catabolism by Repressing Malonyl CoA Decarboxylase.* Mol Cell, 2013. 50(5): p. 686-98.

232. Kusminski, C.M., et al., *MitoNEET-driven alterations in adipocyte mitochondrial activity reveal a crucial adaptive process that preserves insulin sensitivity in obesity.* Nat Med, 2012. 18(10): p. 1539-49.

233. Suganami, T., et al., *Role of the Toll-like receptor 4/NF-kappaB pathway in saturated fatty acid-induced inflammatory changes in the interaction between adipocytes and macrophages.* Arterioscler Thromb Vasc Biol, 2007. 27(1): p. 84-91.

234. Tsukumo, D.M., et al., *Loss-of-function mutation in Toll-like receptor 4 prevents diet-induced obesity and insulin resistance.* Diabetes, 2007. 56(8): p. 1986-98.

235. Koliwad, S.K., et al., *DGAT1-dependent triacylglycerol storage by macrophages protects mice from diet-induced insulin resistance and inflammation.* The Journal of clinical investigation, 2010. 120(3): p. 756-67.

236. Galic, S., et al., *Hematopoietic AMPK beta1 reduces mouse adipose tissue macrophage inflammation and insulin resistance in obesity.* J Clin Invest, 2011. 121(12): p. 4903-15.

237. Sebastian, D., et al., *CPT I overexpression protects L6E9 muscle cells from fatty acid-induced insulin resistance.* American journal of physiology. Endocrinology and metabolism, 2007. 292(3): p. E677-86.

238. Gao, X., et al., *Carnitine palmitoyltransferase 1A prevents fatty acid-induced adipocyte dysfunction through suppression of c-Jun N-terminal kinase.* The Biochemical journal, 2011. 435(3): p. 723-32.

239. Monsenego, J., et al., *Enhancing liver mitochondrial fatty acid oxidation capacity in obese mice improves insulin sensitivity independently of hepatic steatosis.* Journal of hepatology, 2012. 56(3): p. 632-9.

240. Henique, C., et al., *Increased mitochondrial fatty acid oxidation is sufficient to protect skeletal muscle cells from palmitate-induced apoptosis.* The Journal of biological chemistry, 2010. 285(47): p. 36818-27.

241. Seifert, E.L., et al., *Electron transport chain-dependent and -independent mechanisms of mitochondrial H2O2 emission during long-chain fatty acid oxidation.* The Journal of biological chemistry, 2010. 285(8): p. 5748-58.

242. Anderson, E.J., et al., *Mitochondrial H2O2 emission and cellular redox state link excess fat intake to insulin resistance in both rodents and humans.* The Journal of clinical investigation, 2009. 119(3): p. 573-81.

243. Hevener, A.L., et al., *Macrophage PPAR gamma is required for normal skeletal muscle and hepatic insulin sensitivity and full antidiabetic effects of thiazolidinediones.* J Clin Invest, 2007. 117(6): p. 1658-69.

244. Odegaard, J.I., et al., *Macrophage-specific PPARgamma controls alternative activation and improves insulin resistance.* Nature, 2007. 447(7148): p. 1116-20.

245. Kang, K., et al., *Adipocyte-derived Th2 cytokines and myeloid PPARdelta regulate macrophage polarization and insulin sensitivity.* Cell Metab, 2008. 7(6): p. 485-95.

246. Odegaard, J.I., et al., *Alternative M2 activation of Kupffer cells by PPARdelta ameliorates obesity-induced insulin resistance.* Cell Metab, 2008. 7(6): p. 496-507.

247. Vats, D., et al., *Oxidative metabolism and PGC-1beta attenuate macrophage-mediated inflammation.* Cell Metab, 2006. 4(1): p. 13-24.

248. Furuhashi, M., et al., *Treatment of diabetes and atherosclerosis by inhibiting fatty-acid-binding protein aP2.* Nature, 2007. 447(7147): p. 959-65.

249. Makowski, L., et al., *Lack of macrophage fatty-acid-binding protein aP2 protects mice deficient in apolipoprotein E against atherosclerosis.* Nat Med, 2001. 7(6): p. 699-705.

250. Marrades, M.P., et al., *Orchestrated downregulation of genes involved in oxidative metabolic pathways in obese vs. lean high-fat young male consumers.* J Physiol Biochem, 2011. 67(1): p. 15-26.

251. Nadler, S.T., et al., *The expression of adipogenic genes is decreased in obesity and diabetes mellitus.* Proc Natl Acad Sci U S A, 2000. 97(21): p. 11371-6.

252. Dubois, S.G., et al., *Decreased expression of adipogenic genes in obese subjects with type 2 diabetes.* Obesity (Silver Spring), 2006. 14(9): p. 1543-52.

253. Matsuzawa, Y., et al., *Pathophysiology and pathogenesis of visceral fat obesity.* Ann N Y Acad Sci, 1995. 748: p. 399-406.

254. Muoio, D.M. and P.D. Neufer, *Lipid-induced mitochondrial stress and insulin action in muscle.* Cell Metab, 2012. 15(5): p. 595-605.

255. Drynan, L., P.A. Quant, and V.A. Zammit, *Flux control exerted by mitochondrial outer membrane carnitine palmitoyltransferase over beta-oxidation, ketogenesis and tricarboxylic acid cycle activity in hepatocytes isolated from rats in different metabolic states.* Biochem J, 1996. 317 (Pt 3): p. 791-5.

256. Sunny, N.E., et al., *Excessive hepatic mitochondrial TCA cycle and gluconeogenesis in humans with nonalcoholic fatty liver disease.* Cell Metab, 2011. 14(6): p. 804-10.

PUBLICATIONS

Molecular Therapy for Obesity and Diabetes Based on a Long-Term Increase in Hepatic Fatty-Acid Oxidation

Josep M. Orellana-Gavaldà,[1] Laura Herrero,[1] Maria Ida Malandrino,[1] Astrid Pañeda,[2] Maria Sol Rodríguez-Peña,[2] Harald Petry,[2] Guillermina Asins,[1] Sander Van Deventer,[2] Fausto G. Hegardt,[1] and Dolors Serra[1]

Obesity-induced insulin resistance is associated with both ectopic lipid deposition and chronic, low-grade adipose tissue inflammation. Despite their excess fat, obese individuals show lower fatty-acid oxidation (FAO) rates. This has raised the question of whether burning off the excess fat could improve the obese metabolic phenotype. Here we used human-safe nonimmunoreactive adeno-associated viruses (AAV) to mediate long-term hepatic gene transfer of carnitine palmitoyltransferase 1A (CPT1A), the key enzyme in fatty-acid *β*-oxidation, or its permanently active mutant form CPT1AM, to high-fat diet-treated and genetically obese mice. High-fat diet CPT1A- and, to a greater extent, CPT1AM-expressing mice showed an enhanced hepatic FAO which resulted in increased production of CO_2, adenosine triphosphate, and ketone bodies. Notably, the increase in hepatic FAO not only reduced liver triacylglyceride content, inflammation, and reactive oxygen species levels but also systemically affected a decrease in epididymal adipose tissue weight and inflammation and improved insulin signaling in liver, adipose tissue, and muscle. Obesity-induced weight gain, increase in fasting blood glucose and insulin levels, and augmented expression of gluconeogenic genes were restored to normal only 3 months after AAV treatment. Thus, CPT1A- and, to a greater extent, CPT1AM-expressing mice were protected against obesity-induced weight gain, hepatic steatosis, diabetes, and obesity-induced insulin resistance. In addition, genetically obese *db/db* mice that expressed CPT1AM showed reduced glucose and insulin levels and liver steatosis. *Conclusion*: A chronic increase in liver FAO improves the obese metabolic phenotype, which indicates that AAV-mediated CPT1A expression could be a potential molecular therapy for obesity and diabetes. (HEPATOLOGY 2011;53:821-832)

Obesity is a major risk factor for disorders ranging from insulin resistance and type 2 diabetes (T2D) to hepatic steatosis and cardiovascular disease. The incidence of obesity is increasing worldwide and a concerted effort is being made to understand its pathogenesis. Two main mechanisms have been proposed to explain obesity-induced insulin resistance: on the one hand the ectopic deposition of triacylglyceride (TAG) outside the adipose tissue,[1] and on the other, the heightened inflammatory state of the adipose tissue and liver.[2]

However, the ultimate cause of obesity is an energy imbalance between intake and expenditure, leading to the accumulation of excess nutrients in lipid deposits. Therefore, any strategy able to tilt the balance towards fatty-acid oxidation (FAO) could improve obesity-induced disorders. Malonyl-CoA, derived from glucose metabolism and the first intermediate in lipogenesis, regulates FAO by inhibiting carnitine palmitoyltransferase 1 (CPT1). This makes CPT1 the rate-limiting step in mitochondrial fatty-acid *β*-oxidation. Short-

Abbreviations: AAV, adeno-associated viruses; ACC1, acetyl-CoA carboxylase 1; ASP, acid-soluble products; BHB-CoA, β-hydroxybutyryl-CoA; CPT1A, carnitine palmitoyltransferase I liver isoform; DGAT2, diacylglycerol O-acyltransferase homolog 2; GFP, green fluorescent protein; G6Pase, glucose-6-phosphatase; HFD, high-fat diet; HMGS2, hydroxymethylglutaryl-CoA synthase 2; MCD, malonyl-CoA decarboxylase; MCP-1, monocyte chemoattractant protein-1; MTP, microsomal triacylglycerol transfer protein; PDK4, pyruvate dehydrogenase kinase-4; SCD1, stearoyl-Coenzyme A desaturase 1; TAG, triacylglyceride; UCP1, uncoupling protein 1; VLCAD, very long-chain acyl-CoA dehydrogenase.

From the [1]Department of Biochemistry and Molecular Biology, Institut de Biomedicina de la Universitat de Barcelona (IBUB) and CIBER Fisiopatologia de la Obesidad y Nutrición (CIBEROBN), Facultat de Farmacia, Universitat de Barcelona, instead of Faculty of Pharmacy, University of Barcelona, Barcelona, Spain; and [2]Amsterdam Molecular Therapeutics, Amsterdam, The Netherlands.

Supported by the Ministerio de Educaciæn y Ciencia, Spain (Grant SAF2007-61926 to F.G.H.), by Instituto de Salud Carlos III (Grant CB06/03/0026 to F.G.H. and research contract to J.M.O-G), M.I.M. is a recipient of a fellowship from Ministerio de Educacion y Ciencia, Spain.

Current address for Astrid Pañeda: Division of Gene Therapy and Hepatology, Center for Applied Medical Research, University of Navarra, Pamplona, Spain.

term genetic studies that increased FAO in liver showed a decrease in hepatic TAG content[3] and insulin resistance in obese rodents.[4,5] However, to date there is no successful approach to chronically increase FAO and improve whole-animal obesity-induced insulin resistance *in vivo*.

Here we achieved hepatic gene transfer of CPT1A (CPT1 liver isoform) to obese mice by injecting adeno-associated viruses (AAV) into the tail vein. This led to a nonimmunoreactive, long-term increase in lipid oxidation. We also used a mutant but active form of CPT1A (CPT1AM[6]), which is insensitive to malonyl-CoA and therefore leads to a permanent increase in the rate of FAO, independently of the glucose-derived malonyl-CoA levels. Our results show that an increase in hepatic FAO through AAV-mediated gene transfer of CPT1A and CPT1AM reduced obesity-induced hepatic steatosis, weight gain, inflammation, diabetes, and insulin resistance in mice consuming a high-fat diet (HFD). Furthermore, CPT1AM expression also reduced glucose and insulin levels, and liver steatosis in genetically obese *db/db* mice.

Materials and Methods

Adeno-Associated Vectors. AAV vectors, serotype 1, AAV1-AAT-GFP, AAV1-AAT-CPT1A, and AAV1-AAT-CPT1AM were constructed to drive mouse liver expression of green fluorescent protein (GFP), CPT1A, and CPT1AM, respectively. Vector plasmids carried the human albumin enhancer element and the human 1-antitrypsin (EalbAATp) liver-specific promoter described by Kramer et al.[30]; the cDNA sequence of GFP, CPT1A,[31] and CPT1AM[6]; the woodchuck posttranscriptional regulatory element (WPRE, Access. No. AY468-486)[32]; and the bovine growth hormone polyadenosine transcription termination signal [bGH-poly(A)] (bases 2326-2533 GenBank Access. No. M57764). The expression cassette was flanked by two inverted terminal repeats (ITRs) derived from AAV2. AAV1 vectors were produced in insect cells using baculovirus.[33] The vector preparations used had titers of 1×10^{12}, 7.6×10^{11}, and 7.5×10^{11} genome copies (gc)/ml for AAV1-AAT-GFP, AAV1-AAT-CPT1A, and AAV1-AAT-CPT1AM respectively.

Animals. Eight-week-old male C75Bl/6J mice were fed for 10-15 weeks with either NCD (TestDiet D8Y2, 10% Kcal fat) or HFD (TestDiet D8Y1, 60% Kcal fat). Two weeks after diet treatment, AAV1 vectors were administered by tail vein injection in a single dose of 7.5×10^{12} gc/kg of body weight. Mice were killed 4 to 13 weeks after virus injection. Eight-week-old male C75BL/KsJ-*db/db* and C75BL/KsJ-*db*/+ control mice were injected with AAV1 vectors in the tail vein at a single dose of 7.5×10^{12} gc/kg and killed 17 weeks later.

Methods. Primary mouse hepatocytes were isolated by the collagenase method[34] and used to measure FAO to CO_2.[35] Isolation of mitochondria from liver was obtained as described.[36] Measurement of CPT1 activity was determined by the radiometric method.[37] Glucose and pyruvate tolerance tests (2.0 g per kg body weight) were administered by intraperitoneal injection after an overnight fast. Histological examination was done using formalin-fixed, paraffin-embedded tissue sections stained with hematoxylin-eosin at the Pathology Department of the Hospital Clinic of Barcelona.

Statistical Analysis and Other Methods. Data are presented as mean ± SEM. Student *t* test was used for statistical analysis. Differences were considered significant at $P < 0.05$ and complete methods are described in the Supporting Information.

Results

AAV1-Mediated Expression of CPT1A and CPT1AM in Mouse Liver Increases FAO. To deliver CPT1A, CPT1AM, and GFP as a control to the mouse liver we prepared three adeno-associated viruses: AAV1-CPT1A, AAV1-CPT1AM, and AAV1-GFP. The genome of each virus contained the target gene under the control of a liver-specific promoter EalbAATp (Fig. 1A). AAVs were administrated by the tail-vein injection to C57Bl/6J mice that had been feeding for 2 weeks on either normal chow diet (NCD) or HFD. Mice were studied throughout the dietary treatment and killed at either 4 or 13 weeks after AVV administration, for short- or long-term studies, respectively (Fig. 1A). Long-term expression of the virus was evaluated in mice injected with AAV-GFP until they were 33 weeks old (Supporting Fig. 1A-D). Specific

Address reprint requests to: Dolors Serra, Ph.D., Department of Biochemistry and Molecular Biology, Facultat de Farmácia, Universitat de Barcelona, Av. Diagonal 643, E 08028 Barcelona, Spain. E-mail: dserra@ub.edu; fax: (34) 934 024 520.

View this article online at wileyonlinelibrary.com.

DOI 10.1002/hep.24140

Potential conflict of interest: Dr. Van Deventer owns stock in and is a board member of AMT. Dr. Petry is a director at AMT.

Additional Supporting Information may be found in the online version of this article.

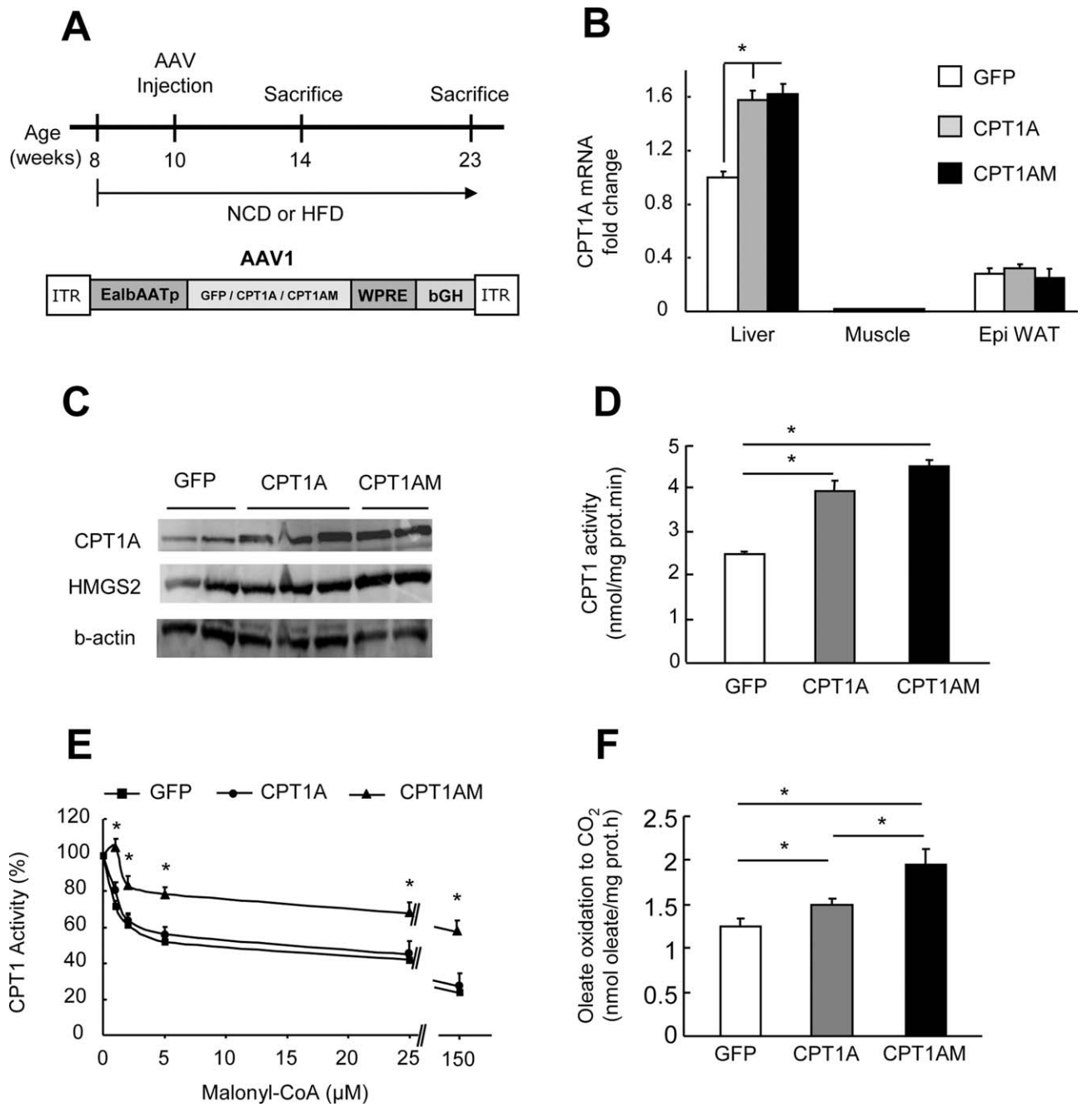

Fig. 1. Increased CPT1A mRNA, protein, activity, and oleate oxidation in CPT1A- and CPT1AM-expressing mice on HFD. (A) Experiment time course and schema of the AAV vectors: AAV-GFP; AAV-CPT1A, and AAV-CPT1AM. The cassettes contain the GFP, CPT1A, or CPT1AM transgene driven by liver specific EalbAATp promoter. (B) CPT1A mRNA expression in liver, epididymal white adipose tissue (epi WAT), and muscle from 14-week-old HFD-treated mice. Primers recognize both CPT1A and CPT1AM sequences. (C) Protein levels from liver mitochondria of HFD mice. (D,E) CPT1 activity from isolated liver mitochondria of HFD-fed mice and CPT1 activity from NCD liver mitochondria enriched cell fractions incubated with different amounts of malonyl-CoA. Data are means ± SEM of six experiments. (F) Oleate oxidation to CO_2 from primary hepatocytes isolated from HFD GFP-, CPT1A-, or CPT1AM-expressing mice. Experiments were done at 4 weeks after the virus treatment. Shown are representative experiments performed in triplicate. n = 6-10. *$P < 0.05$. **$P < 0.05$ versus GFP.

expression of CPT1A and CPT1AM in the liver was measured by quantitative reverse-transcription polymerase chain reaction (qRT-PCR) (Fig. 1B). CPT1A mRNA expression levels were 58% and 62% higher in liver of CPT1A- and CPT1AM-expressing mice, respectively, compared to GFP control mice. No significant differences were seen in other tissues such as muscle or white adipose tissue (Fig. 1B). Liver CPT1 protein and activity levels were increased in those animals injected with AAV-CPT1A and AAV-CPT1AM compared to control AAV-GFP in both HFD (Fig. 1C,D) and NCD (Supporting Fig. 2A,B). Liver

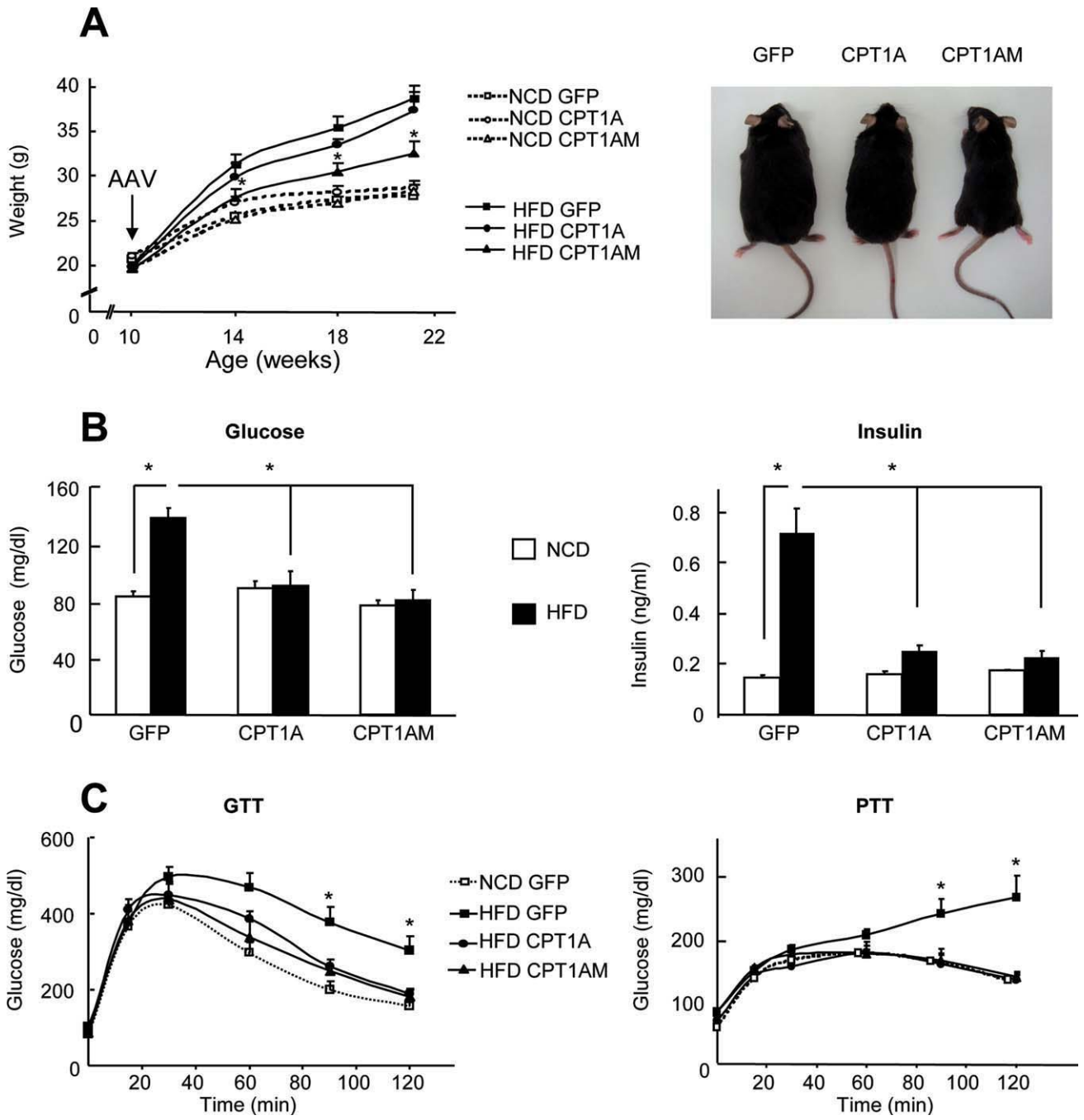

Fig. 2. Metabolic parameters in CPT1A- and CPT1AM-expressing mice. (A) Body weight. *$P < 0.05$ HFD AAV-CPT1AM versus NCD AAV-GFP, left panel and mice receiving CPT1A, and CPT1AM remained leaner than control 3 months after AAV injection and HFD treatment, right panel. (B) Fasting blood glucose, left panel and insulin levels, right panel. (C) Glucose tolerance test, left panel and pyruvate tolerance test, right panel. n = 6-10. *$P < 0.05$.

protein levels increased 3.08 ± 0.2- and 3.01 ± 0.15-fold in HFD CPT1A-, and CPT1AM-expressing mice, respectively, compared to GFP control mice (Supporting Fig. 1E). CPT1 activity was also higher in HFD CPT1A-, and CPT1AM-expressing mice compared to GFP control mice (GFP: 2.51 ± 0.07, CPT1A: 3.96 ± 0.25, and CPT1AM: 4.53 ± 0.15 nmol.mg prot^{-1}.min^{-1}; $P < 0.05$) (Fig. 1D).

CPT1AM is not inhibited by malonyl-CoA in yeast, pancreatic β-cells, muscle cells, or primary rat hepatocytes.[6-9] We measured CPT1 activity in the presence of increasing concentrations of malonyl-CoA in liver mitochondrion-enriched fractions of GFP-, CPT1A-, and CPT1AM-expressing mice. At physiological concentrations of malonyl-CoA (1 to 10 μM), CPT1AM-expressing mice retained up to 78% of their activity,

Table 1. Daily Food Intake and Metabolic Variables in Serum and Liver

	NCD			HFD		
	AAV-GFP	AAV-CPT1A	AAV-CPT1AM	AAV-GFP	AAV-CPT1A	AAV-CPT1AM
Daily food intake (g)	3.43 ± 0.14	3.68 ± 0.12	3.49 ± 0.14	2.72 ± 0.15*	2.91 ± 0.19	2.52 ± 0.13
Serum						
FFA (mM)	0.94 ± 0.1	1.23 ± 0.08	1.24 ± 0.16	1.34 ± 0.08*	1.05 ± 0.07†	1.11 ± 0.08†
TAG (mg/dl)	82.97 ± 6.90	84.31 ± 3.20	78.61 ± 2.70	113.79 ± 10.00*	114.09 ± 9.3	89.96 ± 8.3† ‡
BHB (mM)	1.40 ± 0.04	1.74 ± 0.04†	1.82 ± 0.17†	1.57 ± 0.1*	1.59 ± 0.06	1.90 ± 0.13† ‡
Liver						
BHB-CoA (nmol/g liver)	7.4 ± 0.8	9.7 ± 1.1	12.6 ± 1.3†	6.8 ± 0.9	10.2 ± 1.8	14.6 ± 1.7†
ATP (nmol/g liver)	6.9 ± 0.5	15.4 ± 1.6†	25.1 ± 2.4† ‡	7.2 ± 0.8	16.8 ± 1.2†	23.2 ± 2.8† ‡

Daily food intake and circulating free fatty acids (FFA) and triacylglycerides (TAG) and β-hydroxybutyrate (BHB) and β-hydroxybutyrate-CoA (BHB-CoA) and ATP from 16-week-old overnight fasted mice. Average food intake was calculated for the period between 8 to 14 weeks of age. Data are represented as mean ± S.E.M.

*$P < 0.05$ AAV-GFP HFD versus NCD.

†$P < 0.05$ compared to AAV-GFP on the same diet.

‡$P < 0.05$ compared to AAV-CPT1A versus AAV-CPT1AM on the same diet.

whereas GFP- and CPT1A-expressing mice retained only 48% (Fig. 1E). This indicates that cells expressing CPT1AM will retain most of their CPT1 activity independently of the malonyl-CoA levels. Notably, liver malonyl-CoA levels were similar for GFP-, CPT1A-, and CPT1AM-expressing mice fed on either NCD or HFD (Supporting Fig. 1F).

Next, we examined whether the increase in CPT1 messenger RNA (mRNA), protein, and activity seen in CPT1A- and CPT1AM-expressing mice affected fatty-acid β-oxidation. We isolated primary hepatocytes from GFP-, CPT1A-, and CPT1AM-expressing mice treated with NCD or HFD and measured [1-^{14}C]oleate oxidation to CO_2 and acid-soluble products (ASPs), mainly ketone bodies. In HFD-treated mice, FAO to CO_2 increased by 20.9% ± 0.8%, and 56.4% ± 4.6% in CPT1A- and CPT1AM-expressing mice, respectively, compared to GFP control mice (Fig. 1F). Similar results were obtained for FAO to ASP and total FAO (the sum of oxidation to CO_2 and ASP) in HFD-treated mice (Supporting Fig. 2C,D) and in NCD-treated mice (Supporting Fig. 2E-G). Importantly, oxidation rates were higher in CPT1AM- than in CPT1A-expressing mice, consistent with the higher efficiency of CPT1AM independently of the glucose-derived malonyl-CoA concentrations.

Long-chain fatty-acids undergoing β-oxidation yield acetyl-CoA moieties that have two main possible fates: (1) entry to the Krebs cycle for complete oxidation and adenosine triphosphate (ATP) production, or (2) conversion to ketone bodies. We hypothesized that accelerated β-oxidation due to CPT1A expression could reduce the surplus of acetyl-CoA groups by way of both pathways. Liver ATP levels of CPT1A- and CPT1AM-expressing mice were increased compared to control GFP mice both in NCD and HFD (Table 1). Liver protein levels of mitochondrial hydroxymethylglutaryl-CoA synthase 2 (HMGS2), the rate-limiting enzyme of hepatic ketogenesis, were increased in CPT1A-, and CPT1AM-expressing mice compared to control (Fig. 1C; Supporting Figs. 1E, 2A). Consistent with this, liver and serum levels of ketone bodies such as β-hydroxybutyryl-CoA (BHB-CoA) were higher in CPT1A- and CPT1AM-expressing mice than in GFP control mice both in NCD or HFD (Table 1).

CPT1A and CPT1AM Expression Protected from Obesity-Induced Weight Gain and Insulin Resistance. We next examined the effects of increased β-oxidation on the obese metabolic phenotype. Mice injected with AAV-GFP, AAV-CPT1A, or AAV-CPT1AM were studied under HFD treatment. Although no weight differences were seen in CPT1A- or CPT1AM-expressing mice on NCD, CPT1AM-expressing mice on HFD weighed significantly less than control mice 11 weeks after AAV infection (GFP: 38.7 ± 1.4 g, CPT1AM: 32.5 ± 1.3 g; $P < 0.04$) (Fig. 2A). Interestingly, CPT1AM-expressing mice showed a stronger anti-obesity effect than CPT1A-expressing mice, most likely due to the higher FAO rate observed in the former. The differences in weight gain were not attributable to differences in food consumption because daily rates of food intake were equal in GFP-, CPT1A-, and CPT1AM-expressing mice (Table 1). Notably, fasting blood glucose concentrations (GFP: 128.6 ± 18.0, CPT1A: 87.2 ± 10.7, and CPT1AM: 82.0 ± 7.1 mg/dL; $P < 0.05$) and insulin levels (GFP: 0.72 ± 0.10, CPT1A: 0.25 ± 0.02, and CPT1AM: 0.22 ± 0.02 ng/mL; $P < 0.04$) were lower in both CPT1A-, and CPT1AM-expressing mice than in control mice on HFD, and similar to the levels found

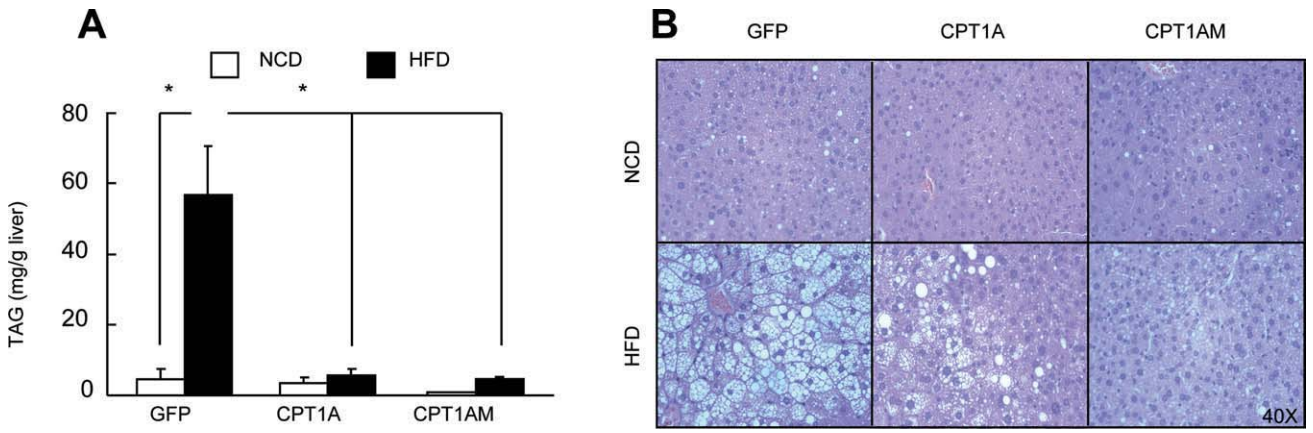

Fig. 3. Liver TAG content and liver histology in CPT1A- and CPT1AM-expressing mice. (A) Liver TAG content of 14-week-old GFP, CPT1A-, and CPT1AM-expressing mice. (B) Liver histological sections (hematoxylin and eosin [H&E] staining) from representative 29-week-old GFP-, CPT1A-, and CPT1AM-expressing littermates. n = 6-10. $*P < 0.05$.

in the mice on NCD (Fig. 2B). Glucose tolerance (measured by way of an intraperitoneal GTT; Fig. 2C, left panel) and gluconeogenesis (measured by way of an intraperitoneal injection of pyruvate; Fig. 2C, right panel) were lower in both CPT1A- and CPT1AM-expressing mice than in HFD control mice. Thus, CPT1A and CPT1AM expression improved the obesity-induced diabetic and insulin-resistant phenotype.

We then examined the effect of the higher FAO levels in CPT1A- and CPT1AM-expressing mice on liver steatosis. Liver TAG content of HFD CPT1A- and CPT1AM-expressing mice was lower than that of HFD control mice (Fig. 3A). Consistent with this, circulating levels of free fatty acids (FFA) and TAG were also reduced (Table 1). Although liver from HFD control mice showed severe centrilobular steatosis, those of CPT1A-, and to a greater extent CPT1AM-expressing mice, were clearly improved (Fig. 3B). CPT1A- and CPT1AM-expression did not affect liver histology in NCD mice (Fig. 3B).

AAV-CPT1A and AAV-CPT1AM-Treatment Reverted the HFD-Induced Increase in Hepatic Gluconeogenesis, Inflammation, and Reactive Oxygen Species (ROS) Levels. We next examined the mechanisms by which accelerated FAO in CPT1A- and CPT1AM-expressing mice improved obesity-induced diabetes and insulin resistance. Four weeks after virus injection hepatic mRNAs levels of genes involved in gluconeogenic, lipogenic, and inflammatory pathways were analyzed. At this short time, glucose (data not shown) and body weight (Fig. 2A) values were already normalized in HFD CPT1AM-expressing mice compared to HFD control mice. mRNA levels of glucose-6-phosphatase (G6Pase) and pyruvate dehydrogenase kinase-4 (PDK4), which are involved in the gluconeogenic and glycolytic pathways, were increased under HFD treatment (Fig. 4A). The increase in G6Pase and PDK4 expression attributed to HFD was restored to NCD values in CPT1A- and CPT1AM-expressing mice. No changes were observed in PEPCK mRNA levels (Supporting Fig. 3A). We next looked at lipogenic enzymes such as acetyl-CoA carboxylase 1 (ACC1), diacylglycerol O-acyltransferase homolog 2 (DGAT2), and the VLDL secretory enzyme microsomal triacylglycerol transfer protein (MTP). ACC1 and DGAT2 expression was lower in the HFD group, but this decrease was restored in CPT1A- and CPT1AM-expressing mice (Fig. 4C). Similar results were seen for other lipogenic genes such as stearoyl-Coenzyme A desaturase 1 (SCD1) and AAC2 mRNA levels (Supporting Fig. 3B,C). Correlating with *de novo* lipogenesis normalization, the HFD-increase of MTP mRNA levels seen in GFP control mice was blunted in CPT1A- and CPT1AM-expressing mice, in which values returned to NCD control levels (Fig. 4C). These results indicated that the increase in liver FAO observed in CPT1A- and CPT1AM-expressing mice improved liver glucose and lipid metabolism.

Obesity-induced insulin resistance has been associated with chronic, low-grade inflammation in liver and adipose tissue.[2] To investigate the involvement of inflammation in the improvement of insulin resistance in CPT1A- and CPT1AM-expressing mice, we measured mRNA levels of several proinflammatory markers. mRNA levels for tumor necrosis factor alpha (TNFα), interleukin (IL)-6, and IL-1β increased 1.56-, 2.30-, and 4.86-fold, respectively, in HFD GFP control mice versus NCD ($P < 0.04$) (Fig. 5A). Importantly, these values were restored to NCD values in both CPT1A- and CPT1AM-expressing mice. Similar results were

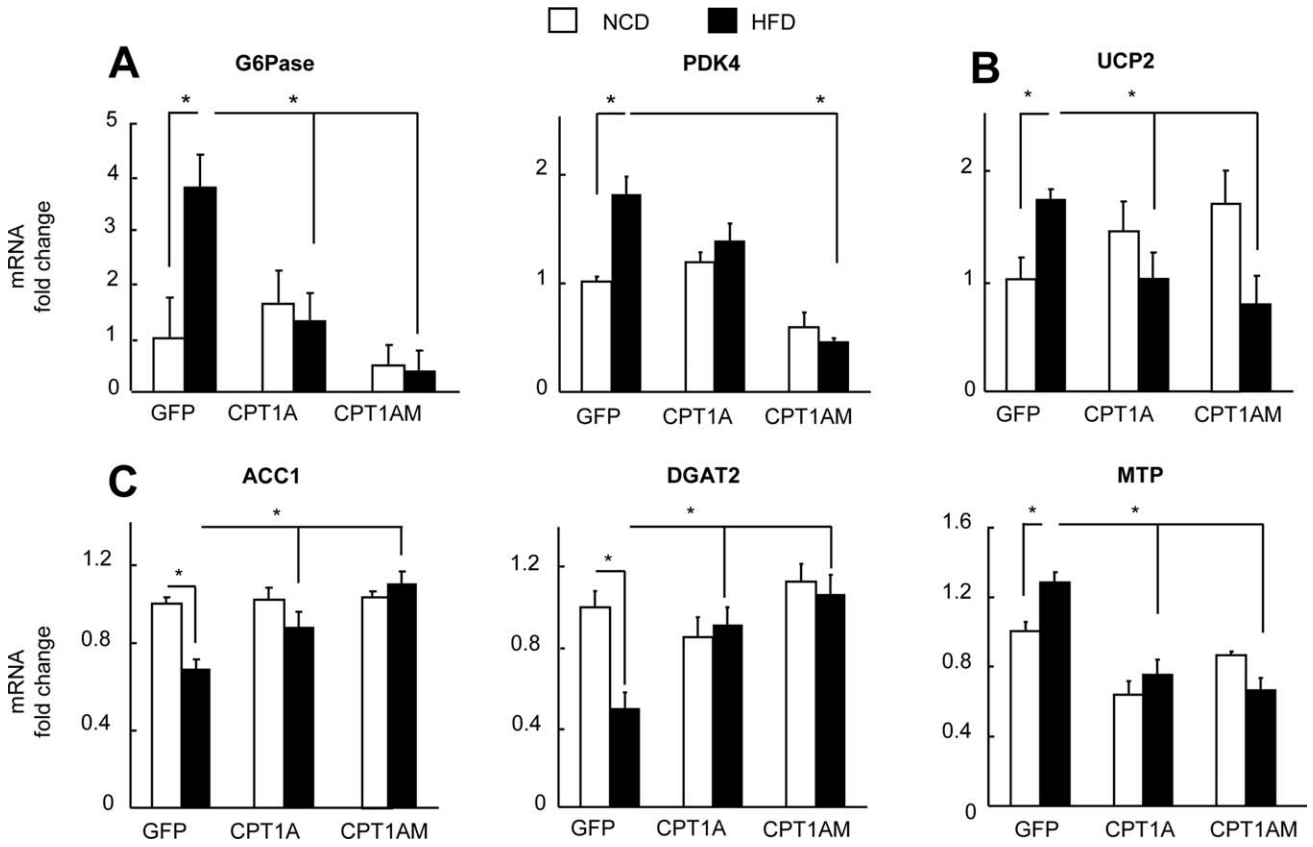

Fig. 4. Liver gene expression. (A-C) mRNA expression in liver of 14-week-old GFP-, CPT1A-, and CPT1AM-expressing mice on NCD (open bars) versus HFD (filled bars). n = 6-10. *$P < 0.05$.

obtained for iNOS, SOCS3, and MCP-1 (Supporting Fig. 3D). Thus, CPT1A and CPT1AM expression and the concomitant increase in FAO reduced obesity-induced inflammatory stress in the liver. Oxidative stress can cause inflammation.[10] Thus, we next evaluated the mRNA expression of the uncoupling protein UCP2, a thermogenic protein and a marker of oxidative stress,[11] and ROS liver levels. Although HFD increased liver UCP2 mRNA levels in control mice, this increase was blunted in CPT1A- and CPT1AM-expressing mice (Fig. 4B). These results are consistent with liver ROS levels analyzed from GFP-, CPT1A-, and CPT1AM-expressing mice under NCD or HFD treatment. HFD increased ROS levels by 77.29% ± 12.33 ($P < 0.05$) in control mice (Fig. 5B). However, ROS levels in CPT1A- and CPT1AM-expressing mice were not significantly different from NCD values.

Altogether, our results indicate that the mechanisms by which CPT1A- and CPT1AM-expressing mice improved obesity-induced insulin resistance and diabetes involve a decrease in gluconeogenesis, restoration of fatty-acid synthesis levels, and decreased inflammatory and ROS levels.

Systemic Effect of Liver CPT1A and CPT1AM Expression. We examined the systemic effect of a chronic increase in liver FAO in adipose tissue. Epididymal adipose tissue weight from CPT1A- and CPT1AM-expressing mice on HFD was reduced by 34.57% ± 7.9%, and 68.15% ± 3.9%, respectively, compared to HFD GFP control mice ($P < 0.01$) (Fig. 6A). The stronger decrease in the epididymal fat pad from CPT1AM-expressing mice is consistent with their higher rate of liver FAO (Fig. 1F). Concordant with the decrease in the adipose tissue weight, leptin serum levels from HFD CPT1A- and CPT1AM-expressing mice were reduced 1.8- and 2.6-fold, respectively, compared to HFD GFP control mice ($P < 0.04$) (Fig. 6B).

Obese adipose tissue is characterized by enlarged adipocytes together with an increase in mononuclear cell infiltration.[12-15] These immune cells surround smaller dying adipocytes forming crown-like structures.[16] Mononuclear cell infiltration was lower in HFD CPT1A-expressing mice, and almost undetectable in HFD CPT1AM-expressing mice (Fig. 6C). Consistent with this, expression of proinflammatory

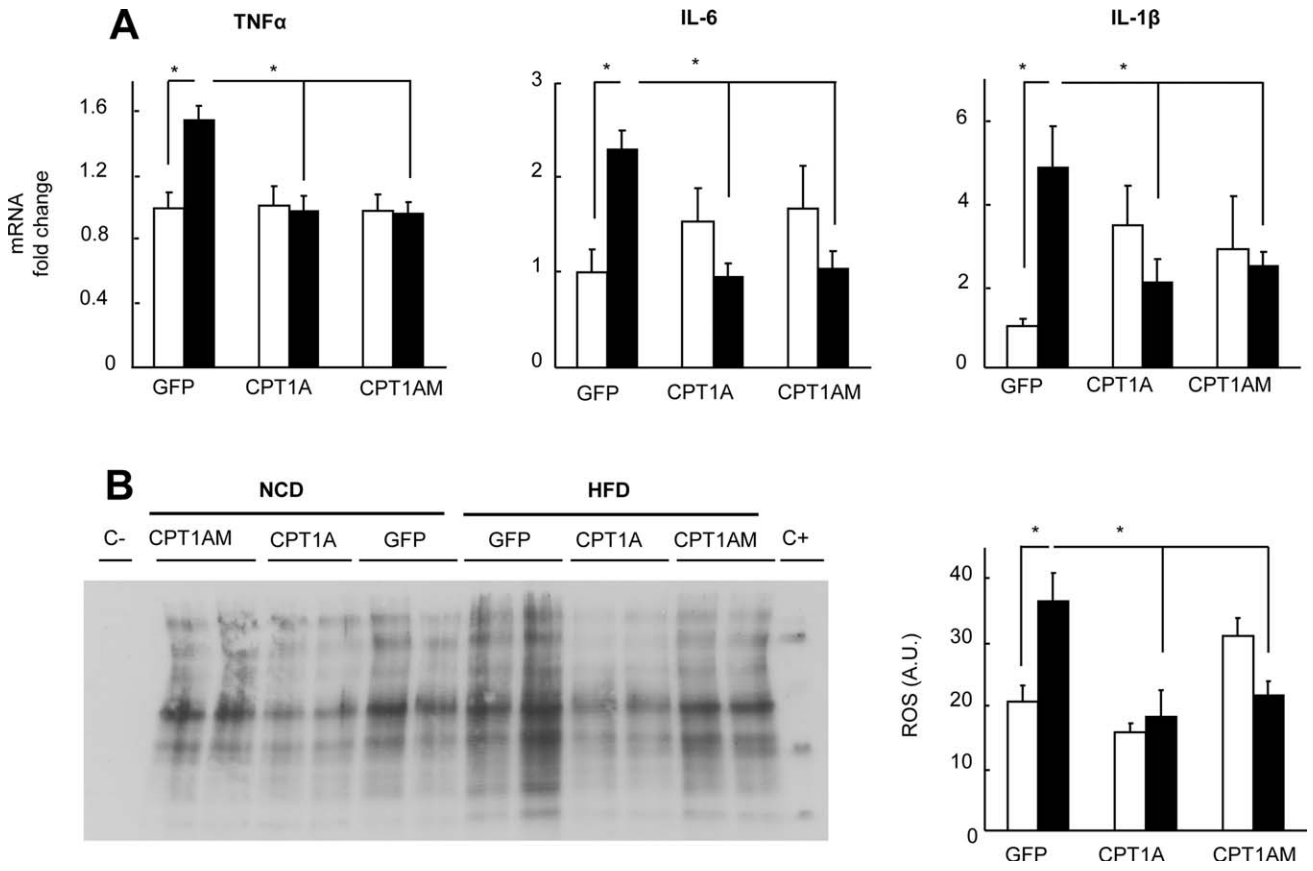

Fig. 5. Liver gene expression and ROS levels. (A) mRNA expression in liver of 14-week-old GFP-, CPT1A-, and CPT1AM-expressing mice on NCD (open bars) versus HFD (filled bars). (B) Analysis and quantification of ROS from liver total extract of 14-week-old GFP-, CPT1A-, and CPT1AM-expressing mice on NCD (open bars) and HFD (filled bars). A.U., arbitrary units. n = 6-10. *$P < 0.05$.

markers such as TNFα, IL-6, and MCP-1 was lower in epididymal fat pads from HFD CPT1A- and CPT1AM-expressing mice than in HFD GFP control mice (Fig. 6D-F).

The effect of an increase in hepatic FAO on insulin signaling was evaluated in liver, adipose tissue, muscle, and spleen. Interestingly, HFD-induced reduction of insulin-stimulated AKT phosphorylation was improved in CPT1A- and CPT1AM-expressing mice not only in liver but also in epididymal adipose tissue and muscle (Fig. 7A). No differences were seen in spleen. This is consistent with the improvements in glucose and insulin levels seen in these mice (Fig. 2B,C).

AAV-CPT1AM-Treatment Improved Obesity-Induced Insulin Resistance and Diabetes in db/db Mice. Because CPT1AM expression gave the strongest effect in terms of FAO, we examined the effect of AAV-CPT1AM-treatment on genetically obese mice. AAV-GFP or AAV-CPT1AM was injected into 8-week-old *db/db* and *db/+* control mice and the metabolic phenotype was analyzed 3 months later. CPT1AM treatment reduced glucose by 41.2% ± 3.5% and insulin levels by 51.3% ± 4.6% in *db/db* mice (Fig. 7B,C). Hepatic steatosis was reduced (Fig. 7D) but no differences were seen in epididymal adipose tissue (Supporting Fig. 3F).

Discussion

It is widely accepted that pharmacological or genetic strategies to enhance FAO may be beneficial for the treatment of obesity and T2D. Shulman and colleagues[1,17] showed that increasing FAO can ameliorate insulin resistance by reducing hepatic and intramyocellular lipid levels. However, increased rates of FAO in muscle have also been associated with skeletal muscle insulin resistance[18,19] due to mitochondrial overload and incomplete FAO.[20] Furthermore, recent studies from Hoehn et al.[21] reported that an increase of FAO has little effect on adiposity and weight gain in mice fed HFD. These findings raise questions about whether strategies that increase FAO *per se* are sufficient to reduce whole-body adiposity *in vivo,* and which are the most appropriate tissue and gene targets. The data presented here support the notion that increased flux of fatty acids exclusively

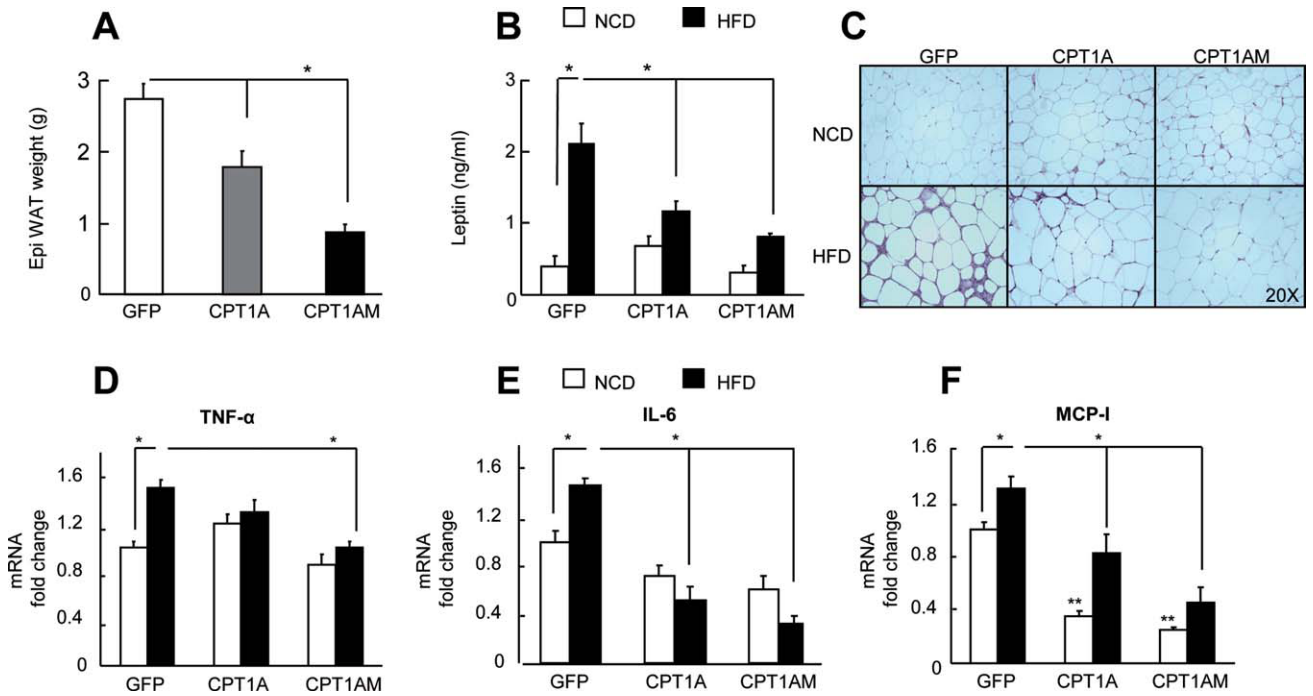

Fig. 6. Adipose tissue weight, circulating leptin, histology, and gene expression. (A) Epididymal white adipose tissue (Epi WAT) weight from GFP-, CPT1A-, and CPT1AM-expressing mice after 11 weeks on HFD. (B) Circulating leptin concentrations from GFP-, CPT1A-, and CPT1AM-expressing mice on NCD (open bars) or HFD (filled bars). (C) Histological sections from epididymal adipose tissue from a representative GFP-, CPT1A-, and CPT1AM-expressing littermates stained with H&E. (D-F) mRNA expression in adipose tissue of 14-week-old GFP-, CPT1A-, and CPT1AM-expressing mice on NCD (open bars) and HFD (filled bars). n = 6-10. *$P < 0.05$. **$P < 0.05$ NCD AAV-GFP versus NCD AAVCPT1A or AAV-CPT1AM.

into liver mitochondria by chronic overexpression of the β-oxidation key enzyme, CPT1A, protects against obesity-induced insulin resistance and T2D.

The beneficial effects of CPT1A and CPT1AM gene transfer reported here were mainly the consequence of three key factors. First, the use of AAV for long-term gene expression. Recombinant AAVs are attractive candidates for use as human gene therapy vehicles because they may overcome the problem of preexisting immunity[22,23] against human AAV serotypes and produce long-term expression of the target genes. Second, the choice of the liver as a target organ, because it plays a central role in both energy expenditure and lipid/glucose homeostasis. And third, the use of a mutant but active form of CPT1A (CPT1AM[6]), which is insensitive to its physiological inhibitor, malonyl-CoA. We and others have shown that expression of CPT1AM leads to a permanent rise in the rate of FAO, independently of the glucose-derived malonyl-CoA levels.[7-9] Overall, the use of AAV-CPT1A and AAV-CPT1AM led to a long-term liver-selective gene transfer that allowed us to evaluate the metabolic impact and underlying mechanisms of increased FAO in HFD and genetically obese mice.

HFD CPT1A- and CPT1AM-expressing mice showed general improvement in hepatic glucose and lipid metabolism as a consequence of increased hepatic fatty acid flux through mitochondria. This, in turn, prevented intracellular lipid accumulation in liver and adipose tissue, especially in CPT1AM-expressing mice. However, increased fatty acid flux in the absence of a concomitant dissipation of FAO metabolites has been associated with enhanced ROS production[24] and a consequent inflammatory state.[10,25,26] Interestingly, CPT1A- and CPT1AM-expressing mice on HFD had normalized liver ROS levels and inflammatory state in both liver and adipose tissue, with a significant decrease in proinflammatory mediators such as TNFα, IL-6, and MCP-1. These results suggest that factors other than a chronic FAO increase *per se* are responsible for ROS production and inflammation. Accumulation of toxic substances (DAG or ceramides),[27] hypoxia,[28] as well as adipose tissue-derived cytokines[2] might participate in the induction of ROS production and inflammation. On the other hand, the beneficial effect of an increased FAO rate observed in HFD CPT1A- and CPT1AM-expressing mice might also be attributed to a concomitant enhancement of hepatic

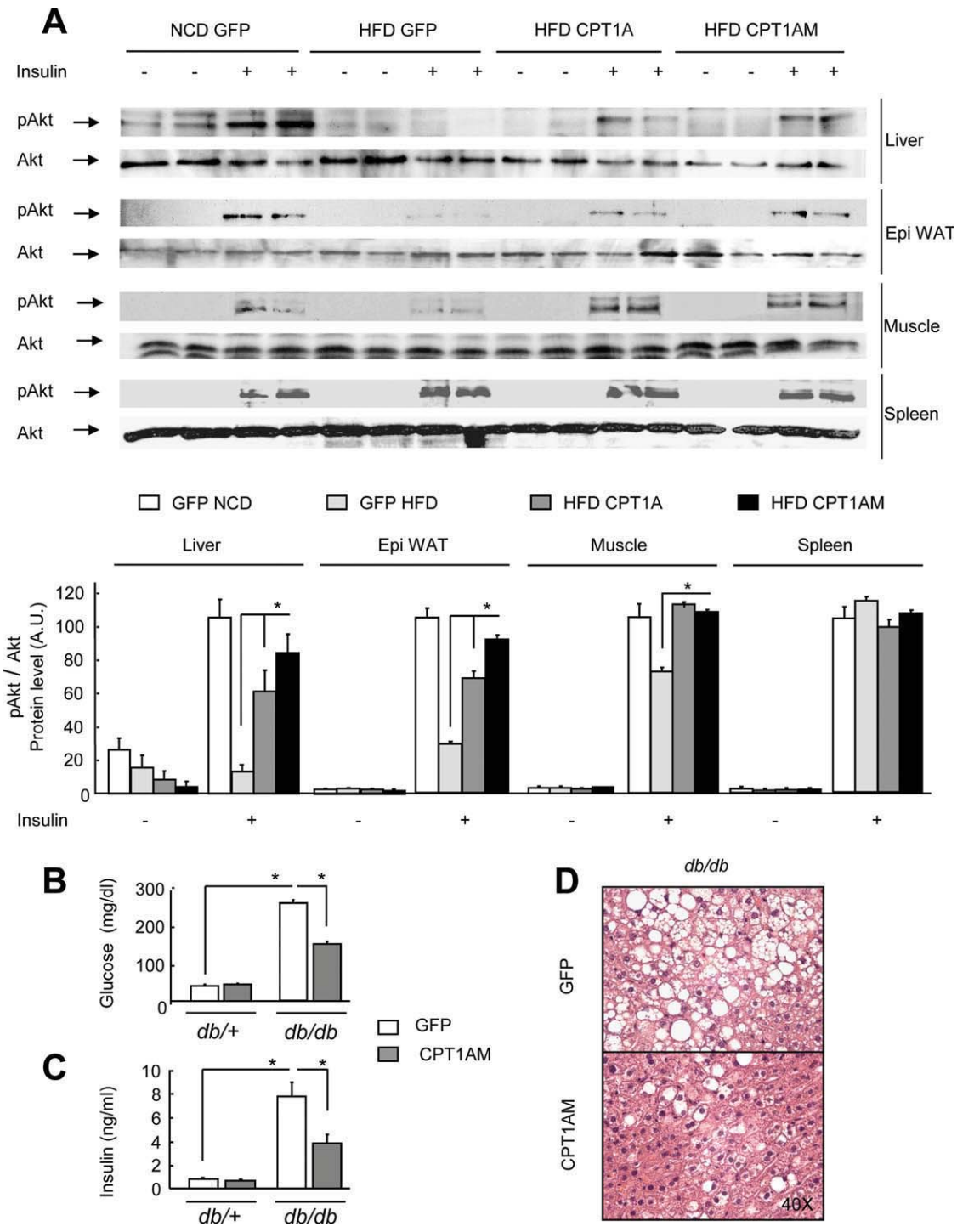

Fig. 7. Improvement of insulin signaling on HFD mice and metabolic parameters in db/db mice. Injected with AAV-CPT1A or AAV-CPT1AM. (A) Insulin signaling in liver and epididymal white adipose tissue (WAT), as indicated by western blotting of insulin-induced AKT phosphorylation (pAKT, Ser473) and quantification of pAKT normalized by total AKT. A.U., arbitrary units. (B) Fasting blood glucose on db/db mice 3 months after AAV injection. (C) Insulin levels on db/db mice 3 months after AAV injection. (D) Liver histological sections from representative db/db mice 3 months after injection with AAV-GFP or AAV-CPT1AM and stained with H&E. n = 8-10. $*P < 0.05$.

ketone body production (present data and[29]). Although to a lesser extent, increased FAO to CO_2, ATP, and ASPs was also observed in NCD CPT1A- and CPT1AM-expressing mice. Importantly, no changes were seen in this case in body weight, hepatic ROS levels, or other hepatic parameters. The present results reinforce the idea that hepatic CPT1A-, and to a greater extent CPT1AM-treatment, is a valid *in vivo* strategy to reduce obesity and improve metabolic parameters without producing undesired alterations on

NCD conditions. However, we cannot rule out possible side effects produced by hepatic FAO induction for periods longer than those tested in this study.

Several authors have focused on treatments to increase FAO in order to reduce hepatic steatosis, such as liver-specific ACC suppression[5] or hepatic MCD overexpression.[4] They reported a decrease in hepatic TAG content and insulin resistance in obese animals, which is consistent with our findings. However, the contribution of an increase in FAO was difficult to discern because these were short-term studies using approaches that also targeted other metabolic functions. In contrast, a direct increase in FAO through adenovirus-mediated overexpression of CPT1A was reported by O'Doherty and colleagues.[3] The latter study also showed a reduction in hepatic TAG levels, although it was too short to reveal any improvement in insulin sensitivity. Our strategy directly and chronically increased FAO in HFD-treated mice. This led to a decrease in hepatic TAG content and circulating FFA and a consequent improvement in insulin signaling, not only in liver but also in muscle and adipose tissue. Thus, AAV-mediated expression of CPT1A, and to a greater extent CPT1AM, protected mice from HFD-induced whole-animal insulin resistance without altering any of these parameters in NCD control mice.

The lack of pathogenicity of the AAV vectors used and the improvement in hepatic steatosis, serum glucose, and insulin levels observed in the severe obesity developed by genetically obese *db/db* mice are encouraging results with which to address new challenges related to this gene transfer system. Further studies will be required to elucidate long-term risks which involve both vector and transgene. Uncertainties surrounding gene transfer such as gene integration, the effects of long latencies, and the probability of subtle effects during long-term gene expression must be studied with care. Furthermore, additional caution is needed regarding the feasibility of extrapolating these data to humans, particularly in nonalcoholic fatty liver disease, which is considered a relatively benign disease.

In summary, we report a novel and efficient gene therapy approach to reduce body weight, liver steatosis, fat accumulation in adipose tissue, and obesity-induced diabetes and insulin resistance in rodents. This was achieved by an AAV-mediated, long-term increase in FAO. These results point towards CPT1A as a new potential therapeutic target against obesity-induced disorders.

Acknowledgment: We thank Gloria Gonzãlez-Aseguinolaza for the supplying EalbAATp promoter, Olga Jãuregui and Eli Bermudo from the Scientific-Technical Services of the University of Barcelona for their technical assistance in the HPLC/MS analysis, and Robin Rycroft of the Language Service for valuable assistance in the preparation of the English manuscript.

References

1. Savage DB, Petersen KF, Shulman GI. Disordered lipid metabolism and the pathogenesis of insulin resistance. Physiol Rev 2007;87: 507-520.
2. Shoelson SE, Herrero L, Naaz A. Obesity, inflammation, and insulin resistance. Gastroenterology 2007;132:2169-2180.
3. Stefanovic-Racic M, Perdomo G, Mantell BS, Sipula IJ, Brown NF, O'Doherty RM. A moderate increase in carnitine palmitoyltransferase 1a activity is sufficient to substantially reduce hepatic triglyceride levels. Am J Physiol Endocrinol Metab 2008;294:E969-E977.
4. An J, Muoio DM, Shiota M, Fujimoto Y, Cline GW, Shulman GI, et al. Hepatic expression of malonyl-CoA decarboxylase reverses muscle, liver and whole-animal insulin resistance. Nat Med 2004;10:268-274.
5. Savage DB, Choi CS, Samuel VT, Liu ZX, Zhang D, Wang A, et al. Reversal of diet-induced hepatic steatosis and hepatic insulin resistance by antisense oligonucleotide inhibitors of acetyl-CoA carboxylases 1 and 2. J Clin Invest 2006;116:817-824.
6. Morillas M, Gomez-Puertas P, Bentebibel A, Selles E, Casals N, Valencia A, et al. Identification of conserved amino acid residues in rat liver carnitine palmitoyltransferase I critical for malonyl-CoA inhibition. Mutation of methionine 593 abolishes malonyl-CoA inhibition. J Biol Chem 2003;278:9058-9063.
7. Herrero L, Rubi B, Sebastian D, Serra D, Asins G, Maechler P, et al. Alteration of the malonyl-CoA/carnitine palmitoyltransferase I interaction in the beta-cell impairs glucose-induced insulin secretion. Diabetes 2005;54:462-471.
8. Sebastian D, Herrero L, Serra D, Asins G, Hegardt FG. CPT I overexpression protects L6E9 muscle cells from fatty acid-induced insulin resistance. Am J Physiol Endocrinol Metab 2007;292:E677-E686.
9. Akkaoui M, Cohen I, Esnous C, Lenoir V, Sournac M, Girard J, et al. Modulation of the hepatic malonyl-CoA-carnitine palmitoyltransferase 1A partnership creates a metabolic switch allowing oxidation of de novo fatty acids. Biochem J 2009;420:429-438.
10. Furukawa S, Fujita T, Shimabukuro M, Iwaki M, Yamada Y, Nakajima Y, et al. Increased oxidative stress in obesity and its impact on metabolic syndrome. J Clin Invest 2004;114:1752-1761.
11. Echtay KS, Roussel D, St-Pierre J, Jekabsons MB, Cadenas S, Stuart JA, et al. Superoxide activates mitochondrial uncoupling proteins. Nature 2002;415:96-99.
12. Weisberg SP, McCann D, Desai M, Rosenbaum M, Leibel RL, Ferrante AW Jr. Obesity is associated with macrophage accumulation in adipose tissue. J Clin Invest 2003;112:1796-1808.
13. Feuerer M, Herrero L, Cipolletta D, Naaz A, Wong J, Nayer A, et al. Lean, but not obese, fat is enriched for a unique population of regulatory T cells that affect metabolic parameters. Nat Med 2009;15: 930-939.
14. Lumeng CN, Maillard I, Saltiel AR. T-ing up inflammation in fat. Nat Med 2009;15:846-847.
15. Liu J, Divoux A, Sun J, Zhang J, Clement K, Glickman JN, et al. Genetic deficiency and pharmacological stabilization of mast cells reduce diet-induced obesity and diabetes in mice. Nat Med 2009;15: 940-945.
16. Strissel KJ, Stancheva Z, Miyoshi H, Perfield JW 2nd, DeFuria J, Jick C, et al. Adipocyte death, adipose tissue remodeling, and obesity complications. Diabetes 2007;56:2910-2918.
17. Choi CS, Savage DB, Abu-Elheiga L, Liu ZX, Kim S, Kulkarni A, et al. Continuous fat oxidation in acetyl-CoA carboxylase 2 knockout mice increases total energy expenditure, reduces fat mass, and improves insulin sensitivity. Proc Natl Acad Sci U S A 2007;104:16480-16485.

18. Finck BN, Bernal-Mizrachi C, Han DH, Coleman T, Sambandam N, LaRiviere LL, et al. A potential link between muscle peroxisome proliferator-activated receptor-alpha signaling and obesity-related diabetes. Cell Metab 2005;1:133-144.
19. Koves TR, Ussher JR, Noland RC, Slentz D, Mosedale M, Ilkayeva O, et al. Mitochondrial overload and incomplete fatty acid oxidation contribute to skeletal muscle insulin resistance. Cell Metab 2008;7: 45-56.
20. Muoio DM, Koves TR. Skeletal muscle adaptation to fatty acid depends on coordinated actions of the PPARs and PGC1 alpha: implications for metabolic disease. Appl Physiol Nutr Metab 2007;32: 874-883.
21. Hoehn KL, Turner N, Swarbrick MM, Wilks D, Preston E, Phua Y, et al. Acute or chronic upregulation of mitochondrial fatty acid oxidation has no net effect on whole-body energy expenditure or adiposity. Cell Metab;11:70-76.
22. Berns KI, Linden RM. The cryptic life style of adeno-associated virus. Bioessays 1995;17:237-245.
23. Zincarelli C, Soltys S, Rengo G, Rabinowitz JE. Analysis of AAV serotypes 1-9 mediated gene expression and tropism in mice after systemic injection. Mol Ther 2008;16:1073-1080.
24. Pessayre D, Fromenty B, Mansouri A. Mitochondrial injury in steatohepatitis. Eur J Gastroenterol Hepatol 2004;16:1095-1105.
25. Lin Y, Berg AH, Iyengar P, Lam TK, Giacca A, Combs TP, et al. The hyperglycemia-induced inflammatory response in adipocytes: the role of reactive oxygen species. J Biol Chem 2005;280:4617-4626.
26. Shoelson SE, Lee J, Goldfine AB. Inflammation and insulin resistance. J Clin Invest 2006;116:1793-1801.
27. Summers SA. Ceramides in insulin resistance and lipotoxicity. Prog Lipid Res 2006;45:42-72.
28. Hosogai N, Fukuhara A, Oshima K, Miyata Y, Tanaka S, Segawa K, et al. Adipose tissue hypoxia in obesity and its impact on adipocytokine dysregulation. Diabetes 2007;56:901-911.
29. Drynan L, Quant PA, Zammit VA. Flux control exerted by mitochondrial outer membrane carnitine palmitoyltransferase over beta-oxidation, ketogenesis and tricarboxylic acid cycle activity in hepatocytes isolated from rats in different metabolic states. Biochem J 1996;317(Pt 3):791-795.
30. Kramer MG, Barajas M, Razquin N, Berraondo P, Rodrigo M, Wu C, et al. In vitro and in vivo comparative study of chimeric liver-specific promoters. Mol Ther 2003;7:375-385.
31. Esser V, Britton CH, Weis BC, Foster DW, McGarry JD. Cloning, sequencing, and expression of a cDNA encoding rat liver carnitine palmitoyltransferase I. Direct evidence that a single polypeptide is involved in inhibitor interaction and catalytic function. J Biol Chem 1993;268: 5817-5822.
32. Donello JE, Loeb JE, Hope TJ. Woodchuck hepatitis virus contains a tripartite posttranscriptional regulatory element. J Virol 1998;72: 5085-5092.
33. Urabe M, Ding C, Kotin RM. Insect cells as factory to produce adeno-associated virus type 2 vectors. Hum Gene Ther 2002;13:1935-1943.
34. Dentin R, Pegorier JP, Benhamed F, Foufelle F, Ferre P, Fauveau V, et al. Hepatic glucokinase is required for the synergistic action of ChREBP and SREBP-1c on glycolytic and lipogenic gene expression. J Biol Chem 2004;279:20314-20326.
35. Veerkamp JH, van Moerkerk TB, Glatz JF, Zuurveld JG, Jacobs AE, Wagenmakers AJ. 14CO2 production is no adequate measure of [14C]fatty acid oxidation. Biochem Med Metab Biol 1986;35:248-259.
36. Rubi B, Antinozzi PA, Herrero L, Ishihara H, Asins G, Serra D, et al. Adenovirus-mediated overexpression of liver carnitine palmitoyltransferase I in INS1E cells: effects on cell metabolism and insulin secretion. Biochem J 2002;364:219-226.
37. Morillas M, Clotet J, Rubi B, Serra D, Asins G, Arino J, et al. Identification of the two histidine residues responsible for the inhibition by malonyl-CoA in peroxisomal carnitine octanoyltransferase from rat liver. FEBS Lett 2000;466:183-186.

ANTIOXIDANTS & REDOX SIGNALING
Volume 00, Number 00, 2012

DOI: 10.1089/ars.2012.4875

FORUM REVIEW ARTICLE

Mitochondrial Fatty Acid Oxidation in Obesity

Dolors Serra, Paula Mera, Maria Ida Malandrino, Joan Francesc Mir, and Laura Herrero

Abstract

Significance: Current lifestyles with high-energy diets and little exercise are triggering an alarming growth in obesity. Excess of adiposity is leading to severe increases in associated pathologies, such as insulin resistance, type 2 diabetes, atherosclerosis, cancer, arthritis, asthma, and hypertension. This, together with the lack of efficient obesity drugs, is the driving force behind much research. ***Recent Advances:*** Traditional anti-obesity strategies focused on reducing food intake and increasing physical activity. However, recent results suggest that enhancing cellular energy expenditure may be an attractive alternative therapy. ***Critical Issues:*** This review evaluates recent discoveries regarding mitochondrial fatty acid oxidation (FAO) and its potential as a therapy for obesity. We focus on the still controversial beneficial effects of increased FAO in liver and muscle, recent studies on how to potentiate adipose tissue energy expenditure, and the different hypotheses involving FAO and the reactive oxygen species production in the hypothalamic control of food intake. ***Future Directions:*** The present review aims to provide an overview of novel anti-obesity strategies that target mitochondrial FAO and that will definitively be of high interest in the future research to fight against obesity-related disorders. *Antioxid. Redox Signal.* 00, 000–000.

Obesity: Molecular and Pathophysiological Features

Obesity is defined as abnormal or excessive fat accumulation in the adipose tissue and other organs. The World Health Organization (WHO) defines overweight as a body mass index (BMI; calculated as weight [kg] divided by height squared [m^2]) equal to or greater than 25 kg/m^2 and obese as a BMI equal to or greater than 30 kg/m^2 (137). Current lifestyle trends and continuous nutrient excess are causing obesity to increase at alarming rates, especially in young people. There are more than 500 million obese people worldwide and, more importantly, overweight and obesity are the fifth leading risk for death globally (137). Humanity is facing a new epidemic already dubbed "Prosperity's Plague" (160). Therefore, significant research is needed in the race to find effective therapies and to minimize the enormous costs of the related healthcare.

Weight gain is influenced by several factors, such as genetics, maternal and perinatal environment, energy-dense diets, and sedentary lifestyle (3). Of great concern are the concurrent and parallel increases in the prevalence of pathological conditions associated with obesity, which include insulin resistance, type 2 diabetes, cardiovascular disease, nonalcoholic fatty liver, polycystic ovary syndrome, asthma, Alzheimer's disease, and some forms of cancer. Elucidating the causes involved in the pathophysiology of obesity-related disorders is one of the most critical endeavors in modern medical research.

Several mechanisms have emerged in the past two decades, during which obesity and especially its connection to insulin resistance have become a top-interest research topic being studied by leading groups in the field.

Ectopic-fat deposition

When the adipose tissue cannot store excess fat, lipids accumulate inappropriately in the liver, muscle, and pancreas. This lipotoxic environment, mainly mediated by diacylglycerols (DAGs), blocks correct glucose transport and insulin signaling (145). Thus, it has been postulated that any strategy that could block the entry of fatty acids (FAs) into the cell, promote fatty acid oxidation (FAO), or convert DAGs into triglycerides (TGs) could prevent insulin resistance (160).

Inflammation

The pathophysiology of obesity-induced insulin resistance has also been correlated with an increase in circulation and tissue inflammation originating in the adipocyte damage and infiltration of immune cells (107, 151). As fat accumulates in adipose tissue, adipocytes overcome their healthy size limit (157, 169) and release inflammatory cytokines and molecules

Department of Biochemistry and Molecular Biology, Facultat de Farmàcia, Universitat de Barcelona, Institut de Biomedicina de la Universitat de Barcelona (IBUB), and CIBER Fisiopatología de la Obesidad y la Nutrición (CIBEROBN), Instituto de Salud Carlos III, Barcelona, Spain.

known as adipokines. The excessive accumulation of lipids in the adipose tissue leads to adipocyte hypoxia (73), endoplasmic reticulum (ER) stress (132), and cell death, and causes FA spillover (145). Infiltrated immune cells also contribute to this chronic low-grade inflammatory milieu, whereby the increase in inflammatory cytokines causes insulin resistance elsewhere in the body. Thus, anti-inflammatory strategies become central as possible new treatments of insulin resistance and other complications of obesity (56).

ER stress

The fundamental role of ER is the integration of multiple metabolic signals and the maintenance of cell homeostasis (26, 58). Under stress conditions that challenge its function, ER triggers an adaptive response called uncoupled protein response (UPR) (97, 178). To resolve ER stress, UPR promotes a decrease in protein synthesis, and at the same time, an increase in protein degradation and chaperone production for protein folding. During the chronic energy surplus associated with obesity, ER cannot recover its normal function and UPR activation contributes to the development of insulin resistance through several mechanisms, such as JNK-Ap1 and NF-Kβ-IKK signaling pathways, inflammation, and oxidative stress (74).

Food intake

The central nervous system, specifically the hypothalamus, is of crucial importance in obesity-induced pathologies, since it plays a major role in the control of food intake and regulation of body weight (177). The discovery of leptin was a major breakthrough for our current knowledge of energy homeostasis (179). This adipocyte-secreted hormone acts on the hypothalamus to inhibit food intake and control body weight and has proved essential in the interaction between the brain and other organs in obesity-related disorders (51). The alteration of the circadian rhythm has also been associated with an increased risk of obesity (63, 76), proving that it is not only what you eat, but also when you eat it. Thus, advances in understanding the molecular mechanisms linking circadian rhythms and metabolism may provide new therapies for obesity and other pathologies associated with the disruption of normal sleep–wake cycles.

Lack of Efficacy of Current Anti-Obesity Drugs

Obesity develops when energy intake exceeds energy expenditure. Thus, any treatment for obesity-induced disorders must reduce energy intake, increase energy expenditure, or have an effect on both. Attempting to lose weight only by caloric restriction comes up against the problem that mammals have evolved mechanisms to store energy to survive during periods of starvation. Such homeostatic mechanisms increase caloric efficiency, thus making further weight loss even more difficult. In recent years, several anti-obesity drugs designed to limit energy intake have been withdrawn from the market due to serious adverse effects (*i.e.,* fenfluramine, dexfenfluramine, sibutramine, and rimonabant) (36). Nowadays, only two drugs are approved specifically for weight loss by the US Food and Drug Administration (FDA): the lipase-inhibitor Orlistat that is also approved by the European Medicines Agency (EMA), but has a limited long-term effectiveness (36), and the recently approved serotonergic Lorcaserin-Belviq (84, 126). Thus, more efforts are needed to develop new anti-obesity agents. In this regard, strategies designed to increase lipid mobilization and oxidation could be very useful in the treatment of obesity and associated diseases.

Mitochondrial FAO and Bioenergetics

Hormones, such as insulin, glucagon, and noradrenaline, control the extracellular uptake and intracellular release of the main cell fuels; namely, carbohydrates and FAs. Once inside the cell, FAs are esterified, metabolized to lipid second messengers, or β-oxidized in mitochondria. The first step of the oxidative pathway is the transport of long-chain FAs (LCFAs) into the mitochondrial matrix (Fig. 1). This step is controlled by the carnitine palmitoyltransferase (CPT) system, which consists of three proteins: CPT1, acylcarnitine translocase (CACT), and CPT2 (109). Malonyl-CoA, a molecule derived from glucose metabolism and the first intermediate in lipogenesis, regulates FAO by inhibiting CPT1, thus making this enzyme the rate-limiting step in mitochondrial oxidation of FAs. Mammal tissues express three isoforms of CPT1: CPT1A (41) (liver), CPT1B (175) (muscle and heart), and CPT1C (138) (brain). Acetyl-CoA carboxylase (ACC), which controls the synthesis of malonyl-CoA; malonyl-CoA decarboxylase

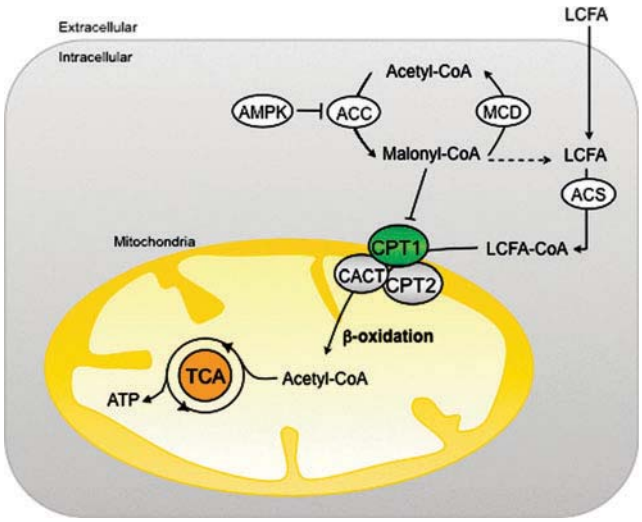

FIG. 1. Mitochondrial fatty acid oxidation (FAO). Long-chain fatty acid (LCFA) catalysis implies activation by acyl-CoA synthase (ACS) of LCFAs into LCFA-CoA, which is a substrate for the mitochondrial carnitine palmitoyltransferase 1 (CPT1) enzyme. The CPT system, which includes CPT1, acylcarnitine translocase (CACT), and CPT2, allows LCFA-CoA to enter the mitochondrial matrix, *via* transesterification reactions, to then be β-oxidized. CPT1 is the rate-limiting enzyme in FAO since its activity is tightly regulated by the glucose-derived malonyl-CoA, generated by acetyl-CoA carboxylase (ACC) during fatty acid (FA) *de novo* formation (in energetically abundant situations) or degraded by malonyl-CoA decarboxylase (MCD) in a process regulated by AMP-activated protein kinase (AMPK). Acetyl-CoA generated in FAO eventually enters the tricarboxylic acid (TCA) cycle to obtain reductive power for cellular respiration and produce ATP. (To see this illustration in color, the reader is referred to the web version of this article at www.liebertpub.com/ars.)

(MCD), which catalyzes malonyl-CoA degradation; and CPT1, which is regulated by malonyl-CoA, are components of a metabolic signaling network that perceives the level of fuel stimuli (109).

One of the main regulators of this network is the AMP-activated protein kinase (AMPK). This protein is the downstream element of a kinase cascade, activated by its phosphorylation in the Thr172 residue of the catalytic subunit (174). In general, AMPK inhibits ATP-consuming processes, while activating catabolic pathways. Active AMPK phosphorylates and inhibits ACC and reduces the expression of FA synthase, thus decreasing the flux of substrates in the FA anabolic pathway (176). In consequence, the reduction in malonyl-CoA levels leads to an increase in CPT1 activity and FAO.

The regulation of AMPK by members of the sirtuin family of NAD^+-dependent protein deacetylases and ADP-ribosyltransferases (sirtuins) has been reported (94). Sirtuin 1 (SIRT1) and SIRT3 stimulate AMPK by deacetylating its upstream activator, kinase LKB1 (94, 135). In turn, the AMPK activity leads to an increase in NAD^+ levels, thereby promoting deacetylation/activation of other SIRT1 targets involved in FAO, like peroxisome proliferator-activated receptor γ coactivator-1α (PGC-1α) (18). In recent years, sirtuins have emerged as critical modulators of lipid metabolism and specifically of FAO. In mammals, the seven identified members of the sirtuin family are differentially located within the cell: SIRT1, 6 and 7 are mainly located in the nucleus; SIRT3, 4 and 5 are located in the mitochondria; and SIRT2 is a cytosolic protein (111). In specific tissues, sirtuins act on different targets promoting FAO (liver and skeletal muscle [SkM]), mitochondrial respiration (brown adipose tissue [BAT]), lipolysis (white adipose tissue [WAT]), and food intake (hypothalamus) (148).

Energy flow in living cells (bioenergetics) takes place mainly in mitochondria. Energy is obtained from FAs and other nutrients in the form of ATP—the chemical currency of life—through the tricarboxylic acid (TCA) cycle, and the electron transport chain (ETC) in a process known as oxidative phosphorylation (162) (Fig. 2). This process is the main source of reactive oxygen species (ROS) in the cell. In the ETC, the energy of electrons from NADH and $FADH_2$ is used to pump protons (H^+) from the mitochondrial matrix to the intermembrane space and generate the electrochemical gradient necessary for ATP synthesis. However, when these electrons escape the ETC, ROS are produced in the mitochondria. Even under physiological conditions, the incomplete electron transfer to O_2, resulting in ROS production, occurs with 0.2%–2% of oxygen molecules (21). Mitochondrial ROS production is highly regulated and important for various cell functions, as ROS can act as signaling molecules. However, high ROS levels are associated with significant cell damage and mitochondrial dysfunction in a process known as oxidative stress (122), usually associated with the etiology of obesity, insulin resistance, and type 2 diabetes (67).

In the mitochondria, the ETC complexes remain electron-bounded when the proton gradient between the mitochondrial matrix and the intermembrane space is high, preventing the outward pumping of H^+ and increasing ROS production. Mitochondrial uncoupling proteins (UCPs) uncouple ATP production from mitochondrial respiration, thereby reducing the H^+ gradient across the inner mitochondrial membrane and relieving the formation of ROS (106). In BAT, UCP1 dissipates energy as heat and plays a key role in adaptive thermogenesis. In other tissues, the UCP homologues (UCP2, 3, and 4) affect ROS production and have crucial roles in energy homeostasis (106).

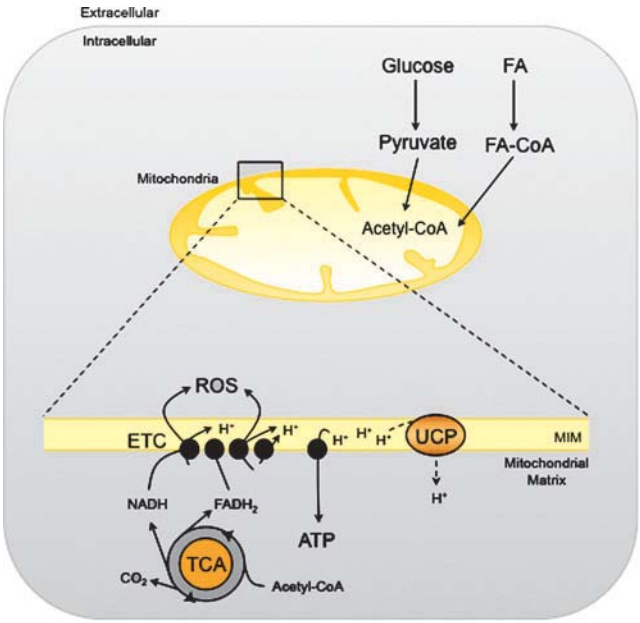

FIG. 2. Bioenergetics and mitochondrial metabolism. The mitochondrial fuels, glucose, and FAs, are converted to acetyl-CoA, which can be further metabolized to obtain energy. The TCA cycle generates protons (H^+) and electrons that are carried by NADH and FADH to the electron transport chain (ETC), where the protons are transported to the mitochondrial intermembrane (MIM) space to generate energy as ATP. Highly reactive electrons may leak from the ETC and generate reactive oxygen species (ROS), which could act physiologically as signaling molecules, but can also cause significant cellular damage when overproduced. Uncoupling proteins (UCPs) dissipate the proton gradient and scavenge ROS accumulation, thus dissipating energy as heat. (To see this illustration in color, the reader is referred to the web version of this article at www.liebertpub.com/ars.)

The Central Role of Liver in Obesity

Fatty liver and nonalcoholic steatohepatitis

The liver plays a central role in both energy expenditure and lipid/glucose homeostasis. In conditions associated with prolonged excess of energy or impaired FA metabolism, the liver stores considerable amounts of lipids in a process that leads to nonalcoholic fatty liver disease (NAFLD). A hallmark of NAFLD is the accumulation of hepatic TGs, which originate in the increased availability of free FAs (FFAs; circulating and from *de novo* lipogenesis), altered FAO and inadequate synthesis and export of VLDL (37, 55). The imbalance between these inputs and outputs results in lipid accumulation in hepatocytes, which causes hepatosteatosis and insulin resistance. The progression of a more severe liver disease triggers nonalcoholic steatohepatitis (NASH), a serious condition of inflamed fatty liver that can further progress to liver fibrosis and cirrhosis (32, 155). The pathogenesis of NAFLD in human and animal models has been reviewed in seminal articles (27, 161). The mechanisms underlying NAFLD to NASH

progression are not completely understood. However, the alteration of FA metabolism and ROS production, which lead to mitochondrial dysfunction, and the induction of proinflammatory cytokines and fibrosis have emerged as key components that ultimately cause this liver disease (47).

Alterations of mitochondrial FAO and ROS production

Mitochondria play a vital role in the oxidation of FAs and ROS production. In the liver, mitochondrial FAO results either in complete oxidation to carbon dioxide or in partial oxidation to ketone bodies, which are exported to provide fuel for other tissues. The key step is catalyzed by CPT1A (109). Data on the rates of mitochondrial FAO and CPT1A activity in NAFLD/NASH are not conclusive, possibly because of the use of different models and parameters. *In vitro* and *in vivo* studies of liver or hepatocytes exposed to high FFA concentrations show both increased (25, 44, 112, 116) and decreased (43) mitochondrial FAO. Similarly controversial results were obtained with CPT1A expression and activity. An increase in CPT1A expression has been reported in several rodent models (14, 134). However, a considerable decrease in the expression of this enzyme was observed in NAFLD patients (123). Several mechanisms may explain these controversial data: (i) the variation of malonyl-CoA levels that depend on the expression and activity of AAC/MCD enzymes (24, 39); (ii) the loss of CPT1 sensitivity to malonyl-CoA, which alters CPT1 activity (29, 133); and (iii) the increased pool of FFAs or lipid derivatives in hepatocytes may activate transcription factors, such as PPARs (PPARα, PPARβ/δ), which in turn may enhance CPT1 expression and FAO (19, 20, 22, 83). However, the transcriptional effect of PPARα on liver CPT1 remains controversial, since some studies have suggested that long-chain FFA regulates CPT1 expression through a PPARα-independent pathway (96, 101). Interestingly, another mechanism that modulates the CPT1 activity has recently been proposed (150). In this study, a NASH rat model fed a methionine-choline-deficient diet had a notable reduction in CPT1A activity and mitochondrial FAO despite increased CPT1A mRNA expression. The formation of a 4-hydroxynonenal-CPT1 adduct caused by lipid peroxidation as a consequence of ROS overproduction is the main cause of impaired FAO and lipid removal from hepatocytes. ROS can attack polyunsaturated FAs, initiating lipid peroxidation and the formation of aldehyde by-products (ahydroxy-2-nonenal [HNE] and malondialdehyde [MDA]), which have longer half-lives than ROS and are able to spread from their site of origin to reach distant intracellular and extracellular targets, thereby amplifiying the effects of oxidative stress (44, 170). The observations listed above suggest that CPT1 overexpression and increased CPT1 activity occur in liver during the onset of steatosis as a mechanism to compensate for increased FA levels. Accelerated mitochondrial FAO might cause excessive electron flux in the ETC and ROS overproduction. As lipids, proteins, and mitochondrial DNA are the main ROS targets, increased ROS might initiate lipid peroxidation, damage mitochondrial DNA and proteins, and alter mitochondrial morphology and function. The post-translational modifications of CPT1 caused by lipid peroxidation could, subsequently, decrease CPT1 activity and reverse initially activated FAO. This notion raises the question of whether interventions aimed at promoting mitochondrial FAO in liver would be beneficial to the treatment of NAFLD/NASH.

Several strategies have been used to promote FAO, including the use of PPAR agonists (7, 114), AMPK agonists [metformin (180), AICAR (166)], and ACC antagonists (62, 108). Genetic aproaches specifically promoting liver FAO are of considerable interest. An improvement in high-fat diet (HFD)-induced liver insulin resistance has been described in rodents, in which, FAO was indirectly enhanced by the reduction of malonyl-CoA levels through the modulation of ACC (146) and MCD (4). More interesting are the results obtained with a direct enhancement of mitochondrial FAO by increasing CPT1A expression in liver. Recent studies (117, 130) overexpressing an active and malonyl-CoA-insensitive mutant form of CPT1A (CPT1AM) (118) in obese rodents show that permanently enhanced liver FAO not only rescues impaired hepatic, muscle, and WAT insulin signaling in these animals, but also reduces steatosis, inflammation, and adiposity (Fig. 3). Furthermore, in these studies, enhanced

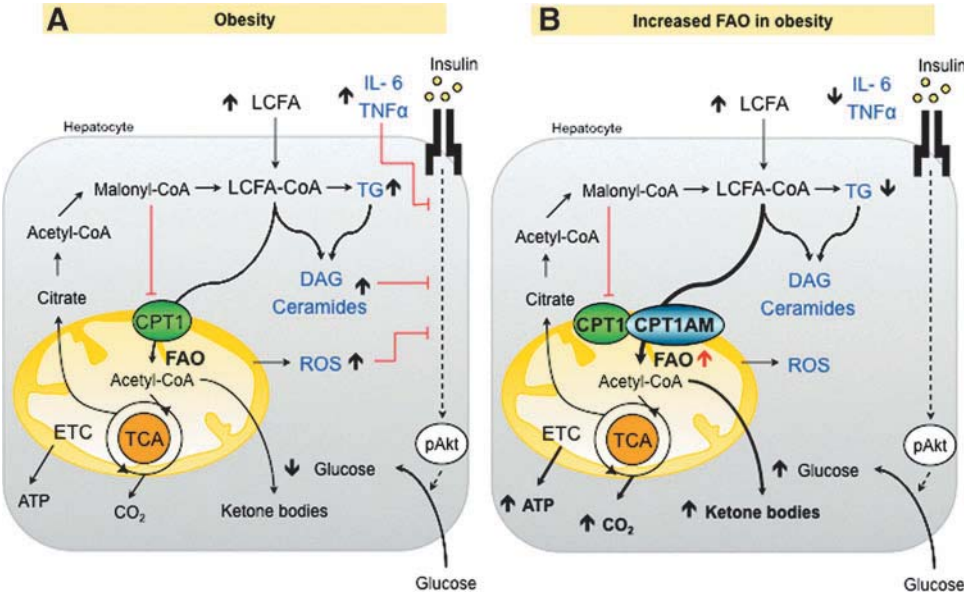

FIG. 3. Effects of enhanced FAO in fatty liver. (A) Obesity increases FA uptake, triglyceride (TG), diacylglycerol (DAG), ceramides, and other lipid derivatives that may inhibit insulin signaling. FA accumulation induces mitochondrial dysfunction and increased ROS production, oxidative stress, and inflammation that could also disrupt insulin signaling. **(B)** Enhancing FAO by the overexpression of CPT1AM (117, 130) increases the production of ketone bodies, ATP, and CO_2. The reduction of lipid content re-establishes lipid metabolism, insulin signaling, and decreases inflammation and ROS production.

mitochondrial FAO did not increase ROS derivatives or liver injury. Taken together, these results highlight an increase of CPT1A as a new strategy for the treatment of NAFLD/NASH pathologies. Alternatively, it has been reported that the administration of CPT1 inhibitors reduces gluconeogenesis and improves glucose homeostasis, although chronic treatments on HFD-treated mice caused hepatic steatosis (28, 53). This side effect has interrupted the development of other systemic inhibitors, such as etomoxir and 2-tetradecylglycidic acid, as a therapeutic tool. Taken together, these data support the idea that any strategy able to switch liver FA's fate from esterification toward oxidation produces a beneficial effect on the liver and on the whole body. It seems that the liver can deal with an increased flux of FA into the mitochondria, thus escaping from liver injury. This is due to the ability of liver to flip the balance from complete oxidation to ketone body production (88). The ketone bodies produced by enhanced FAO are easily consumed by other tissues, increasing the flux of carbons from liver to other organs. Recently, a new hepatic factor, fibroblast growth factor 21 (FGF21), has emerged as a key regulator in FAO and ketogenic activation. FGF21 is induced in the liver during fasting (136) and has been increasingly pointed to as a potential therapeutic agent in obesity-induced insulin-resistant states (78).

WAT Meets Inflammation and Metabolic Disorders in Obesity

WAT has long been recognized as the main storage site for lipids derived from food intake (142). This long-term energy reservoir stores lipids mainly in the form of TGs, which can be mobilized and used to generate ATP through the mitochondrial β-oxidation pathway in peripheral organs during periods of caloric need.

WAT is composed mainly by adipocytes, but also by immune cells, such as macrophages, T cells, and mast cells (68, 104). Thus, WAT is an active and endocrine organ that secretes a large number of adipokines, cytokines, and chemokines (*i.e.*, leptin, adiponectin, resistin, TNFα, IL-6, MCP-1, and IL-10), and plays a key role in regulating whole-body glucose and lipid metabolism (46, 151).

WAT, obesity, and inflammation

Obesity is characterized by the expansion of WAT mass due to an increase in both adipocyte number (hyperplasia) and size (hypertrophy), and it is closely associated with insulin resistance in peripheral tissues, such as SkM and liver. In fact, under excess caloric intake, WAT reaches its upper limit for further lipid storage (157, 169). Consequently, adipocytes exceed their oxygen diffusion limit, thereby promoting hypoxia (73), ER stress (132), and cell death, and increased circulating FFA and TG accumulation in ectopic sites is produced (145). The combination of microhypoxia and lipid overload triggers the recruitment of immune cells, such as macrophages in the adipose tissue and their activation (103, 129, 171). Obese adipocytes and infiltrated immune cells secrete a large amount of inflammatory mediators that promote a proinflammatory state through the activation of IKKβ-NF-Kβ and the JNK-Ap1 signaling pathways (151). The induction of JNK leads to serine phosphorylation of IRS-1 and 2, crucial molecules in insulin signaling, and consequently inhibits insulin action. These events cause insulin resistance in adipocytes, exacerbation of the inflammatory state, and systemic insulin resistance (59, 147) (Fig. 4).

FFAs, inflammation, and ROS

Physiological ROS production in adipocytes is a relevant cellular signaling mechanism in the insulin response and it depends mainly on the NADPH oxidase (NOX) family activity (9). In obesity, the excess of FFAs increases NOX-mediated ROS generation. Recently, it has been demonstrated that increased ROS in adipocytes exposed to an excess of FFAs does not depend on enhanced mitochondrial flux, but on high levels of TNFα and ER stress as well as the upregulation of aforementioned NOX enzymes (8, 60). ROS have the capacity to interfere with insulin signaling, since they activate several downstream pathways involving MAPK, JNK/IKKβ, and

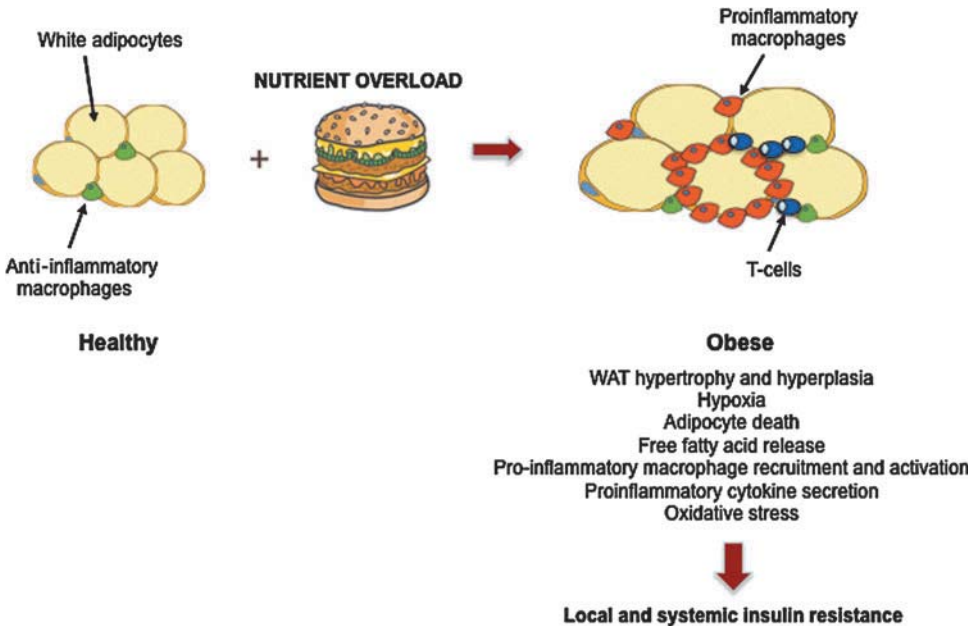

FIG. 4. White adipose tissue (WAT), obesity, and insulin resistance. Nutrient overload, weight gain, and obesity result in increased adipose tissue mass and adipocyte size. The expansion of the adipose tissue leads to adipocyte hypoxia, death, and free fatty acid (FFA) release into circulation. These events trigger the recruitment and activation of immune cells, such as macrophages and T cells, in the adipose tissue. Infiltrated and activated immune cells and adipocytes secrete large amounts of proinflammatory cytokines, which promote the inhibition of insulin signaling with an ensuing local and systemic resistance (147).

JAK/STAT, which are key contributors to the development of insulin resistance in obesity and type 2 diabetes (8, 75).

Enhanced FAO and improvement in insulin sensitivity

The imbalance between lipid storage and lipid utilization predisposes to adipocyte dysfunction and FFAs promote the proinflammatory response and ROS production involved in severe metabolic disorders. Although the exact physiological role of FAO in WAT remains to be determined, recent studies have shown beneficial effects of increased FAO and lipolysis in adipocytes, through direct CPT1A overexpression. In fact, this rise in lipid utilization improves insulin sensitivity in these cells and suppresses inflammatory signaling (50). However, there is still no evidence that increasing adipose tissue FAO would decrease FFA-induced ROS production. Thus, further research is required to elucidate these mechanisms and to evaluate the potential benefit of this strategy to prevent or reverse obesity and related metabolic diseases.

BAT, Turning Up the Heat

BAT morphology and function

In addition to energy-storing WAT, human fat consists of thermogenic controlling BAT. The latter has traditionally received less attention than WAT since it is less abundant and was considered exclusive to rodents and children. However, more recently, BAT have gained relevance in the mechanisms involved in obesity-related disorders.

BAT thermogenesis takes place in its numerous, densely packed mitochondria, which contain the BAT-specific UCP1. Activation of this protein uncouples aerobic respiration by producing heat instead of ATP (162). Brown adipocytes are also differentiated from white adipocytes because of their high expression of type 2 iodothyronnine deiodinase (DIO2), the transcription coregulators, PRDM16 and PGC-1α, and the lipolytic regulator, Cidea (52, 131). In rodents, BAT generates heat mainly for two reasons; namely, to protect against cold exposure *via* nonshivering thermogenesis and to burn the excess calories and reduce fat accumulation (54, 72). Therefore, BAT plays a crucial role in protecting mice from diet-induced obesity.

Rediscovery of human BAT

The fusion of positron emission tomography (PET) and computed tomography (CT) images allowed radiologists to see both functional and structural information in a single image. In the course of using PET-CT to detect and stage tumors in humans, active BAT was observed to increase after cold exposure (124).

However, the real breakthrough arrived in 2009 when five independent groups used PET-CT to identify the presence and study the relevance of BAT in adult humans (30, 143, 165, 168, 181). All the groups showed major depots of metabolically active fat in the cervical–supraclavicular region, a slightly different site from that in rodents and children, where BAT is found mainly situated in the interscapular area. The expression of UCP1, DIO2, and the β3-adrenergic receptor was also reported, thereby indicating the potential responsiveness of human BAT to both hormonal and pharmacological stimuli.

Interestingly, human studies showed that BAT is reduced in obese and diabetic patients, thus indicating that this tissue participates in both cold-induced and diet-induced thermogenesis (30). These observations made BAT a major breakthrough, since any strategy able to increase the mass or activity of this tissue could potentially provide hope for obese and diabetic patients.

BAT bioenergetics and mitochondrial metabolism

BAT is the only tissue to express UCP1, a protein found in the inner mitochondrial membrane that orchestrates the uncoupled reaction of allowing protons to re-enter the mitochondrial matrix without generating ATP. The dissipation of energy as heat confers BAT with the capacity to control thermogenesis. In fact, altered UCP1 expression (UCP1-deficient or transgenic mice) leads to dysregulated sensitivity to cold exposure and body weight control (40, 42, 86, 87, 98).

Body temperature changes stimulate norepinephrine release by sympathetic nervous endings that activate β-adrenergic receptors and trigger a signal transduction cascade that converts nutrients into acetyl-CoA. The TCA cycle uses this mitochondrial fuel to produce protons and electrons, which generate ATP through the ETC. However, in BAT, UCP1 allows protons to enter the mitochondrial matrix without generating ATP, that is, uncoupled, and heat is produced in this process. Thus, BAT burning power intensely clears and oxidizes circulating lipids and glucose to generate heat (17). This observation thus highlights BAT thermogenesis as an attractive therapeutic anti-obesity target.

Enhancing BAT burning power and browning of WAT as an anti-obesity strategy

Recent landmark studies have identified novel secreted proteins, such as liver FGF21 (72), cardiac natriuretic peptides (11), and irisin (12), that stimulate brown adipocyte thermogenesis. Interestingly, a moderate increase (threefold) in irisin blood levels in mice enhanced energy expenditure and improved obesity and glucose homeostasis (12). In addition, recent articles reported that macrophages (125) and the bone morphogenetic protein BMP8B (172) have also the capacity to regulate BAT thermogenesis. Therefore, promoting BAT activation and/or brown adipocyte recruitment in white fat (browning) are approaches of considerable interest by which to develop pharmacological strategies to improve systemic metabolism by increasing energy expenditure (Fig. 5).

Role of FAO in Muscle Insulin Sensitivity During Obesity

SkM is vital for the maintenance of glucose homeostasis. It accounts for $\sim$80% of total glucose uptake after insulin stimulation (34) and its transition to an insulin-resistant state is central for the pathogenesis of type 2 diabetes (152). Various pathways trigger obesity-induced insulin resistance (147). Both the action of fat-derived cytokines (adipocytokines) and ectopic accumulation of lipid deposition impair SkM function and play a critical role in insulin sensitivity. Obesity is characterized by a greater breakdown and uptake of FAs. Parallel with the increase in circulating lipids, the intramyocellular (IMC) lipid content appears to increase proportionally in obese humans (105) and rodents (23). The lipotoxic hypothesis proposes that FAs and their metabolites (such as DAG and

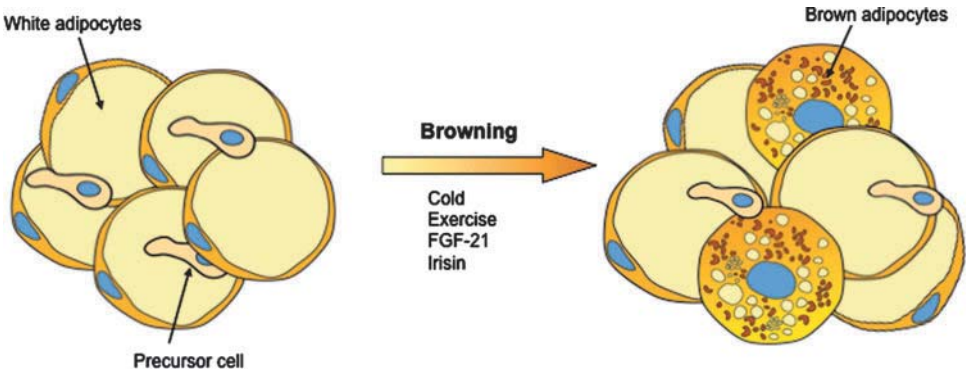

FIG. 5. Stimulation of brown adipose tissue (BAT) thermogenesis. Cold exposure, exercise, and some secreted proteins, such as fibroblast growth factor-21 (FGF-21) (72) and irisin (12), enhance BAT burning power by promoting brown adipocyte recruitment in white fat (browning).

ceramides) are important contributors to lipid-induced insulin resistance in SkM. These molecules activate proinflammatory and nutrient-sensing pathways that lead to the impairment of insulin action (Fig. 6A) [for further information, readers are referred to additional reviews (144, 159)].

Muscle FAO in obesity: two sides of the same coin

Several strategies have been designed to prevent IMC lipid accumulation and its deleterious effects. In SkM, these are mainly focused on the inhibition of FA uptake and esterification and/or the increase in FAO. However, whether the metabolic shift toward fat oxidation ameliorates lipid-induced SkM dysfunction is still open to debate.

Different laboratories have demonstrated that a decrease in the size and number of mitochondria, the activity of proteins in the ETC and, in general, impaired oxidative capacity in SkM are associated with obesity and insulin resistance in humans and animals (102, 139, 153). Given these observations, it is postulated that increased mitochondrial FAO could prevent lipid accumulation and, thus, improve insulin sensitivity in SkM (Fig. 6B). Several lines of evidence support this idea: (i) exercise in obese humans increases muscle mitochondrial FAO and improves glucose tolerance and insulin sensitivity (16). This effect is probably due to increased CPT1 expression and activity during exercise (163); (ii) direct CPT1 overexpression in animals and SkM cells protects muscle from FA-induced insulin resistance and apoptosis (15, 66, 149); and (iii) indirect SkM CPT1 activation, by the use of AMPK activators (77) or the ACC2 knockout (1), ameliorates insulin-stimulated glucose uptake in rodents.

Despite all the above points, the idea of mitochondrial deficiency as the main cause of diet-induced insulin resistance has been challenged in recent years. First, it is known that SkM's capacity to oxidize substrates is far in excess of what is needed to supply the energy demands of resting muscle (5). With this in mind, it seems clear that the mild (≈30%) reduction in mitochondrial content observed in obese patients does not affect the ability of resting muscle to oxidize fat. Further, despite the reduction in the mitochondrial content, insulin-resistant SkM has normal mitochondrial function (13). Secondly, since FA and glucose compete as metabolic substrates, the decrease in FAO would produce enhanced glucose utilization instead of insulin resistance. In fact, patients with severe mitochondrial deficiency have an increase in glucose uptake despite the large accumulation of IMC lipids (61). And finally, a HFD causes insulin resistance in rodents, while inducing an increase in SkM mitochondrial biogenesis and β-oxidation (164). This suggests that FAO might already be enhanced during obesity, contributing to the development of insulin resistance (121).

The main problems associated with an increase in FAO are: (i) the high rates of incomplete fat oxidation and (ii) the increase in oxidative stress associated with a mitochondrial overload (Fig. 6C) (89). Koves *et al.* (89) postulated that HFD induces the expression of FAO-related genes, but not those associated with the ETC and TCA cycle. This causes a mismatch between FAO and TCA cycle activity, thus leading to the accumulation of incomplete FAs and other intermediates (*i.e.*, acylcarnitines) that correlate negatively with glucose tolerance (2). How these intermediates mediate the onset of insulin resistance is still unknown. However, studies linking overnutrition with the acylation of mitochondrial proteins are relevant to this topic and suggest a role for acylcarnitines (70). Mitochondrial members of the sirtuin family are known to deacetylate/activate several proteins involved in fat oxidation. This along with the observation that SIRT3 knockout mice have high acylcarnitines and increased acylated mitochondrial proteins and develop metabolic syndrome, implies that mitochondrial accumulation of FAO intermediates triggers metabolic complications *via* protein modification (71, 80).

Role of ROS in muscle insulin signaling

FAO intermediates may also create an unfavorable environment in the mitochondria, which contributes to the formation of ROS and the development of oxidative stress (119, 120). High levels of ROS and systemic oxidative stress have been associated with obesity and insulin resistance (45). However, these molecules are produced normally during mitochondrial respiration and are essential signal transducers that regulate several cell processes in SkM (8), including the insulin pathway (64, 65). Due to its dual role in insulin sensitivity, modulation of redox balance is crucial for correct cell function. On the one hand, under physiological conditions, ROS are generated in response to insulin and are required for its action (69), since the activity of different enzymes that participate in the insulin cascade are dependent on their oxidation state. In particular, the phosphatases that negatively modulate the insulin pathway are the main targets for oxidative inhibition by ROS (35). It has also been reported that ROS enhance insulin sensitivity in HFD mice (100). These molecules are also crucial for the SkM remodeling that occurs in response to exercise (31). ROS show insulin-like effects, stimulating SkM glucose uptake during muscle contraction *via* the activation of AMPK (81) and the induction of PGC-1α

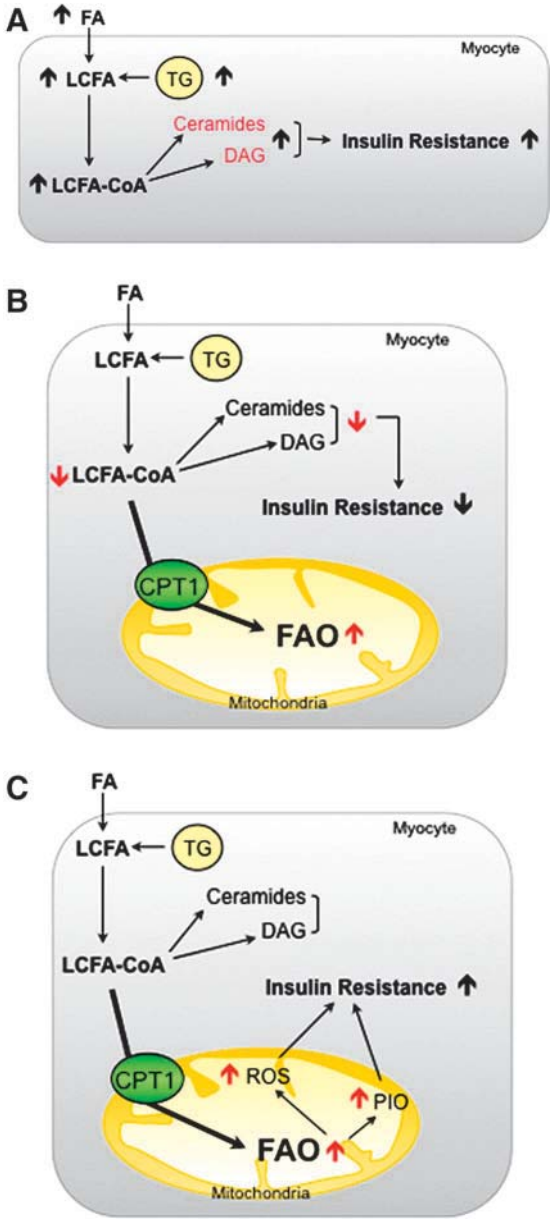

FIG. 6. Two hypotheses for the role of FAO in the development of obese-induced insulin resistance in skeletal muscle (SkM). (A) During obesity, intramyocellular lipid accumulation leads to a decrease in insulin-stimulated glucose uptake in SkM (144). **(B)** An increase in FAO may decrease LCFAs, ceramide, and DAG content, thus enhancing insulin action (15, 66, 149). **(C)** However, an increase in FAO may augment ROS production and enhance the accumulation of products of incomplete β-oxidation (PIO), which are hypothesized to decrease insulin signaling through the activation of various stress kinases (89).

expression *in vitro* and *in vivo* (57, 79). On the other hand, during a pathophysiological state, abundant evidence indicates that a large and sustained increase in ROS impairs insulin action, through the activation of stress signaling pathways (*i.e.,* MAPK and JNK) (85, 154), contributing to the pathogenesis of diet-induced insulin resistance (67). Therefore, clarifying the role of mitochondrial FAO, and the ROS production derived from it, in diet-induced SkM insulin-resistance is crucial to the development of new therapeutic strategies to fight against obesity and its related metabolic complications.

Hypothalamic FAO in the Regulation of Food Intake

Excess food intake in obesity is related to behavioral processes controlled by the central nervous system. Specific hypothalamic nuclei, which sense nutrients and modify energy intake and expenditure to maintain a balance, are responsible for regulating this intake (48). The mechanisms for sensing the nutritional state have not been fully discovered and less is known about lipid than glucose sensing. Nonetheless, there are two classic hypotheses on nutritional state metabolic mediators, involving malonyl-CoA and LCFA-CoA.

CPT1A on food intake control: linking the malonyl-CoA and LCFA-CoA hypotheses

Strong evidence shows that increased malonyl-CoA levels, which are generated by activated (*i.e.,* dephosphorylated) ACC, act as abundance indicators, thereby diminishing food intake and consequently body weight (173). During starvation, ACC phosphorylation is mainly controlled by the well-known energy sensor, AMPK (115), which acts also as an important hub, integrating in-cell energetic state sensing and its modulation due to different circulating hormones. Concretely, ghrelin-mediated activation (*i.e.,* phosphorylation) of AMPK is done *via* SIRT1-mediated activation (*i.e.,* deacetylation) of p53. It is known that the SIRT1 activity is increased in hypothalamus during starvation with high ghrelin levels (167). The mechanism of leptin action also appears to be related to increases in physiological malonyl-CoA in the arcuate nucleus, which promotes a reduction in food intake and body weight, using different mechanisms to those previously reported for ghrelin action, during energetically wealthy states (49, 141).

In addition, LCFA-CoA levels have also been put forward as mediators in nutritional state sensing. During starvation, circulating FFA increase can be sensed in hypothalamic nuclei through in-cell activation to LCFA-CoA. This increase, previous to active ghrelin rise, is an early reporter of a deficient nutritional state (156). However, unfortunately, no cytoplasmic LCFA-CoA increase in hypothalamus has been found. Even so, in the last decade, pharmacological and genetic inhibition of hypothalamic CPT1A has been reported to reduce the food intake (10, 110, 127), potentially as a result of LCFA-CoA cytoplasmic accumulation. Furthermore, the role of malonyl-CoA as a CPT1 inhibitor is worth noting, to link the two hypotheses.

Regardless of whether malonyl-CoA or LCFA-CoA is the main actor, changes in feeding behavior and peripheral metabolism are conducted *via* the action of neuropeptides, such as agouti-related protein (AgRP), neuropeptide Y (NPY), and melanocortins. Transcription factors affected by changes in hypothalamic FAO, such as CREB, FoxO1, and BSX, are involved in ghrelin-induced expression of NPY and AgRP (92). However, it is still unknown whether high levels of LCFA-CoA trigger NPY and AgRP *via* BSX and subsequent transcription factors. Probably, neither malonyl-CoA nor LCFA-CoA act as key molecular mediators *per se* to induce the expression of the different food intake-controller neuropeptides,

but they are just two of the several pieces involved in the highly complex hypothalamic nutritional state sensing system, which is still not fully understood.

The relevance of FAO in neuronal cells is controversial because glucose is the brain's primary energy source. However, basal levels of FAO enzymes and FA transport proteins (such as FATP-1, FATP-4, and FAT/CD36) are expressed in hypothalamic neurons (93, 95). Additionally, the presence of such small, but functional FAO could be explained by its essential role in neuronal FA turnover and its action as a lipid-sensing mediator for energy homeostasis (113). There is also another controversy regarding fasting, because during fasting, high blood FFA levels presumably reach hypothalamic nuclei. This does not fit in with the satiety effect observed in early experiments with high LCFA concentration in the hypothalamus (128). Nonetheless, the direct correlation observed between fasting and FFA levels (156) and the capacity of hypothalamic neurons to sense glucose and FFA simultaneously and to integrate other nutritional and hormonal inputs (95, 99) seem to throw light on how important FAO really is in hypothalamic nuclei.

ROS, third in discord

Along with malonyl-CoA and LCFA-CoA, mitochondrial ROS have been put forward as a mediator in response to nutrient availability (140) (Fig. 7). ROS in the hypothalamus are produced chiefly in mitochondria ECT complexes. Concretely, some authors pointed to complex I as the most relevant site for single electron reduction in brain mitochondria (90). Various kinases and transcription factors, involved in neuropeptide regulation, have been reported to be modulated by redox signaling (33, 91). Further, the signaling under different levels of ROS may imply dissimilar pathophysiological changes in proteins, depending on their redox state (33). A certain level of ROS, without being excessive, is probably required to trigger neuropeptide expression. This notion may explain the importance of UCP2 as a ROS scavenger to keep a physiological ROS level that allows correct NPY and AgRP expression in the hypothalamus (6). In addition to all these considerations, the recent finding that hypothalamic autophagy is a source of endogenous FFA to regulate AgRP levels (82) could be explained by increased mitochondrial FAO and ROS signaling. However, further research is needed to establish the contribution of ROS to the hypothalamic control of food intake.

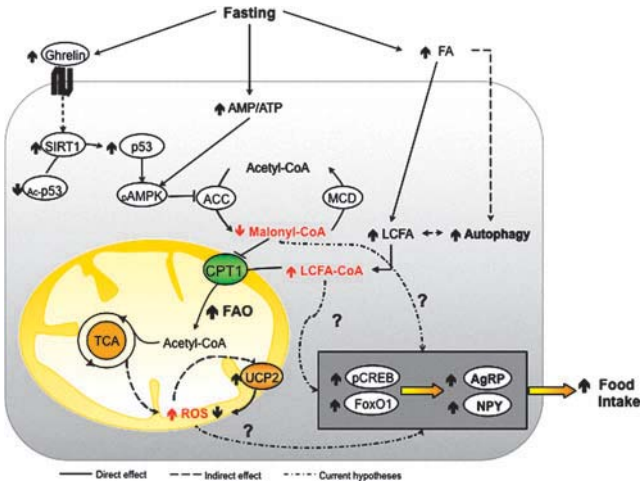

FIG. 7. Hypotheses involving FAO in the regulation of food intake. During fasting, the effects of ghrelin, AMP, and FAs act in hypothalamic nuclei to increase the expression of orexigenic neuropeptides (48). The mechanisms involved in this process appear to be related to an increase in LCFA-CoA, diminished malonyl-CoA, and a certain level of ROS. Excessive ROS production is controlled by UCP2 with a negative feed-back. CPT1A is postulated to be involved in all the three approaches.

Conclusions

Despite considerable current efforts, the prevalence of obesity and associated diseases is rising exponentially in both industrialized and developing countries worldwide. This is especially worrying in the young. Current therapeutic strategies, focused mainly on controlling food intake, have met limited success, probably due to the inherent resistance of the human body to weight loss. However, recent approaches targeting energy expenditure and mitochondrial FAO shed light on new therapies to fight obesity.

Mitochondrial FAO is the cell source of energy from FAs. Since an excess of lipids is found in obesity and associated pathologies, a lot of research studies how to eliminate them through an increase in FAO. Beneficial effects of an increase in energy expenditure in obesity have been described in several tissues, including liver, muscle, WAT, and BAT. On the contrary, FAO therapeutic inhibition in hypothalamus seems to reduce food intake. Whether or not FAO should be modulated in the above-mentioned tissues to improve insulin resistance or to lose weight is still a subject of debate. There is no doubt regarding the involvement of ROS in pathophysiological processes related to obesity, and CPT1 seems to be a good molecular target for ROS and FAO modulation. However, several questions still need to be answered before FAO can become an obesity therapy. First, it is not known whether a long-term increase in energy expenditure would cause an enhancement of appetite as a compensatory mechanism. Second, an increase in FAO could induce pathological levels of ROS and/or other incomplete oxidation products. Third, it is not known whether FAO enhancement might reach a limit in a specific tissue, such as in BAT, in which thermogenesis is tightly adjusted to the environmental temperature. Finally, since increasing flux through β-oxidation would only make sense together with a corresponding enhancement in energy demand (121), the physiological relevance of improved mitochondrial FAO might be questioned if the individual remains sedentary (muscle, WAT, or liver) or warm (BAT). Potential mechanisms to explain the beneficial effects of targeting mitochondrial FAO could be the concomitant enhancement of hepatic ketone bodies, CO_2, acid soluble products, ATP production, and endergonic processes (*e.g.*, gluconeogenesis) seen in previous publications (38, 130, 158). Increased FAO may also decrease glucose oxidation to maintain energy homeostasis, augment mitochondrial burning capacity through an increase in the number of mitochondria and/or the increased expression of UCPs, and thus dissipate the excess of energy as heat and ATP. All of these could well alleviate the mitochondrial pressure found in lipid overload states. Thus, an increase in energy expenditure could

indeed be the underlying protective mechanism against obesity-induced metabolic abnormalities.

Although more research is needed, we are encouraged that targeting of FAO and cell energy expenditure may be available in the near future as therapies to treat obesity and its associated severe diseases.

Innovation

Recent results suggest that enhancing cellular energy expenditure may be an attractive therapy to prevent or reverse the exponential growth of obesity-related disorders. We reviewed those recent discoveries regarding mitochondrial FAO and its potential as a therapy for obesity.

Acknowledgments

We thank Professor Fausto G. Hegardt for helpful, inspiring, and wise discussions and the Language Service of the University of Barcelona for valuable assistance in the preparation of the English manuscript. This study was supported by the Spanish Ministry of Science and Innovation (Grant SAF2010-20039 to L.H., Grant SAF2011-30520-C02-01 to D.S., and doctoral fellowships to M.I.M. and J.F.M.), by the CIBER Fisiopatología de la Obesidad y la Nutrición (CIBEROBN), Instituto de Salud Carlos III (Grant CB06/03/0026 to D.S. and research contract to P.M.), and by the EFSD/Lilly and EFSD/Janssen (research fellowships to L.H.).

References

1. Abu-Elheiga L, Oh W, Kordari P, and Wakil SJ. Acetyl-CoA carboxylase 2 mutant mice are protected against obesity and diabetes induced by high-fat/high-carbohydrate diets. *Proc Natl Acad Sci U S A* 100: 10207–10212, 2003.
2. Adams SH, Hoppel CL, Lok KH, Zhao L, Wong SW, Minkler PE, Hwang DH, Newman JW, and Garvey WT. Plasma acylcarnitine profiles suggest incomplete long-chain fatty acid beta-oxidation and altered tricarboxylic acid cycle activity in type 2 diabetic African-American women. *J Nutr* 139: 1073–1081, 2009.
3. Ahima RS. Digging deeper into obesity. *J Clin Invest* 121: 2076–2079, 2011.
4. An J, Muoio DM, Shiota M, Fujimoto Y, Cline GW, Shulman GI, Koves TR, Stevens R, Millington D, and Newgard CB. Hepatic expression of malonyl-CoA decarboxylase reverses muscle, liver and whole-animal insulin resistance. *Nat Med* 10: 268–274, 2004.
5. Andersen P and Saltin B. Maximal perfusion of skeletal muscle in man. *J Physiol* 366: 233–249, 1985.
6. Andrews ZB, Liu ZW, Walllingford N, Erion DM, Borok E, Friedman JM, Tschop MH, Shanabrough M, Cline G, Shulman GI, Coppola A, Gao XB, Horvath TL, and Diano S. UCP2 mediates ghrelin's action on NPY/AgRP neurons by lowering free radicals. *Nature* 454: 846–851, 2008.
7. Barroso E, Rodriguez-Calvo R, Serrano-Marco L, Astudillo AM, Balsinde J, Palomer X, and Vazquez-Carrera M. The PPARbeta/delta activator GW501516 prevents the down-regulation of AMPK caused by a high-fat diet in liver and amplifies the PGC-1alpha-Lipin 1-PPARalpha pathway leading to increased fatty acid oxidation. *Endocrinology* 152: 1848–1859, 2011.
8. Bashan N, Kovsan J, Kachko I, Ovadia H, and Rudich A. Positive and negative regulation of insulin signaling by reactive oxygen and nitrogen species. *Physiol Rev* 89: 27–71, 2009.
9. Bedard K and Krause KH. The NOX family of ROS-generating NADPH oxidases: physiology and pathophysiology. *Physiol Rev* 87: 245–313, 2007.
10. Bentebibel A, Sebastian D, Herrero L, Lopez-Vinas E, Serra D, Asins G, Gomez-Puertas P, and Hegardt FG. Novel effect of C75 on carnitine palmitoyltransferase I activity and palmitate oxidation. *Biochemistry* 45: 4339–4350, 2006.
11. Bordicchia M, Liu D, Amri EZ, Ailhaud G, Dessi-Fulgheri P, Zhang C, Takahashi N, Sarzani R, and Collins S. Cardiac natriuretic peptides act via p38 MAPK to induce the brown fat thermogenic program in mouse and human adipocytes. *J Clin Invest* 122: 1022–1036, 2012.
12. Bostrom P, Wu J, Jedrychowski MP, Korde A, Ye L, Lo JC, Rasbach KA, Bostrom EA, Choi JH, Long JZ, Kajimura S, Zingaretti MC, Vind BF, Tu H, Cinti S, Hojlund K, Gygi SP, and Spiegelman BM. A PGC1-alpha-dependent myokine that drives brown-fat-like development of white fat and thermogenesis. *Nature* 481: 463–468, 2012.
13. Boushel R, Gnaiger E, Schjerling P, Skovbro M, Kraunsoe R, and Dela F. Patients with type 2 diabetes have normal mitochondrial function in skeletal muscle. *Diabetologia* 50: 790–796, 2007.
14. Brady LJ, Brady PS, Romsos DR, and Hoppel CL. Elevated hepatic mitochondrial and peroxisomal oxidative capacities in fed and starved adult obese (ob/ob) mice. *Biochem J* 231: 439–444, 1985.
15. Bruce CR, Hoy AJ, Turner N, Watt MJ, Allen TL, Carpenter K, Cooney GJ, Febbraio MA, and Kraegen EW. Overexpression of carnitine palmitoyltransferase-1 in skeletal muscle is sufficient to enhance fatty acid oxidation and improve high-fat diet-induced insulin resistance. *Diabetes* 58: 550–558, 2009.
16. Bruce CR, Thrush AB, Mertz VA, Bezaire V, Chabowski A, Heigenhauser GJ, and Dyck DJ. Endurance training in obese humans improves glucose tolerance and mitochondrial fatty acid oxidation and alters muscle lipid content. *Am J Physiol Endocrinol Metab* 291: E99–E107, 2006.
17. Cannon B and Nedergaard J. Brown adipose tissue: function and physiological significance. *Physiol Rev* 84: 277–359, 2004.
18. Canto C, Gerhart-Hines Z, Feige JN, Lagouge M, Noriega L, Milne JC, Elliott PJ, Puigserver P, and Auwerx J. AMPK regulates energy expenditure by modulating NAD+ metabolism and SIRT1 activity. *Nature* 458: 1056–1060, 2009.
19. Chakravarthy MV, Lodhi IJ, Yin L, Malapaka RR, Xu HE, Turk J, and Semenkovich CF. Identification of a physiologically relevant endogenous ligand for PPARalpha in liver. *Cell* 138: 476–488, 2009.
20. Chakravarthy MV, Pan Z, Zhu Y, Tordjman K, Schneider JG, Coleman T, Turk J, and Semenkovich CF. "New" hepatic fat activates PPARalpha to maintain glucose, lipid, and cholesterol homeostasis. *Cell Metab* 1: 309–322, 2005.
21. Chance B, Sies H, and Boveris A. Hydroperoxide metabolism in mammalian organs. *Physiol Rev* 59: 527–605, 1979.
22. Chatelain F, Kohl C, Esser V, McGarry JD, Girard J, and Pegorier JP. Cyclic AMP and fatty acids increase carnitine palmitoyltransferase I gene transcription in cultured fetal rat hepatocytes. *Eur J Biochem* 235: 789–798, 1996.
23. Chen MT, Kaufman LN, Spennetta T, and Shrago E. Effects of high fat-feeding to rats on the interrelationship of body weight, plasma insulin, and fatty acyl-coenzyme A esters in liver and skeletal muscle. *Metabolism* 41: 564–569, 1992.
24. Choi CS, Savage DB, Abu-Elheiga L, Liu ZX, Kim S, Kulkarni A, Distefano A, Hwang YJ, Reznick RM, Codella R, Zhang D, Cline GW, Wakil SJ, and Shulman GI. Con-

tinuous fat oxidation in acetyl-CoA carboxylase 2 knockout mice increases total energy expenditure, reduces fat mass, and improves insulin sensitivity. *Proc Natl Acad Sci U S A* 104: 16480–16485, 2007.
25. Ciapaite J, van den Broek NM, Te Brinke H, Nicolay K, Jeneson JA, Houten SM, and Prompers JJ. Differential effects of short- and long-term high-fat diet feeding on hepatic fatty acid metabolism in rats. *Biochim Biophys Acta* 1811: 441–451, 2011.
26. Cnop M, Foufelle F, and Velloso LA. Endoplasmic reticulum stress, obesity and diabetes. *Trends Mol Med* 18: 59–68, 2012.
27. Cohen JC, Horton JD, and Hobbs HH. Human fatty liver disease: old questions and new insights. *Science* 332: 1519–1523, 2011.
28. Conti R, Mannucci E, Pessotto P, Tassoni E, Carminati P, Giannessi F, and Arduini A. Selective reversible inhibition of liver carnitine palmitoyl-transferase 1 by teglicar reduces gluconeogenesis and improves glucose homeostasis. *Diabetes* 60: 644–651, 2011.
29. Cook GA and Gamble MS. Regulation of carnitine palmitoyltransferase by insulin results in decreased activity and decreased apparent Ki values for malonyl-CoA. *J Biol Chem* 262: 2050–2055, 1987.
30. Cypess AM, Lehman S, Williams G, Tal I, Rodman D, Goldfine AB, Kuo FC, Palmer EL, Tseng YH, Doria A, Kolodny GM, and Kahn CR. Identification and importance of brown adipose tissue in adult humans. *N Engl J Med* 360: 1509–1517, 2009.
31. Davies KJ, Quintanilha AT, Brooks GA, and Packer L. Free radicals and tissue damage produced by exercise. *Biochem Biophys Res Commun* 107: 1198–1205, 1982.
32. Day CP and James OF. Steatohepatitis: a tale of two "hits"? *Gastroenterology* 114: 842–845, 1998.
33. de Keizer PL, Burgering BM, and Dansen TB. Forkhead box o as a sensor, mediator, and regulator of redox signaling. *Antioxid Redox Signal* 14: 1093–1106, 2010.
34. DeFronzo RA, Jacot E, Jequier E, Maeder E, Wahren J, and Felber JP. The effect of insulin on the disposal of intravenous glucose. Results from indirect calorimetry and hepatic and femoral venous catheterization. *Diabetes* 30: 1000–1007, 1981.
35. Denu JM and Tanner KG. Redox regulation of protein tyrosine phosphatases by hydrogen peroxide: detecting sulfenic acid intermediates and examining reversible inactivation. *Methods Enzymol* 348: 297–305, 2002.
36. Derosa G and Maffioli P. Anti-obesity drugs: a review about their effects and their safety. *Expert Opin Drug Saf* 11: 459–471, 2012.
37. Donnelly KL, Smith CI, Schwarzenberg SJ, Jessurun J, Boldt MD, and Parks EJ. Sources of fatty acids stored in liver and secreted via lipoproteins in patients with nonalcoholic fatty liver disease. *J Clin Invest* 115: 1343–1351, 2005.
38. Drynan L, Quant PA, and Zammit VA. Flux control exerted by mitochondrial outer membrane carnitine palmitoyltransferase over beta-oxidation, ketogenesis and tricarboxylic acid cycle activity in hepatocytes isolated from rats in different metabolic states. *Biochem J* 317: 791–795, 1996.
39. Dyck JR, Berthiaume LG, Thomas PD, Kantor PF, Barr AJ, Barr R, Singh D, Hopkins TA, Voilley N, Prentki M, and Lopaschuk GD. Characterization of rat liver malonyl-CoA decarboxylase and the study of its role in regulating fatty acid metabolism. *Biochem J* 350: 599–608, 2000.
40. Enerback S, Jacobsson A, Simpson EM, Guerra C, Yamashita H, Harper ME, and Kozak LP. Mice lacking mitochondrial uncoupling protein are cold-sensitive but not obese. *Nature* 387: 90–94, 1997.
41. Esser V, Britton CH, Weis BC, Foster DW, and McGarry JD. Cloning, sequencing, and expression of a cDNA encoding rat liver carnitine palmitoyltransferase I. Direct evidence that a single polypeptide is involved in inhibitor interaction and catalytic function. *J Biol Chem* 268: 5817–5822, 1993.
42. Feldmann HM, Golozoubova V, Cannon B, and Nedergaard J. UCP1 ablation induces obesity and abolishes diet-induced thermogenesis in mice exempt from thermal stress by living at thermoneutrality. *Cell Metab* 9: 203–209, 2009.
43. Fromenty B and Pessayre D. Inhibition of mitochondrial beta-oxidation as a mechanism of hepatotoxicity. *Pharmacol Ther* 67: 101–154, 1995.
44. Fromenty B, Robin MA, Igoudjil A, Mansouri A, and Pessayre D. The ins and outs of mitochondrial dysfunction in NASH. *Diabetes Metab* 30: 121–138, 2004.
45. Furukawa S, Fujita T, Shimabukuro M, Iwaki M, Yamada Y, Nakajima Y, Nakayama O, Makishima M, Matsuda M, and Shimomura I. Increased oxidative stress in obesity and its impact on metabolic syndrome. *J Clin Invest* 114: 1752–1761, 2004.
46. Galic S, Oakhill JS, and Steinberg GR. Adipose tissue as an endocrine organ. *Mol Cell Endocrinol* 316: 129–139, 2010.
47. Gambino R, Musso G, and Cassader M. Redox balance in the pathogenesis of nonalcoholic fatty liver disease: mechanisms and therapeutic opportunities. *Antioxid Redox Signal* 15: 1325–1365, 2011.
48. Gao Q and Horvath TL. Neurobiology of feeding and energy expenditure. *Annu Rev Neurosci* 30: 367–398, 2007.
49. Gao S, Kinzig KP, Aja S, Scott KA, Keung W, Kelly S, Strynadka K, Chohnan S, Smith WW, Tamashiro KL, Ladenheim EE, Ronnett GV, Tu Y, Birnbaum MJ, Lopaschuk GD, and Moran TH. Leptin activates hypothalamic acetyl-CoA carboxylase to inhibit food intake. *Proc Natl Acad Sci U S A* 104: 17358–17363, 2007.
50. Gao X, Li K, Hui X, Kong X, Sweeney G, Wang Y, Xu A, Teng M, Liu P, and Wu D. Carnitine palmitoyltransferase 1A prevents fatty acid-induced adipocyte dysfunction through suppression of c-Jun N-terminal kinase. *Biochem J* 435: 723–732, 2011.
51. Gautron L and Elmquist JK. Sixteen years and counting: an update on leptin in energy balance. *J Clin Invest* 121: 2087–2093, 2011.
52. Gesta S, Tseng YH, and Kahn CR. Developmental origin of fat: tracking obesity to its source. *Cell* 131: 242–256, 2007.
53. Giannessi F, Pessotto P, Tassoni E, Chiodi P, Conti R, De Angelis F, Dell'Uomo N, Catini R, Deias R, Tinti MO, Carminati P, and Arduini A. Discovery of a long-chain carbamoyl aminocarnitine derivative, a reversible carnitine palmitoyltransferase inhibitor with antiketotic and antidiabetic activity. *J Med Chem* 46: 303–309, 2003.
54. Giralt A, Hondares E, Villena JA, Ribas F, Diaz-Delfin J, Giralt M, Iglesias R, and Villarroya F. Peroxisome proliferator-activated receptor-gamma coactivator-1alpha controls transcription of the Sirt3 gene, an essential component of the thermogenic brown adipocyte phenotype. *J Biol Chem* 286: 16958–16966, 2011.
55. Goldberg IJ and Ginsberg HN. Ins and outs modulating hepatic triglyceride and development of nonalcoholic fatty liver disease. *Gastroenterology* 130: 1343–1346, 2006.
56. Goldfine AB, Fonseca V, and Shoelson SE. Therapeutic approaches to target inflammation in type 2 diabetes. *Clin Chem* 57: 162–167, 2011.

57. Gomez-Cabrera MC, Domenech E, Romagnoli M, Arduini A, Borras C, Pallardo FV, Sastre J, and Vina J. Oral administration of vitamin C decreases muscle mitochondrial biogenesis and hampers training-induced adaptations in endurance performance. *Am J Clin Nutr* 87: 142–149, 2008.
58. Gregor MF and Hotamisligil GS. Thematic review series: Adipocyte Biology. Adipocyte stress: the endoplasmic reticulum and metabolic disease. *J Lipid Res* 48: 1905–1914, 2007.
59. Guilherme A, Virbasius JV, Puri V, and Czech MP. Adipocyte dysfunctions linking obesity to insulin resistance and type 2 diabetes. *Nat Rev Mol Cell Biol* 9: 367–377, 2008.
60. Han CY, Umemoto T, Omer M, Den Hartigh LJ, Chiba T, Leboeuf R, Buller CL, Sweet IR, Pennathur S, Abel ED, and Chait A. NADPH Oxidase-derived Reactive Oxygen Species Increases Expression of Monocyte Chemotactic Factor Genes in Cultured Adipocytes. *J Biol Chem* 287: 10379–10393, 2012.
61. Han DH, Nolte LA, Ju JS, Coleman T, Holloszy JO, and Semenkovich CF. UCP-mediated energy depletion in skeletal muscle increases glucose transport despite lipid accumulation and mitochondrial dysfunction. *Am J Physiol Endocrinol Metab* 286: E347–E353, 2004.
62. Harwood HJ, Jr., Petras SF, Shelly LD, Zaccaro LM, Perry DA, Makowski MR, Hargrove DM, Martin KA, Tracey WR, Chapman JG, Magee WP, Dalvie DK, Soliman VF, Martin WH, Mularski CJ, and Eisenbeis SA. Isozyme-nonselective N-substituted bipiperidylcarboxamide acetyl-CoA carboxylase inhibitors reduce tissue malonyl-CoA concentrations, inhibit fatty acid synthesis, and increase fatty acid oxidation in cultured cells and in experimental animals. *J Biol Chem* 278: 37099–37111, 2003.
63. Hatori M, Vollmers C, Zarrinpar A, Ditacchio L, Bushong EA, Gill S, Leblanc M, Chaix A, Joens M, Fitzpatrick JA, Ellisman MH, and Panda S. Time-restricted feeding without reducing caloric intake prevents metabolic diseases in mice fed a high-fat diet. *Cell Metab* 15: 848–860, 2012.
64. Hayes GR and Lockwood DH. Role of insulin receptor phosphorylation in the insulinomimetic effects of hydrogen peroxide. *Proc Natl Acad Sci U S A* 84: 8115–8119, 1987.
65. Heffetz D, Bushkin I, Dror R, and Zick Y. The insulinomimetic agents H2O2 and vanadate stimulate protein tyrosine phosphorylation in intact cells. *J Biol Chem* 265: 2896–2902, 1990.
66. Henique C, Mansouri A, Fumey G, Lenoir V, Girard J, Bouillaud F, Prip-Buus C, and Cohen I. Increased mitochondrial fatty acid oxidation is sufficient to protect skeletal muscle cells from palmitate-induced apoptosis. *J Biol Chem* 285: 36818–36827, 2010.
67. Henriksen EJ, Diamond-Stanic MK, and Marchionne EM. Oxidative stress and the etiology of insulin resistance and type 2 diabetes. *Free Radic Biol Med* 51: 993–999, 2011.
68. Herrero L, Shapiro H, Nayer A, Lee J, and Shoelson SE. Inflammation and adipose tissue macrophages in lipodystrophic mice. *Proc Natl Acad Sci U S A* 107: 240–245, 2010.
69. Higaki Y, Mikami T, Fujii N, Hirshman MF, Koyama K, Seino T, Tanaka K, and Goodyear LJ. Oxidative stress stimulates skeletal muscle glucose uptake through a phosphatidylinositol 3-kinase-dependent pathway. *Am J Physiol Endocrinol Metab* 294: E889–E897, 2008.
70. Hirschey MD, Shimazu T, Huang JY, and Verdin E. Acetylation of mitochondrial proteins. *Methods Enzymol* 457: 137–147, 2009.
71. Hirschey MD, Shimazu T, Jing E, Grueter CA, Collins AM, Aouizerat B, Stancakova A, Goetzman E, Lam MM, Schwer B, Stevens RD, Muehlbauer MJ, Kakar S, Bass NM, Kuusisto J, Laakso M, Alt FW, Newgard CB, Farese RV Jr., Kahn CR, and Verdin E. SIRT3 deficiency and mitochondrial protein hyperacetylation accelerate the development of the metabolic syndrome. *Mol Cell* 44: 177–190, 2011.
72. Hondares E, Rosell M, Gonzalez FJ, Giralt M, Iglesias R, and Villarroya F. Hepatic FGF21 expression is induced at birth via PPARalpha in response to milk intake and contributes to thermogenic activation of neonatal brown fat. *Cell Metab* 11: 206–212, 2010.
73. Hosogai N, Fukuhara A, Oshima K, Miyata Y, Tanaka S, Segawa K, Furukawa S, Tochino Y, Komuro R, Matsuda M, and Shimomura I. Adipose tissue hypoxia in obesity and its impact on adipocytokine dysregulation. *Diabetes* 56: 901–911, 2007.
74. Hotamisligil GS. Endoplasmic reticulum stress and the inflammatory basis of metabolic disease. *Cell* 140: 900–917, 2010.
75. Houstis N, Rosen ED, and Lander ES. Reactive oxygen species have a causal role in multiple forms of insulin resistance. *Nature* 440: 944–948, 2006.
76. Huang W, Ramsey KM, Marcheva B, and Bass J. Circadian rhythms, sleep, and metabolism. *J Clin Invest* 121: 2133–2141, 2011.
77. Iglesias MA, Ye JM, Frangioudakis G, Saha AK, Tomas E, Ruderman NB, Cooney GJ, and Kraegen EW. AICAR administration causes an apparent enhancement of muscle and liver insulin action in insulin-resistant high-fat-fed rats. *Diabetes* 51: 2886–2894, 2002.
78. Iglesias P, Selgas R, Romero S, and Diez JJ. Biological role. Clinical significance and therapeutic possibilities of the recently discovered metabolic hormone fibroblastic growth factor 21. *Eur J Endocrinol* 167: 301–309, 2012.
79. Irrcher I, Ljubicic V, and Hood DA. Interactions between ROS and AMP kinase activity in the regulation of PGC-1alpha transcription in skeletal muscle cells. *Am J Physiol Cell Physiol* 296: C116–C123, 2009.
80. Jing E, Emanuelli B, Hirschey MD, Boucher J, Lee KY, Lombard D, Verdin EM, and Kahn CR. Sirtuin-3 (Sirt3) regulates skeletal muscle metabolism and insulin signaling via altered mitochondrial oxidation and reactive oxygen species production. *Proc Natl Acad Sci U S A* 108: 14608–14613, 2011.
81. Katz A. Modulation of glucose transport in skeletal muscle by reactive oxygen species. *J Appl Physiol* 102: 1671–1676, 2007.
82. Kaushik S, Rodriguez-Navarro JA, Arias E, Kiffin R, Sahu S, Schwartz GJ, Cuervo AM, and Singh R. Autophagy in hypothalamic AgRP neurons regulates food intake and energy balance. *Cell Metab* 14: 173–183, 2011.
83. Keller H, Dreyer C, Medin J, Mahfoudi A, Ozato K, and Wahli W. Fatty acids and retinoids control lipid metabolism through activation of peroxisome proliferator-activated receptor-retinoid X receptor heterodimers. *Proc Natl Acad Sci U S A* 90: 2160–2164, 1993.
84. Khan A, Raza S, Khan Y, Aksoy T, Khan M, Weinberger Y, and Goldman J. Current updates in the medical management of obesity. *Recent Pat Endocr Metab* 6: 117–128, 2012.
85. Kim JS, Saengsirisuwan V, Sloniger JA, Teachey MK, and Henriksen EJ. Oxidant stress and skeletal muscle glucose transport: roles of insulin signaling and p38 MAPK. *Free Radic Biol Med* 41: 818–824, 2006.
86. Kontani Y, Wang Y, Kimura K, Inokuma KI, Saito M, Suzuki-Miura T, Wang Z, Sato Y, Mori N, and Yamashita H. UCP1 deficiency increases susceptibility to diet-induced obesity with age. *Aging Cell* 4: 147–155, 2005.
87. Kopecky J, Clarke G, Enerback S, Spiegelman B, and Kozak LP. Expression of the mitochondrial uncoupling protein

gene from the aP2 gene promoter prevents genetic obesity. *J Clin Invest* 96: 2914–2923, 1995.
88. Kotronen A, Seppala-Lindroos A, Vehkavaara S, Bergholm R, Frayn KN, Fielding BA, and Yki-Jarvinen H. Liver fat and lipid oxidation in humans. *Liver Int* 29: 1439–1446, 2009.
89. Koves TR, Ussher JR, Noland RC, Slentz D, Mosedale M, Ilkayeva O, Bain J, Stevens R, Dyck JR, Newgard CB, Lopaschuk GD, and Muoio DM. Mitochondrial overload and incomplete fatty acid oxidation contribute to skeletal muscle insulin resistance. *Cell Metab* 7: 45–56, 2008.
90. Kudin AP, Malinska D, and Kunz WS. Sites of generation of reactive oxygen species in homogenates of brain tissue determined with the use of respiratory substrates and inhibitors. *Biochim Biophys Acta* 1777: 689–695, 2008.
91. Kuo DY, Chen PN, Yang SF, Chu SC, Chen CH, Kuo MH, Yu CH, and Hsieh YS. Role of reactive oxygen species-related enzymes in neuropeptide y and proopiomelanocortin-mediated appetite control: a study using atypical protein kinase C knockdown. *Antioxid Redox Signal* 15: 2147–2159, 2011.
92. Lage R, Vazquez MJ, Varela L, Saha AK, Vidal-Puig A, Nogueiras R, Dieguez C, and Lopez M. Ghrelin effects on neuropeptides in the rat hypothalamus depend on fatty acid metabolism actions on BSX but not on gender. *FASEB J* 24: 2670–2679, 2010.
93. Lam TK, Schwartz GJ, and Rossetti L. Hypothalamic sensing of fatty acids. *Nat Neurosci* 8: 579–584, 2005.
94. Lan F, Cacicedo JM, Ruderman N, and Ido Y. SIRT1 modulation of the acetylation status, cytosolic localization, and activity of LKB1. Possible role in AMP-activated protein kinase activation. *J Biol Chem* 283: 27628–27635, 2008.
95. Le Foll C, Irani BG, Magnan C, Dunn-Meynell AA, and Levin BE. Characteristics and mechanisms of hypothalamic neuronal fatty acid sensing. *Am J Physiol Regul Integr Comp Physiol* 297: R655–R664, 2009.
96. Le May C, Cauzac M, Diradourian C, Perdereau D, Girard J, Burnol AF, and Pegorier JP. Fatty acids induce L-CPT I gene expression through a PPARalpha-independent mechanism in rat hepatoma cells. *J Nutr* 135: 2313–2319, 2005.
97. Lee AH, Scapa EF, Cohen DE, and Glimcher LH. Regulation of hepatic lipogenesis by the transcription factor XBP1. *Science* 320: 1492–1496, 2008.
98. Leonardsson G, Steel JH, Christian M, Pocock V, Milligan S, Bell J, So PW, Medina-Gomez G, Vidal-Puig A, White R, and Parker MG. Nuclear receptor corepressor RIP140 regulates fat accumulation. *Proc Natl Acad Sci U S A* 101: 8437–8442, 2004.
99. Levin BE. Metabolic sensors: viewing glucosensing neurons from a broader perspective. *Physiol Behav* 76: 397–401, 2002.
100. Loh K, Deng H, Fukushima A, Cai X, Boivin B, Galic S, Bruce C, Shields BJ, Skiba B, Ooms LM, Stepto N, Wu B, Mitchell CA, Tonks NK, Watt MJ, Febbraio MA, Crack PJ, Andrikopoulos S, and Tiganis T. Reactive oxygen species enhance insulin sensitivity. *Cell Metab* 10: 260–272, 2009.
101. Louet JF, Chatelain F, Decaux JF, Park EA, Kohl C, Pineau T, Girard J, and Pegorier JP. Long-chain fatty acids regulate liver carnitine palmitoyltransferase I gene (L-CPT I) expression through a peroxisome-proliferator-activated receptor alpha (PPARalpha)-independent pathway. *Biochem J* 354: 189–197, 2001.
102. Lowell BB and Shulman GI. Mitochondrial dysfunction and type 2 diabetes. *Science* 307: 384–387, 2005.
103. Lumeng CN, Bodzin JL, and Saltiel AR. Obesity induces a phenotypic switch in adipose tissue macrophage polarization. *J Clin Invest* 117: 175–184, 2007.
104. Lumeng CN, Maillard I, and Saltiel AR. T-ing up inflammation in fat. *Nat Med* 15: 846–847, 2009.
105. Machann J, Bachmann OP, Brechtel K, Dahl DB, Wietek B, Klumpp B, Haring HU, Claussen CD, Jacob S, and Schick F. Lipid content in the musculature of the lower leg assessed by fat selective MRI: intra- and interindividual differences and correlation with anthropometric and metabolic data. *J Magn Reson Imaging* 17: 350–357, 2003.
106. Mailloux RJ and Harper ME. Uncoupling proteins and the control of mitochondrial reactive oxygen species production. *Free Radic Biol Med* 51: 1106–1115, 2011.
107. Mathis D and Shoelson SE. Immunometabolism: an emerging frontier. *Nat Rev Immunol* 11: 81, 2011.
108. McCune SA and Harris RA. Mechanism responsible for 5-(tetradecyloxy)-2-furoic acid inhibition of hepatic lipogenesis. *J Biol Chem* 254: 10095–10101, 1979.
109. McGarry JD and Brown NF. The mitochondrial carnitine palmitoyltransferase system. From concept to molecular analysis. *Eur J Biochem* 244: 1–14, 1997.
110. Mera P, Bentebibel A, Lopez-Vinas E, Cordente AG, Gurunathan C, Sebastian D, Vazquez I, Herrero L, Ariza X, Gomez-Puertas P, Asins G, Serra D, Garcia J, and Hegardt FG. C75 is converted to C75-CoA in the hypothalamus, where it inhibits carnitine palmitoyltransferase 1 and decreases food intake and body weight. *Biochem Pharmacol* 77: 1084–1095, 2009.
111. Michan S and Sinclair D. Sirtuins in mammals: insights into their biological function. *Biochem J* 404: 1–13, 2007.
112. Miele L, Grieco A, Armuzzi A, Candelli M, Forgione A, Gasbarrini A, and Gasbarrini G. Hepatic mitochondrial beta-oxidation in patients with nonalcoholic steatohepatitis assessed by 13C-octanoate breath test. *Am J Gastroenterol* 98: 2335–2336, 2003.
113. Migrenne S, Le Foll C, Levin BE, and Magnan C. Brain lipid sensing and nervous control of energy balance. *Diabetes Metab* 37: 83–88, 2011.
114. Minnich A, Tian N, Byan L, and Bilder G. A potent PPARalpha agonist stimulates mitochondrial fatty acid beta-oxidation in liver and skeletal muscle. *Am J Physiol Endocrinol Metab* 280: E270–E279, 2001.
115. Minokoshi Y, Alquier T, Furukawa N, Kim YB, Lee A, Xue B, Mu J, Foufelle F, Ferre P, Birnbaum MJ, Stuck BJ, and Kahn BB. AMP-kinase regulates food intake by responding to hormonal and nutrient signals in the hypothalamus. *Nature* 428: 569–574, 2004.
116. Mollica MP, Iossa S, Liverini G, and Soboll S. Steady state changes in mitochondrial electrical potential and proton gradient in perfused liver from rats fed a high fat diet. *Mol Cell Biochem* 178: 213–217, 1998.
117. Monsenego J, Mansouri A, Akkaoui M, Lenoir V, Esnous C, Fauveau V, Tavernier V, Girard J, and Prip-Buus C. Enhancing liver mitochondrial fatty acid oxidation capacity in obese mice improves insulin sensitivity independently of hepatic steatosis. *J Hepatol* 56: 632–639, 2012.
118. Morillas M, Gomez-Puertas P, Bentebibel A, Selles E, Casals N, Valencia A, Hegardt FG, Asins G, and Serra D. Identification of conserved amino acid residues in rat liver carnitine palmitoyltransferase I critical for malonyl-CoA inhibition. Mutation of methionine 593 abolishes malonyl-CoA inhibition. *J Biol Chem* 278: 9058–9063, 2003.
119. Muoio DM. Intramuscular triacylglycerol and insulin resistance: guilty as charged or wrongly accused? *Biochim Biophys Acta* 1801: 281–288, 2010.
120. Muoio DM and Koves TR. Skeletal muscle adaptation to fatty acid depends on coordinated actions of the PPARs

and PGC1 alpha: implications for metabolic disease. *Appl Physiol Nutr Metab* 32: 874–883, 2007.
121. Muoio DM and Neufer PD. Lipid-induced mitochondrial stress and insulin action in muscle. *Cell Metab* 15: 595–605, 2012.
122. Murphy MP. How mitochondria produce reactive oxygen species. *Biochem J* 417: 1–13, 2009.
123. Nakamuta M, Kohjima M, Morizono S, Kotoh K, Yoshimoto T, Miyagi I, and Enjoji M. Evaluation of fatty acid metabolism-related gene expression in nonalcoholic fatty liver disease. *Int J Mol Med* 16: 631–635, 2005.
124. Nedergaard J, Bengtsson T, and Cannon B. Unexpected evidence for active brown adipose tissue in adult humans. *Am J Physiol Endocrinol Metab* 293: E444–E452, 2007.
125. Nguyen KD, Qiu Y, Cui X, Goh YP, Mwangi J, David T, Mukundan L, Brombacher F, Locksley RM, and Chawla A. Alternatively activated macrophages produce catecholamines to sustain adaptive thermogenesis. *Nature* 480: 104–108, 2011.
126. O'Neil PM, Smith SR, Weissman NJ, Fidler MC, Sanchez M, Zhang J, Raether B, Anderson CM, and Shanahan WR. Randomized placebo-controlled clinical trial of lorcaserin for weight loss in type 2 diabetes mellitus: The BLOOM-DM Study. *Obesity* 20: 1426–1436, 2012.
127. Obici S, Feng Z, Arduini A, Conti R, and Rossetti L. Inhibition of hypothalamic carnitine palmitoyltransferase-1 decreases food intake and glucose production. *Nat Med* 9: 756–761, 2003.
128. Obici S, Feng Z, Morgan K, Stein D, Karkanias G, and Rossetti L. Central administration of oleic acid inhibits glucose production and food intake. *Diabetes* 51: 271–275, 2002.
129. Olefsky JM and Glass CK. Macrophages, inflammation, and insulin resistance. *Annu Rev Physiol* 72: 219–246, 2010.
130. Orellana-Gavalda JM, Herrero L, Malandrino MI, Paneda A, Sol Rodriguez-Pena M, Petry H, Asins G, Van Deventer S, Hegardt FG, and Serra D. Molecular therapy for obesity and diabetes based on a long-term increase in hepatic fatty-acid oxidation. *Hepatology* 53: 821–832, 2011.
131. Ortega FJ, Jilkova ZM, Moreno-Navarrete JM, Pavelka S, Rodriguez-Hermosa JI, Kopeck Ygrave J, and Fernandez-Real JM. Type I iodothyronine 5′-deiodinase mRNA and activity is increased in adipose tissue of obese subjects. *Int J Obes* 36: 320–324, 2011.
132. Ozcan U, Cao Q, Yilmaz E, Lee AH, Iwakoshi NN, Ozdelen E, Tuncman G, Gorgun C, Glimcher LH, and Hotamisligil GS. Endoplasmic reticulum stress links obesity, insulin action, and type 2 diabetes. *Science* 306: 457–461, 2004.
133. Park EA, Mynatt RL, Cook GA, and Kashfi K. Insulin regulates enzyme activity, malonyl-CoA sensitivity and mRNA abundance of hepatic carnitine palmitoyltransferase-I. *Biochem J* 310: 853–858, 1995.
134. Paterson JM, Morton NM, Fievet C, Kenyon CJ, Holmes MC, Staels B, Seckl JR, and Mullins JJ. Metabolic syndrome without obesity: Hepatic overexpression of 11beta-hydroxysteroid dehydrogenase type 1 in transgenic mice. *Proc Natl Acad Sci U S A* 101: 7088–7093, 2004.
135. Pillai VB, Sundaresan NR, Kim G, Gupta M, Rajamohan SB, Pillai JB, Samant S, Ravindra PV, Isbatan A, and Gupta MP. Exogenous NAD blocks cardiac hypertrophic response via activation of the SIRT3-LKB1-AMP-activated kinase pathway. *J Biol Chem* 285: 3133–3144, 2010.
136. Pissios P and Maratos-Flier E. More than satiety: central serotonin signaling and glucose homeostasis. *Cell Metab* 6: 345–347, 2007.
137. Pizer ES, Jackisch C, Wood FD, Pasternack GR, Davidson NE, and Kuhajda FP. Inhibition of fatty acid synthesis induces programmed cell death in human breast cancer cells. *Cancer Res* 56: 2745–2747, 1996.
138. Price N, van der Leij F, Jackson V, Corstorphine C, Thomson R, Sorensen A, and Zammit V. A novel brain-expressed protein related to carnitine palmitoyltransferase I. *Genomics* 80: 433–442, 2002.
139. Ritov VB, Menshikova EV, Azuma K, Wood R, Toledo FG, Goodpaster BH, Ruderman NB, and Kelley DE. Deficiency of electron transport chain in human skeletal muscle mitochondria in type 2 diabetes mellitus and obesity. *Am J Physiol Endocrinol Metab* 298: E49–E58, 2009
140. Rochford JJ, Myers MG, Jr., and Heisler LK. Setting the tone: reactive oxygen species and the control of appetitive melanocortin neurons. *Cell Metab* 14: 573–574, 2011.
141. Roman EA, Reis D, Romanatto T, Maimoni D, Ferreira EA, Santos GA, Torsoni AS, Velloso LA, and Torsoni MA. Central leptin action improves skeletal muscle AKT, AMPK, and PGC1 alpha activation by hypothalamic PI3K-dependent mechanism. *Mol Cell Endocrinol* 314: 62–69, 2010.
142. Rosen ED and Spiegelman BM. Adipocytes as regulators of energy balance and glucose homeostasis. *Nature* 444: 847–853, 2006.
143. Saito M, Okamatsu-Ogura Y, Matsushita M, Watanabe K, Yoneshiro T, Nio-Kobayashi J, Iwanaga T, Miyagawa M, Kameya T, Nakada K, Kawai Y, and Tsujisaki M. High incidence of metabolically active brown adipose tissue in healthy adult humans: effects of cold exposure and adiposity. *Diabetes* 58: 1526–1531, 2009.
144. Samuel VT, Petersen KF, and Shulman GI. Lipid-induced insulin resistance: unravelling the mechanism. *Lancet* 375: 2267–2277, 2010.
145. Samuel VT and Shulman GI. Mechanisms for insulin resistance: common threads and missing links. *Cell* 148: 852–871, 2012.
146. Savage DB, Choi CS, Samuel VT, Liu ZX, Zhang D, Wang A, Zhang XM, Cline GW, Yu XX, Geisler JG, Bhanot S, Monia BP, and Shulman GI. Reversal of diet-induced hepatic steatosis and hepatic insulin resistance by antisense oligonucleotide inhibitors of acetyl-CoA carboxylases 1 and 2. *J Clin Invest* 116: 817–824, 2006.
147. Schenk S, Saberi M, and Olefsky JM. Insulin sensitivity: modulation by nutrients and inflammation. *J Clin Invest* 118: 2992–3002, 2008.
148. Schug TT and Li X. Sirtuin 1 in lipid metabolism and obesity. *Ann Med* 43: 198–211, 2011.
149. Sebastian D, Herrero L, Serra D, Asins G, and Hegardt FG. CPT I overexpression protects L6E9 muscle cells from fatty acid-induced insulin resistance. *Am J Physiol Endocrinol Metab* 292: E677–E686, 2007.
150. Serviddio G, Giudetti AM, Bellanti F, Priore P, Rollo T, Tamborra R, Siculella L, Vendemiale G, Altomare E, and Gnoni GV. Oxidation of hepatic carnitine palmitoyl transferase-I (CPT-I) impairs fatty acid beta-oxidation in rats fed a methionine-choline deficient diet. *PloS One* 6: e24084, 2011.
151. Shoelson SE, Herrero L, and Naaz A. Obesity, inflammation, and insulin resistance. *Gastroenterology* 132: 2169–2180, 2007.
152. Shulman GI, Rothman DL, Jue T, Stein P, DeFronzo RA, and Shulman RG. Quantitation of muscle glycogen synthesis in normal subjects and subjects with non-insulin-dependent diabetes by 13C nuclear magnetic resonance spectroscopy. *N Engl J Med* 322: 223–228, 1990.

153. Simoneau JA, Veerkamp JH, Turcotte LP, and Kelley DE. Markers of capacity to utilize fatty acids in human skeletal muscle: relation to insulin resistance and obesity and effects of weight loss. *FASEB J* 13: 2051–2060, 1999.
154. Solinas G and Karin M. JNK1 and IKKbeta: molecular links between obesity and metabolic dysfunction. *FASEB J* 24: 2596–2611, 2010.
155. Starley BQ, Calcagno CJ, and Harrison SA. Nonalcoholic fatty liver disease and hepatocellular carcinoma: a weighty connection. *Hepatology* 51: 1820–1832, 2010.
156. Steyn FJ, Leong JW, Huang L, Tan HY, Xie TY, Nelson C, Waters MJ, Veldhuis JD, Epelbaum J, and Chen C. GH does not modulate the early fasting-induced release of free fatty acids in mice. *Endocrinology* 153: 273–282, 2012.
157. Sun K, Kusminski CM, and Scherer PE. Adipose tissue remodeling and obesity. *J Clin Invest* 121: 2094–2101, 2011.
158. Sunny NE, Parks EJ, Browning JD, and Burgess SC. Excessive hepatic mitochondrial TCA cycle and gluconeogenesis in humans with nonalcoholic fatty liver disease. *Cell Metab* 14: 804–810, 2011.
159. Taube A, Eckardt K, and Eckel J. Role of lipid-derived mediators in skeletal muscle insulin resistance. *Am J Physiol Endocrinol Metab* 297: E1004–E1012, 2009.
160. Taubes G. Insulin resistance. Prosperity's plague. *Science* 325: 256–260, 2009.
161. Tiniakos DG, Vos MB, and Brunt EM. Nonalcoholic fatty liver disease: pathology and pathogenesis. *Annu Rev Pathol* 5: 145–171, 2010.
162. Tseng YH, Cypess AM, and Kahn CR. Cellular bioenergetics as a target for obesity therapy. *Nat Rev Drug Discov* 9: 465–482, 2010.
163. Tunstall RJ, Mehan KA, Wadley GD, Collier GR, Bonen A, Hargreaves M, and Cameron-Smith D. Exercise training increases lipid metabolism gene expression in human skeletal muscle. *Am J Physiol Endocrinol Metab* 283: E66–E72, 2002.
164. Turner N, Bruce CR, Beale SM, Hoehn KL, So T, Rolph MS, and Cooney GJ. Excess lipid availability increases mitochondrial fatty acid oxidative capacity in muscle: evidence against a role for reduced fatty acid oxidation in lipid-induced insulin resistance in rodents. *Diabetes* 56: 2085–2092, 2007.
165. van Marken Lichtenbelt WD, Vanhommerig JW, Smulders NM, Drossaerts JM, Kemerink GJ, Bouvy ND, Schrauwen P, and Teule GJ. Cold-activated brown adipose tissue in healthy men. *N Engl J Med* 360: 1500–1508, 2009.
166. Velasco G, Geelen MJ, and Guzman M. Control of hepatic fatty acid oxidation by 5'-AMP-activated protein kinase involves a malonyl-CoA-dependent and a malonyl-CoA-independent mechanism. *Arch Biochem Biophys* 337: 169–175, 1997.
167. Velasquez DA, Martinez G, Romero A, Vazquez MJ, Boit KD, Dopeso-Reyes IG, Lopez M, Vidal A, Nogueiras R, and Dieguez C. The central Sirtuin 1/p53 pathway is essential for the orexigenic action of ghrelin. *Diabetes* 60: 1177–1185, 2011.
168. Virtanen KA, Lidell ME, Orava J, Heglind M, Westergren R, Niemi T, Taittonen M, Laine J, Savisto NJ, Enerback S, and Nuutila P. Functional brown adipose tissue in healthy adults. *N Engl J Med* 360: 1518–1525, 2009.
169. Virtue S and Vidal-Puig A. Adipose tissue expandability, lipotoxicity and the Metabolic Syndrome—an allostatic perspective. *Biochim Biophys Acta* 1801: 338–349, 2010.
170. Wagner BA, Buettner GR, and Burns CP. Free radical-mediated lipid peroxidation in cells: oxidizability is a function of cell lipid bis-allylic hydrogen content. *Biochemistry* 33: 4449–4453, 1994.
171. Weisberg SP, McCann D, Desai M, Rosenbaum M, Leibel RL, and Ferrante AW, Jr. Obesity is associated with macrophage accumulation in adipose tissue. *J Clin Invest* 112: 1796–1808, 2003.
172. Whittle AJ, Carobbio S, Martins L, Slawik M, Hondares E, Vazquez MJ, Morgan D, Csikasz RI, Gallego R, Rodriguez-Cuenca S, Dale M, Virtue S, Villarroya F, Cannon B, Rahmouni K, Lopez M, and Vidal-Puig A. BMP8B increases brown adipose tissue thermogenesis through both central and peripheral actions. *Cell* 149: 871–885, 2012.
173. Wolfgang MJ, Cha SH, Sidhaye A, Chohnan S, Cline G, Shulman GI, and Lane MD. Regulation of hypothalamic malonyl-CoA by central glucose and leptin. *Proc Natl Acad Sci U S A* 104: 19285–19290, 2007.
174. Woods A, Johnstone SR, Dickerson K, Leiper FC, Fryer LG, Neumann D, Schlattner U, Wallimann T, Carlson M, and Carling D. LKB1 is the upstream kinase in the AMP-activated protein kinase cascade. *Curr Biol* 13: 2004–2008, 2003.
175. Yamazaki N, Shinohara Y, Shima A, and Terada H. High expression of a novel carnitine palmitoyltransferase I like protein in rat brown adipose tissue and heart: isolation and characterization of its cDNA clone. *FEBS Lett* 363: 41–45, 1995.
176. Yeh LA, Lee KH, and Kim KH. Regulation of rat liver acetyl-CoA carboxylase. Regulation of phosphorylation and inactivation of acetyl-CoA carboxylase by the adenylate energy charge. *J Biol Chem* 255: 2308–2314, 1980.
177. Yue JT and Lam TK. Lipid sensing and insulin resistance in the brain. *Cell Metab* 15: 646–655, 2012.
178. Zeng L, Lu M, Mori K, Luo S, Lee AS, Zhu Y, and Shyy JY. ATF6 modulates SREBP2-mediated lipogenesis. *EMBO J* 23: 950–958, 2004.
179. Zhang Y, Proenca R, Maffei M, Barone M, Leopold L, and Friedman JM. Positional cloning of the mouse obese gene and its human homologue. *Nature* 372: 425–432, 1994.
180. Zhou G, Myers R, Li Y, Chen Y, Shen X, Fenyk-Melody J, Wu M, Ventre J, Doebber T, Fujii N, Musi N, Hirshman MF, Goodyear LJ, and Moller DE. Role of AMP-activated protein kinase in mechanism of metformin action. *J Clin Invest* 108: 1167–1174, 2001.
181. Zingaretti MC, Crosta F, Vitali A, Guerrieri M, Frontini A, Cannon B, Nedergaard J, and Cinti S. The presence of UCP1 demonstrates that metabolically active adipose tissue in the neck of adult humans truly represents brown adipose tissue. *FASEB J* 23: 3113–3120, 2009.

Address correspondence to:
Dr. Laura Herrero
Department of Biochemistry and Molecular Biology
School of Pharmacy
University of Barcelona
Av. Diagonal, 643
E-08028 Barcelona
Spain

E-mail: lherrero@ub.edu

Date of first submission to ARS Central, August 11, 2012; date of acceptance, August 19, 2012.

Abbreviations Used

ACC = acetyl-CoA carboxylase
AgRP = agouti-related protein
AMPK = AMP-activated protein kinase
BAT = brown adipose tissue
BMI = body mass index
CACT = acylcarnitine translocase
CPT1 = carnitine palmitoyltransferase 1
CPT1A = liver CPT1
CT = computed tomography
DAG = diacylglycerol
ETC = electron transport chain
FA = fatty acid
FAO = fatty acid oxidation
FAS = fatty acid synthase
FFA = free fatty acid
FGF21 = fibroblast growth factor 21
HFD = high-fat diet
IMC = intramyocellular
LCFA-CoA = long-chain fatty acid-CoA
MCD = malonyl-CoA decarboxylase
NAFLD = nonalcoholic fatty liver disease
NASH = nonalcoholic steatohepatitis
NPY = neuropeptide Y
PET = positron-emission tomography
ROS = reactive oxygen species
SkM = skeletal muscle
TCA = tricarboxylic acid
TG = triglyceride
UCPs = uncoupling proteins
UPR = uncoupled protein response
WAT = white adipose tissue